



Coastline Assessment to Support Ecological and Economic Resilience of a Tribal Community on the Northern Washington Coast

By

George M. Kaminsky, Hannah Drummond, Amanda Hacking,
Heather M. Weiner, and Diana McCandless

For the

Shorelands and Environmental Assistance Program

Washington State Department of Ecology

Olympia, Washington

November 2022, Publication 22-06-007

Publication Information

This document is available on the Department of Ecology's website at:

<http://ecyapfaff/Biblio2/SummaryPages/2206007.html>

Suggested Citation

Kaminsky, G.M., Drummond, H., Hacking, A., Weiner, H.M., and McCandless, D. 2022. Coastline Assessment to Support Ecological and Economic Resilience of a Tribal Community on the Northern Washington Coast, Publication 22-06-007. Washington State Department of Ecology, Olympia. <http://ecyapfaff/Biblio2/SummaryPages/2206007.html>.

Related Information

- Washington Coast Restoration and Resiliency Initiative RCO PRISM Project #18-2137
- WebMap: [Makah Bay Coastal Change \(arcgis.com\)](#)

Contact Information

Coastal Monitoring & Analysis Program Unit Shorelands and Environmental Assistance Program

George Kaminsky, PhD, PE
Senior Coastal Engineer
george.kaminsky@ecy.wa.gov

P.O. Box 47600
Olympia, WA 98504-7600
Phone: 360-407-6600

Website¹: [Washington State Department of Ecology](#)

ADA Accessibility

The Department of Ecology is committed to providing people with disabilities access to information and services by meeting or exceeding the requirements of the Americans with Disabilities Act (ADA), Section 504 and 508 of the Rehabilitation Act, and Washington State Policy #188.

To request an ADA accommodation, contact Ecology by phone at 360-407-6831 or email at ecyadacoordinator@ecy.wa.gov. For Washington Relay Service or TTY call 711 or 877-833-6341. Visit Ecology's website for more information.

¹ www.ecology.wa.gov/contact

Department of Ecology's Regional Offices

Map of Counties Served



Southwest Region 360-407-6300	Northwest Region 206-594-0000	Central Region 509-575-2490	Eastern Region 509-329-3400
---	---	---------------------------------------	---------------------------------------

Region	Counties Served	Mailing Address	Phone
Southwest	Clallam, Clark, Cowlitz, Grays Harbor, Jefferson, Mason, Lewis, Pacific, Pierce, Skamania, Thurston, Wahkiakum	PO Box 47775 Olympia, WA 98504	360-407-6300
Northwest	Island, King, Kitsap, San Juan, Skagit, Snohomish, Whatcom	PO Box 330316 Shoreline, WA 98133	206-594-0000
Central	Benton, Chelan, Douglas, Kittitas, Klickitat, Okanogan, Yakima	1250 W Alder St Union Gap, WA 98903	509-575-2490
Eastern	Adams, Asotin, Columbia, Ferry, Franklin, Garfield, Grant, Lincoln, Pend Oreille, Spokane, Stevens, Walla Walla, Whitman	4601 N Monroe Spokane, WA 99205	509-329-3400
Headquarters	Across Washington	PO Box 46700 Olympia, WA 98504	360-407-6000

This page is purposely left blank

Coastline Assessment to Support Ecological and Economic Resilience of a Tribal Community on the Northern Washington Coast

By

George M. Kaminsky, Hannah Drummond, Amanda Hacking,
Heather M. Weiner, and Diana McCandless

Shorelands and Environmental Assistance Program

Washington State Department of Ecology
Olympia, WA

November 2022 | Publication 22-06-007



DEPARTMENT OF
ECOLOGY
State of Washington

Table of Contents

List of Figures and Tables	5
Figures.....	5
Tables.....	9
Acknowledgements	13
Executive Summary	14
Introduction	17
Background.....	17
Site overview.....	17
Methods	21
Historical coastline change.....	23
Biennial topo-bathymetric change.....	31
Makah Bay Results	41
Overview.....	41
Hobuck Beach.....	48
Tsoo-Yess Beach.....	60
Synthesis of results.....	66
Ozette Sub-region Results	73
Overview.....	73
Historical coastline change.....	73
Synthesis of Results.....	80
Discussion	82
Makah Bay.....	83
Ozette Reservation.....	86
Conclusion	93
References	96
Appendix A. Assessment of Measurement Uncertainties	101
Base station monument.....	101
Positional uncertainty.....	101
Topographic measurement uncertainty.....	103
Bathymetric measurement uncertainty.....	104

Total measurement uncertainty 105

Appendix B. Historical Vegetation Line Change Tables, Makah Bay..... 109

Appendix C. Historical Shoreline Change Tables, Makah Bay 109

Appendix D. Historical Coastline Change Tables, Ozette Sub-region 139

Appendix E. Topo-bathymetric Map of Makah Bay..... 158

List of Figures and Tables

Figures

Figure 1. General vicinity map of the Makah Reservation and project sub-regions: Hobuck Beach, Tsoo-Yess Beach, and the Ozette Reservation..... **18**

Figure 2. Aerial imagery of Hobuck Beach with project site outlined in yellow (2017 NAIP)..... **19**

Figure 3. Aerial imagery of Tsoo-Yess Beach with project site outlined in yellow (2017 NAIP). . **20**

Figure 4. Aerial imagery of the Ozette sub-region with project site outlined in yellow (2015 NAIP)..... **21**

Figure 5. Example of registration error between the 2013 and 2011 NAIP imagery in a southern reach of Hobuck Beach, and example of an area where shadows and tree cover obscure the vegetation line in a southern reach of Tsoo-Yess Beach. **27**

Figure 6. Method used to calculate an average localized beach slope to make horizontal adjustments to the digitized shoreline. **28**

Figure 7. Method used to determine the horizontal adjustment applied to the digitized mean high water tide plus wave runup shoreline, resulting in a derived shoreline position..... **28**

Figure 8. Google Street View photo showing an example of the seaward extent of the sand wedge that was digitized at the Ozette Reservation as another feature to determine coastline change..... **29**

Figure 9. Calculation and display of coastline change analysis results, shown here as change at the vegetation line. **30**

Figure 10. Cluster boundaries identified by a multivariate cluster analysis based on historical coastline change rates..... **31**

Figure 11. Planned survey coverage of Makah Bay with polygons delineating approximate survey boundaries and types of data collected for the topo-bathymetric surveys: multibeam echosounder (MBES; sonar), mobile laser scanning (MLS; boat-based lidar); and GNSS topography (Topo) including transects (black lines) **32**

Figure 12. Topo-bathymetric data collection techniques. A) GNSS Base station. B) Topographic data collection using GNSS mounted on backpacks. C) Topographic surface mapping using a GNSS mounted on an ATV. D) R/V George Davidson collecting MBES in the nearshore. E) Lidar target being surveyed..... **33**

Figure 13. Combined topo-bathymetric data coverage of Makah Bay from CMAP’s 2019 and 2021 surveys (2017 NAIP imagery). **34**

Figure 14. DEM topo-bathymetric coverage of Makah Bay from the 2019 surveys, gridded at 0.5 m (2017 NAIP imagery)..... **36**

Figure 15. Change surface from September 2019 to July 2021, with the 2021 MLLW contour for context (2017 NAIP imagery). **37**

Figure 16. Change surface from September 2019 to July 2021 with zones used for analysis. Zones were roughly defined by following contours of no change..... **38**

Figure 17. Cross-shore shoreface change swaths centered on clusters defined by the historical vegetation line change rates for comparative analyses. **39**

Figure 18. Makah Bay average shoreline and vegetation line change rates by cluster, with the overall average 10-year and long-term change rates in Makah Bay for the vegetation line and shoreline. **43**

Figure 19 Makah Bay average vegetation line change rates by cluster, and average based on the 10-m transects. Accretion is indicated by positive change rate values and erosion is indicated by negative change rate values. **44**

Figure 20. Change surface from September 2019 to July 2021 with zones showing net volume change and net elevation change (cm). **46**

Figure 21. Long-term (1952-2019) and recent 10-year (2009-2019) coastline change rates at 10-m transect intervals along Hobuck Beach, based on digitized shorelines and vegetation lines from aerial imagery..... **48**

Figure 22. Select vegetation lines digitized from aerial imagery in Cluster 3 and 4, near Hobuck Creek and the Hobuck RV Campground..... **50**

Figure 23. Hobuck Creek channel thalwegs crossing Hobuck Beach digitized from aerial imagery with select years of imagery between 1985 and 2017 showing key instances of Hobuck Creek thalweg migration from south to north. **51**

Figure 24. Normalized Difference Vegetation Index (NDVI) enhanced aerial imagery overlain on true color imagery to display the removal of trees between 2011 and 2013 followed by significant vegetation line retreat between 2013 and 2015 at the Hobuck RV Campground..... **52**

Figure 25. Vegetation lines digitized from aerial imagery at the mouth of the Tsoo-Yess River, with select years of imagery between 1985 and 2019 showing vegetation line progradation and increase in vegetation density through time..... **53**

Figure 26. Vegetation lines digitized from aerial imagery at the mouth of the Wa'atch River, with select years of imagery between 1964 and 2019 displaying the vegetation line progradation..... **54**

Figure 27. Hobuck Beach 2019 topo-bathymetric DEM with MLLW contour and 5-m NAVD88 contours overlaid for reference, with transects A and B measured between the -10 m contour and MLLW contour for shoreface width comparison..... **55**

Figure 28. Hobuck Beach change surface from September 2019 to July 2021 with 2021 MLLW contour and 1-m NAVD88 contours overlaid. **57**

Figure 29. Hobuck Creek 2019 DEM, 2021 DEM, and change surface, with respective years' MLLW and 1-m NAVD88 contours..... **58**

Figure 30. Google Earth imagery from August 19, 2016 showing intertidal bar and trough complexity fronting the Hobuck RV Campground..... **58**

Figure 31. Hobuck Beach change surface from September 2019 to July 2021 with change zone boundaries overlaid showing gross positive and negative volume change in 1000 m3. **59**

Figure 32. Long-term and 10-year shoreline and vegetation line change rates at 10-m transect intervals along Tsoo-Yess Beach..... **61**

Figure 33. Tsoo-Yess Beach 2019 topo-bathymetric DEM with MLLW contour and 5-m NAVD88 contours overlaid for reference. **63**

Figure 34. Tsoo-Yess Beach change surface from September 2019 to July 2021 with 2021 MLLW contour and 1-m NAVD88 contours overlaid. **64**

Figure 35. Tsoo-Yess Beach change surface from September 2019 to July 2021 with change zone boundaries overlaid showing gross positive and negative volume change in 1000 m3. **65**

Figure 36. Cluster-based shoreface change from 150 m-wide swaths from the 2019-2021 topobathymetric difference surface; MHHW and MLLW. **68**

Figure 37. Integrated coastline change rates based on the average of vegetation line and shoreline change along Hobuck Beach with trendlines divided at Hobuck Creek **70**

Figure 38. Integrated coastline change rates based on the average of vegetation line and shoreline change along Tsoo-Yess Beach. **71**

Figure 39. Ozette sub-region shoreline and seaward edge of the sand wedge average change rates by cluster, with the overall averaged indicated for comparison..... **75**

Figure 40. Ozette sub-region shoreline, sand wedge, and vegetation line average change rates by cluster, with overall averages calculated from the 10-m transects. 76

Figure 41. Ozette sub-region number of transects, alongshore lengths, 10-year shoreline change, and standard deviation of the 10-year shoreline change per cluster. 77

Figure 42. Photos from Washington Department of Ecology Oblique Shoreline Photo Viewer showing examples of qualitative observations characterizing vegetation line change at the Ozette Reservation and sub-region. 79

Figure 43. Google Street View photos showing erosion along the Ozette sub-region near the boundary of Cluster 43 and 44 and Cluster 46. 80

Figure 44. Ozette sub-region reaches based on 10-year cluster-average shoreline rates and geomorphic features on the coastline. 81

Figure 45. Conceptual dynamic cobble revetment and bank stabilization approach to counter coastal erosion at North Cove, Washington. 85

Figure 46. Example of large wood energy dissipaters installed along drainage ditch mouth to control channel meandering across the beach at North Cove, Washington. 86

Figure 47. WDNR 2018 digital elevation model of the Ozette Reservation coastline with blue and tan colors showing the intertidal zone and beach, and shades of green showing the upland topography. 88

Figure 48. Google Street View photos looking alongshore along the Ozette Reservation and sub-region used to characterize beach conditions. 89

Figure 49. Photos taken at the Ozette Reservation showing beach conditions. 90

Figure 50. Depiction of the creation of a beach terrace through construction of a rock ridge along the low tide line on a bedrock or rocky slope. 92

Figure 51. Conceptual drawing of the setting and beach dynamics at Makah Bay and the Ozette Reservation. 94

Figure A-1. Boxplot showing distribution of elevation measurements at the Bahobohosh survey monument from the 2019 survey and 2021 survey. 103

Figure E-1. Topo-bathymetric digital elevation model of Makah Bay with contours indicating elevation relative to mean lower low water (MLLW). 159

Tables

Table 1. Information describing the 12 sets of imagery used in the historical coastline change analysis for Makah Bay including the date, source, spatial resolution (pixel size), root mean square error (RMSE) for photos that were georeferenced, and description of the imagery type. **24**

Table 2. Information describing the 9 sets of imagery and 2 sets of lidar data used in the historical coastline change analysis for the Ozette Reservation including the date, source, spatial resolution (pixel size), and root mean square error (RMSE) for photos that were georeferenced, and description of the imagery type. **25**

Table 3. Volume and elevation changes derived from September 2019 and July 2021 topo-bathymetric surveys for zones shown in Figure 16 and Figure 20. **47**

Table A-1. Local geographic coordinates for epoxy monument, Bahobohosh, in NAD83 (2011) with ellipsoid height relative to GRS80, meters. **101**

Table A-2. Grid coordinates for epoxy monument, Bahobohosh, in Washington State Plane North, NAD83 (2011), meters, with elevation relative to NAVD88 (GEOID12B), meters. **101**

Table A-3. Summary of topography data used to assess the vertical precision of the topographic DEMs. **104**

Table A-4. Summary of survey lines and survey area used to assess the vertical precision of the bathymetric survey. **104**

Table A-5. Gross accretion and erosion sub-areas, volume changes, and propagated errors derived from September 2019 and July 2021 topo-bathymetric surveys for zones shown in Figure 16 and Figure 20. **106**

Table A-6. Gross accretion and erosion sub-areas, volume changes, and propagated errors derived from September 2019 and July 2021 topo-bathymetric surveys for zones shown in Figure 16 and Figure 21 (continued). **107**

Table B-1. Historical vegetation line change rates in Makah Bay based on the 10-m average transects in Cluster 1. **109**

Table B-2. Historical vegetation line change rates in Makah Bay based on the 10-m average transects in Cluster 2a. **110**

Table B-3. Historical vegetation line change rates in Makah Bay based on the 10-m average transects in Cluster 2b. **111**

Table B-4. Historical vegetation line change rates in Makah Bay based on the 10-m average transects in Cluster 2c. **112**

Table B-5. Historical vegetation line change rates in Makah Bay based on the 10-m average transects in Clusters 3, 4, and 5..... **113**

Table B-6. Historical vegetation line change rates in Makah Bay based on the 10-m average transects in Clusters 6 and 7. **114**

Table B-7. Historical vegetation line change rates in Makah Bay based on the 10-m average transects in Cluster 8..... **115**

Table B-8. Historical vegetation line change rates in Makah Bay based on the 10-m average transects in Cluster 9..... **116**

Table B-9. Historical vegetation line change rates in Makah Bay based on the 10-m average transects in Cluster 9, continued..... **117**

Table B-10. Historical vegetation line change rates in Makah Bay based on the 10-m average transects in Cluster 10a. **118**

Table B-11. Historical vegetation line change rates in Makah Bay based on the 10-m average transects in Cluster 10b. **119**

Table B-12. Historical vegetation line change rates in Makah Bay based on the 10-m average transects in Cluster 10b, continued. **120**

Table B-13. Historical vegetation line change rates in Makah Bay based on the 10-m average transects in Cluster 10c. **121**

Table B-14. Historical vegetation line change rates in Makah Bay based on the 10-m average transects in Cluster 11. **122**

Table B-15. Historical vegetation line change rates in Makah Bay based on the 10-m average transects in Cluster 11, continued..... **123**

Table B-16. Historical vegetation line and shoreline change rates in Makah Bay based on the 10-m average transects in Cluster 12. **124**

Table C-1. Historical shoreline change rates in Makah Bay based on the 10-m average transects in Cluster 1. **125**

Table C-2. Historical shoreline change rates in Makah Bay based on the 10-m average transects in Cluster 2a..... **126**

Table C-3. Historical shoreline change rates in Makah Bay based on the 10-m average transects in Cluster 2b. **127**

Table C-4. Historical shoreline change rates in Makah Bay based on the 10-m average transects in Cluster 2c..... **128**

Table C-5. Historical shoreline change rates in Makah Bay based on the 10-m average transects in Clusters 3, 4, and 5. **129**

Table C-6. Historical shoreline change rates in Makah Bay based on the 10-m average transects in Clusters 6 and 7. **130**

Table C-7. Historical shoreline change rates in Makah Bay based on the 10-m average transects in Cluster 8. **131**

Table C-8. Historical shoreline change rates in Makah Bay based on the 10-m average transects in Cluster 9. **132**

Table C-9. Historical shoreline change rates in Makah Bay based on the 10-m average transects in Cluster 9, continued. **133**

Table C-10. Historical shoreline change rates in Makah Bay based on the 10-m average transects in Cluster 10a. **134**

Table C-11. Historical shoreline change rates in Makah Bay based on the 10-m average transects in Cluster 10b. **135**

Table C-12. Historical shoreline change rates in Makah Bay based on the 10-m average transects in Cluster 10b, continued. **136**

Table C-13. Historical shoreline change rates in Makah Bay based on the 10-m average transects in Cluster 10c. **137**

Table C-14. Historical shoreline change rates in Makah Bay based on the 10-m average transects in Cluster 11. **138**

Table C-15. Historical shoreline change rates in Makah Bay based on the 10-m average transects in Cluster 11, continued. **139**

Table D-1. Summary of imagery years used in each cluster average change rate reported for the Ozette sub-region. This table shows clusters 21-36. **141**

Table D-2. Summary of imagery years used in each cluster average change rate reported for the Ozette sub-region. This table shows clusters 37-49. **142**

Table D-3. Historical shoreline change rates in the Ozette sub-region based on the 10-m average transects in Clusters 21 to 25. **143**

Table D-4. Historical shoreline change rates in the Ozette sub-region based on the 10-m average transects in Cluster 26. **144**

Table D-5. Historical shoreline and vegetation line change rates in the Ozette sub-region based on the 10-m average transects in Cluster 26 (continued) through Cluster 29. **145**

Table D-6. Historical shoreline and vegetation line change rates in the Ozette sub-region based on the 10-m average transects in Clusters 30 and 31. **146**

Table D-7. Historical shoreline change rates in the Ozette sub-region based on 10-m average transects in Clusters 32 and 33. **147**

Table D-8. Historical shoreline and vegetation line change rates in the Ozette sub-region based on the 10-m average transects in Clusters 34 and 35. **148**

Table D-9. Historical shoreline, sand wedge, and vegetation line change rates in the Ozette sub-region based on the 10-m average transects in Cluster 36..... **149**

Table D-10. Historical shoreline, sand wedge, and vegetation line change rates in the Ozette sub-region based on the 10-m average transects in Cluster 37. **150**

Table D-11. Historical shoreline and sand wedge change rates in the Ozette sub-region based on the 10-m average transects in Cluster 37 to 40. **151**

Table D-12. Historical shoreline and sand wedge change rates in the Ozette sub-region based on the 10-m average transects in Cluster 41..... **152**

Table D-13. Historical shoreline and sand wedge change rates in the Ozette sub-region based on the 10-m average transects in Cluster 42 and 43..... **153**

Table D-14. Historical shoreline and sand wedge change rates in the Ozette sub-region based on the 10-m average transects in Cluster 44 and 45..... **154**

Table D-15. Historical shoreline and sand wedge change rates in the Ozette sub-region based on the 10-m average transects in Cluster 45 (continued) through 47. **155**

Table D-16. Historical shoreline and sand wedge change rates in the Ozette sub-region based on the 10-m average transects in Cluster 48..... **156**

Table D-17. Historical shoreline and sand wedge change rates in the Ozette sub-region based on the 10-m average transects in Cluster 49..... **157**

Table D-18. Historical shoreline and sand wedge change rates in the Ozette sub-region based on the 10-m average transects in Cluster 49 (continued)..... **158**

Acknowledgements

This project was funded by Washington Coastal Conservation and Restoration Initiative Project 18-2137, Makah Coastline Assessment and Restoration Design

The authors of this report thank the following people for their contribution to this study:

- Makah Tribe for access to their land and accommodation during COVID restrictions
- Adrienne Akmajian and Katie Wrubel from Makah Fisheries Management for project management and coordination
- Ian Miller from the Washington Sea Grant Program at the University of Washington for collaborative efforts throughout the project including helping with the beach topography data collection in 2019
- Gabrielle Alampay (Ecology CMAP) for beach topography data collection in 2021, historical photo inventory and organization, georeferencing and mosaicking, and vegetation line delineation
- Delaney Stokes (Ecology CMAP) for photo georeferencing and mosaicking
- Members of the Makah tribal staff, Angelina Woods and Cole Svec for helping with beach topography data collection in 2019
- Volunteers Ryan Anderson, Sky Richardson, and Matt Weiner for helping with beach topography data collection in 2021
- Alena Reynolds (Ecology CMAP) for helping with the beach topography data collection in 2019

This page is purposely left blank

Executive Summary

A comprehensive coastline assessment of the Makah Reservation and Ozette (Makah) Reservation in northwest Washington was conducted by the Washington State Department of Ecology Coastal Monitoring & Analysis Program. The overarching goal of this project is to increase the Makah Tribe's ability to restore and increase the resilience of coastal areas on the reservation from coastal erosion and other hazards. The results will inform an engineered restoration design at a known erosional area that addresses the underlying causes of erosion to protect the ecological, economic, and cultural function of the site, aiming for long-term restoration of the beach dunes using nature-based approaches.

The assessment consists of two parts: 1) a historical coastline change analysis to understand how Hobuck, Tsoo-Yess, and Ozette (Makah) Reservation beaches have changed over the past several decades and 2) high-resolution topographic/bathymetric surveys of Makah Bay and the adjacent beaches to help identify bathymetric controls on beach erosion and accretion cycles and detect recent morphology changes.

The results of data collection and analysis reveal that the beaches of Makah Bay have grown seaward by sediment accretion processes since 1952. Since 2009, the average rates of beach accretion are generally higher than the long-term average rates, except at the Hobuck Beach Resort's RV Campground. This area is subject to localized processes—creek flow that undercuts the dune toe, northward creek channel migration that lowers the beach profile to allow more wave interaction with the dunes, and northward growth of the beach and dunes south of the creek outlet to reduce southward migration of the creek channel.

The historical assessment of coastal change at the Ozette (Makah) Reservation found that the shoreline has been changing at relatively low rates since 1977, with both erosion and accretion occurring locally, but with an average trend of erosion over time. Since 2009, the average rate of erosion has been higher than the longer-term average rate since 1977. Both the coastal geomorphology and remoteness of the Ozette (Makah) Reservation present a unique set of challenges for implementing strategies that reduce the erosion impacts.

In both cases, continued monitoring and assessment is recommended to integrate observations and management of these Reservation beaches as resilience strategies are implemented.

This page is purposely left blank

Introduction

Background

In recent years, erosion and inundation of certain coastal areas of the Makah Reservation, namely an area adjacent to the Hobuck Beach Resort's RV Campground (hereafter "Hobuck RV Campground") and along the shoreline of the Ozette (Makah) Reservation (hereafter "Ozette Reservation"), has impacted recreational use areas, housing, and archeological sites. An analysis of coastline change trends is needed to better understand the dynamics of these areas and to protect their ecological, economic, and cultural functions.

Hobuck Beach draws visitors from around the world, generating approximately \$1 million for the Tribe annually. The Hobuck Beach Resort is one of the few locations for lodging on the remote northwest Washington coast. During the winter of 2017-2018, the Tribe witnessed as much as 20-30 feet of erosion of the beach at the Hobuck RV Campground with a steep dune scarp fronting the resort, posing a risk to public safety and infrastructure. The Makah Tribe used beach nourishment in December 2017 as a preventative measure to reduce further erosion at this site; however, the sand began to erode, and they were unable to perform annual nourishment. In the winter of 2018-2019, rock rip rap was placed along the dune scarp to thwart further erosion of the upland (see cover photo).

In addition to the erosion at Hobuck Beach, the Makah Tribe has also experienced erosion at the Ozette Reservation for the past several years, a site that is culturally and archeologically important to the Tribe and registered under the U.S. National Register of Historic Places. With little information known about this remote part of the Washington coast, this study aims to better understand the erosion dynamics at the Ozette Reservation and inform potential restoration of this culturally rich site.

This project provides insight into recent erosion trends through historical coastline change analyses at the three major coastal beaches of the Makah Reservation (Hobuck, Tsoo-Yess, and Ozette) and an assessment of recent morphology change of Makah Bay and the adjacent beaches. The results will allow the Makah Tribe to develop strategies for shoreline protection with the goal of increasing the resilience of these areas to coastal erosion and other hazards.

Site overview

The project occurs at three sub-regions within the Makah Reservation near Neah Bay, Washington: Hobuck, Tsoo-Yess, and the Ozette Reservation beaches (Figure 1). The Reservation is 47 square miles and is located on the Olympic Peninsula in the northwest corner of Washington State, bounded by the Pacific Ocean to the west and the Strait of Juan de Fuca to the north. The marine waters off this coastline include approximately 1,550 square miles of the Tribe's Usual and Accustomed (U&A) Fishing Area, which overlaps with a portion of the Olympic Coast National Marine Sanctuary (OCNMS). The surrounding land on the coastal portion of the Reservation is part of Olympic National Park.

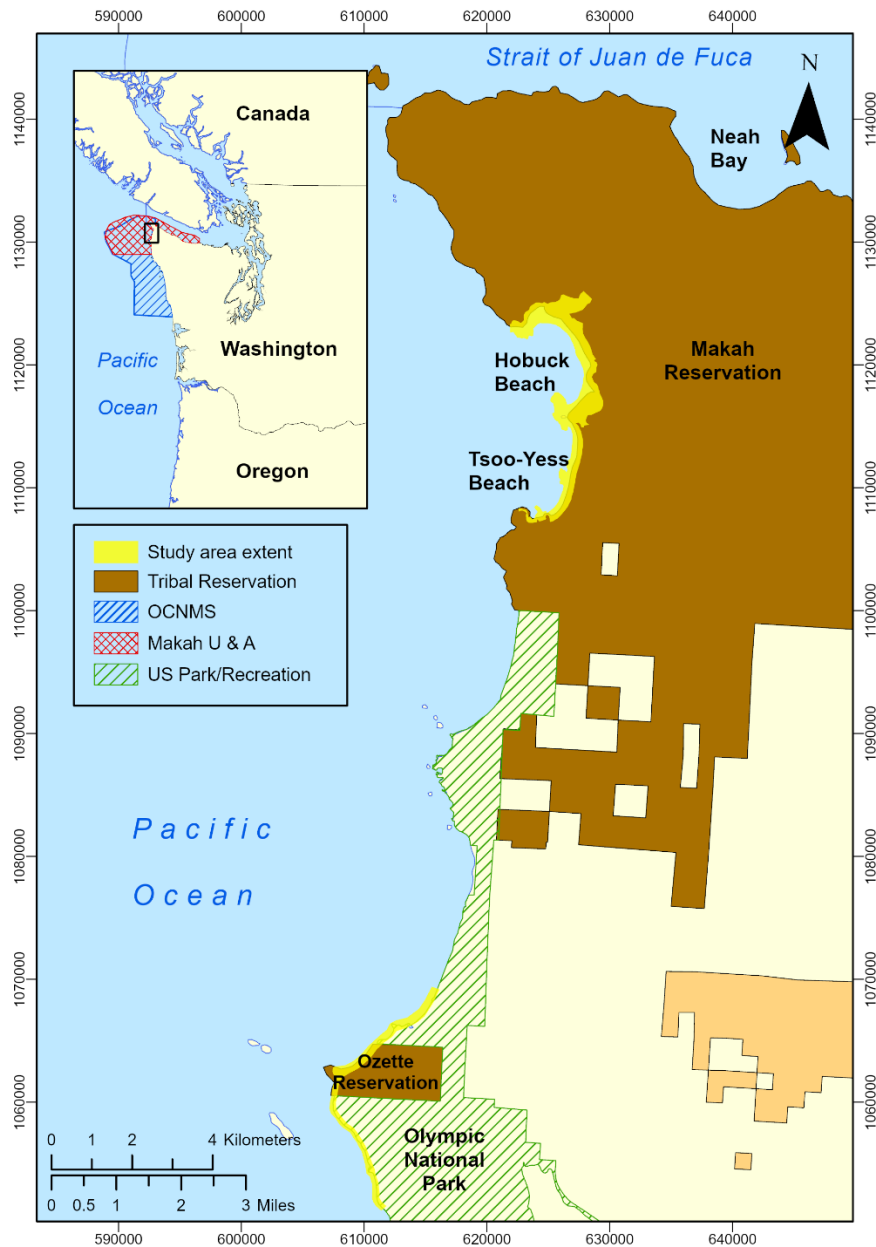


Figure 1. General vicinity map of the Makah Reservation and project sub-regions, showing the three beach locations (alongshore extent highlighted in yellow) included in the change analyses: Hobuck Beach, Tsoo-Yess Beach, and the Ozette Reservation.

Hobuck Beach

Hobuck Beach is located at the north end of Makah Bay. This sandy, western-facing shoreline makes a crescent shape bounded by Wa'atch Point to the north and a rocky headland to the south², both of which include expansive rocky intertidal reefs and outcrops (Figure 2). Two rivers drain through Hobuck Beach: the Wa'atch River at the north end, and the Tsoo-Yess River near the south end. North of where the Tsoo-Yess River drains onto the beach, there is a rocky outcrop extending from land known as Bahobohosh Point. A small unnamed stream, herein referred to as Hobuck Creek, drains onto the beach between Bahobohosh Point and the Hobuck RV Campground.

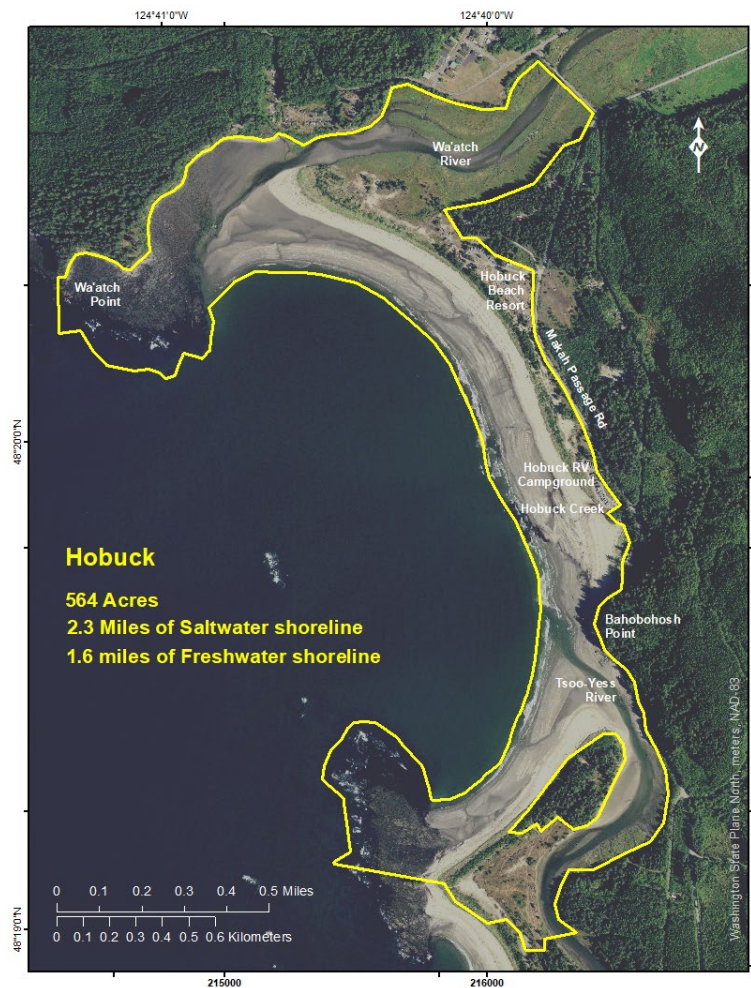


Figure 2. Aerial imagery of Hobuck Beach with project site outlined in yellow (2017 NAIP).

² Based on overall geomorphology and geologic control, the division between Hobuck Beach and Tsoo-Yess Beach is defined herein at the approximate center of the rocky outcrop and shoreline near the middle of Makah Bay. Other studies may define the division between these two beaches at the mouth of the Tsoo-Yess River.

Tsoo-Yess Beach

The southern half of the Makah Bay shoreline, south of the rocky headland and outcrops, is known as Tsoo-Yess Beach (Figure 3). The beach is backed by low-lying sand dunes and trees on the northern half, which transition to vegetated bluff at the south end of the bay. A small, unnamed creek empties into Makah Bay at the south end of the beach. While most of the beach is sandy, there is an area of rock outcroppings and rocky intertidal reef offshore in the center part of the beach. There is a small pocket beach at the far south end, separated from the north-south oriented Tsoo-Yess Beach by a rocky outcrop that extends from the upland into the water and is impassable at high tide.

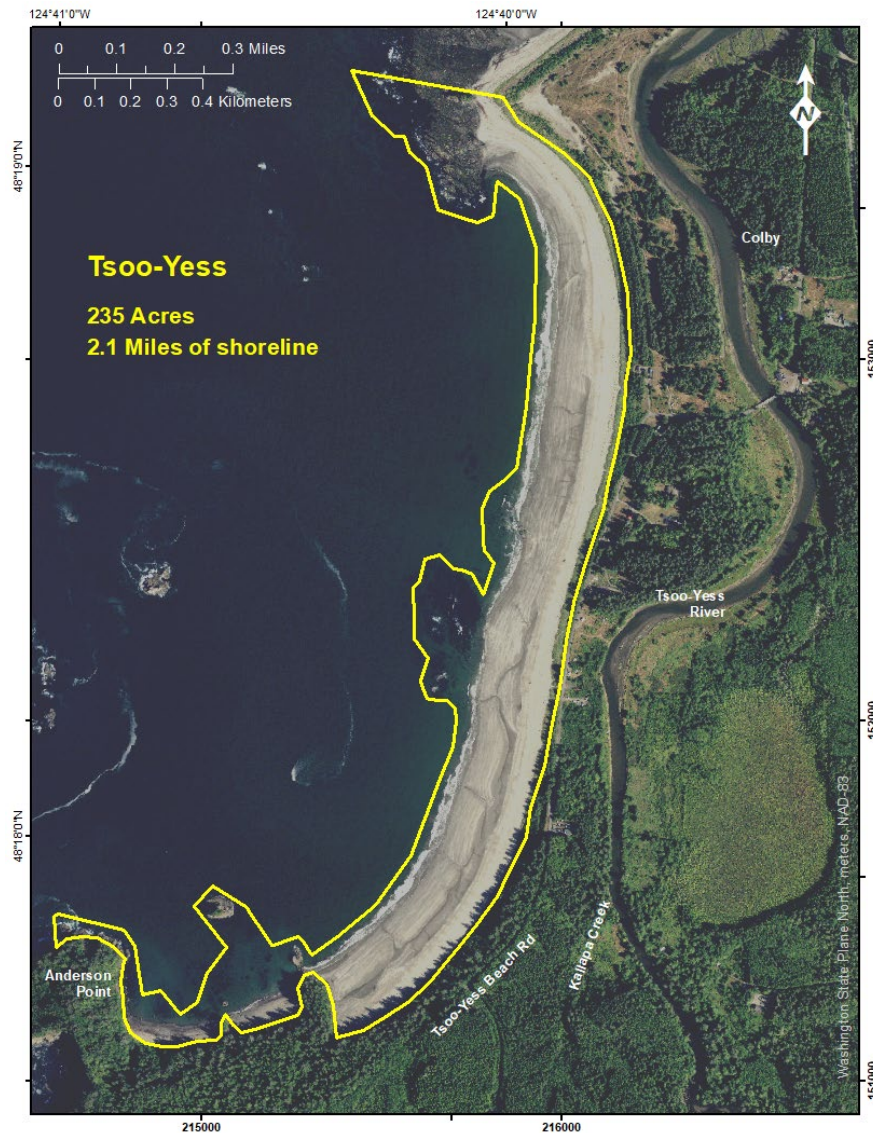


Figure 3. Aerial imagery of Tsoo-Yess Beach with project site outlined in yellow (2017 NAIP).

Ozette Reservation

The Ozette Reservation is located about 10 mi (16 km) south of Makah Bay on a remote stretch of the Olympic Coast (Figure 4). This sub-region was extended beyond the Ozette Reservation boundaries north and south into the Olympic National Park to aid in larger scale interpretations. The study area including the coastline of the Ozette Reservation and adjacent Olympic National Park is herein referred to as the Ozette sub-region. The beach is composed of sand on the lower beach face and a mix of cobbles and pebbles on the upper beach and is backed by coastal bluffs (Riedel et al., 2021). Converging longshore drift directions at Cape Alava resulted in the formation of a tombolo, connecting the land to a large sea stack, called Tskawahyah (Cannonball) Island. The coast has an extensive rocky intertidal platform and is partially protected by Ozette Island, Bodehteh Islands, and the offshore rocks.

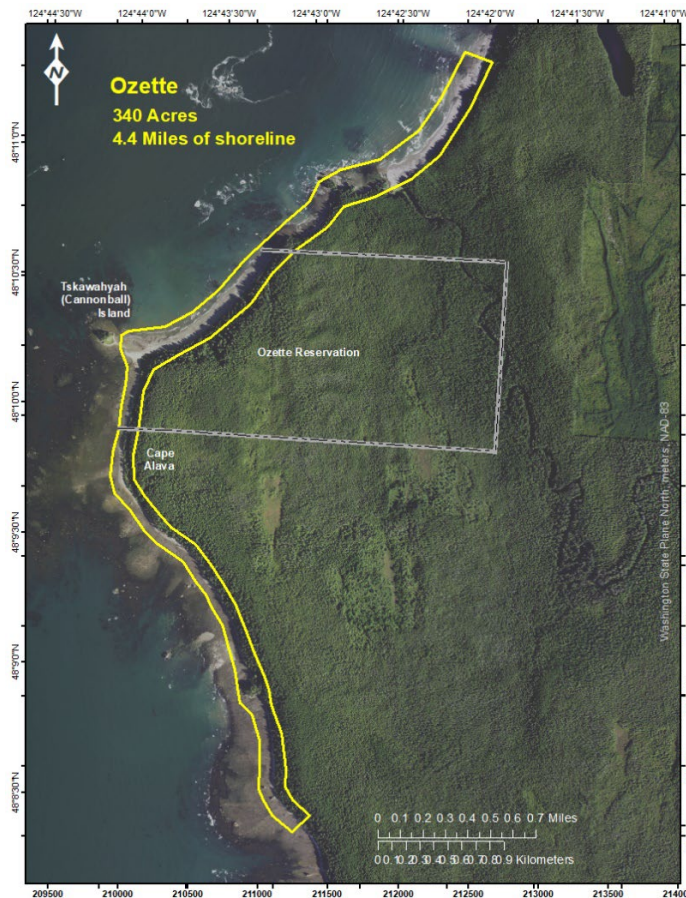


Figure 4. Aerial imagery of the Ozette sub-region with project site outlined in yellow (2015 NAIP).

The Ozette Reservation is archeologically and culturally important to the Makah Tribe. Several hundred years ago, a mudslide inundated the area, covering and preserving the Ozette Village Site. The site was re-discovered in the late 1960s when artifacts were exposed from coastal erosion, resulting in an 11-year excavation effort (Daugherty and Fryxell, 1967; Friedman, 1976). Recent erosion is threatening this cultural site.

This page is purposely left blank

Methods

A comprehensive coastal change assessment was performed for the Pacific coastline of the Makah Reservation. Two separate assessments were conducted, one for Makah Bay, which included Hobuck and Tsoo-Yess beaches, and one for the Ozette Reservation. For Makah Bay, the assessment includes both a historical coastline change analysis to understand how the shoreline and vegetation line has changed over multi-decadal timescales and high-resolution topographic/bathymetric (topo-bathymetric) surveys that help to identify exchanges of sediment between the shallow sub-tidal zone and intertidal beach. These surveys complement and provide spatial and temporal context to ongoing seasonal beach profile monitoring performed by the Makah Tribe. For the Ozette Reservation, the assessment consists solely of a historical coastline change analysis.

Historical coastline change

Source data

Historical coastline change analyses provide information on how the coast has changed over multi-decadal timescales by examining existing aerial imagery, oblique shoreline photographs, and aerial lidar datasets.

Five sets of historical aerial photographs supplied by the Washington Department of Natural Resources (WDNR) collected between 1952 and 1997 were georeferenced and mosaicked for analysis. These were used in conjunction with seven sets of Washington statewide imagery from the National Agricultural Imagery Program (NAIP) available for 2006 to 2019. Most images were collected between July and September, showing late summer beach conditions. The spatial resolution of the images ranged between 13.8 ft in 1952 and 1 ft in 2019; however, all imagery sets between 1964 and 2019 had a resolution between 1 ft and 3 ft (Table 1). Photo mosaics from 1952, 1964, and 1985 were excluded for the Ozette Reservation because of poor image quality or poor image alignment.

Table 1. Information describing the 12 sets of imagery used in the historical coastline change analysis for Makah Bay including the date, source, spatial resolution (pixel size), root mean square error (RMSE) for photos that were georeferenced, and description of the imagery type.

Year	Month, Day	Source	Resolution (feet)	RMSE (feet)	Description
1952	June 8	WDNR	13.8	31.5	One band photo mosaic
1964	May 15	WDNR	1.7	8.9	One band photo mosaic
1977	July 18	WDNR	1.9	9.5	One band photo mosaic
1985	July 2	WDNR	1.7	5.6	One band photo mosaic
1997	August 1	WDNR	1.9	8.5	One band photo mosaic
2006	June 24	NAIP	1.5	n/a	Three band aerial imagery
2009	September 11	NAIP	3	n/a	Four band aerial imagery
2011	September 2	NAIP	3	n/a	Four band aerial imagery
2013	September 10	NAIP	3	n/a	Four band aerial imagery
2015	September 27	NAIP	3	n/a	Four band aerial imagery
2017	August 17	NAIP	3	n/a	Four band aerial imagery
2019	October 9	NAIP	1	n/a	Four band aerial imagery

To aid in shoreline positioning at the Ozette Reservation, digital elevation models (DEMs) derived from aerial lidar data from 2016 and 2018 were downloaded from the WDNR Lidar Portal (available online at: <https://lidarportal.dnr.wa.gov>; Table 2). The lidar DEMs were not used for direct shoreline extraction because the delineated features are based on visual cues in the imagery. In addition, the lidar DEMs do not adequately resolve either the precise location of breaks in slope such as the bluff toe or finer scale beach texture and morphology that are important to delineating coastline features. However, beach slopes were extracted from the lidar DEMs at select cross-shore profiles to aid in estimating water levels and adjusting the location of the digitized shoreline.

Table 2. Information describing the 9 sets of imagery and 2 sets of lidar data used in the historical coastline change analysis for the Ozette Reservation including the date, source, spatial resolution (pixel size), and root mean square error (RMSE) for photos that were georeferenced, and description of the imagery type.

Year	Month, Day	Source	Resolution (feet)	RMSE (feet)	Description
1977	July 18	WDNR	1.9	8.5	One band photo mosaic
1997	August 1	WDNR	1.9	3.6	One band photo mosaic
2006	June 24	NAIP	1.5	n/a	Three band aerial imagery
2009	September 11	NAIP	3	n/a	Four band aerial imagery
2011	September 2	NAIP	3	n/a	Four band aerial imagery
2013	September 10	NAIP	3	n/a	Four band aerial imagery
2015	September 27	NAIP	3	n/a	Four band aerial imagery
2016	April 30 through May 1	WDNR/ Dewberry	3	n/a	Airborne Lidar DEM
2017	August 17	NAIP	3	n/a	Four band aerial imagery
2018	January 2	WDNR/ Quantum Spatial	3	n/a	Airborne Lidar DEM
2019	October 9	NAIP	1	n/a	Four band aerial imagery

Oblique shoreline photos from the Washington Department of Ecology Coastal Atlas (available online at: <https://apps.ecology.wa.gov/shorephotoviewer/Map/ShorelinePhotoViewer>) were used for a qualitative assessment of shoreline conditions at the Ozette Reservation. A total of 13 photo points taken in 1997, 2002, 2006, and 2016 spanning the study area at the Ozette Reservation were viewed. Comparing vegetation and morphological indicators in the photos from each point through time offered a qualitative assessment to support findings from the quantitative analysis. Additionally, these photos were used during shoreline delineation to help resolve beach features that were obscured in the aerial imagery.

Feature delineation

Two alongshore features were chosen for analysis to provide complementary measures of coastal change: the vegetation line, which is a good proxy of the long-term stability of the coastline; and the shoreline, defined as the average high-water mark or the horizontal excursion of water, including wave run-up, during a mean high water (MHW) event. These features and the methodology used to delineate them are consistent with those described in Kaminsky et al. (1999).

Coastline features were delineated at Hobuck Beach and Tsoo-Yess Beach using each of the 12 sets of aerial imagery in Table 1 and at the Ozette Reservation using each of the 9 sets of aerial imagery in Table 2. The vegetation line was digitized at the seaward extent of stable vegetation, which was defined as terrestrial vegetation (i.e., trees or shrubs) or well-established dune grass with greater than 50% ground cover. Other visual cues of the physical condition of the beach in the imagery were used to constrain the digitized location of the shoreline. The shoreline location was delineated based on visual interpretation of the following features:

- landward of smooth sand caused by recent swash activity,
- seaward of wind-rippled sand that represented longer aerial exposure,
- along a line of fresh beach wrack or driftwood, and
- along the dewatering line when the photo was taken during a falling tide.

These visual interpretations were further constrained by accounting for tidal elevations and the amount of time passed since the previous high tide. The timestamp on each photo was used to determine the three most recent high tide levels based on observed water levels at the National Oceanic and Atmospheric Administration (NOAA) tide station 9442396 at La Push, Quillayute River. The wet sand line and most prominent beach wrack line were used to determine the extent of wave runup from the most recent high tide, and the previous two high tides were related to dry beach wrack lines if they were higher than the most recent high tide. The difference in elevation between the three previous high tide levels and MHW was calculated. Using the relative distances of the high tides as guides to indicate horizontal scale (i.e., beach slope), the shoreline was positioned proportionally landward or seaward of a recent high tide position depending on whether the high tide was lower or higher than MHW, respectively. Rocky outcrops were omitted from the historical coastline change analysis because of increased image distortion in these high-relief areas and a decreased change signal.

Image quality factors that may affect the outcome of the analysis were considered while delineating features. In areas where overhanging vegetation obstructed the view of the vegetation line, including Hobuck Creek and south Tsoo-Yess Beach, the position of the vegetation line was estimated using the location of the tree trunks as a guide. To help resolve dark imagery due to shade from vegetation and rocks, image brightness and gamma were adjusted. A Normalized Difference Vegetation Index (NDVI) layer was generated for imagery between 2009 and 2019 to aid in resolving the vegetation extent; however, these layers were not found to be useful for interpreting areas obscured by shadows. Image distortion and clarity were also considered on a case-by-case basis. Areas were omitted from analysis if the registration error of the imagery was greater than the estimated magnitude of change, or if the imagery was too dark to resolve features with moderate or high confidence (Figure 5).

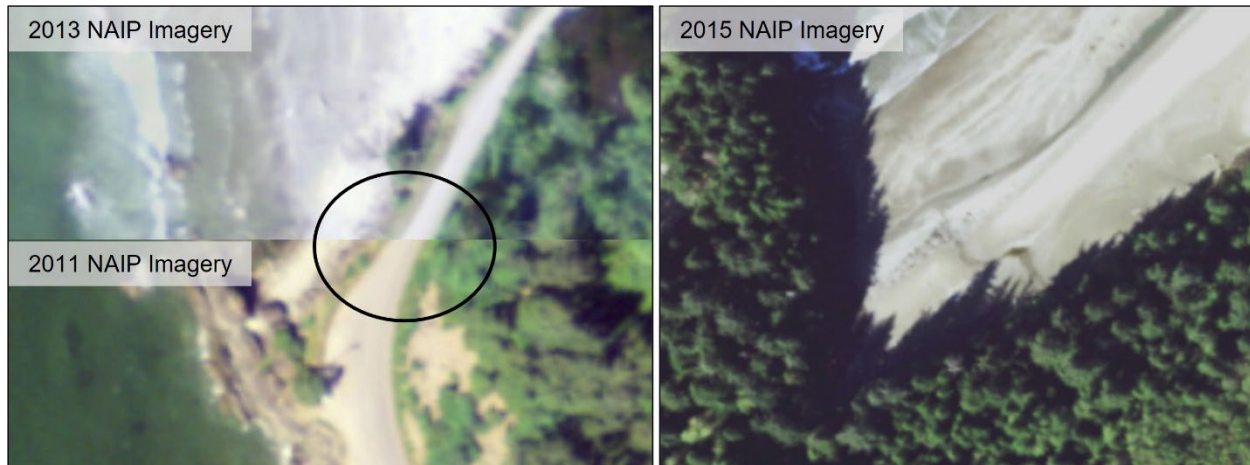


Figure 5. Example of registration error between the 2013 and 2011 NAIP imagery in a southern reach of Hobuck Beach where the road is offset by 2.5 m (left), and example of an area where shadows and tree cover obscure the vegetation line in a southern reach of Tsoo-Yess Beach (right).

The vegetation line was indiscernible for most years along the Ozette sub-region due to shaded imagery, vegetation cover, and a complex beach face. The vegetation lines could only be evaluated in six clusters which account for 24.5% (1,601 m) of the entire Ozette sub-region. Within the Ozette Reservation, long-term vegetation line change rates were evaluated for 46.8% (861 m) of the coastline.

To estimate the shoreline position and minimize digitizing error caused by the complexity of beach topography and texture in the Ozette sub-region, WDNR DEMs from 2016 and 2018 were used to aid in shoreline positioning. Elevations from the two DEMs were extracted at fixed points with 1-m spacing along 1-m spaced cross-shore transects. The mean elevation between the two datasets was calculated at each point and used to plot an average beach profile, which were assumed to be representative of typical beach conditions at each cross-shore transect. The highest and lowest of the previous three high tides, based on timestamps of the imagery and the La Push tide station, were plotted along each averaged profile and used as endpoints for calculating beach slope (Figure 6). The elevation difference between the most recent high tide and MHW was used with the beach slope to calculate the horizontal adjustment applied to the digitized shoreline. The resulting adjusted shorelines were used in analysis (Figure 7).

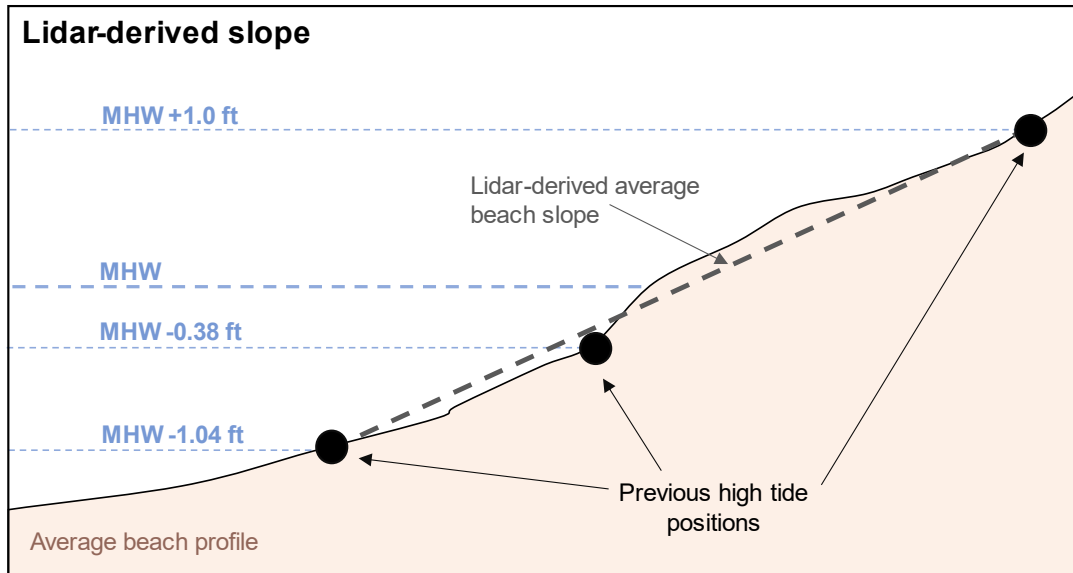


Figure 6. Method used to calculate an average localized beach slope to make horizontal adjustments to the digitized shoreline. Slope was calculated between the highest and lowest of the previous three high tide levels determined by correlating imagery timestamps to observed water levels at the La Push tide station.

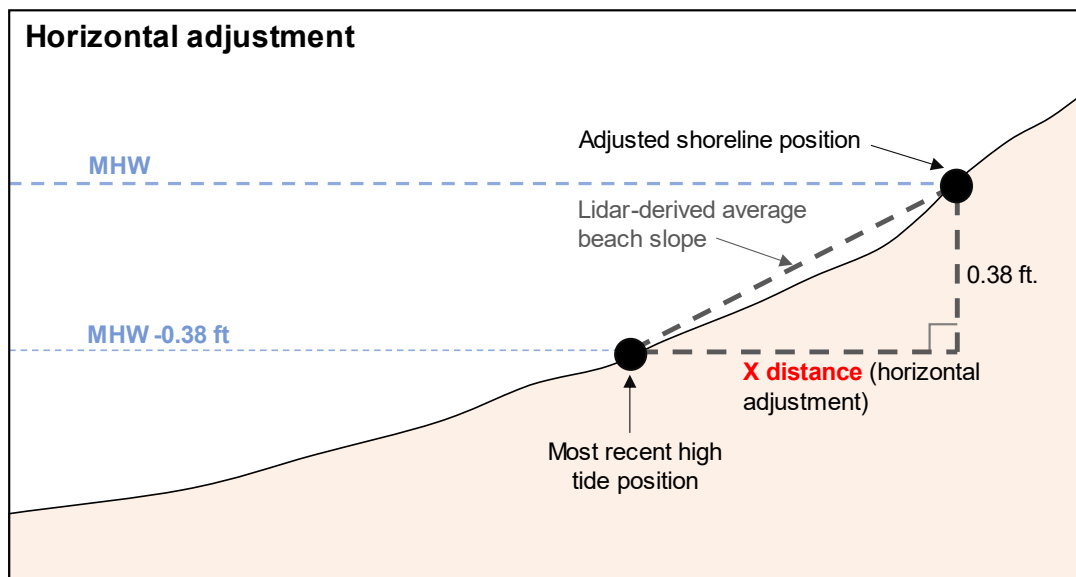


Figure 7. Method used to determine the horizontal adjustment applied to the digitized mean high water tide plus wave runup shoreline, resulting in a derived shoreline position. Horizontal adjustments of the digitized shoreline were calculated by right angle geometry.

In addition to the two features previously described, the boundary between the rocky or mixed-sediment low-tide terrace and the seaward extent of the beach sand wedge was also digitized for another measure of coastal change along the complex Ozette sub-region coastline (Figure 8). However, the sand wedge could not be discerned in the imagery for all locations and years. In imagery from 2009, 2011, 2013, 2015, and 2017, the seaward edge of the sand wedge was obscured by water covering the lower beach. The seaward edge of the sand wedge could not be

digitized from the 2019 imagery due to wrack covering its position. As a result, sand wedge change could only be calculated for long term (1977-2019) rates from approximately Tskawahyah (Cannonball) Island southward and for 10-yr (2009-2019) rates southward from Cape Alava (Figure 4).

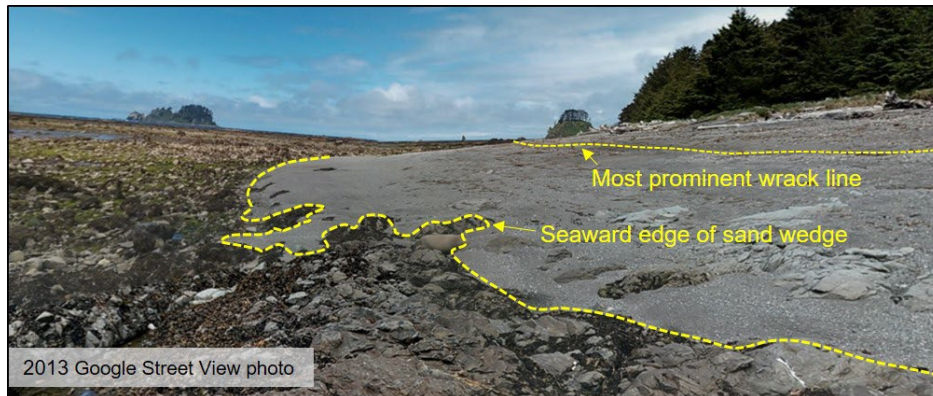


Figure 8. Google Street View photo showing an example of the seaward extent of the sand wedge that was digitized at the Ozette Reservation as another feature to determine coastline change. The most prominent wrack line, used as a visual cue to generate a shoreline position, is shown in the background.

Data analysis

The average position of all vegetation lines and shorelines was calculated for each sub-region to create a reference vegetation line and reference shoreline. Transects with 1-m spacing were generated along the resultant reference lines, oriented perpendicular to the average feature position to reflect the primary direction of change. Endpoint rates along the 1-m spaced transects were calculated for all digitized features between consecutive years (using the decimal year for a more precise time interval). Due to discontinuous digitized features caused by image quality being too poor to resolve beach conditions, rates between consecutive years are not reported for the Ozette Reservation.

The average position of the reference vegetation line and reference shoreline was calculated, and 10-m spaced transects were generated perpendicular to the average of both reference lines. The 10-m transects were used to divide the reference vegetation line and reference shoreline into alongshore segments centered around each transect, resulting in approximate 10-m alongshore segments that could be related between features by a common 10-m transect. The change rates calculated along the 1-m transects were averaged within each 10-m alongshore segment, resulting in a robust set of rates each representing the average of approximately 10 measurements (Figure 9). This method of change rate calculation was selected to minimize the error associated with imagery resolution and digitizing by averaging over anomalous error, and change rates presented here are estimated to be within ± 25 cm/yr accuracy.

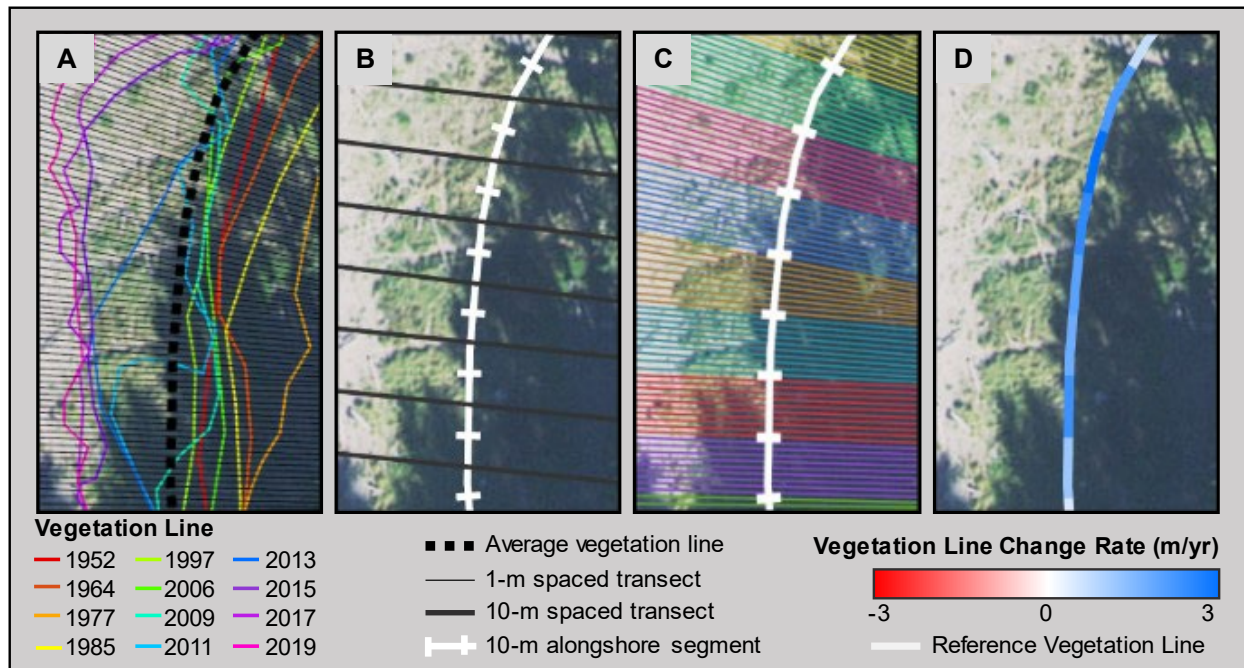


Figure 9. Calculation and display of coastline change analysis results, shown here as change at the vegetation line. A) The average position of all vegetation lines was calculated and used to generate perpendicular transects with 1-m spacing. B) 10-m spaced transects were generated along the average position of all digitized alongshore features (herein, shoreline and vegetation line), and were used to divide the reference line into 10-m alongshore segments. C) Change rates calculated along the 1-m transects were binned and averaged by the intersecting alongshore reference line. D) The resulting final change rates are displayed along 10-m segments and colored to depict magnitude of change.

An ordinary least squares linear regression was used to calculate a 10-year average rate between 2009 and 2019 and long-term average historical rates since 1952 (or 1977 at the Ozette sub-region) for vegetation line and shoreline change in Makah Bay and vegetation line, shoreline, and sand wedge change at the Ozette sub-region. The Spatially Constrained Multivariate Cluster Analysis tool in ArcGIS Pro was used to perform a cluster analysis for both Makah Bay and the Ozette sub-region. This analysis technique identifies spatially contiguous transects with minimal within-cluster variability and maximum between-cluster variability. In Makah Bay, the long-term average vegetation line change rates were selected for the input analysis field and the tool was run without any constraints using 100 permutations, resulting in 12 clusters. To maintain a higher spatial resolution, 3 sub-clusters were identified for each of the two largest clusters, which brought the total number of cluster units to 16 for Makah Bay (Figure 10). For the Ozette sub-region, the short-term average shoreline change rates, which are assumed to be the most accurate rates in this sub-region, were selected for the input analysis field. A minimum cluster size threshold of two transects was required to achieve statistically distinct clusters due to complexity in the Ozette sub-region with no other constraints. The tool was run with 100 permutations and identified 29 clusters used to guide

analysis and interpretations (Figure 10). Seven of the identified clusters are fully or partially within the Ozette Reservation.

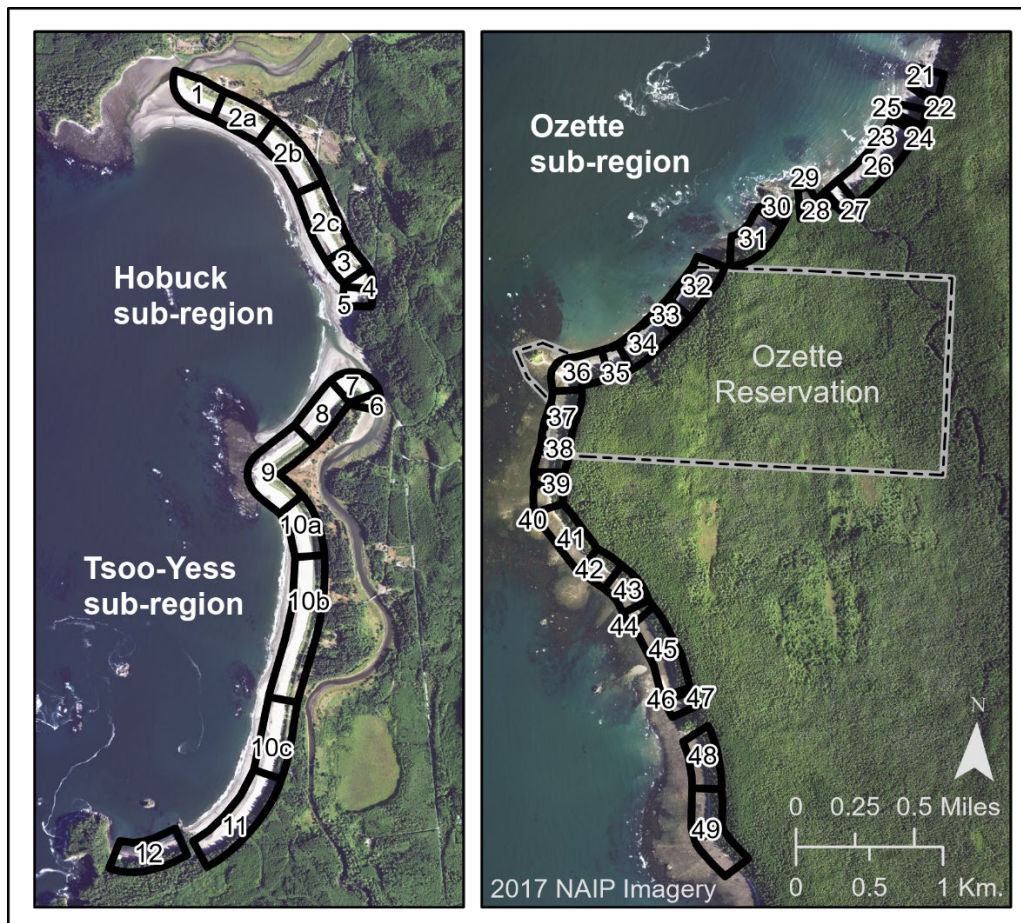


Figure 10. Cluster boundaries identified by a multivariate cluster analysis based on historical coastline change rates. Clusters in Makah Bay were identified using historical vegetation line change rates, and the clusters in the Ozette sub-region were identified using historical shoreline change rates. Makah Bay and Ozette sub-regions are displayed at the same scale.

Biennial topo-bathymetric change

Data collection

Two high-resolution topographic/bathymetric surveys were conducted of Makah Bay, Hobuck Beach, and Tsoo-Yess Beach during September 4-14, 2019 and July 7-16, 2021. The surveys consisted of ground-based surface mapping using Global Navigation Satellite Systems (GNSS), boat-based lidar scanning, and multibeam sonar mapping from Wa'atch Point to Anderson Point, including the entire bay, beaches, outcrops, islands, and parts of the Wa'atch and Tsoo-Yess rivers and floodplains (Figure 11). All positional data were referenced to a local GNSS base station set up on an epoxy monument installed on Bahobohosh Point for the purpose of this study (Figure 12A and Appendix A).

GNSS topographic surface mapping consisted of cross-shore profiles at approximately 50-m spacing, topographic feature mapping, and alongshore mapping at approximately 20-m spacing (Figure 11). The data were collected using GNSS backpack and ATV survey platforms (Figure 12B - Figure 12C).

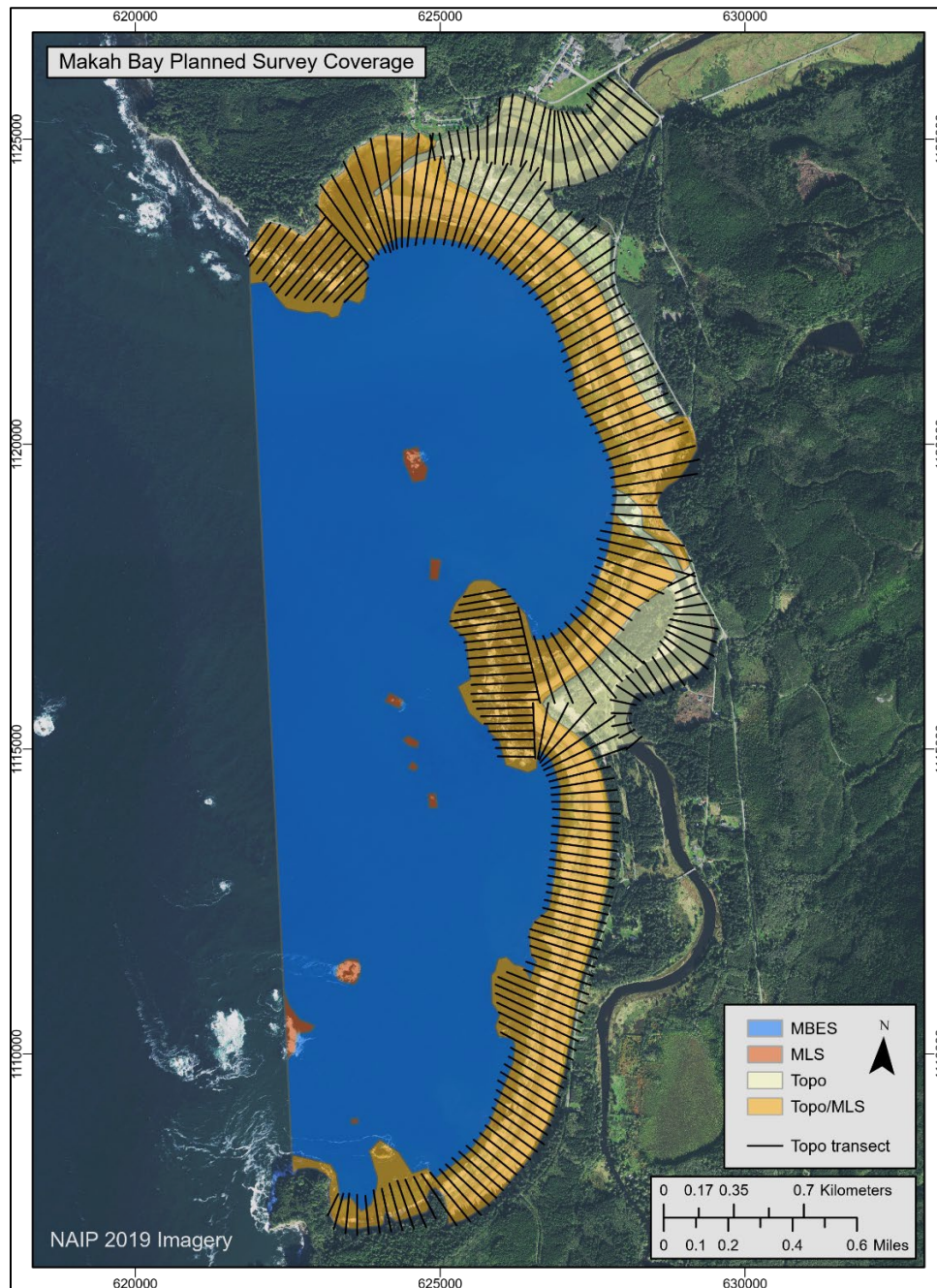


Figure 11. Planned survey coverage of Makah Bay with polygons delineating approximate survey boundaries and types of data collected for the topo-bathymetric surveys: multibeam echosounder (MBES; sonar), mobile laser scanning (MLS; boat-based lidar); and GNSS

topography (Topo) including transects (black lines), which are independent from those derived for coastline change analyses.

Boat-based lidar scanning of the beach and uplands was conducted along the shoreline of Makah Bay from the R/V George Davidson (Figure 12D). Lidar targets of 1-m² sheet metal and 2-ft (0.6-m) diameter spheres on the beach were jointly surveyed using GNSS topography equipment to assess the positional accuracy of the lidar data (Figure 12E).



Figure 12. Topo-bathymetric data collection techniques. A) GNSS Base station. B) Topographic data collection using GNSS mounted on backpacks. C) Topographic surface mapping using a GNSS mounted on an ATV. D) R/V George Davidson collecting MBES in the nearshore. E) Lidar target being surveyed.

Multibeam sonar mapping of the seafloor of Makah Bay was conducted from the R/V George Davidson. In 2019, the multibeam dataset covered as much of Makah Bay as was navigable during the survey, whereas in 2021 the scope was limited to sandy areas most likely to exhibit change up to the interface with rocky substrate, as identified in the 2019 dataset. The combined data coverages from multibeam, lidar, and GNSS collection is shown in Figure 13.

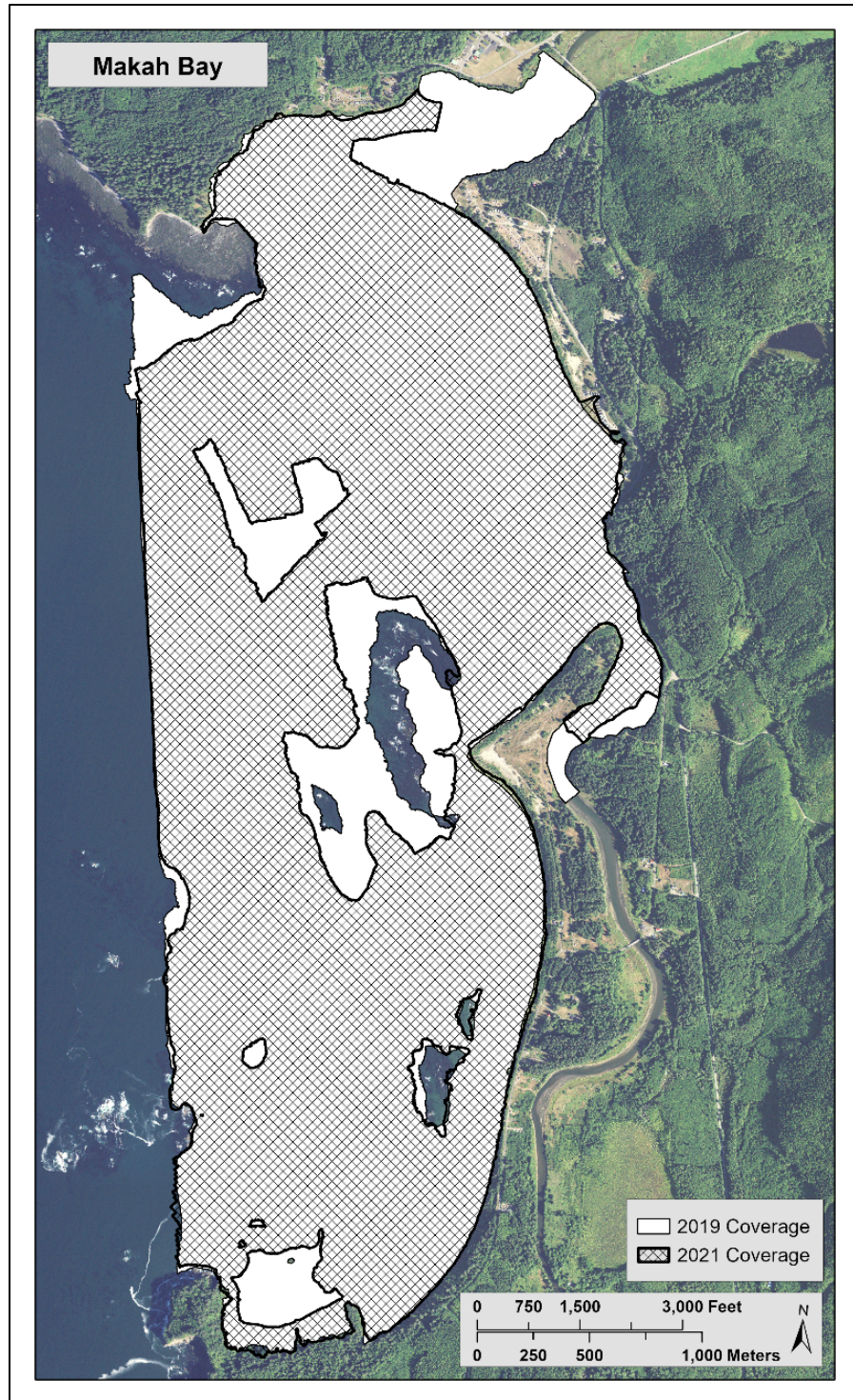


Figure 13. Combined topo-bathymetric data coverage of Makah Bay from CMAP’s 2019 and 2021 surveys (2017 NAIP imagery).

Data processing

All data were post-processed relative to a final position of the monument on Bahobohosh Point, derived from 11 occupations (115.3 hours) during the 2019 survey (Appendix A).

GNSS surface topography data were vertically adjusted to account for offsets between surveyors due to varying antenna heights.

Boat-based lidar data were corrected for vessel motion and cleaned manually in QPS Qimera, a hydrographic data processing software, to remove returns from vegetation, buildings, water surface, and noise. The lidar dataset was vertically adjusted to match GNSS surface topography data and gridded with the GNSS surface data using a bin average.

Multibeam sonar data were corrected for vessel motion, the speed of sound through the water column, and angular offsets between the sonars and the motion system. The data were manually cleaned in QPS Qimera to remove soundings from vegetation and noise, then gridded using a Combined Uncertainty Bathymetric Estimator (CUBE) algorithm, which accounts for the uncertainty of each sounding to find the most likely depth for each grid cell (Calder, 2003).

The multibeam grid and lidar/GNSS grid of each survey were combined and interpolated using a Triangulated Irregular Network (or TIN) in ArcGIS Pro using the Create TIN tool, resulting in a digital elevation model (DEM) of the beach and seafloor. Data gaps that caused interpolation artifacts such as visual triangular patterns or distortion around data edges were manually removed from the final datasets, and all edges of the datasets were manually edited to avoid extrapolation beyond the bounds of the data. Figure 14 shows the DEM created from the combined topographic and bathymetric data collected during the 2019 survey (in meters relative to NAVD88). A topo-bathymetric map of this DEM coverage with elevation contours in feet relative to mean lower low water (MLLW) is provided in Appendix E.

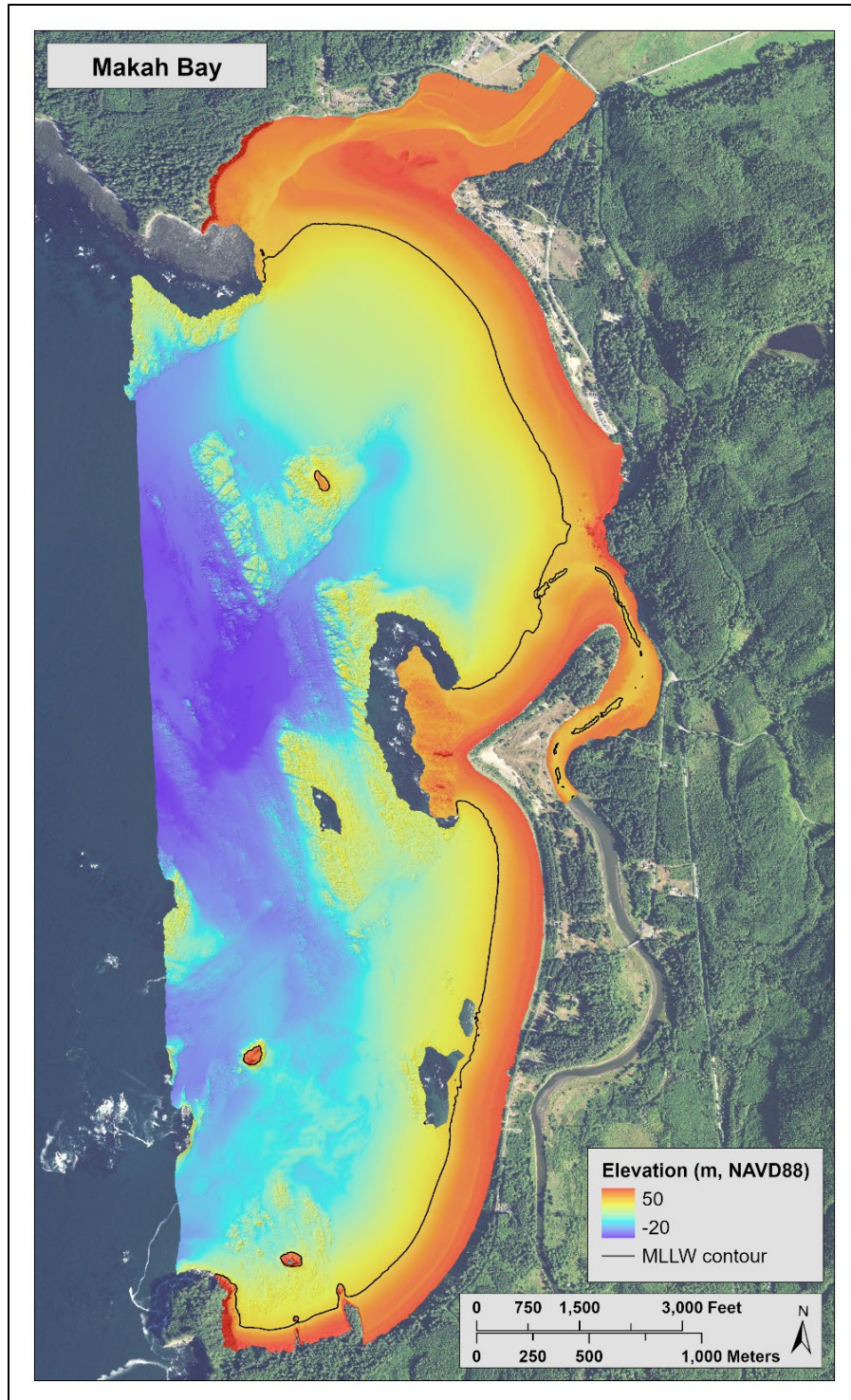


Figure 14. DEM topo-bathymetric coverage of Makah Bay from the 2019 surveys, gridded at 0.5 m (2017 NAIP imagery).

Data analysis

The 2019 DEM was subtracted from the 2021 DEM to create a difference surface of all of Makah Bay showing areas of erosion (red) or accretion (blue) that took place between the two surveys (Figure 15). Areas of white indicate no change ± 10 cm.

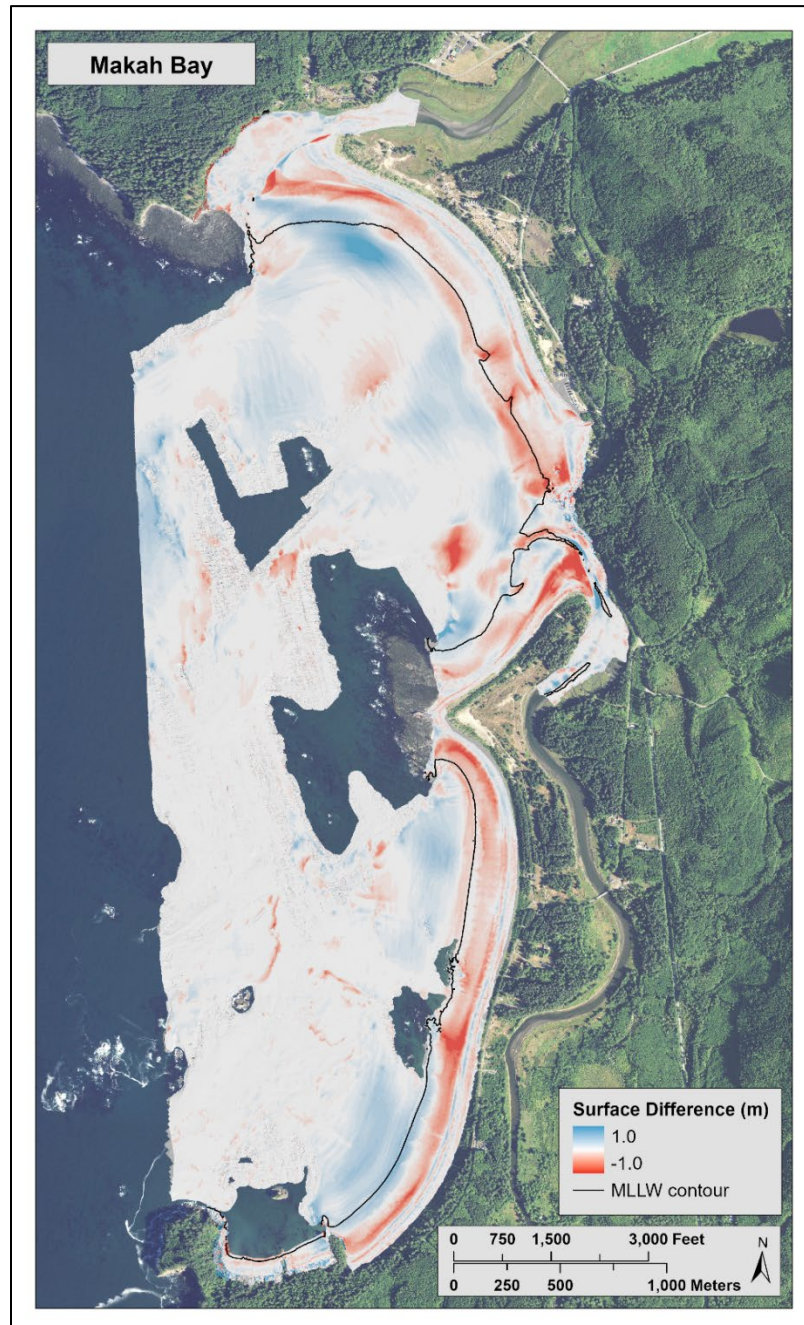


Figure 15. Change surface from September 2019 to July 2021, with the 2021 MLLW contour for context (2017 NAIP imagery). Areas of white indicate no change ± 10 cm.

Zones of morphologic change were manually digitized from the change surface with cross-shore boundaries including the seaward extent of change associated with the intertidal zone and an upper limit of intertidal change for the length of the bay. These zones roughly follow contours of no change, rather than elevation contours, in order to relate areas of similar change signal. Alongshore extents of each zone were determined through a mix of morphology, morphology change patterns, and areas of interest (Figure 16).

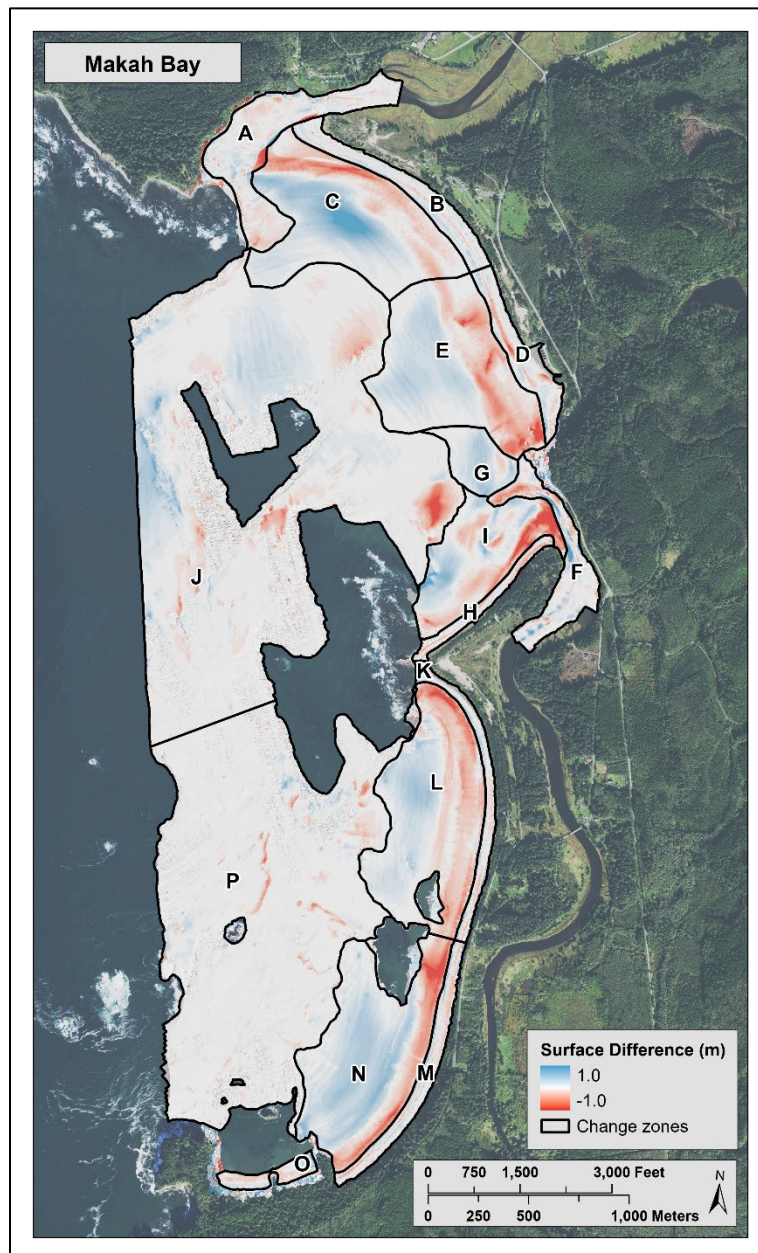


Figure 16. Change surface from September 2019 to July 2021 with zones used for analysis. Zones were roughly defined by following contours of no change. Areas of white indicate no change ± 10 cm.

In an attempt to relate the biennial topo-bathymetric shoreface change to longer-term shoreline and vegetation line change, the clusters derived from the historical vegetation line change analysis were used to create 150 m-wide swaths that extend from the upper beach through the seaward depth of closure on the shoreface (Figure 17). While the swaths were located preferentially in the center of each sub-cluster, some were adjusted alongshore to avoid data gaps, rocky outcrops, and overlap with adjacent sub-clusters. Swaths were omitted from analysis if they were unable to be adjusted to a location with a direct offshore-onshore connection uninterrupted by rocky outcrops or another portion of the coastline, resulting in a total of nine swaths used for analysis.

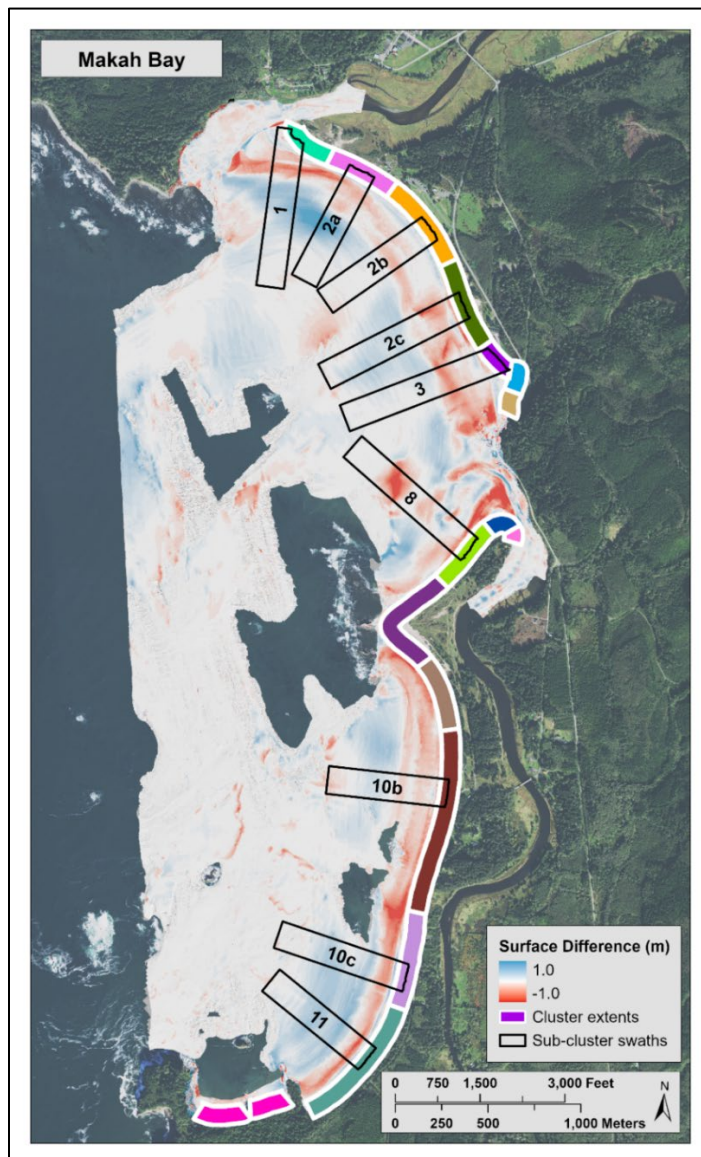


Figure 17. Cross-shore shoreface change swaths centered on clusters defined by the historical vegetation line change rates for comparative analyses. Change swaths that were truncated by rocky outcrops or other obstructions were excluded. Areas of white indicate no change ± 10 cm.

Measurement uncertainty

There are two types of errors reflected in uncertainty of measurements: systematic and random. Systematic errors are those related to any environmental, instrumental, methodological, or operational process that can bias the elevation measurement from the true value. Random errors may be caused by small unpredictable fluctuations that result in variations in precision of the measurements.

Measurement uncertainties for topo-bathymetric change analysis correspond to three different instrumentation and techniques used in specific survey locations. The positional uncertainty, topographic measurement uncertainty, and sonar measurement uncertainty are calculated individually. Calculations for estimating these three measurement uncertainties are discussed in Appendix A.

Depending on which survey techniques are used for each specific location, individual measurement uncertainties are propagated to obtain the total uncertainty for that specific location. Using this approach, the estimated total uncertainty for interpolated topographic DEMs in this study can be calculated by propagating the positional and topographic uncertainties resulting in a combined uncertainty of 10.2 cm at the 95% confidence interval. This is consistent with ± 10 cm that appears as a white band in the surface difference figures (e.g., Figure 15, Figure 16, and Figure 17), which indicates no detectable change.

Similarly, the estimated total uncertainty in measurements of offshore areas (Figure 16, Zones J and P) can be calculated by propagating the positional and sonar head uncertainties resulting in a combined uncertainty of 2.1 cm at the 95% interval. The propagated uncertainty for areas combining both topography and sonar measurements (Zones C, E, G, I, L, and N in Figure 16) can be calculated by propagating the positional, sonar head, and topography uncertainties resulting in a combined uncertainty of 10.4 cm at the 95% interval.

Makah Bay Results

Results from the Hobuck and Tsoo-Yess beach sub-regions are reported separately and combined for a complete analysis of Makah Bay. The historical coastline change assessment results created context for interpreting the biennial topo-bathymetric change.

Overview

Historical coastline change

Both shoreline change and vegetation line change rates were used to characterize historical coastline change for the long-term average (1952-2019 in Makah Bay and 1977-2019 at the Ozette Reservation) and recent 10-year average (2009-2019). Vegetation line change rates in Makah Bay were generally low with gradual changes temporally and spatially. Shoreline change rates were more variable with a larger magnitude due to sand migration and bar morphology on the mid and lower beaches. This result is consistent with Ruggerio et al. (2003) that found minimal variability at the vegetation line and increasing variability with decreasing beach elevation across the beach profile. Similarly, Miller and Akmajian (2022) found no seasonal pattern of erosion and accretion observed at the dune toe (4.0 m NAVD88) at Hobuck and Tsoo-Yess beaches, whereas the mean higher high water (MHHW) contour fluctuated horizontally by an average of 35 m/yr, and was typically influenced by the formation of a beach berm approximately 20-m wide during summer months. In comparison, Miller and Akmajian (2022) found the average elevation of the dune grass vegetation to be 4.12 m NAVD88 at Hobuck Beach. As such the dune toe changes reported by Miller and Akmajian (2022) derived from beach profile data are essentially equivalent to vegetation line changes derived here from aerial imagery (i.e., the dune toe at elevation 4.0 m NAVD88 is at nearly same location at the vegetation line at 4.12 m NAVD88 such that changes measured by either the dune toe elevation or the vegetation line location would be taken from features within close proximity). For these reasons, this assessment focuses analysis on vegetation line change as the proxy most directly relating to upland stability, and shoreline change to support observations of beach dynamics that drive overall coastline change. Further, shoreline change data are analyzed herein primarily based on cluster averages and long-term and 10-year trends rather than interannual fluctuations.

Both vegetation line and shoreline change in Makah Bay show an overall pattern of accretion with localized areas of erosion, and higher erosion rates primarily occurring in the most recent 10-year period (Figure 18). The average vegetation line change in Makah Bay for all years is 0.52 m/yr of accretion and the average shoreline change rate for all years is 0.64 m/yr of accretion. The 10-year average vegetation line change rate was 0.68 m/yr of accretion and the 10-year average shoreline change was 0.38 m/yr of accretion (Figure 18). The most widespread erosion with some of the highest erosion rates occurred between 2015 and 2017 (Figure 19) with an average of -0.2 m/yr vegetation line change. Historical change rates between 1952 and 2006 had a generally lower magnitude than recent rates between 2006 and 2019, possibly due to a

sampling bias from data being available only every 9 years, on average, before 2006 and every 2 to 3 years after 2006.

Results reported by cluster revealed spatial patterns of change. Vegetation line and shoreline trends are not always consistent with each other within each cluster over the same time period. Cluster 7 at the Tsoo-Yess River mouth shows the largest disparity in both the 10-year average and long-term average rates between the vegetation line and shoreline trends (Figure 18). The 10-year average rates reveal a vegetation line accretion trend throughout the bay in most clusters; however, Cluster 3 in front of the Hobuck RV Campground eroded during this time period (2009–2019) by 1 m/yr (Figure 19).

Appendix B provides the 10-m spaced vegetation line change rates calculated from the average of 1-m spaced transects as shown in Figure 9, and Appendix C provides the same for shoreline change rates. The aerial photos, shorelines, vegetation lines, shoreline change rates and vegetation line change rates are also provided in an interactive online map, [Makah Bay Coastal Change \(arcgis.com\)](https://wacyy.maps.arcgis.com/apps/webappviewer/index.html?id=8c3798dde9ee4be0a0835eee3572c50c)³. The map default view displays the 10-year average change rates in Makah Bay and offers the ability to pan, zoom, and select any segment to view the associated average and individual change rates. Additional layers including the shoreline change rates, digitized features, and NAIP imagery, can be viewed by turning them on using the “Layers” dropdown option.

³ The web map listed can be found at:
<https://wacyy.maps.arcgis.com/apps/webappviewer/index.html?id=8c3798dde9ee4be0a0835eee3572c50c>

Figure 18. Makah Bay average shoreline and vegetation line change rates by cluster (black polygons with change shown as red and blue bars), with the overall average 10-year and long-term change rates in Makah Bay for the vegetation line (solid black line) and shoreline (dotted black line). Accretion is indicated by positive change values (blue bars) and erosion is indicated by negative change values (red bars).

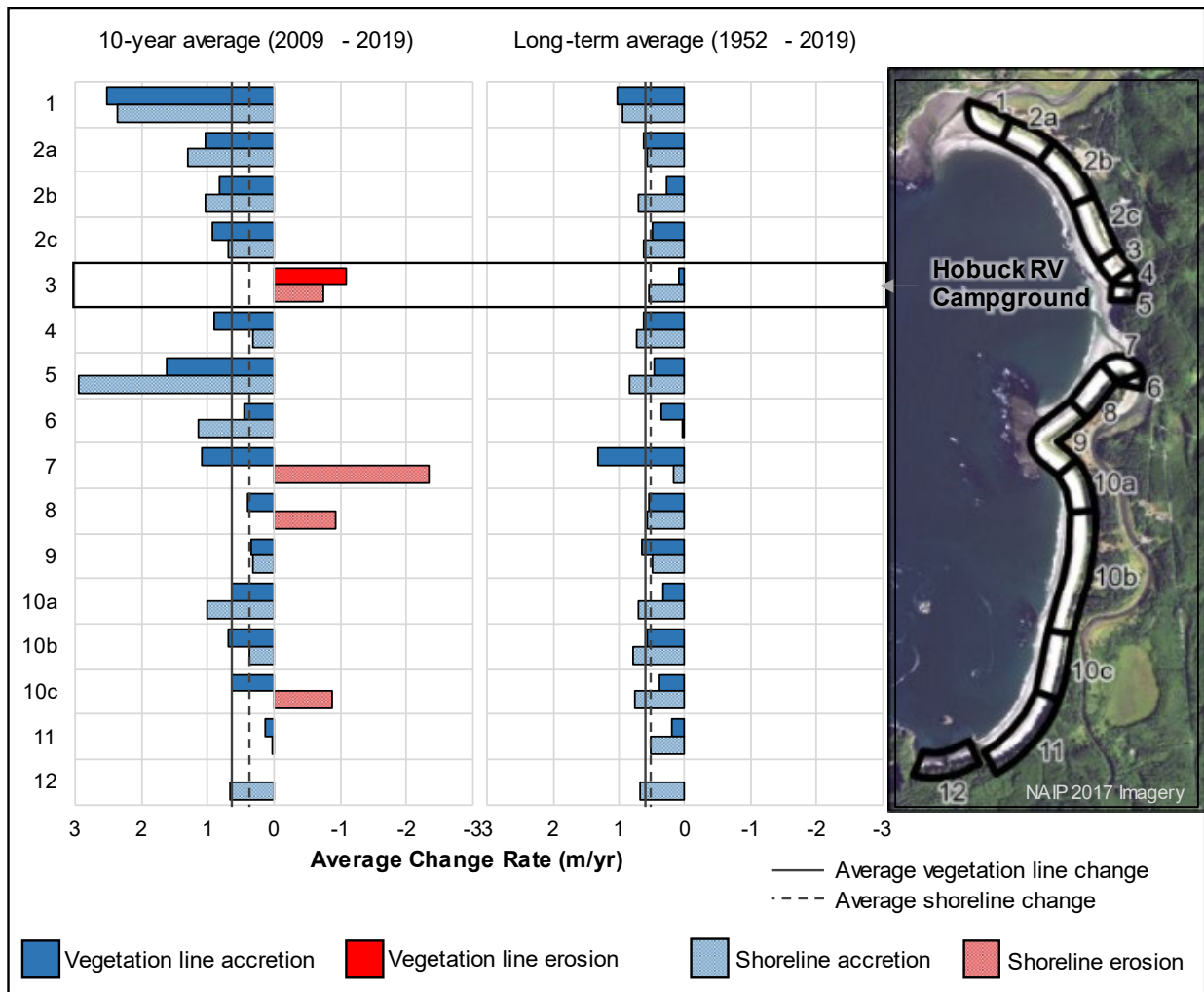
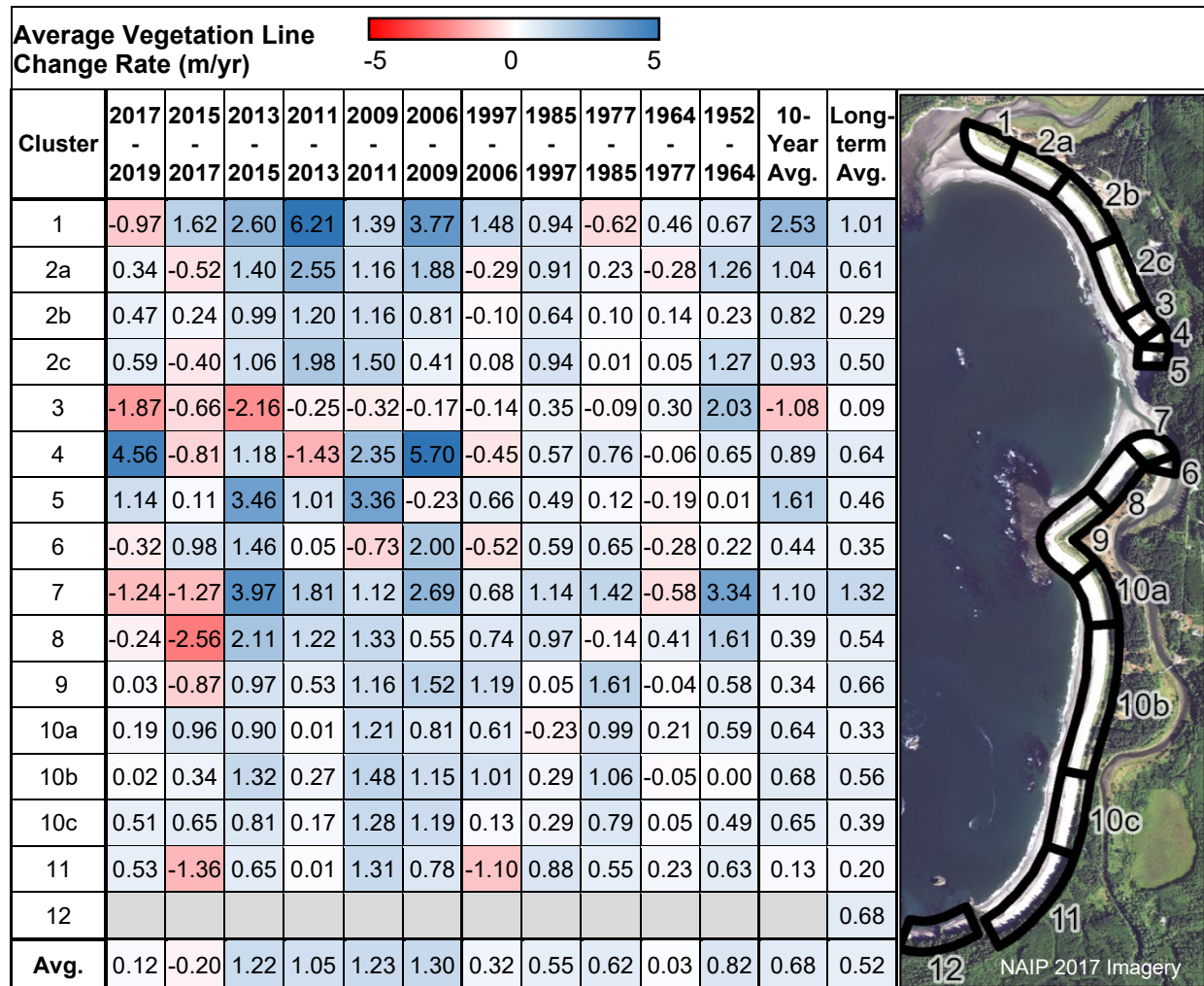


Figure 19. Makah Bay average vegetation line change rates by cluster (black polygons), and average based on the 10-m transects. Accretion is indicated by positive change rate values (blue) and erosion is indicated by negative change rate values (red). Interannual change rates are not reported for Cluster 12 due to a discontinuous time-series of vegetation line change in this area.



Biennial topo-bathymetric change

Between 2019 and 2021 Makah Bay had a net volume change of +93k m³, which equates to an average of 1 cm of accretion over the entire survey area (7.3 km²) (Figure 20 and Table 3). The largest magnitudes of change between the 2019 and 2021 surveys were seen in the lower beach and nearshore, with less change in the upper beach and deep bay.

Wa’atch and Tsoo-Yess rivers both showed localized channel migration of varying magnitudes up to 2.5 m of elevation change. The upper beach away from rivers was characterized by narrow bands of alternating erosion and accretion, mostly limited to the area above MHW (2.1

m NAVD88). The bands were 20-50 m wide and had elevation change magnitudes less than 2 m of either erosion or accretion.

The intertidal and sub-tidal areas contained the largest change in volume throughout the bay, characterized by a 100-200 m wide band of erosion on the beachface and dispersed accretion in the nearshore. Most of the beach-influenced change was limited to depths shallower than 10 m and within 500 m of the shoreline. The deep areas of the bay showed relatively less change and mostly along sand-rock boundaries, with localized erosion or accretion on the order of ± 1.5 m (Table 3).

Estimates of the uncertainty in volume change based on the propagation of measurement error for each accretion and erosion area are provided in Appendix A. The average error at the 95th percent confidence interval for each is approximately 17%.

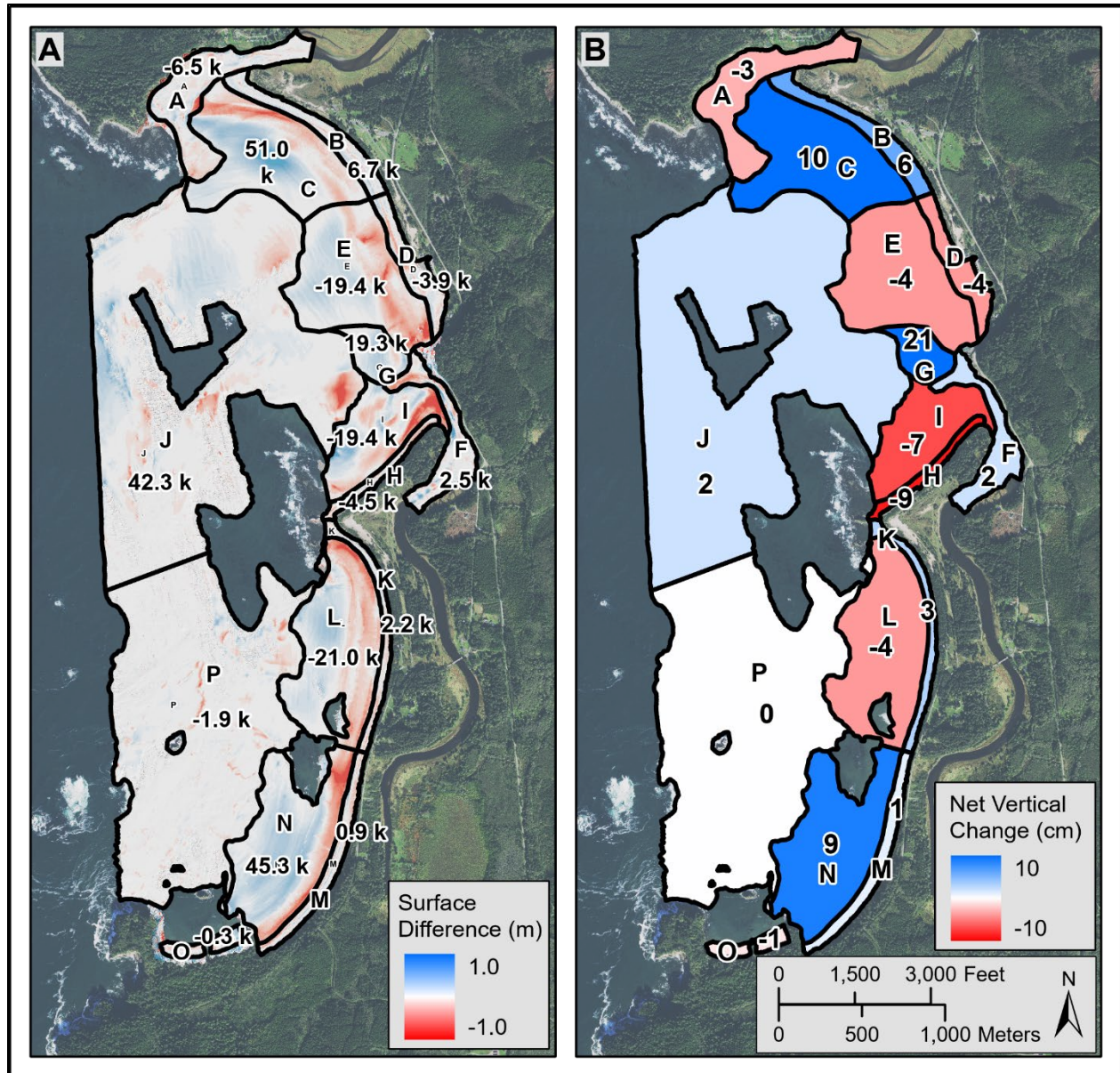


Figure 20. A) Change surface from September 2019 to July 2021 with zones showing net volume change (1000 m³) and B) showing net elevation change (cm). Areas of white indicate no change ± 10 cm.

Table 3. Volume and elevation changes derived from September 2019 and July 2021 topobathymetric surveys for zones shown in Figure 16 and Figure 20. *99.99th and 0.01th percentiles used for maximum accretion and erosion, respectively, to avoid the potential for outlying data artifacts.

Location	Zone	Area (m ²)	Gross Accretion Volume (1000 m ³)	Max Accretion (m)	Gross Erosion Volume (1000 m ³)	Max Erosion (m)	Net Volume Change (1000 m ³)	Net Vertical Change (cm)
Wa'atch River	A	248,664	14.9	1.2	-21.4	-1.7	-6.5	-3
Hobuck North Upper	B	116,830	11.3	0.8	-4.5	-0.9	6.7	6
Hobuck North Tidal	C	502,475	102.1	1.3	-51.1	-1.4	51.0	10
Hobuck Central Upper	D	97,344	7.2	1.9	-11.1	-1.4	-3.9	-4
Hobuck Central Tidal	E	491,049	54.6	1.8	-74.0	-1.9	-19.4	-4
Tsoo-Yess River Upper*	F	140,256	16.2	2.4	-13.6	-1.4	2.5	2
Tsoo-Yess River Tidal	G	92,406	20.5	0.9	-1.2	-0.4	19.3	21
Hobuck South Upper	H	47,710	2.2	0.5	-6.6	-1.0	-4.5	-9
Hobuck South Tidal	I	273,559	33.7	1.7	-53.1	-2.1	-19.4	-7
Hobuck Offshore*	J	2,286,400	149.1	1.6	-106.8	-1.7	42.3	2
Hobuck North	A-C	867,969	128.3	1.3	-77.1	-1.7	51.2	6
Hobuck South	D-I	1,044,980	127.0	2.4	-148.5	-2.1	-21.4	-2
Hobuck Beach	A-I	4,296,692	262.5	2.4	-236.7	-2.1	25.9	1
Hobuck Bay	A-J	4,296,692	411.6	2.4	-343.4	-2.1	68.2	2
Tsoo-Yess North Upper	K	68,991	6.7	0.8	-4.5	-0.8	2.2	3
Tsoo-Yess North Tidal*	L	494,090	53.9	0.8	-74.9	-1.3	-21.0	-4
Tsoo-Yess South Upper	M	100,010	9.7	0.9	-8.9	-0.7	0.9	1
Tsoo-Yess South Tidal	N	500,204	109.2	1.4	-63.9	-1.4	45.3	9
Secret Beach	O	39,728	4.0	1.8	-4.3	-1.5	-0.3	-1
Tsoo-Yess Offshore*	P	1,755,740	52.1	1.1	-54.0	-1.2	-1.9	0
Tsoo-Yess North	K-L	563,081	60.6	0.8	-79.4	-1.3	-18.8	-3
Tsoo-Yess South	M-O	639,942	122.9	1.8	-77.0	-1.5	45.9	7
Tsoo-Yess Beach	K-O	1,203,022	172.8	1.8	-147.6	-1.5	27.1	2
Tsoo-Yess Bay	K-P	2,958,762	235.6	1.8	-210.4	-1.5	25.2	1
Makah Beach	A-I, K-O	3,213,314	446.1	2.4	-393.1	-2.1	53.0	2
Makah Bay	A-P	7,255,454	647.2	2.4	-553.8	-2.1	93.4	1

Hobuck Beach

Hobuck Beach historical coastline change

The historical coastline change analyses at Hobuck Beach revealed a pattern largely of accretion, however localized areas of erosion were observed. The average long-term vegetation line change at Hobuck Beach was 0.59 m/yr and the average shoreline change for all years was 0.60 m/yr. (Figure 21). The 10-year average vegetation line change was 0.84 m/yr and the 10-year average shoreline change was 0.48 m/yr (Figure 21). 1.0% of the reported average vegetation line change rates were erosion, 89.6% were accretion, and 9.4% were lower than ± 0.25 m/yr, which was considered within the noise level of input data (Appendix B). Similarly, 2.2% of the reported average shoreline change rates were erosion, 92.2% were accretion, and 5.6% were lower than ± 0.25 m/yr (Appendix C).

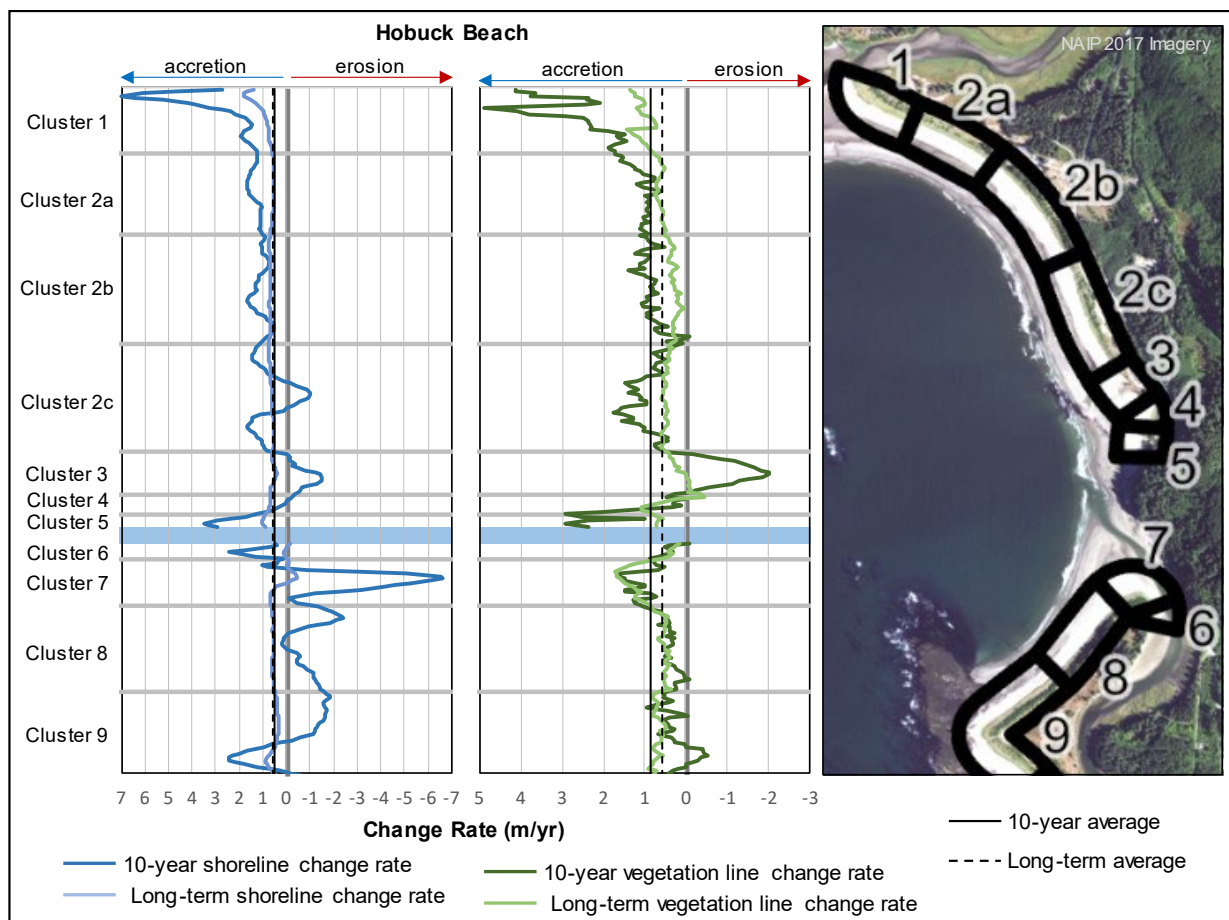


Figure 21. Long-term (1952-2019) and recent 10-year (2009-2019) coastline change rates at 10-m transect intervals along Hobuck Beach, based on digitized shorelines and vegetation lines from aerial imagery.

Both historical and recent coastline change rates revealed three dominant areas of change in the Hobuck sub-region—near Hobuck Creek and at the Tsoo-Yess and Wa’atch river mouths.

Near Hobuck Creek, Clusters 3 and 4 had erosion and accretion signals in both the vegetation line and shoreline that shifted spatially through time, driven by lateral migration of Hobuck Creek across the beach face. Between 1977 and 1985, the vegetation line trend in Cluster 5 switched from eroding to largely accreting, and the vegetation line change rates in Cluster 3 at the Hobuck RV Campground switched from accreting to eroding (Figure 19 and Figure 22). The consistent interannual trend of vegetation line accretion in Cluster 5 and erosion in Cluster 3 since 2009 (Figure 19) has occurred within the context of a long-term trend of net northward migration of the Hobuck Creek thalweg (i.e., deepest path of the creek channel crossing the beach) since 1952 (Figure 23). While the meander of the creek has been observed to fluctuate on short-time scales, the historical aerial imagery indicate a propensity for the creek channel to cross the beach farther to the north since 2011 compared to previous decades.

The recent erosion trend directly north of Hobuck Creek in Cluster 3 is seen in both the vegetation line and shoreline average change rates (Figure 21), with an erosion hotspot occurring directly in front of the south side of the Hobuck RV Campground (Figure 22). The 10-year average shoreline change rates show a second shoreline erosion area approximately 400 m north along the beach in Cluster 2c, however this trend is not reflected in the vegetation line rates (Figure 21).

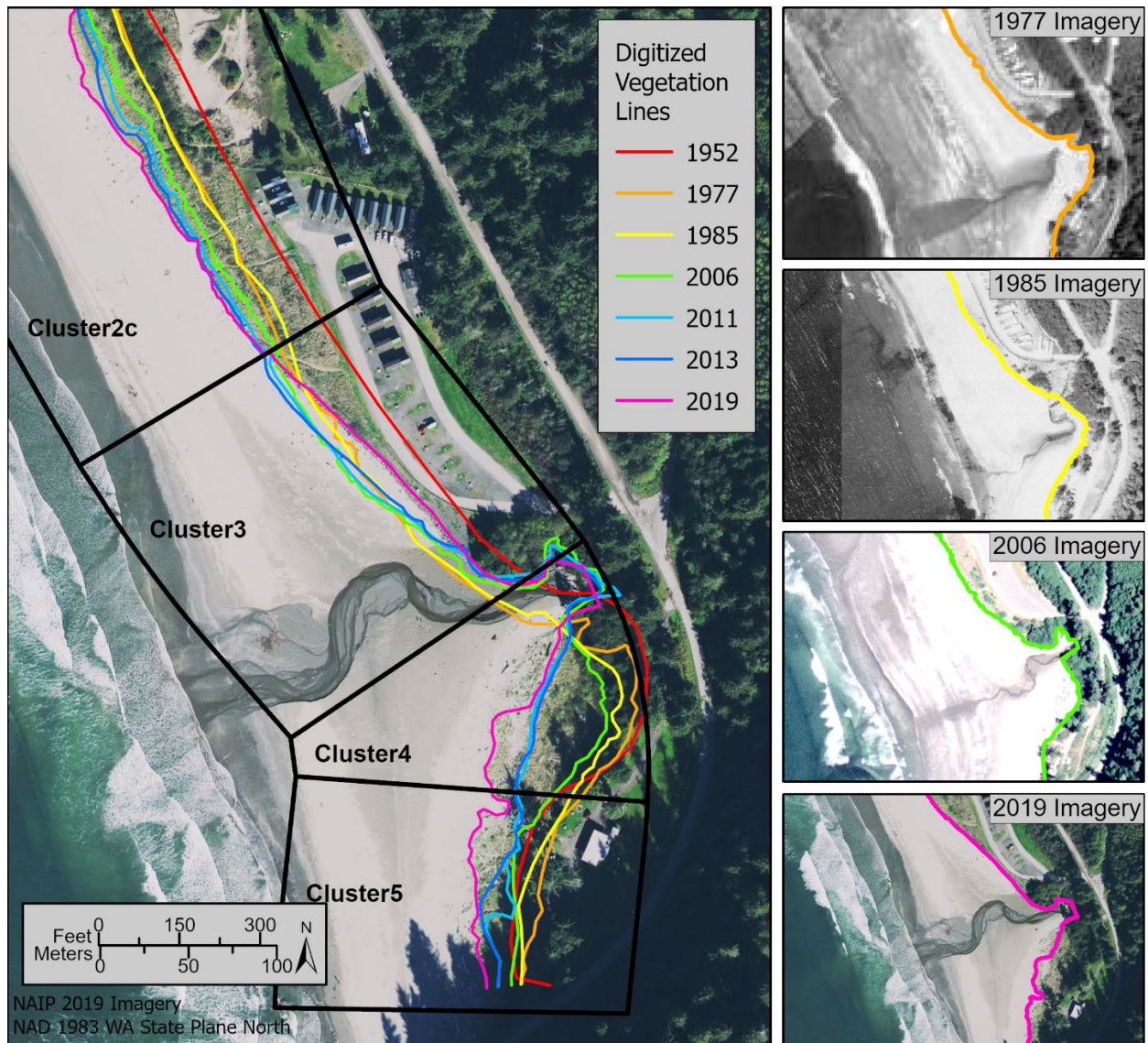


Figure 22. Select vegetation lines digitized from aerial imagery in Cluster 3 and 4, near Hobuck Creek and the Hobuck RV Campground (left). Selected years of aerial imagery between 1977 and 2019 (right) show vegetation line progradation south of Hobuck Creek and vegetation line retreat north of Hobuck Creek.

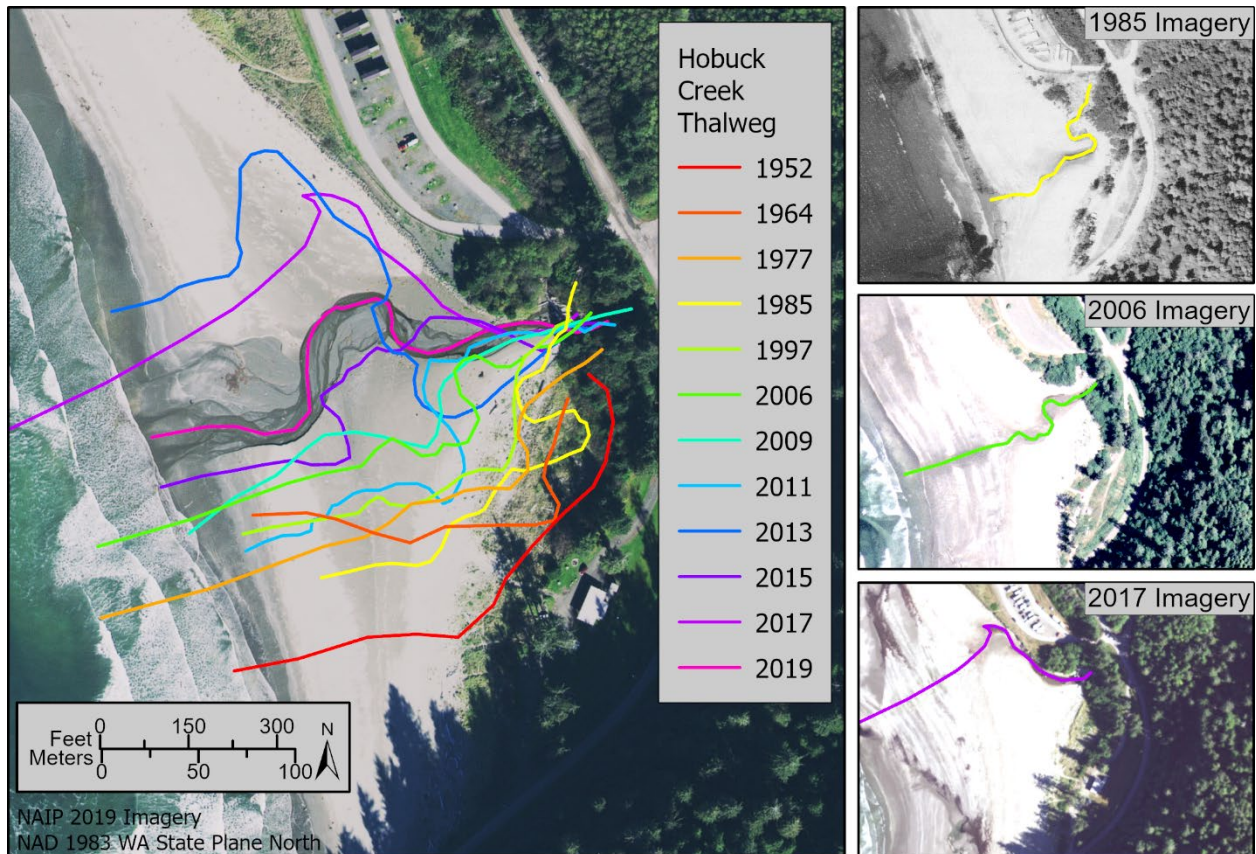


Figure 23. Hobuck Creek channel thalwegs crossing Hobuck Beach digitized from aerial imagery (left) with select years of imagery between 1985 and 2017 (right) showing key instances of Hobuck Creek thalweg migration from south to north.

The highest erosion rates in Cluster 3 occurred between 2013 and 2015 with a consistent erosion trend through 2019 (Figure 19, Appendix B, and Appendix C). The increased erosion occurred after the manual removal of trees between 2011 and 2013 fronting the Hobuck RV Campground, which was observed using imagery overlaid on an NDVI surface to enhance the vegetation visibility (Figure 24). It is possible that the vegetation may have provided some resistance to undercutting of the bank by the creek, and then after trees were removed, there may have been less resistance to combined stream flow and wave runup. Only one tree remained in this area in 2015 out of the several that were apparent in 2011 (Figure 25). By contrast, the area of dense tree vegetation directly south of Hobuck RV Campground has stayed generally stable since 2006, including in 2015 when the creek thalweg was directly adjacent to this stand of trees (Figure 22 and Figure 24).

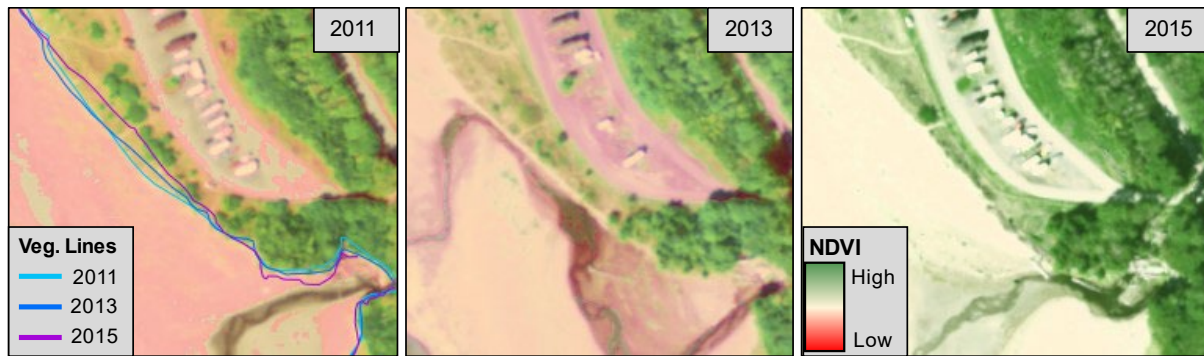


Figure 24. Normalized Difference Vegetation Index (NDVI) enhanced aerial imagery overlain on true color imagery to display the removal of trees between 2011 and 2013 followed by significant vegetation line retreat between 2013 and 2015 at the Hobuck RV Campground. High NDVI values indicate high density or healthy vegetation (green) and low values indicate unvegetated areas such as beach sediment or water (yellow and red).

At the Tsoo-Yess and Wa'atch river mouths, dune grass has propagated seaward reflecting beach accretion, likely driven by sediment outputs from the rivers (Figure 25 and Figure 26).

The Tsoo-Yess River mouth is approximately 500 m south of Hobuck Creek with its northeast side constrained by the Bahobohosh Point rocky outcrop (Figure 2). The southwest shore of the Tsoo-Yess River mouth at Cluster 7 has the highest long-term vegetation line accretion rate of 1.3 m/yr (Figure 18 and Figure 19). The peak accretion extends northward along the axis of the river channel and decreases to the southwest with distance from the mouth (Figure 25). The 10-year average shoreline change in Cluster 7 is likely influenced by the seaward-most beach extent in 2011 eroding significantly by 2013 and continuing to erode until 2015, however the shoreline erosion trend was not consistent through time (Appendix C). The vegetation line during this time accreted through 2015, then eroded through 2019, while still retaining a 10-yr accretion rate of 1.1 m/yr (Figure 18 and Figure 19). Future beach profile monitoring is needed to determine if a reversal in trend of the decadal-scale accretion trend at the vegetation line has begun, or if the recent erosion reflects shorter term fluctuations.

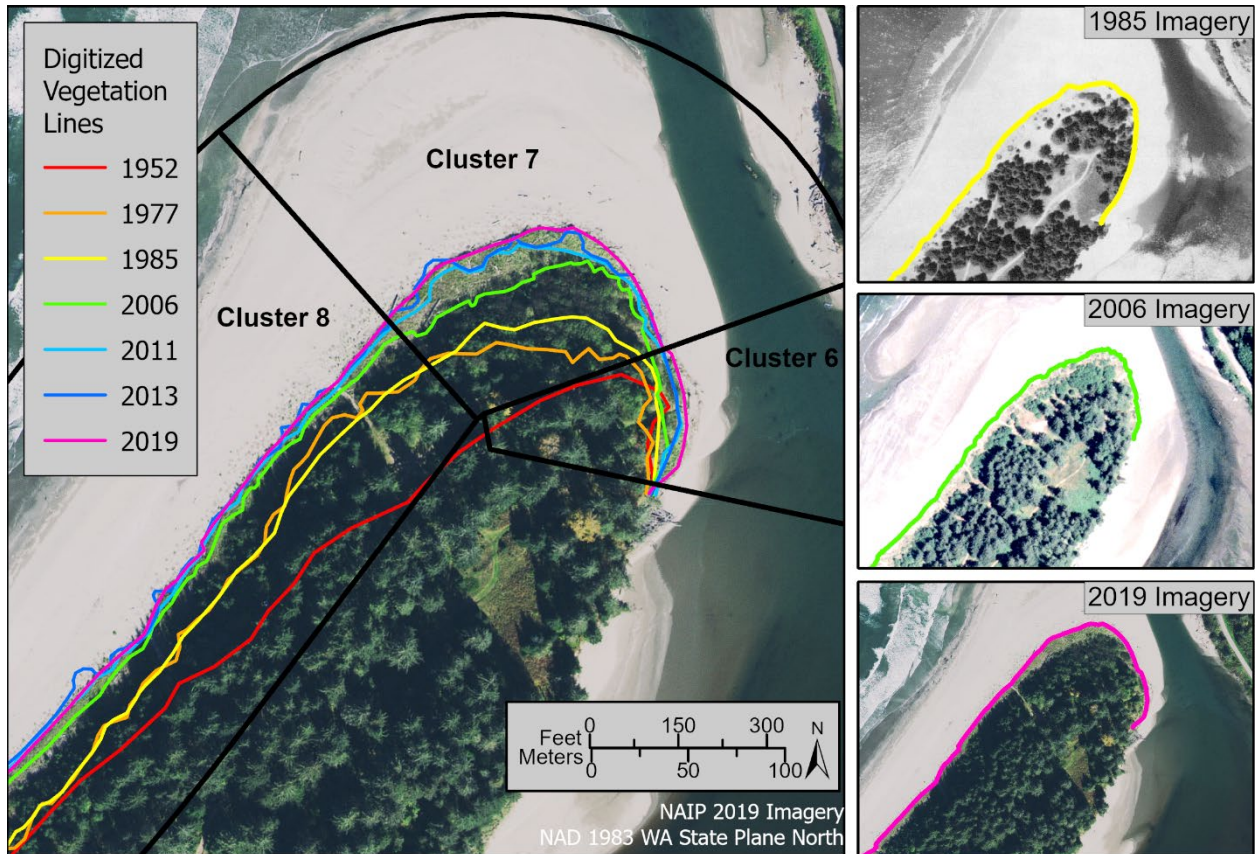


Figure 25. Vegetation lines digitized from aerial imagery at the mouth of the Tsoo-Yess River (left), with select years of imagery between 1985 and 2019 showing vegetation line progradation and increase in vegetation density through time (right).

At the mouth of the Wa’atch River, the vegetation line has prograded a maximum distance of 213 m since 1952, and the vegetation line prograded 68 m since 2006 (Figure 26). Cluster 1 has the highest recent 10-yr (2009-2019) vegetation line accretion rate of 2.5 m/yr and the second highest long-term (1952-2019) accretion rate of 1 m/yr (Figure 18 and Figure 19).

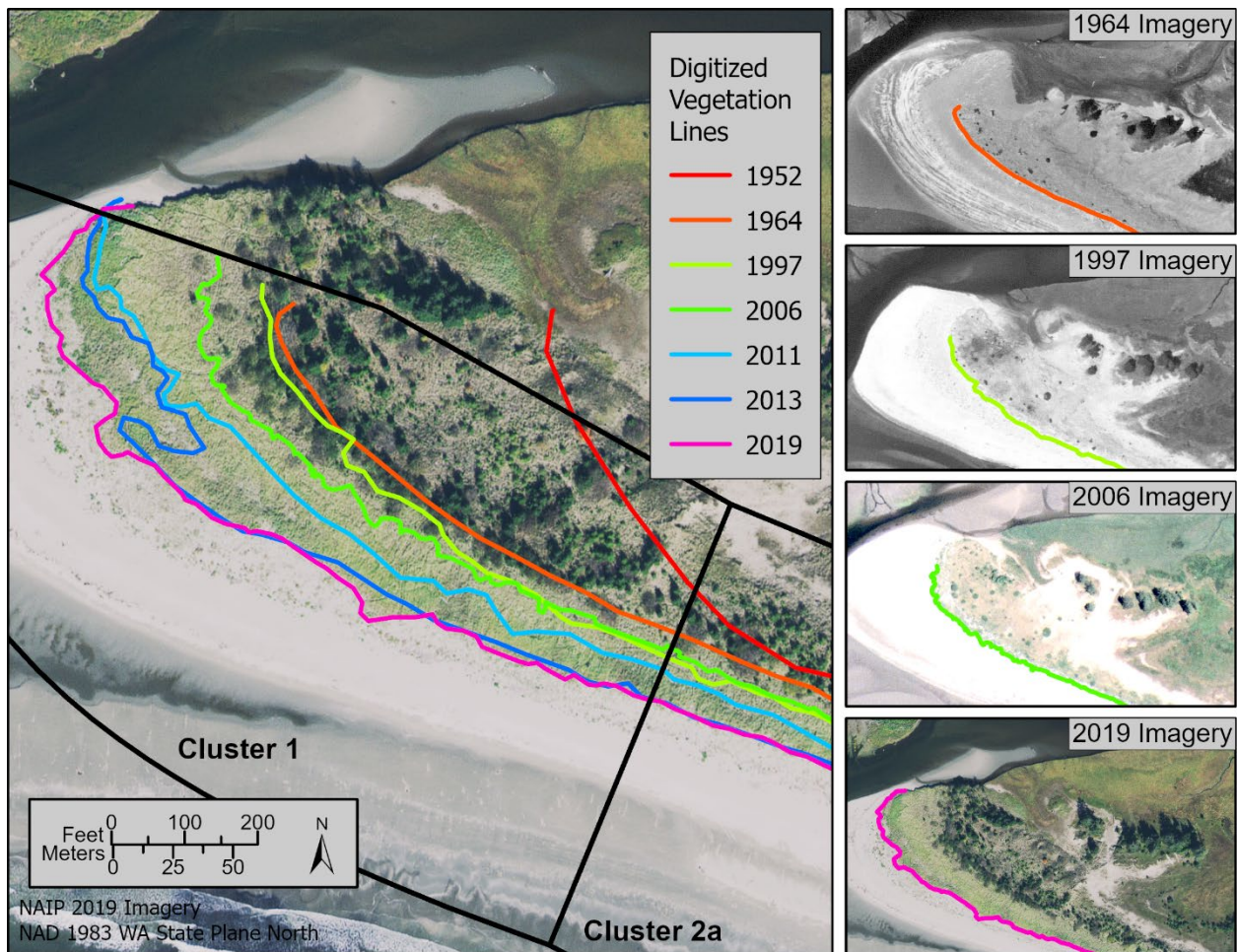


Figure 26. Vegetation lines digitized from aerial imagery at the mouth of the Wa'atch River, with select years of imagery between 1964 and 2019 displaying the vegetation line progradation.

Hobuck Beach biennial topo-bathymetric change

The high-resolution topo-bathymetric survey of the Hobuck Beach sub-region reveals a large embayment with extensive rocky outcrops interfacing with seafloor sediments (Figure 27). A ~100 m-wide channel-oriented SW-NE passes between shallow rocky platforms and bifurcates northward and southward wrapping around the edges of the platforms. A progressively shallower smooth surface toward shore is indicative of a sandy shoreface. As measured by the -10-m NAVD88 contour to the MLLW contour, the width of shoreface in the southern half of Hobuck Beach is approximately 760 m at its widest point and approximately 500 m at its narrowest point, however the northern half of the beach is approximately 1,015 m wide (Figure 27). The narrower shoreface along the southern half of Hobuck Beach implies that it receives greater wave energy near the shoreline, which would drive sediments northward along Hobuck Beach.

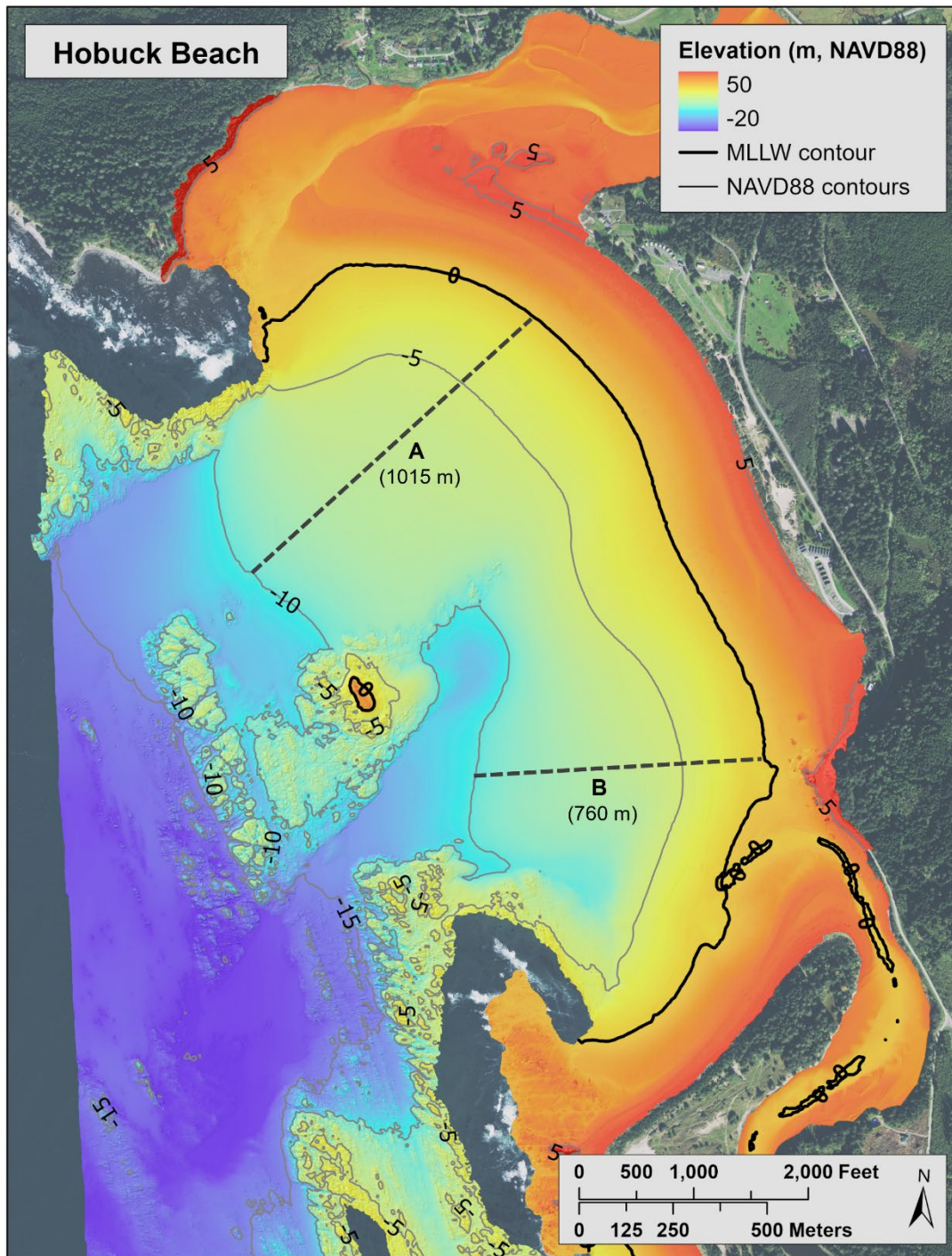


Figure 27. Hobuck Beach 2019 topo-bathymetric DEM with MLLW contour and 5-m NAVD88 contours overlaid for reference, with transects A and B measured between the -10 m contour and MLLW contour for shoreface width comparison (dashed lines).

Figure 28 shows the elevation changes between the September 2019 and July 2021 surveys along with the 2021 elevation contours. A bend in the -2 to -5-m contours toward shoreline at

the Hobuck RV Campground is indicative of wave refraction in this area (spreading and bending toward the north and south shallower areas) but also having relatively higher energy closer to the shoreline associated with the narrower, steeper shoreface. In contrast, the northern Hobuck shoreface has a remarkably wide and gentle slope between the -6 and -8 m contours which would serve to reduce the height of large incoming waves through frictional dissipation (Wright and Short, 1984). The deepest shoreface deposition extends to nearly -10 m NAVD88 landward of mid-bay rocky outcrops, where the -10 m contour reaches landward and the shoreface is most narrow.

The seaward bend of the -3 to -6 m contours in the central part of Hobuck Beach suggest a zone that may be dominated by both wave focusing and offshore sediment transport. While the general pattern of beach erosion and nearshore accretion may be indicative of seasonal to interannual fluctuations, the convex-shaped shoreface contours at mid-Hobuck Beach are shown in both the 2019 and 2021 surveys (Figure 29). It is likely that this shoreface configuration is a persistent feature due to both diffraction as waves bend around the mid-bay rocky outcrop and pass through the openings to the north and south and wave refraction as waves bend toward the shallower bathymetry landward of the outcrop and converge from both the north and south.

This alongshore variability in wave energy distribution and wave direction can set up circulation cells within the bay. Net northerly sediment transport at the Hobuck RV Campground may lead to net offshore transport a few hundred meters to the north, maintained by a local convergence of wave energy and wave direction from both the north and the south. This process may also be aided by Hobuck Creek meandering northward and lowering the beach profile such that it sets up local intertidal troughs that drain northward and seaward. This may explain the difference in the 10-year average shoreline change and vegetation line change shown in Figure 21 where the shoreline change shows an erosion area in the middle of Cluster 2c and the vegetation line show accretion. In this case, the vegetation line accretes due to the northward transport of sand by marine and aeolian processes to feed the dunes approximately 400 m north along the beach in Cluster 2c, while a divergence of sediment transport in the offshore direction is driven by seaward flows from intertidal troughs during falling tides. Figure 29 shows this beach morphology by MLLW contour indentations that are co-located with darker red lower elevations extending landward, which indicate the locations of outflow channels from intertidal troughs during the July 2021 survey. An example of the complexity of the intertidal beach morphology in this area is shown in Figure 30.

Figure 31 shows the gross volume changes between the September 2019 and July 2021 surveys in the Hobuck sub-region, which correspond to the geomorphic data interpretations above. The southern sub-regional shoreface Zone E, reveals a net loss of 19,400 m³ of sediment while the northern shoreface Zone C had a net gain of 51,000 m³ of sediment (Figure 31 and Table 3). These results indicate net northward transport of sediment between the 2019 and 2021 surveys. The 19,300 m³ of gain of sediment in Zone G is interpreted to be most directly associated with the Tsoo-Yess River mouth as a delta feature, with the 19,400 m³ of loss of sediment in Zone I part of a northward shift of sediments probably influenced by changes in

river flow. The entire Hobuck Beach survey area had over 340,000 m³ of sediment exchange between zones, resulting in a net positive 68,200 m³ and average vertical accretion of 2 cm (Table 3).

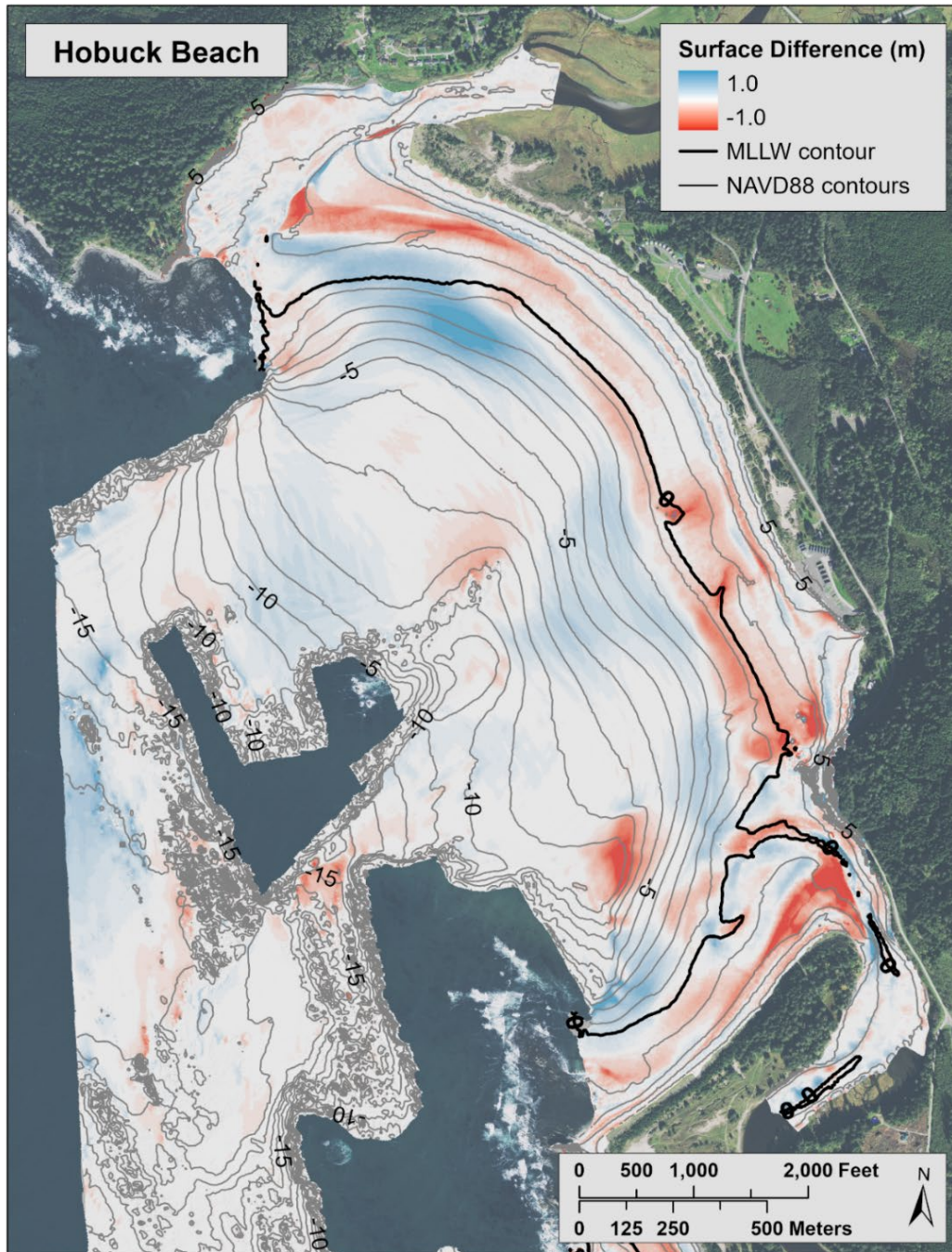


Figure 28. Hobuck Beach change surface from September 2019 to July 2021 with 2021 MLLW contour and 1-m NAVD88 contours overlaid. Areas of white indicate no change ± 10 cm.

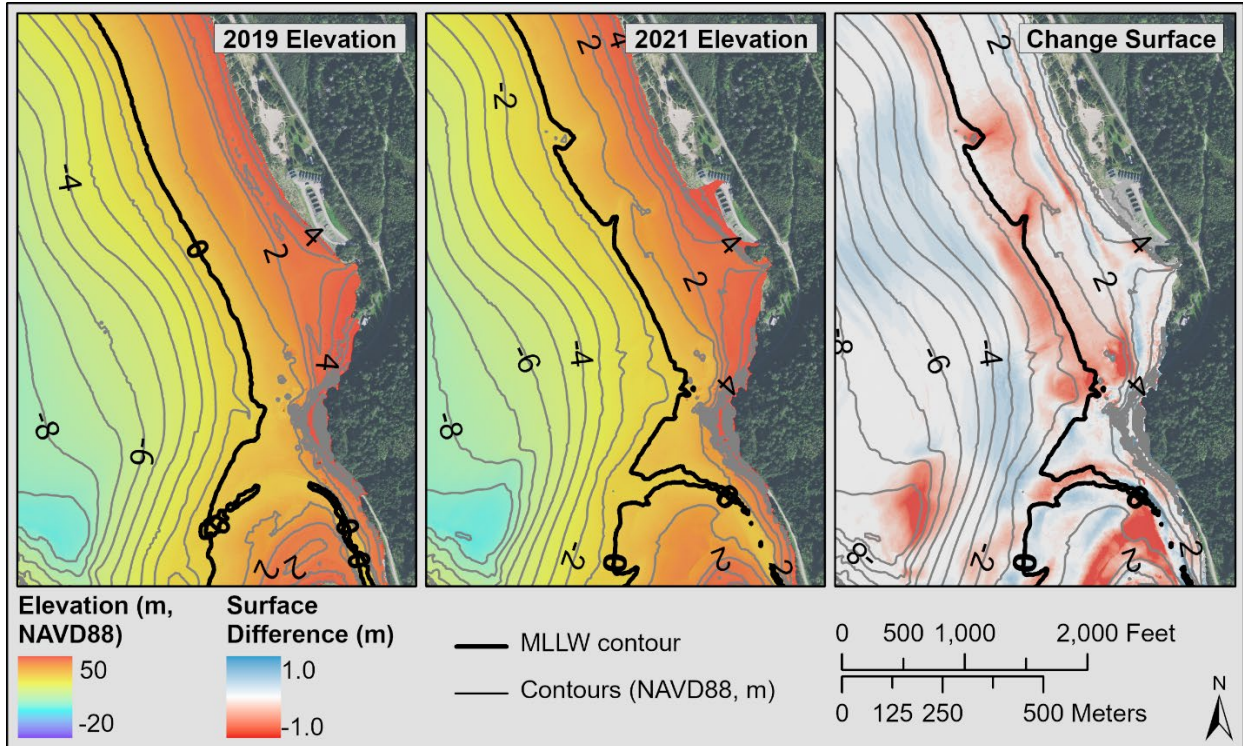


Figure 29. Hobuck Creek 2019 DEM (left), 2021 DEM (middle), and change surface (right), with respective years' MLLW and 1-m NAVD88 contours. Areas of white indicate no change ± 10 cm.

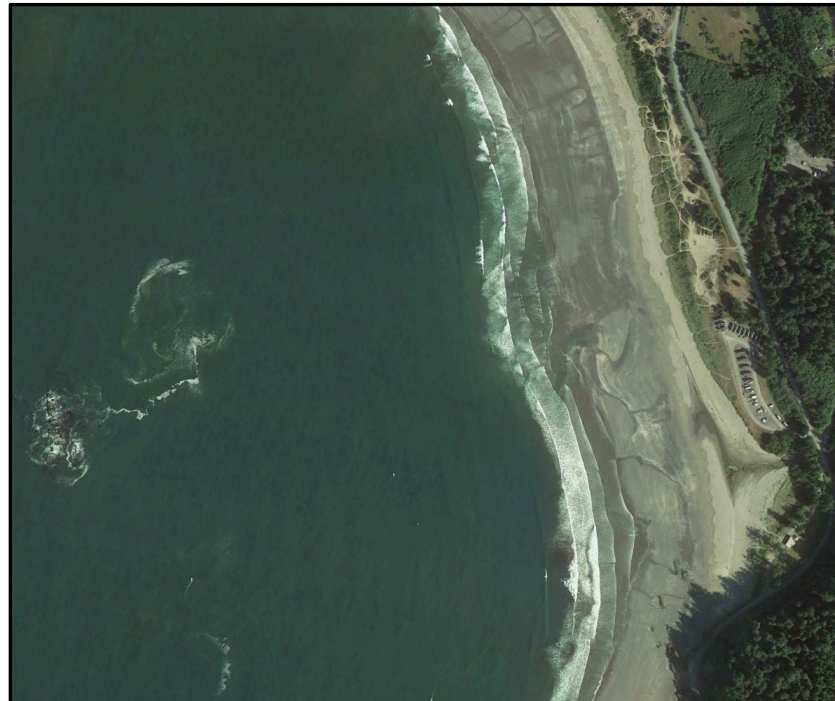


Figure 30. Google Earth imagery from August 19, 2016 showing intertidal bar and trough complexity fronting the Hobuck RV Campground.

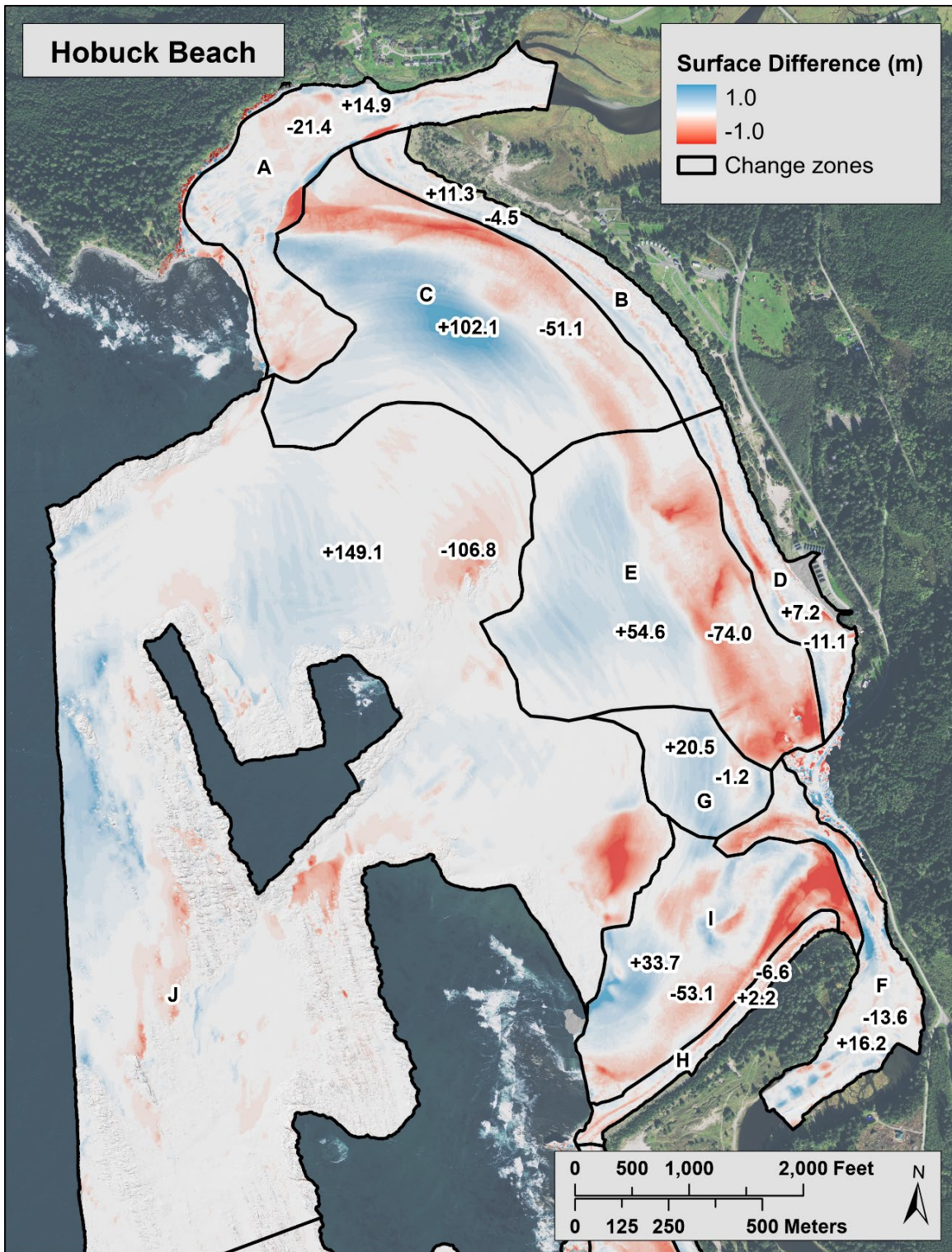


Figure 31. Hobuck Beach change surface from September 2019 to July 2021 with change zone boundaries overlaid showing gross positive and negative volume change in 1000 m³. Areas of white indicate no change ±10 cm.

Tsoo-Yess Beach

Tsoo-Yess Beach historical coastline change

Change rates at Tsoo-Yess Beach show a generally lower magnitude than those at Hobuck Beach, however rates reflect a similar overall pattern of accretion. The average long-term vegetation line change at Tsoo-Yess Beach was 0.41 m/yr and the average long-term shoreline change was 0.68 m/yr (Figure 32). The 10-year average vegetation line change was 0.51 m/yr and the 10-year average shoreline change was 0.28 m/yr (Figure 32). None of the long-term vegetation line change rates were erosion, 79.1% of vegetation line change rates were accretion, and 20.9% of vegetation line change rates were lower than ± 0.25 m/yr. Only 10.6% of long-term average shoreline change rates were less than ± 0.5 m/yr but 98.8% of long-term average rates were less than ± 1.0 m/yr (Appendix C).

Imagery quality was dark with poor positional accuracy at the pocket beach at the south end of Tsoo-Yess Beach (Cluster 12), making shoreline and vegetation lines indistinguishable in most sets of source imagery. This area was interpreted separately from Tsoo-Yess Beach using qualitative observations to supplement the quantitative change rates. Cluster 12 appears to be a relatively thin layer of sand overlaying bedrock that is exposed around the edges of the beach. This area is cut off from the rest of Tsoo-Yess Beach by a rocky outcrop at the north of Cluster 12, so smaller fluctuations in the sediment availability may have translated to large changes in shoreline position.

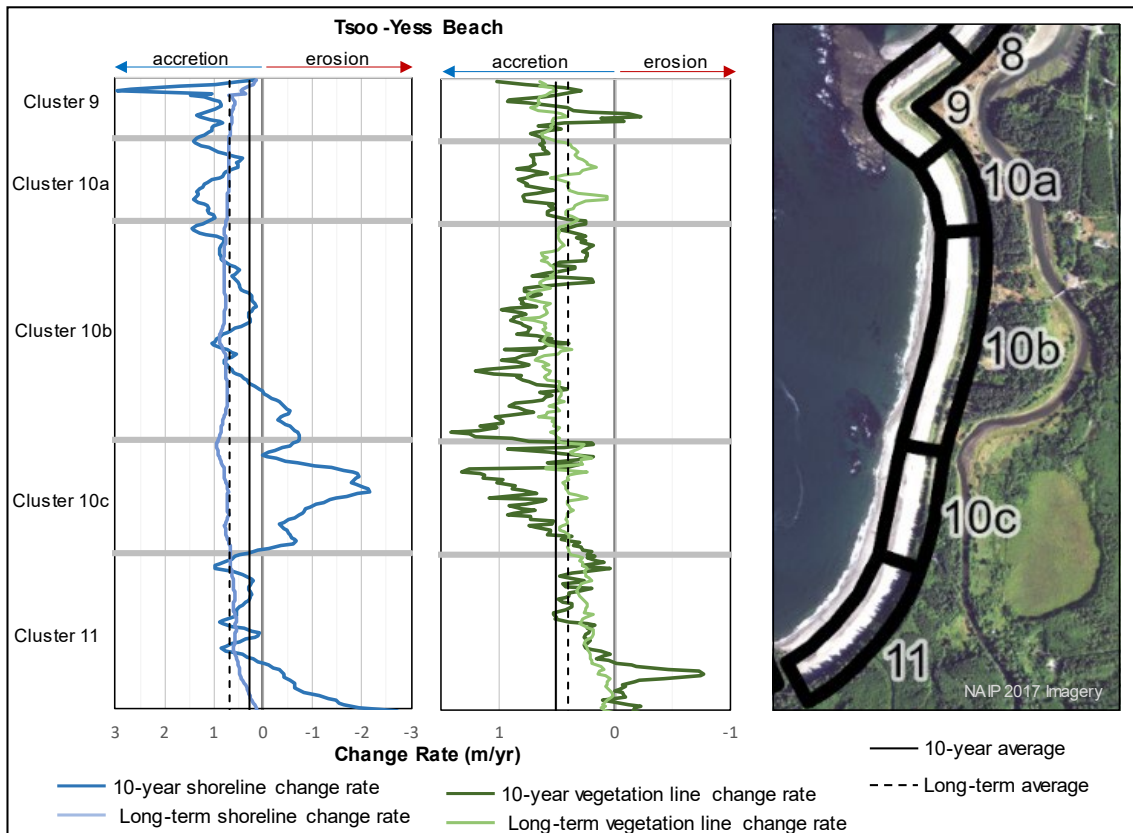


Figure 32. Long-term and 10-year shoreline and vegetation line change rates at 10-m transect intervals along Tsoo-Yess Beach.

Tsoo-Yess Beach biennial topo-bathymetric change

Compared to the Hobuck shoreface, the Tsoo-Yess shoreface is significantly narrower as measured from the -10 m NAVD88 contour to the MLLW contour (Figure 33). The narrowest portion of the Hobuck shoreface of approximately 500 m in width is about the same as the widest portion of the Tsoo-Yess shoreface. The narrowest section of the Tsoo-Yess shoreface is approximately 375 m in width toward the southern part of Makah Bay. In contrast, much of the southern half of Makah Bay is shallower than 15 m with deeper water only reaching into the bay in small pockets from the northwest corner and between rocky outcrops and islands along the offshore boundary of the survey area. As such, Tsoo-Yess Beach is relatively more protected from ocean waves, despite the narrower shoreface landward of the -10 m NAVD88 contour. Similar to Hobuck Beach, the narrower shoreface along the southern half of Tsoo-Yess Beach implies that it receives greater wave energy near the shoreline, which would drive sediments northward along Tsoo-Yess Beach. However, given the complexity of the offshore bathymetry and sheltering from islands and outcrops (Figure 33), a process-based model would need to be applied to provide a more robust assessment of wave energy and sediment transport distribution patterns along Tsoo-Yess Beach.

Figure 34 shows the elevation changes between the September 2019 and July 2021 surveys along with the 2021 elevation contours. The deepest change extends to about -10 m NAVD88 in

the southern half of the bay where the shoreface is steeper and narrower than the northern half. A localized bend in the -2 to -5-m contours toward shoreline at in the southern half of Tsoo-Yess Beach is indicative of wave divergence and refraction toward the north and south. This southern shoreface is also narrower and steeper compared to the northern half of Tsoo-Yess Beach, which has a wider and more dissipative shoreface.

The gross shoreface accretion of 109,000 m³ in the southern half of Tsoo-Yess shoreface (Figure 35, Zone N) is roughly double the 53,900 m³ gross accretion in the northern half (Zone L). This suggests a dominant cross-shore transport of sediment relative to longshore transport of sediment. The entire Tsoo-Yess Beach survey area had over 210,000 m³ of sediment exchange between zones, resulting in a net positive 25,200 m³ and an average vertical accretion of 1 cm (Table 3).

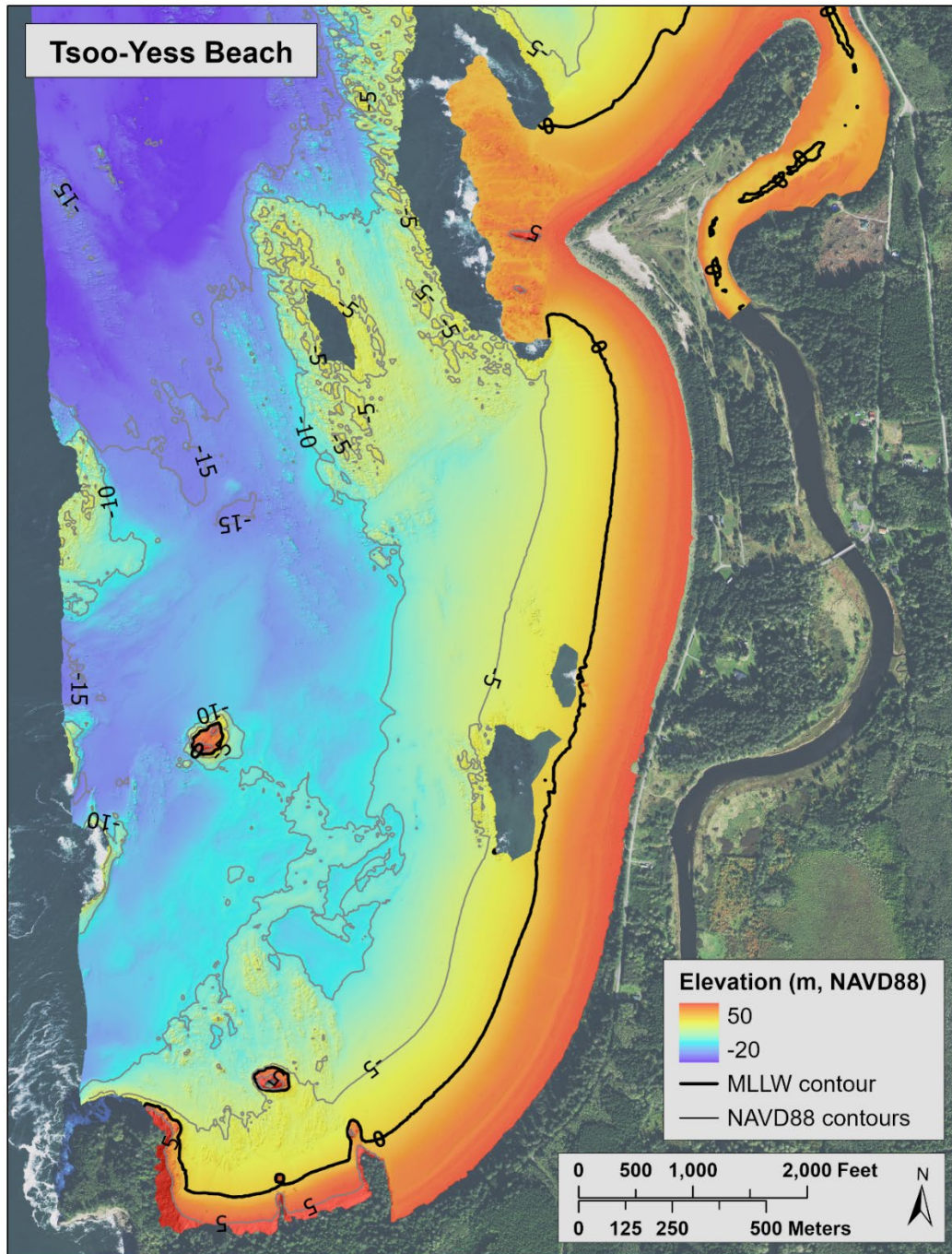


Figure 33. Tsoo-Yess Beach 2019 topo-bathymetric DEM with MLLW contour and 5-m NAVD88 contours overlaid for reference.

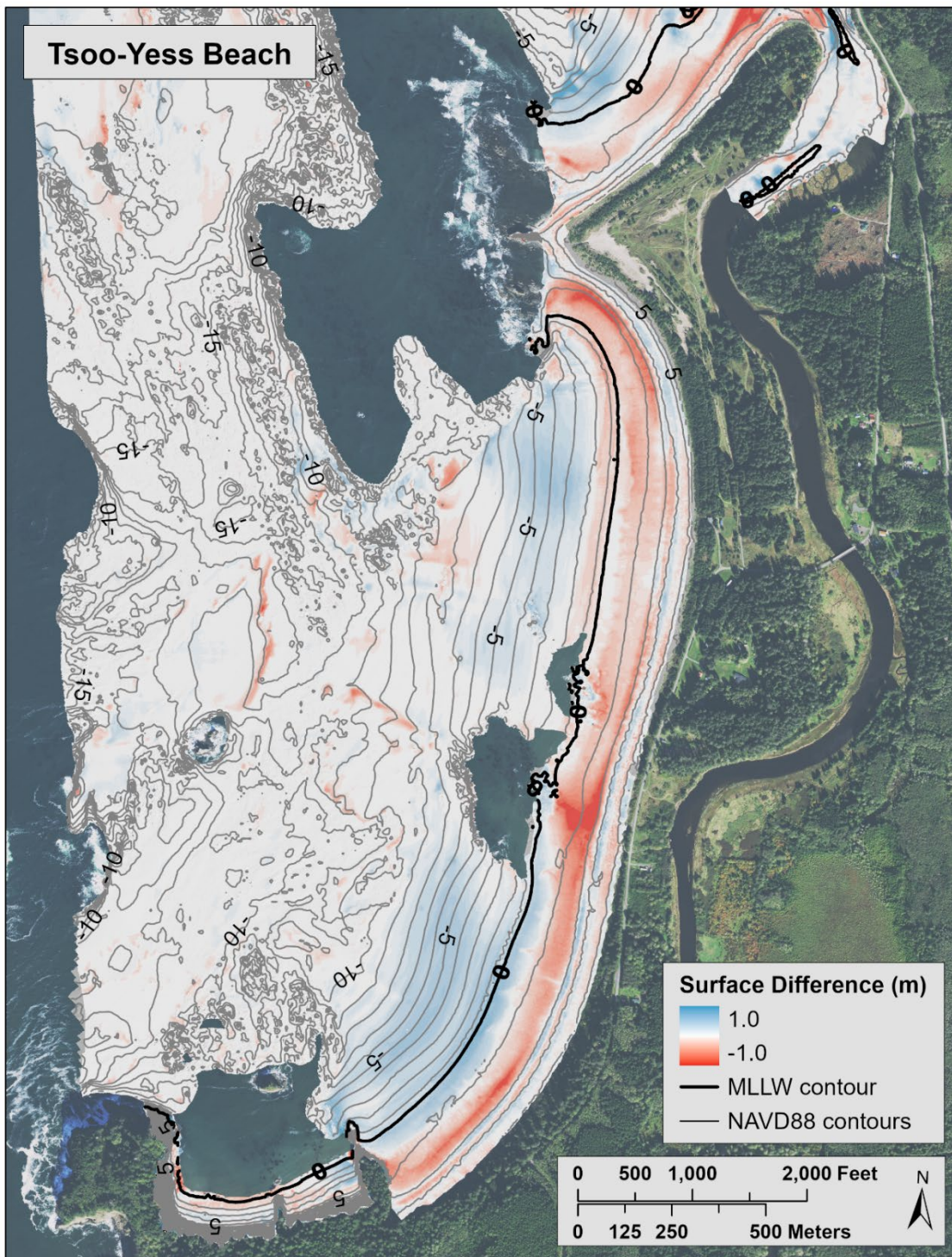


Figure 34. Tsoo-Yess Beach change surface from September 2019 to July 2021 with 2021 MLLW contour and 1-m NAVD88 contours overlaid. Areas of white indicate no change ± 10 cm.

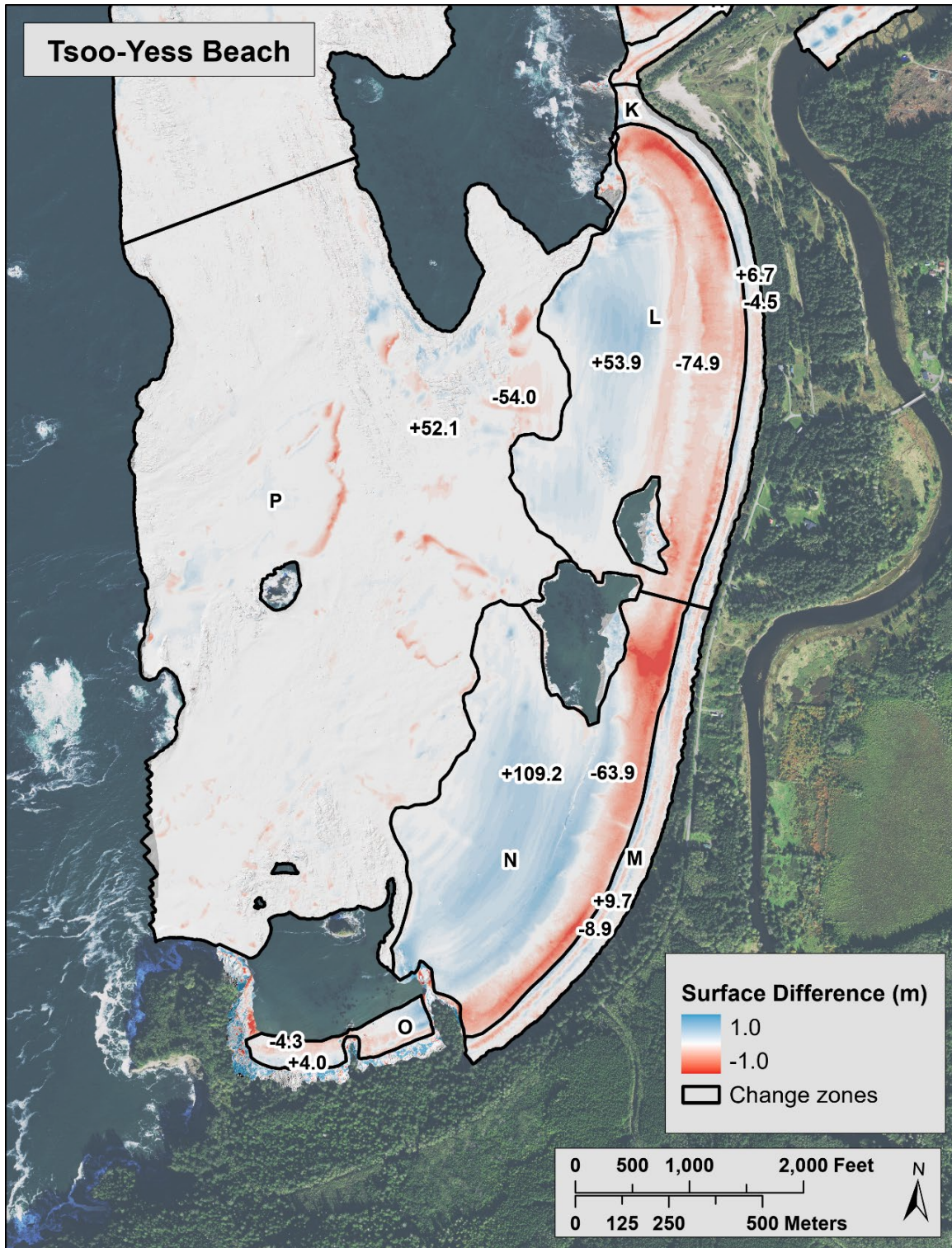


Figure 35. Tsoo-Yess Beach change surface from September 2019 to July 2021 with change zone boundaries overlaid showing gross positive and negative volume change in 1000 m³. Areas of white indicate no change ±10 cm.

Synthesis of results

The biennial topo-bathymetric surface and volume change analyses reveal both cross-shore and alongshore compartments with similar change patterns from which we can infer morphodynamic controls and behavior of the beach and nearshore.

Similar to the seasonal and annual changes discussed above for the beach compared to the dune toe, the magnitude of morphology change and variability increases across the intertidal zone and shoreface due to waves and surf zone processes. The shoreface on the energetic Washington coast is typically characterized by significant spatial and temporal variability with nearshore sandbars that can contain significantly more volume of sediment than the sand dunes backing the beaches (Ruggiero et al., 2016). As such, the topo-bathymetric changes observed between September 2019 and July 2021 provide insight to the seasonal to interannual scales of shoreface change. The consistent pattern of lower beach erosion and nearshore accretion observed in the difference surfaces primarily reflect typical seasonal fluctuations rather than a long-term trend. In particular, this pattern is expected given that the beach accretion typically peaks in September, whereas significant onshore sediment transport and sub-tidal bar migration is actively occurring during July.

These findings are consistent with Ruggiero et al. (2005) that found the seasonal cycle of relatively higher waves and water levels in the winter compared to summer results in significant seasonal transfer of sand between the beach and shoreface, with onshore sediment transport and migration of nearshore sandbars leading to beach accretion dominating change in the summer. The welding of intertidal bars to the beach face in summer contributes to beach progradation and the building of sand berms above MHW, which then contributes to dune growth through increasing wind and aeolian transport in the fall and winter (Cohn et al., 2018).

To explore the potential connection between the backshore vegetation line change identified by cluster analysis and cross-shore shoreface change, a 150m-wide swath of data from the biennial topo-bathymetric change surface is plotted for cluster sections free of rocky outcrops (Figure 17 and Figure 36). These data swaths help to elucidate how the shoreface profile change varies spatially throughout Makah Bay, and how patterns of cross-shore and longshore sediment movement may affect shoreline changes. As waves enter the bay, the offshore islands and outcrops cause wave refraction such that a relationship between shoreface and shoreline change is expected due to the variable wave-energy distribution.

Figure 36 reveals that both Hobuck and Tsoo-Yess beaches, except for Clusters 3 and 11, show beach accretion above 4 m NAVD88. Cluster 3 is backed by rip rap at the Hobuck RV Campground and Cluster 11 at the south end of Tsoo-Yess Beach is backed by a low bluff, whereas other beaches are backed by dunes. The absence of backshore and dune accretion in these two clusters is mirrored by the 10-year average 1.08 m/yr erosion trend, and lowest long-term average 0.09 m/yr accretion trend in Cluster 3, and the lowest 10-year average 0.13 m/yr accretion trend and second-lowest long-term average 0.20 m/yr accretion trend in Cluster 11 compared to all other Makah Bay cluster averages (Figure 19). The depressed backshore

accretion rates may be due to wave reflection off the rip rap and low bluff during elevated water levels, which can cause accentuated erosion and offshore sediment transport at the toe of these steep-faced features.

Above 2-m elevation, Clusters 3, 8, and 11 have the largest magnitude in beach erosion as measured by a decrease in beach elevation up to or exceeding 1 m. Across the intertidal beach between MLLW and MHHW, Cluster 2C north of the Hobuck RV Campground shows the most beach erosion, with up to approximately 1 m of beach elevation loss, and Cluster 3 at the Hobuck RV Campground shows slightly less beach erosion with elevation lowering up to approximately 0.75 m.

Most beaches show the largest changes in beach elevation gain or loss across the intertidal zone spanning MLLW to MHHW. The intertidal to sub-tidal beach profile change pattern with generally decreasing beach elevations above 1 m elevation and increasing beach elevations below 1 m elevation as shown in Clusters 1, 8, 10c, and 11 (Figure 36) are expected given seasonal trends of offshore sediment transport during the winter and onshore bar migration during the early to late summer (Ruggiero et al., 2005; Cohn et al., 2018). In other words, the observed cross-shore changes may be partially due to the seasonal cycle between the surveys conducted in September and July (2019 and 2021, respectively), in which the July condition represents a beach in its seasonal transition toward summer recovery.

The shoreface change signature in Cluster 3 is similar to that in Cluster 2b, with both experiencing minimal shoreface accretion lower on the profile to closure depth (Figure 36). This may be due to wave refraction and convergence toward Cluster 2c from both Cluster 3 and Cluster 2b. These clusters contrast with the relatively larger shoreface accretion of sediment below either 0 m or -2 m on all other profiles, except for Cluster 8, which appears to be influenced by Tsoo-Yess river-flow and includes a depression of erosion of up to -1.5 m of lowering at -8 m NAVD88.

Based on the shoreface changes shown in Figure 36, it appears that the highest wave energy is focused on Clusters 2c, 3, 10c, and 11, where the profile depth of closure is approximately -10 m NAVD88. This is the inferred depth to which sediment from the beachface is moved offshore on annual time scales, and which defines the most morphologically active shoreface profile. In contrast, Clusters 1, 2a, 2b, and 10b had shallower shoreface closure depths of approximately -6 m NAVD88. These northern clusters of each sub-bay are presumed to receive relatively lower wave energy than the southern sub-bay Clusters 2c, 3, 10c, and 11. As such, net sediment transport within the bay is expected to go from these higher energy clusters toward the lower energy Clusters 1, 2a and 10b.

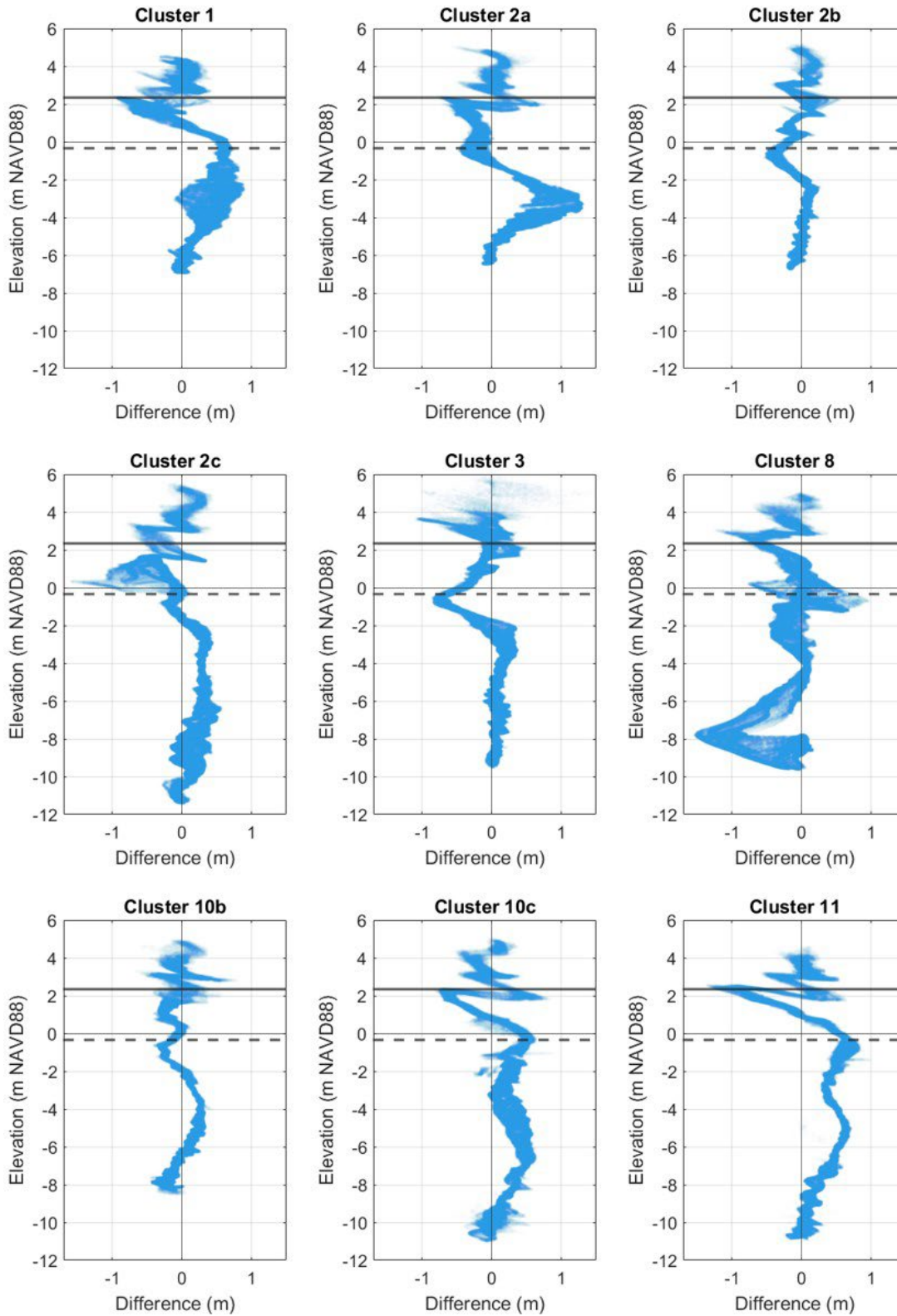


Figure 36. Cluster-based shoreface change from 150 m-wide swaths from the 2019-2021 topobathymetric difference surface; MHW (solid line) and MLLW (dashed line).

The trend of sediment transport moving from the inferred higher energy clusters to lower energy clusters is reflected in the historical shoreline and vegetation line change analysis. A metric of integrated coastline change—the average of shoreline and vegetation line change—shows a gradient of lower change rates in the south of each bay with increasing accretion in northern clusters (Figure 37 and Figure 38). There is also a local increase in accretion rates southward from Cluster 3 at the Hobuck RV Campground to Cluster 5 just north of Bahobohosh Point (Figure 37). This trend may be associated with wave refraction toward the convex bulge in shoreface contours in Cluster 2C in the north and toward Bahobohosh Point and the Tsoo-Yess River mouth in the south, leading to a divergence of waves away from Cluster 4 and creating a more depositional environment within the embayment south of Hobuck Creek (Figure 28 and Figure 29). Based on the difference surfaces, there is no evidence for a direct sediment transport pathway from the Tsoo-Yess River mouth to the beach north of Bahobohosh Point at Clusters 5 and 4. Bahobohosh Point appears to impinge upon the upper shoreface and disrupt littoral transport and deposition along the rocky point. Figure 29 and Figure 31 reveal an irregular pattern of sediment deposition and erosion across the rocky beachface with an abrupt erosional pattern across the intertidal beach on the north side of the point where the beach is the narrowest. Nevertheless, it is conceivable that fluvial sediment supply from the Tsoo-Yess River may affect sediment deposition at this embayment south of Hobuck Creek, and therefore influence Hobuck Creek migration. If there is a relationship between the Tsoo-Yess sediment supply and Hobuck Creek migration, then we would expect greater sediment discharge to have occurred since 2006 when the highest rates of beach accretion occurred.

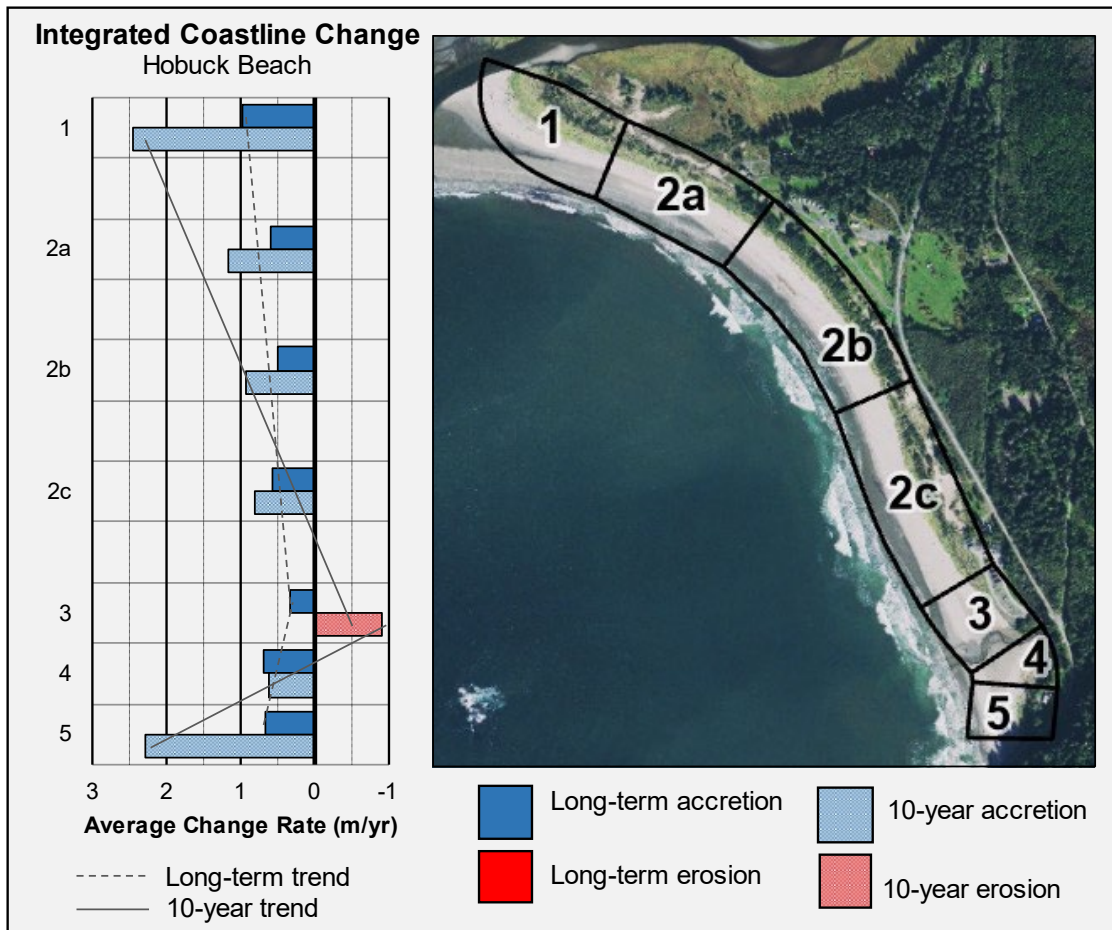


Figure 37. Integrated coastline change rates based on the average of vegetation line and shoreline change along Hobuck Beach with trendlines divided at Hobuck Creek (Cluster 3) to indicate increasing accretion rates to both the north and south with distance from Cluster 3 in both the long-term trend (1952-2019; dotted line) and recent 10-year average trend (2009-2019; solid line), which includes erosion at Cluster 3.

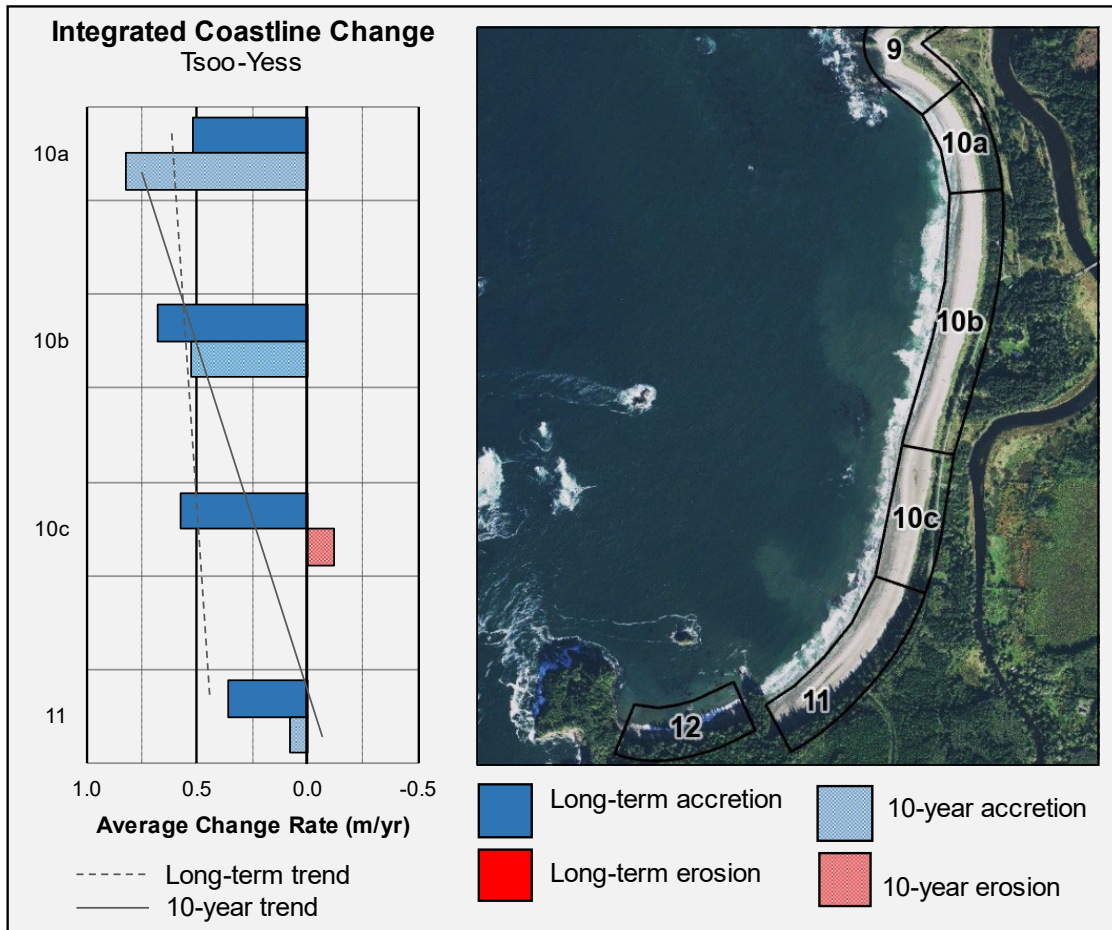


Figure 38. Integrated coastline change rates based on the average of vegetation line and shoreline change along Tsoo-Yess Beach. Trendlines plotted on the bar graph indicate a northward increase in the accretion rate in both the long-term trend (1952-2019; dotted line) and recent 10-year average trend (2009-2019; solid line).

This page is purposely left blank

Ozette Sub-region Results

The Ozette sub-region was analyzed independently from Makah Bay, as it has a different geomorphic context and presents a unique set of conditions and change assessment challenges.

Overview

Makah Bay and Ozette historical shoreline change analysis areas are both similar alongshore lengths (roughly 7 km), and run with more or less the same parameters for the cluster analysis, however, have very different results. This contrast is reflective of the complexity and variability at Ozette as compared to Makah Bay. Only seven of these clusters are within the Ozette Reservation (6 wholly, and 1 partially), however we studied a much larger area for context.

Historical long-term (1977-2019) coastline change rates along the Ozette sub-region were generally low and more broadly extensive compared to Makah Bay. Cluster averages showed the highest shoreline erosion rates occurring north of Tskawahyah (Cannonball) Island (Clusters 21 through 36), and spanning the coastline of the Ozette Reservation (Clusters 32 through the northern portion of 38). Only six of the 29 clusters accreted on average in the recent 10-year period (2009-2019; Figure 39 and Figure 40).

Historical coastline change

The overall coastline change from both shoreline and sand wedge change analyses at the Ozette sub-region shows an erosion trend. Based on the 10-m coastline change transects, the average long-term shoreline change between 1977 and 2019 along the Ozette sub-region was -0.06 m/yr and the average seaward edge of the sand wedge long-term change was -0.24 m/yr (Figure 39). The 10-year average shoreline change between 2009 and 2019 was -0.77 m/yr and the 10-year average seaward edge of the sand wedge change was -0.46 m/yr. 9.8% of long-term average shoreline change rates were erosion, 1.4% of shoreline rates were accretion, and 88.8% of shoreline rates were lower than ± 0.25 m/yr. 43.9% of long-term average change rates derived from the seaward edge of the sand wedge were erosion, 0.6% of sand wedge rates were accretion, and 55.5% of sand wedge rates were lower than ± 0.25 m/yr (Appendix D). The distribution of cluster-average coastline feature change rates, including vegetation line where available, is shown in Figure 40.

The cluster with the highest 10-year shoreline erosion rate (-2.22 m/yr) was at the mouth of the Ozette River and the southern end of a pocket beach (Cluster 27), while the cluster with the highest 10-year shoreline accretion rate (1.72 m/yr) was at the northern end of the same pocket beach (Cluster 25). Cluster-average erosion rates were generally lower in the southern portion of the sub-region, with the exception of Cluster 43, which had a 10-year sand wedge erosion rate of -1.37 (Figure 40), and the area directly north of Wedding Rocks, which had a 10-year shoreline erosion rate of -1.73 m/yr (Cluster 46). Photos from Google Street View reveal a backcountry campsite along the Pacific Northwest National Scenic Trail at the location of Cluster 46. The anomalously high change rate in Cluster 46, which includes only three transects

(covering roughly 30 m alongshore), may be due to increased human traffic that has loosened sediment on the beach, making this area more susceptible to shoreline erosion.

The Ozette Reservation contained some of the highest erosion rates in the sub-region. Based on the 10-m transects, the Ozette Reservation had an average 10-year shoreline change between 2009 and 2019 of -1.29 m/yr, which is an erosion rate 0.52 m/yr more than the Ozette sub-region average. The long-term average change rate between 1977 and 2019 was 0.01 m/yr. The long-term average sand wedge change between 1977 and 2017 was -0.46 m/yr, which is nearly double the average sand-wedge change for the entire Ozette sub-region. The long-term average vegetation line change between 1977 and 2019 was -0.06 m/yr in the Ozette Reservation.

The pattern of higher erosion rates within the Ozette Reservation is also reflected in the cluster averages, including along the Ozette Village Archeological Site (Cluster 36 and Cluster 37) with 10-year average erosion rates of -2.10 m/yr and -1.21 respectively (Figure 40). Despite Clusters 32, 33, and 34 showing accretion in the long-term average, their 10-year averages showed significant erosion (-0.55 m/yr, -1.78 m/yr, and -1.06 m/yr respectively), suggesting increased erosion since 2009. Vegetation line change within the Ozette Reservation could only be evaluated at Clusters 36 and 37, at and directly south of Tskawahya (Cannonball) Island. Both clusters showed a slight erosion trend reflective of their relatively high shoreline erosion rates.

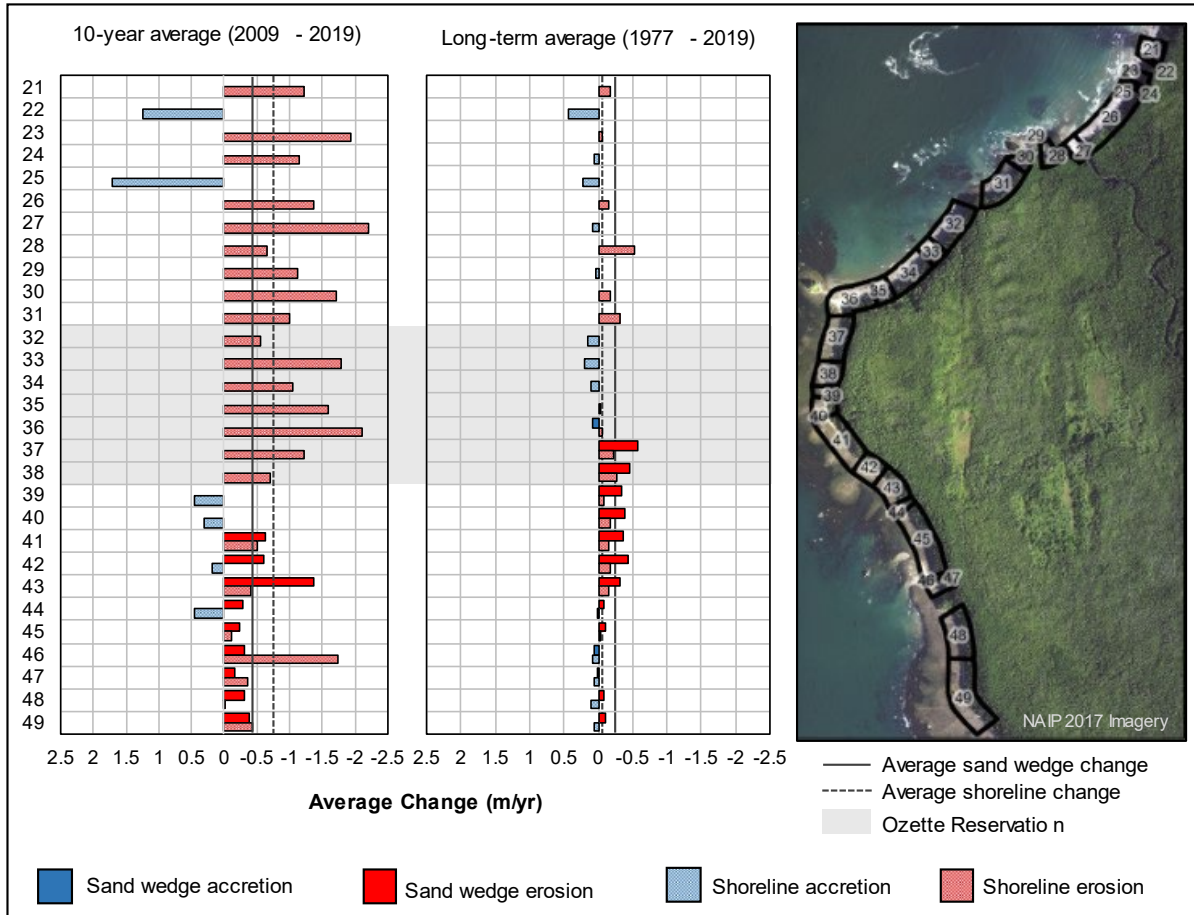


Figure 39. Ozette sub-region shoreline and seaward edge of the sand wedge average change rates by cluster (red and blue bars), with the overall averaged indicated for comparison (dotted and solid black lines). The sand wedge was only evaluated where present, primarily south of Tskawahyah (Cannonball) Island. Clusters that are fully or partially within the Ozette Reservation boundary are indicated with gray shading.

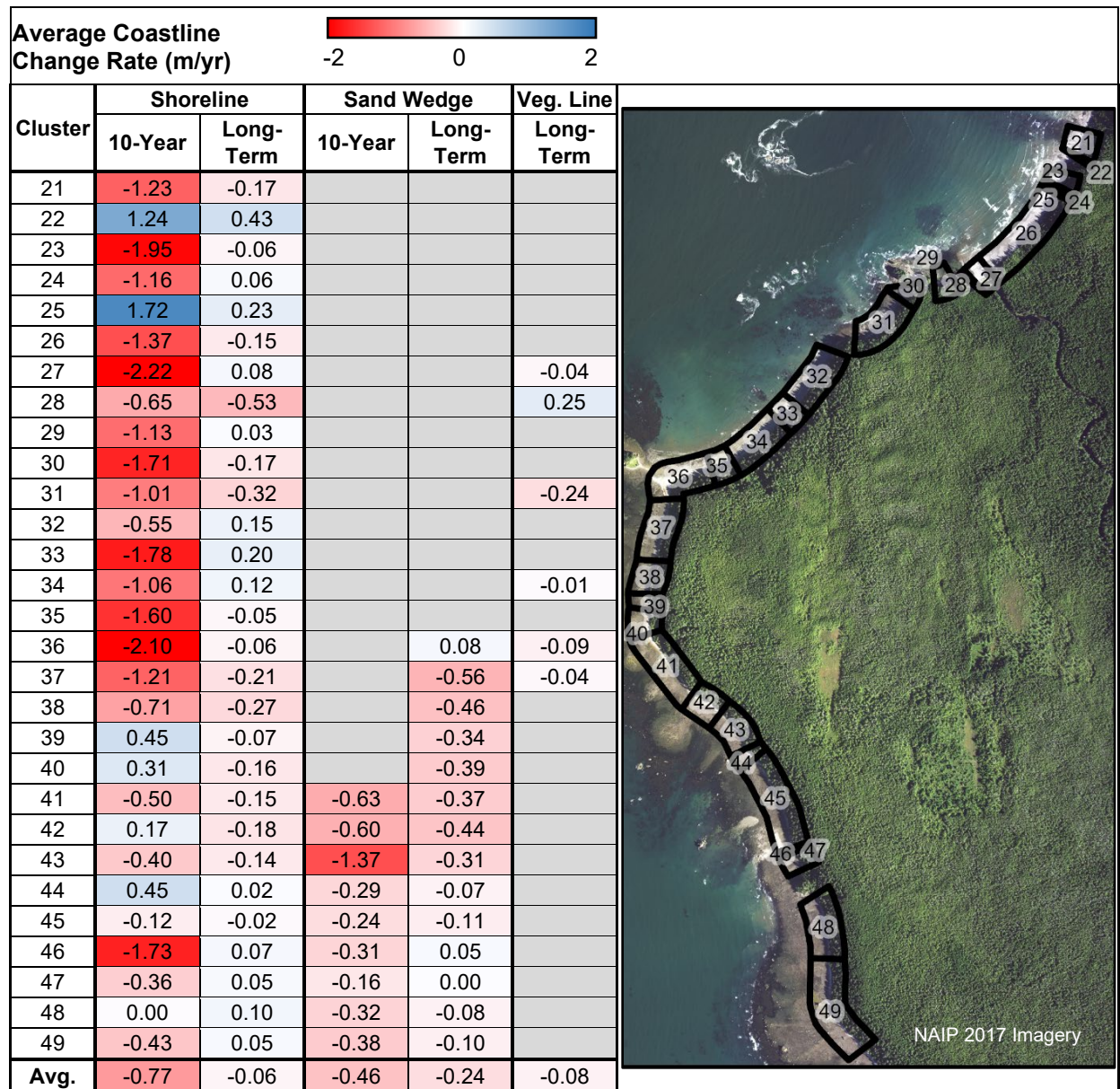


Figure 40. Ozette sub-region shoreline, sand wedge, and vegetation line average change rates by cluster, with overall averages calculated from the 10-m transects. Gray boxes indicate areas in which the change rates could not be evaluated either because the sand wedge was not present, or because the vegetation line was unresolvable in the imagery.

Figure 41 presents the cluster length, number of transects per cluster, and the difference in change rate relative to the adjacent cluster to the north. The average number of transects per cluster at the Ozette sub-region is 22 (median = 15), and average distance based on the vegetation line measurement is 225 m (median = 140 m; Figure 41). Only Cluster 39 and 40 have a difference in change rate below 0.25 m/yr, which is the estimated uncertainty from the historical coastline change analysis. Therefore, all but these two clusters are significantly different in change rate such that combining them would dilute the resolution of the results. However, it is apparent that clusters with somewhat similar characteristics can be grouped

based on their 10-year change rates. These groupings, discussed in the synthesis section, can help to characterize larger scale dynamics throughout the sub-region.

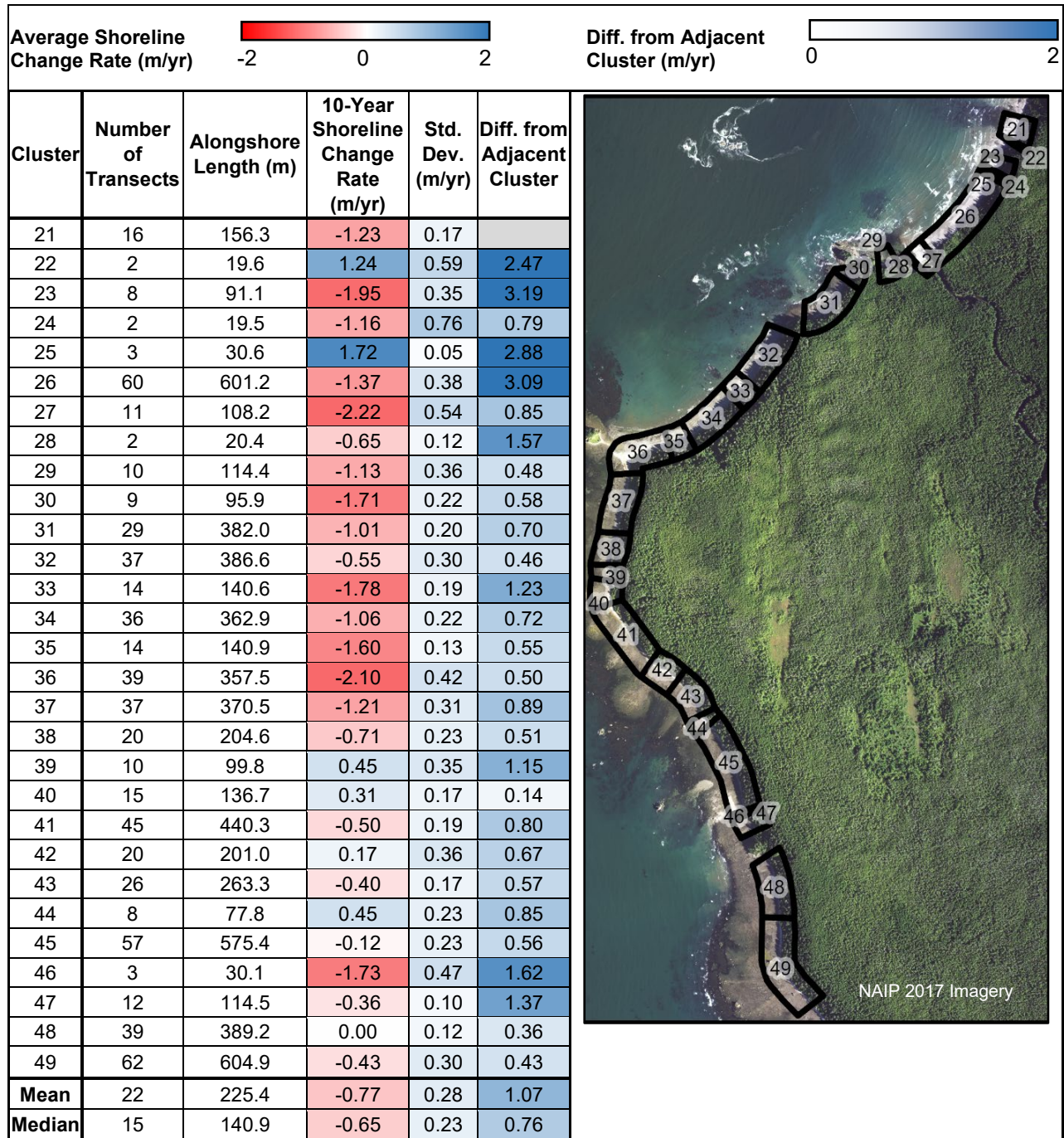


Figure 41. Ozette sub-region number of transects, alongshore lengths, 10-year shoreline change, and standard deviation of the 10-year shoreline change per cluster. The difference in 10-year average shoreline change from the adjacent cluster to the north is recorded to show significant distinctions between all clusters aside from Clusters 39 and 40. Standard deviations and mean 10-year shoreline change is derived from 10-m spaced transects.

Based on observations from the aerial imagery, Google Earth, and oblique shoreline photos, the substrate ranges from sand to large cobble with variability both alongshore and in the cross-shore, while the shore geometry is also highly variable (Figure 42 and Figure 43). Beach complexity in this area is reflected in the output from the cluster analysis, where the Ozette sub-region resulted in 29 clusters. By contrast, the analysis in Makah Bay includes roughly the same alongshore distance as the Ozette sub-region (both 4.4 miles) and similar parameters were used to run the analysis, however Makah Bay only resulted in 12 initial clusters, with additional clusters added to maintain a high spatial resolution. The increased number of clusters at the Ozette sub-region is reflective of higher alongshore complexity as compared to Makah Bay. Additionally, the clusters did not appear to reveal strong trends through space and cluster-averages changed unpredictably from one cluster to the next (Figure 39).

To help characterize the vegetation line stability in the Ozette sub-region where quantitative change rates were largely excluded, qualitative observations from oblique shoreline photos and publicly sourced photos available on Google Street View were collected. The scarp fronting the Ozette Village Archeological Site moved landward between 1990 and 2006, indicated in the oblique shoreline photos by a tree present in 1990 that had fallen onto the beach by 2000 and washed away by 2016 (Figure 42). On the ground photos from Google Maps showed tree roots overhanging on the beach, recently fallen trees, and stands of trees at the scarp edge leaning seaward, suggesting a pattern of bluff toe erosion under the tree roots causing trees to lean and ultimately fall (Figure 43). This pattern was observed throughout the sub-region in oblique shoreline photos taken in 1990, 2000, and 2016, showing a widespread vegetation line erosion trend at least since 1990.

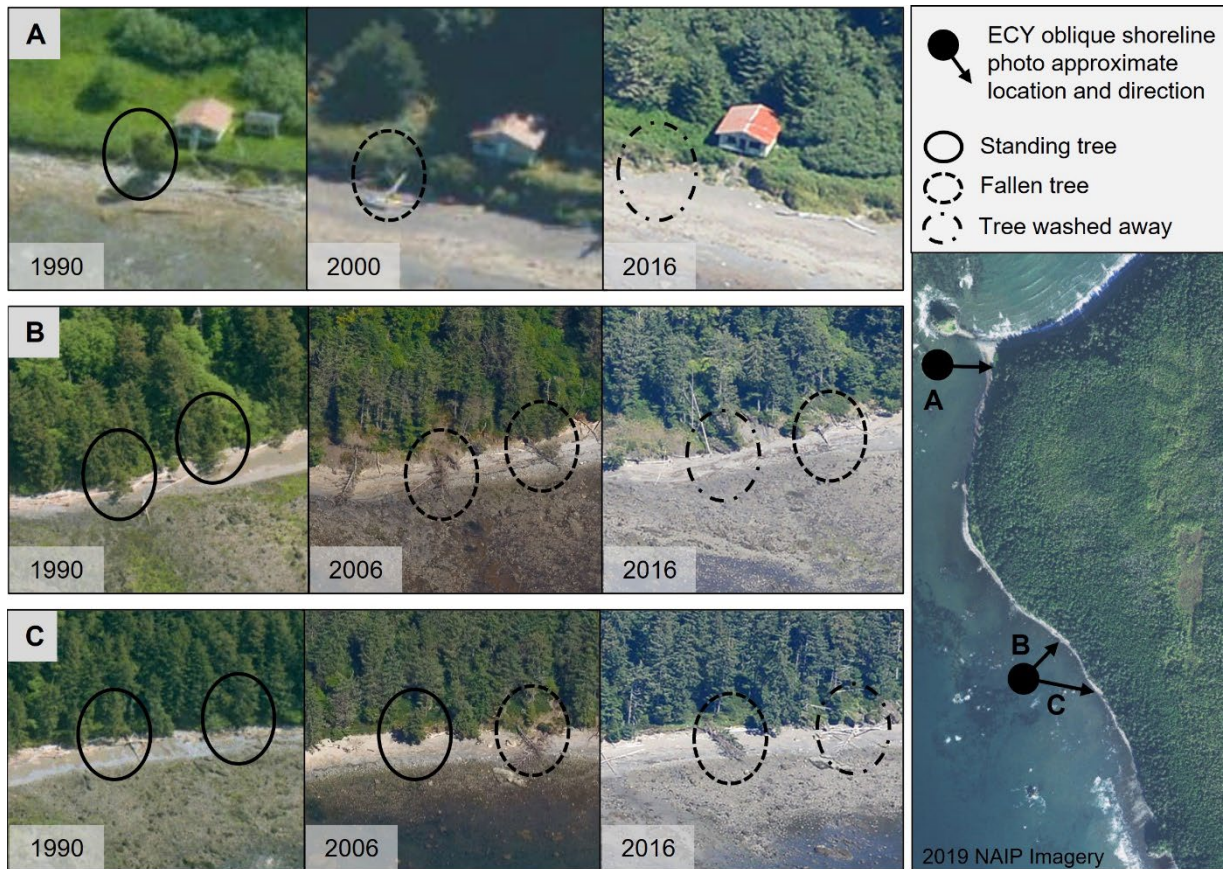


Figure 42. Photos from Washington Department of Ecology Oblique Shoreline Photo Viewer showing examples of qualitative observations characterizing vegetation line change at the Ozette Reservation and sub-region. Photos are of Cluster 37 in the Ozette Reservation (A), Cluster 43 (B), and Cluster 45 (C).



Figure 43. Google Street View photos showing erosion along the Ozette sub-region near the boundary of Cluster 43 and 44 (A) and Cluster 46 (B; Google, n.d.).

Synthesis of Results

To assess larger-scale trends within the sub-region, clusters can be grouped by similar dynamics and their geomorphic boundaries. Based on the long-term (1977-2019) average shoreline change rates, the Ozette sub-region can be separated into 5 shoreline reaches: Cluster 21 to 27 bound by rocky headlands and with low rates of change, Cluster 28 to 31 also bound by rocky headlands with higher erosion rates, Cluster 32 to 36 with lower rates of change and a northwest facing coastline, Cluster 37 to 43 with higher erosion rates, and Cluster 44 to 49 with low change rates. The groupings roughly alternate between low or no significant change and relatively higher rates of erosion; however, since 25 of the 29 clusters have long-term (1977-2019) average change rates of less than the estimated significance level (± 0.25 m/yr), these groups may not be useful for interpreting results.

Based on the 10-year (2009-2019) average shoreline rates and geomorphic boundaries, there are 3 identifiable shoreline reaches: Cluster 21 through Cluster 31 in the north, Cluster 32 through Cluster 38 in the middle, and Cluster 39 through Cluster 49 in the south. The northern reach contains a series of pocket beaches which can be characterized as having high erosion rates with relatively high local variability (Figure 42 and Figure 44). The middle reach spans the coastline of the Ozette Reservation and contains high erosion rates with relatively low local

variability (Figure 42 and Figure 44). The southern reach is a southwest facing coastline with relatively low erosion rates (Figure 42 and Figure 44).

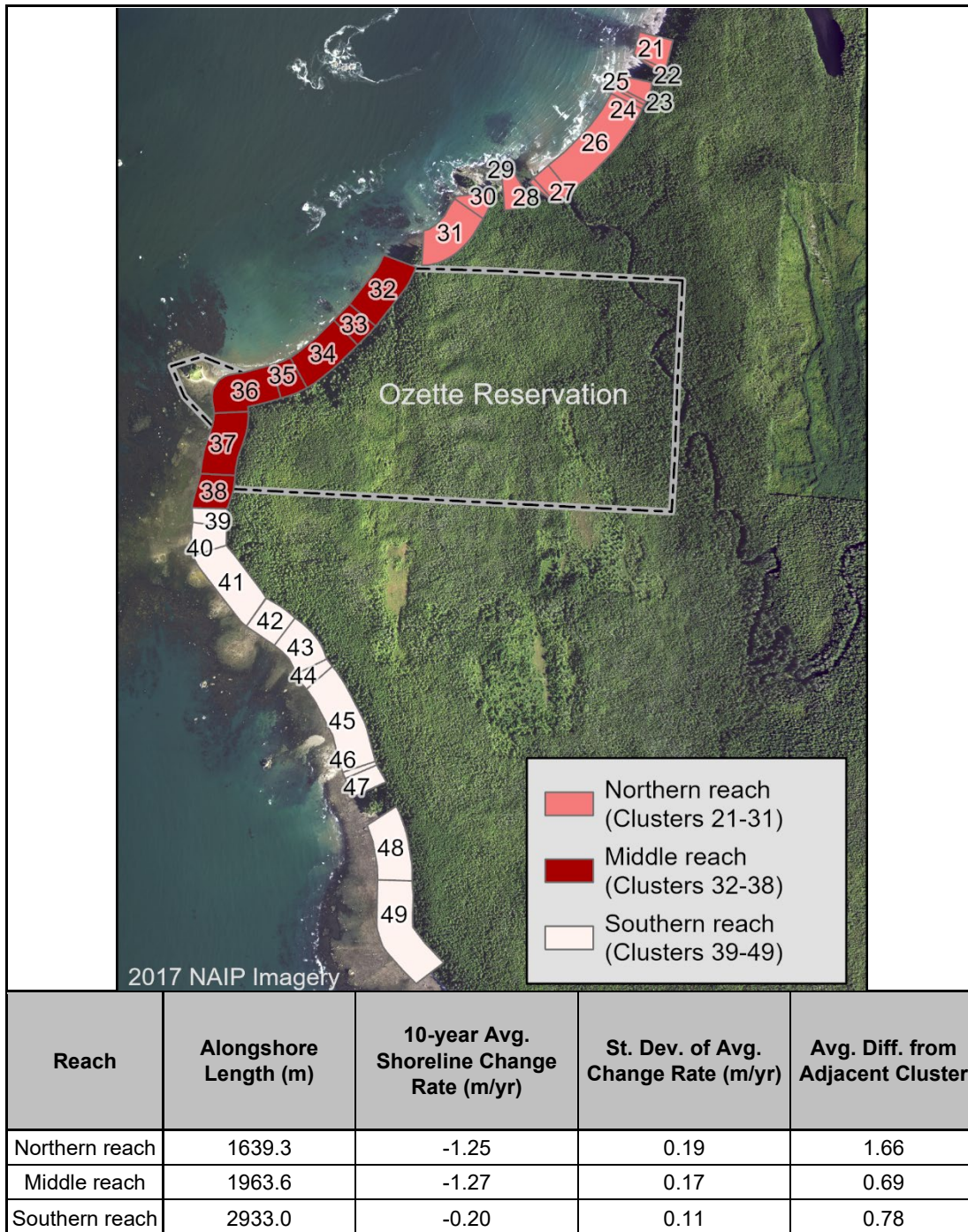


Figure 44. Ozette sub-region reaches based on 10-year cluster-average shoreline rates and geomorphic features on the coastline. The alongshore length, 10-year average shoreline change rate based on the 10-m transects, and standard deviation of 10-m transect rates are shown in the table.

This page is purposely left blank

Discussion

Makah Bay

Discussion of study results

Data analyses revealed several insights important for understanding beach and sediment dynamics in Makah Bay. The bay is a confined littoral cell with essentially two large and complex crescent-shaped pocket beaches, Hobuck Beach to the north and Tsoo-Yess Beach to the south, separated just offshore of the beach in the middle of the bay by an extensive rocky outcrop. The bay is bound by prominent headlands, Wa'atch Point to the north and Anderson Point to the south. The exchange of sediment between the beach and shoreface is confined well within the offshore boundaries of the bay.

Throughout the bay are rocky outcrops and islands (Figure 14, Appendix E) that both filter and focus incoming waves into the bay and influence the configuration of the sandy shoreface and wave refraction patterns that affect sediment transport and form the crescent-shaped beaches extending between the rocky outcrops. There appears to be a net northward transport and accumulation of sediment along both Hobuck Beach and Tsoo-Yess Beach, though southward transport may be locally dominant due to wave refraction and variable energy distribution depending on incoming wave conditions. As such, the shoreline and beach conditions may be more dominated by localized geomorphology and geologic controls as well as seasonal to interannual cross-shore sediment transport processes rather than longshore transport processes. Wave energy and sediment transport distribution patterns are complex, and a process-based model would be needed to determine sediment transport rates and directions and the resulting morphology change over a range of temporal and spatial scales.

Two rivers, the Wa'atch River at the north end of Hobuck Beach and the Tsoo-Yess River near the south end of Hobuck Beach, appear to feed sediment to Makah Bay. Hobuck Creek drains onto the beach just south of the Hobuck RV Campground and occasionally undercuts the adjacent dune fronting the RV Campground to the north as it migrates across the upper beach. Over the past decade Hobuck Creek migration has trended more northward than southward from its outlet to the beach.

Given this context, Makah Bay and the adjacent coastline conserve coastal sediments and receive additional sediment supply from the rivers such that there is a net increase of sediment within the bay over time. This condition is further enhanced by a relative fall in sea level through tectonically driven land uplift (Miller et al., 2018). These combined factors enable the coast to generally accumulate sediment and grow seaward, while morphology at the river and creek mouths remain dynamically active in response to changes in river flow, coastal hydrodynamics, and sediment transport.

The general pattern of higher accretion rates toward the northern ends of both Hobuck Beach and Tsoo-Yess Beach that imply a net northward transport of sediment raise the question as to whether there is sufficient supply of sediment at the south ends of these beaches to prevent an erosion trend from occurring in the future. While the Tsoo-Yess River likely provides sediment to the south end of Hobuck Beach, we cannot determine from the data developed in this study whether sediment supply from the Tsoo-Yess River would be sufficient to prevent erosion in the future associated with net northward sediment transport. Similarly, the data at the small pocket beach at the far south end of Tsoo-Yess Beach was limited yet suggest there is a relatively small volume of sediment in this pocket beach and potential sediment supply from offshore may also be limited.

The erosion trend at the Hobuck RV Campground is only about 200 m in length but significant in magnitude, averaging 1 m/yr of shoreline retreat from 2009 to 2019. All data and analyses in this study point to a combination of creek flow, wave refraction patterns, and growth of the beach and dunes to the south of Hobuck Creek contributing to dune erosion at the Hobuck RV Campground.

Discussion of applications

The continuation of beach monitoring throughout Makah Bay is recommended to improve the understanding of coastal processes that affect both episodic changes and long-term trends. This will enhance the knowledge of how variable conditions in waves and water levels measured by others at select locations relate to the observed coastal changes in the bay.

While undermining of the existing rip rap during the 2021-2022 winter appears to be primarily caused by creek flow at the toe of the structure, the combined effects of higher water levels and waves that allow direct interaction with the rip rap may cause additional toe scour and endpoint erosion, since hard armor tends to reflect and deflect energy to the adjacent beach and dune and reduce the potential for recovery. In addition, wave collision and overtopping may scour sediment from below the large rock causing slumping and additional structural failure. In contrast, nature-based solutions are inherently designed to absorb and dissipate energy, reduce the potential for adjacent erosion, and enhance the potential for sediment deposition and may be a viable, long-term alternative in this location.

By way of example and comparison, an erosional site at North Cove, Washington (e.g., Kaminsky et al., 2010; Talebi et al., 2017) had an average shoreline retreat rate of nearly 13 m/yr in the decade prior to installation of a dynamic revetment (quarry spall cobble berm, Figure 45), which developed a stable shoreline over the past few years following the installation. The project has been monitored and evaluated since 2018 (e.g., Weiner et al., 2019; Kaminsky et al., 2020; Drummond et al., 2021; Bayle et al., 2021; and Bayle et al., 2023). Elements of the North Cove project include cobble berms, large wood material, engineered log structures, and vegetation to form an integrated nature-based system to counter wave-induced erosion, stream flow and channel meandering, and promote sediment deposition, restore backshore habitat, and enhance public access to the beach. Hobuck Beach has much lower rates of erosion that could be dealt with in a similar manner.

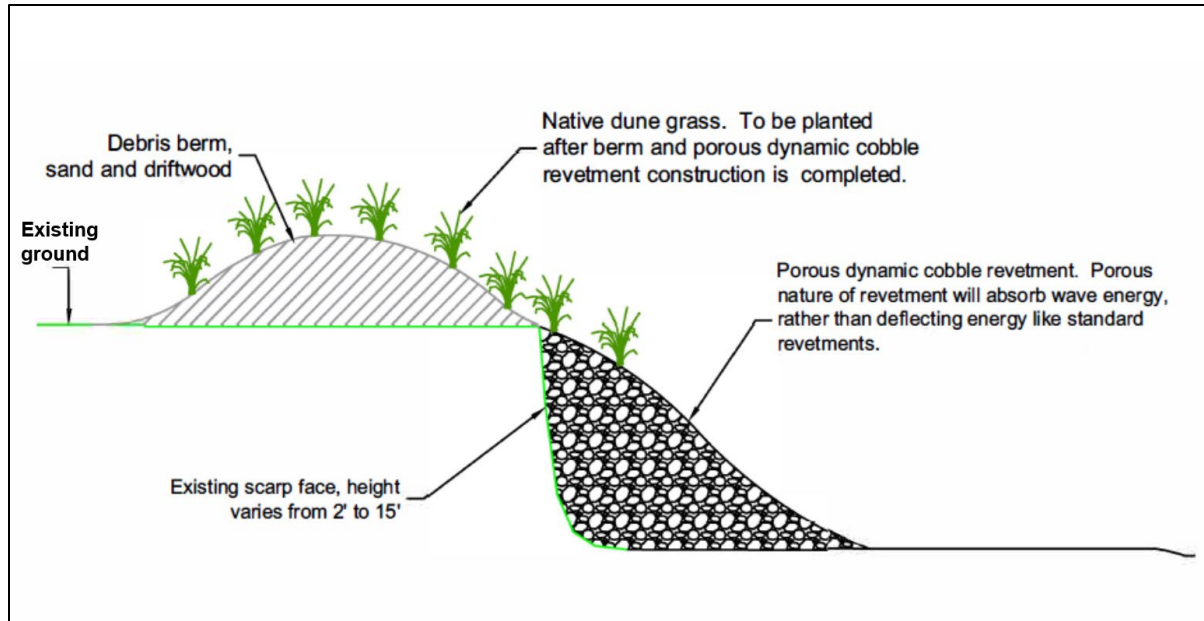


Figure 45. Conceptual dynamic cobble revetment and bank stabilization approach to counter coastal erosion at North Cove, Washington. From Pacific Conservation District, 2018.

The Pacific County Drainage District 1 has been actively managing channel meandering similar to Hobuck Creek that occurs downstream of their drainage ditch outflow to the beach at North Cove (David Cottrell, personal communication). For decades, flows from the ditch have migrated to each side, contributing to undercutting of adjacent banks and meandering across the beach in ways that accentuate wave-induced erosion due to a lowered beach profile across a wider area. Recent applications with strategic use of engineered log features, cobble, gravel, sandy sediments, and vegetation have stabilized the channel and lead to the development of protective sandbar and embayment to effectively eliminate erosion problems (Figure 46).

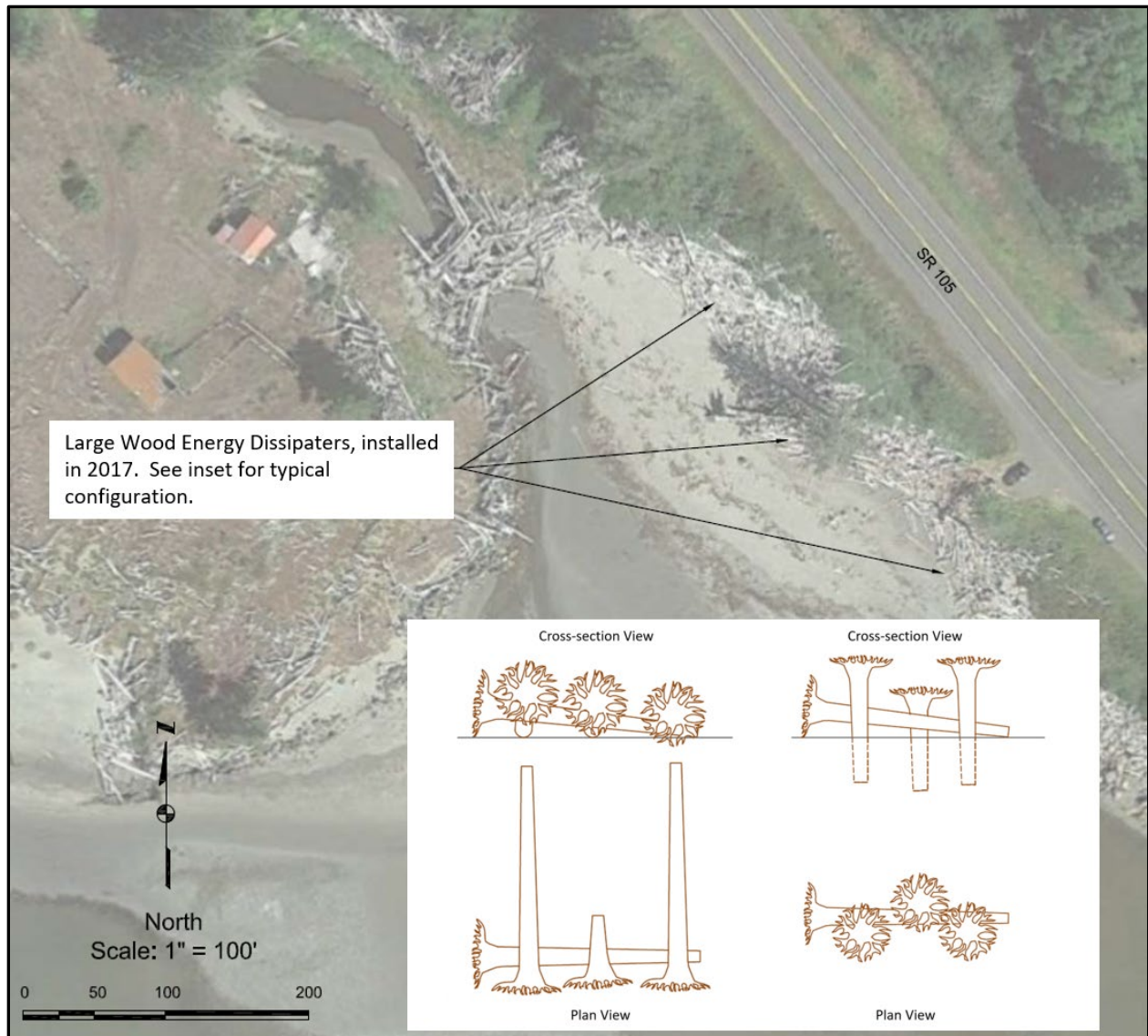


Figure 46. Example of large wood energy dissipaters installed along drainage ditch mouth to control channel meandering across the beach at North Cove, Washington. Modified from Pacific Conservation District, 2018.

Ozette Reservation

Discussion of the coastal setting

In contrast to the sand-rich Hobuck and Tsoo-Yess beaches, the Ozette Reservation beaches are limited to a thin wedge-shape deposit of sand and mixed-sediments overlying a nearly level wave-cut marine platform of Tertiary rocks composed of predominantly marine conglomerates, siltstones, and sandstones (Weisenborn and Snavely 1968). This platform is only partly veneered with modern marine sediment and provides for rich intertidal resources and tide pools which draw birds, fish, and mammals to feed (Janda, 1971; Samuels and Daugherty, 1991;

Wessen, 1982). The platform extends to maximum width of approximately 3 km and is composed of sea stacks and rocks exposed to an average width of about 500 m at low tide and submerged or partially submerged at high tide, in addition to islands, the largest of which include Ozette Island, Tskawahyah (Cannonball) Island, and the Bodeltch Islands--collectively referred to as Flattery Rocks (Weissenborn and Snaveley 1968; Wessen, 1982). The offshore islands form a sheltering arc to protect the coast from large ocean swells and waves to maintain relatively calm nearshore conditions in all but the heaviest storms (Samuels and Daugherty, 1991).

To the northeast of Tskawahyah (Cannonball) Island, the thinly veneered modern beach sand displays prominent sand waves that are nearly parallel to the shoreline (Janda, 1971). Several small crescent beaches are relatively protected and have accumulated sand and gravel deposits from 30 to 60 cm thick (Samuels and Daugherty, 1991). The Ozette River discharges sediments at the mouth, but there is little deltaic development due to the low sediment load as a result of the low-lying Lake Ozette functioning as a settling basin (Samuels and Daugherty, 1991). Holocene and Pleistocene landslide debris with seaward movement join the beach sediment along the backshore zone along an approximately 1 km reach between the base of the Tskawahyah (Cannonball) Island tombolo and a buttress of sandstone with minor siltstone conglomerate (Snaveley et al., 1989).

To the south of Tskawahyah (Cannonball) Island, wind and wave conditions combine to produce a northward longshore sediment drift (Samuels and Daugherty, 1991; Reidel et al., 2021). This movement has stripped most intertidal sediments from the south and west sides of the Ozette Reservation leaving most of the platform an exposed rocky pavement (Samuels and Daugherty, 1991). The beach is narrow and gravelly, perched against an upland bench approximately 30-m wide and between 1 and 5 m in elevation above high tide that parallels the beach (Samuels and Daugherty, 1991). In February 1970, a severe coastal storm with energetic waves undercut this bench causing slumps and triggering an 11-year archaeological excavation project from 1970 to 1981 (Samuels and Daugherty, 1991). Figure 47 illustrates this coastal topography at the Ozette Reservation, with the light green color showing the upland bench, a narrow strip of relatively flat land between the beach and the toe of the steeply sloped hillside.

Figure 48 and Figure 49 further illustrate the complex variability of the Ozette Reservation beaches over a distance of approximately 3 km. Except for the sandy tombolo beach landward of Tskawahyah (Cannonball) Island, the beaches are narrow and composed of sand, gravel and cobble, and the fronting rocky intertidal platform is a broad rough terrace of bedrock, boulders, cobble and mixed sediments with patches of sand.

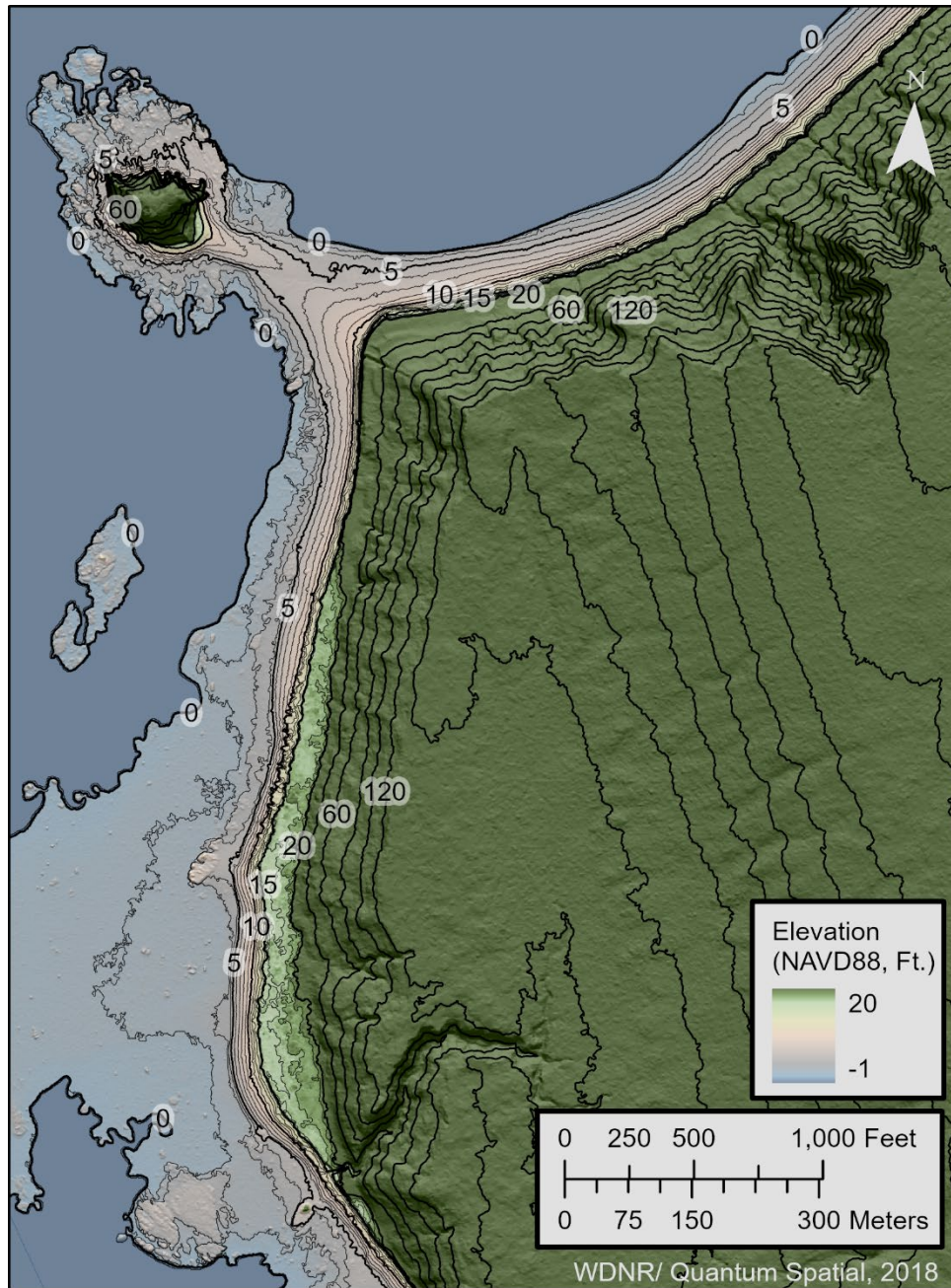


Figure 47. WDNR 2018 digital elevation model of the Ozette Reservation coastline with blue and tan colors showing the intertidal zone and beach, and shades of green showing the upland topography.

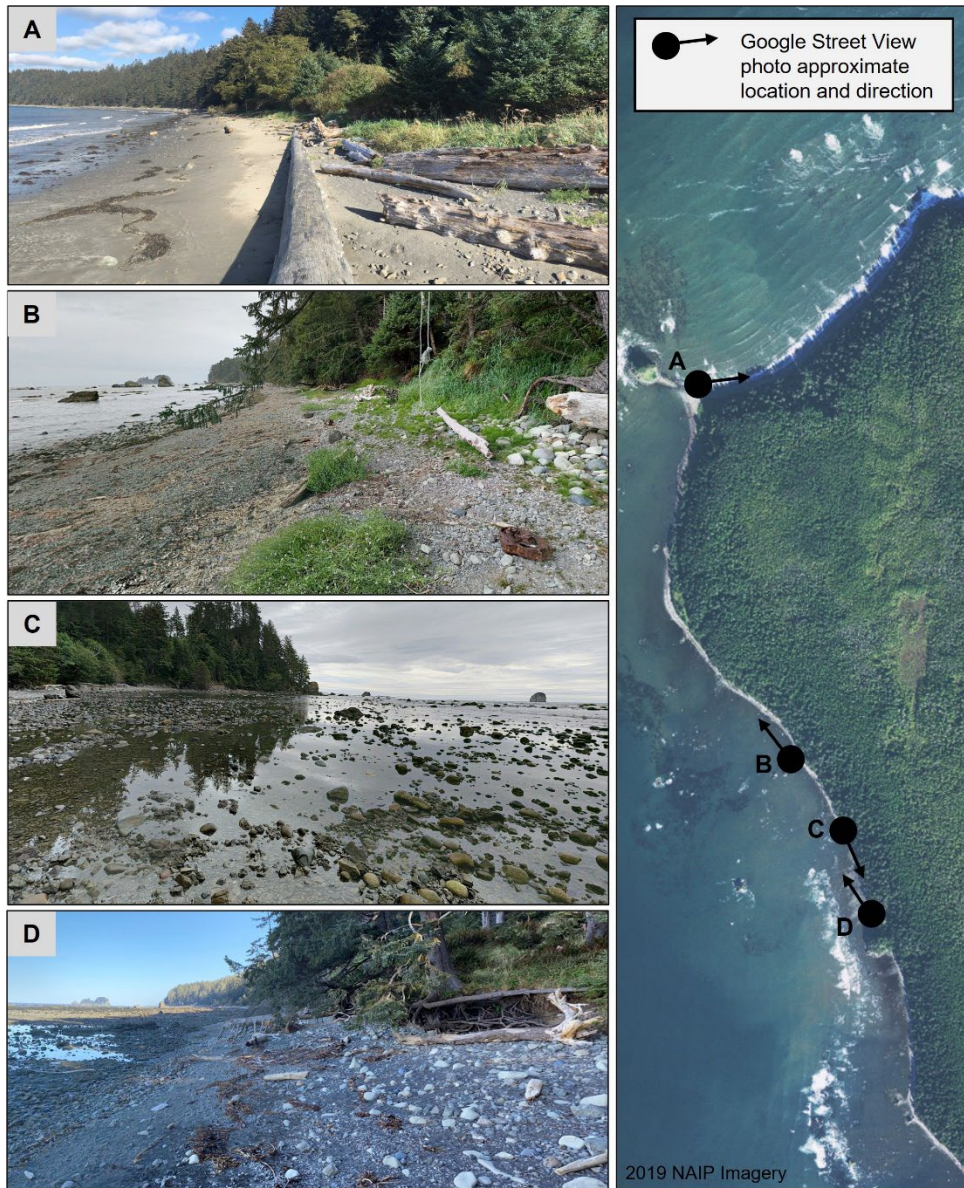


Figure 48. Google Street View photos looking alongshore along the Ozette Reservation and sub-region used to characterize beach conditions (Google, n.d.).

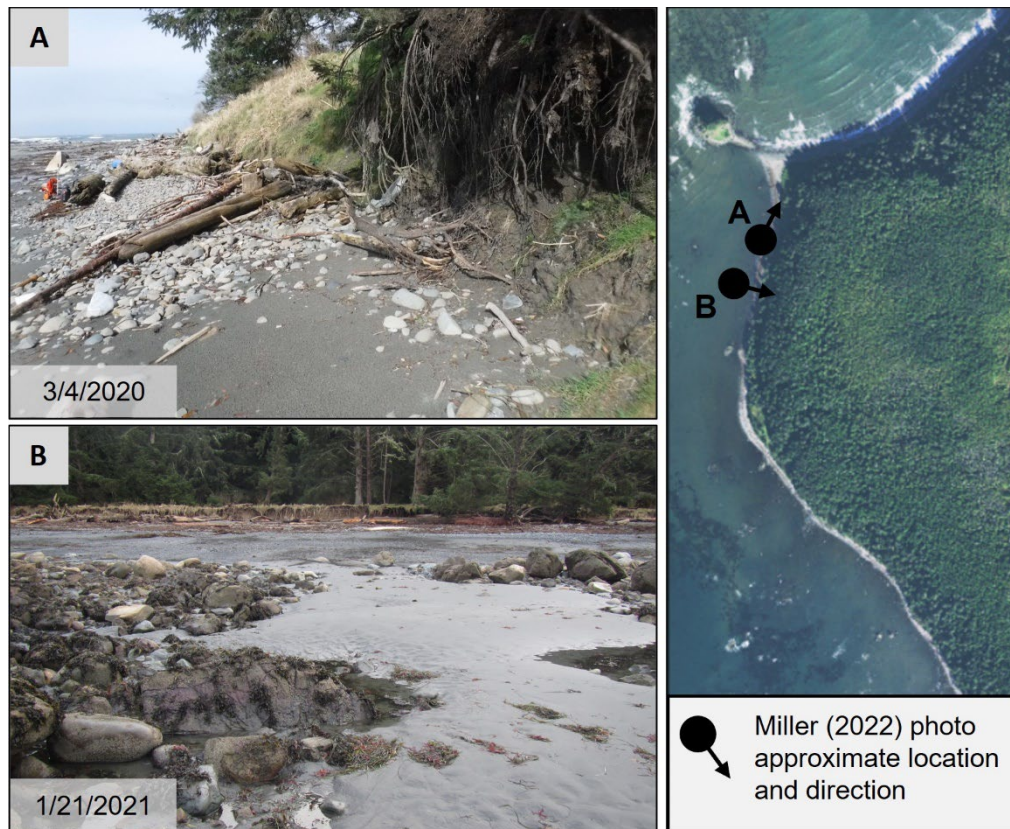


Figure 49. Photos taken on the ground at the Ozette Reservation showing beach conditions (Miller and Akmajian, 2022).

Discussion of applications

Ongoing beach monitoring as well as additional study at the Ozette Reservation will be essential for making a more rigorous assessment of both the evolving erosion conditions as well as the scoping of potential solutions to reduce or halt continuation of erosion. Existing data compiled and analyzed herein as well as by Miller and Akmajian (2022) document a sustained erosion trend manifesting as a retreat of the upland bench and bluff described above.

There are a few factors that suggest the erosion trend at the Ozette Reservation will continue without either human intervention or management.

1. The sustained, near-vertical erosion scarp shown by the beach profiles in Miller and Akmajian (2022) indicate erosion and scarp maintenance through wave reflection.
2. The significant bench and bluff volume loss and absence of beach volume gain indicate sediment supplied by the bench and bluff is transported away from the area being monitored (Miller and Akmajian, 2022).
3. The rocky wave-cut platform as described and reported by others is interpreted to be a potential sink or bypass for beach sediments transported offshore during times of wave-

induced bench and bluff erosion. The net offshore sediment transport may be primarily driven by wave reflection off the near-vertical erosion scarp, causing toe scour and seaward momentum for transporting sediment away from the beach. Sediment can then ephemerally settle among low points and disperse across the wave-cut platform. Such sediment dispersion is expected due to the shallowness of the platform and high turbulence during high waves and water levels to prevent additional sediment accumulation.

4. Relative sea level appears to be stable or rising slightly at the Ozette Reservation (Miller et al., 2018).

Although more assessment and study is required, it is worth considering alternatives that may be feasible to reduce or halt erosion along the Ozette Reservation shoreline. Among the considerations are the remoteness and challenges for equipment and material transport and limitations for access to the beach by both land and sea. Most likely helicopter support would be required to transport equipment and supplies to the site. Another challenge is the apparent limited sediment supply available to develop a more resilient backshore condition to be resilient to erosion. Yet another matter is the need to develop an environmentally acceptable solution that is compatible with the landscape and protects the ecological, cultural, and economic function the Ozette Reservation.

There are several approaches to shoreline restoration that may allow for reducing erosion and loss of cultural artifacts and building up shoreline while maintaining recreational and cultural use of the site. One approach that allows for these functions is the creation of an intertidal boulder and cobble ridge commensurate with indigenous construction of clam gardens, in which several in the Southern Gulf Islands extend over 1 km in length (Grier et al., 2017). The general concept of the clam garden is shown in Figure 50. These intertidal rock ridges or berms effectively trap sediment carried by waves and gradually create a terraced beach deposit on the landward side. This approach serves at least three functions significant to the setting at the Ozette Reservation. It creates space for sediment accumulation; it captures sediment from both marine and terrestrial sides; and it creates a perched beach as foundation for complementary constructions such as a cobble dynamic revetment to further dissipate wave energy and reduce wave reflection from the upland bench scarp, which is essential to maintain an accreted beach profile at this location. Furthermore, to the extent desired, this approach could be iterative, additive, adaptive, managerial, and relational (Grier, 2022).

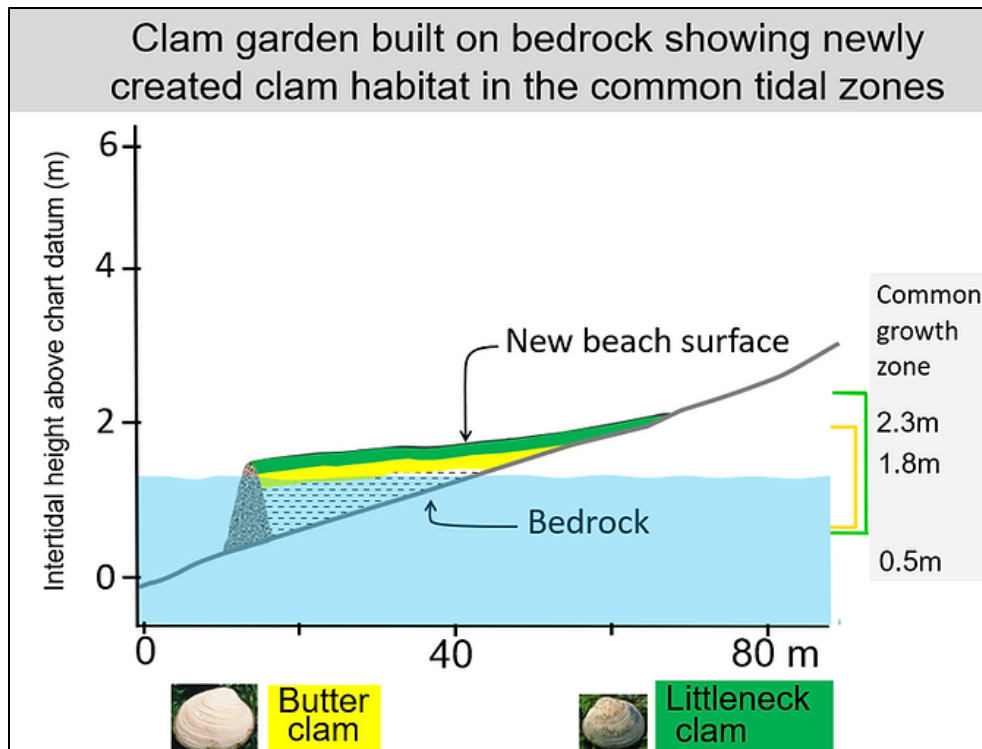


Figure 50. Depiction of the creation of a beach terrace through construction of a rock ridge along the low tide line on a bedrock or rocky slope. Diagram created by Dana Lepofsky, Clam Garden Network.

Conclusion

A coastline assessment of the Makah Reservation and the Ozette Reservation was accomplished. The study included a historical coastline change spanning 1952-2019 at Makah Bay and 1977-2019 at the Ozette Reservation, and a comprehensive topo-bathymetric mapping and change assessment of Makah Bay and coastline from two high-resolution surveys conducted in 2019 and 2021. The surveys provided the first detailed mapping of Makah Bay, and provided volumetric change measurements associated with sediment transport, erosion and deposition. The results provide insight on how sediment is shared, conserved, and added to this coastal littoral cell bounded by rocky headlands and outcrops on each end of the bay.

The results of the both the historical shoreline and recent morphology change assessment for Makah Bay reveal that the amount of sediment in the coastal cell has increased over time. Between 2019 and 2021 Makah Bay had a net volume increase of 93,000 m³, which equates to an average of 1 cm of accretion over the entire survey area (7.3 km²).

Throughout the bay there is a long-term trend of accretion as averaged from 1952 to 2019. When data is averaged over the most recent 10 years from 2009 to 2019, there is a higher rate of accretion for most areas, except for at the Hobuck RV Campground which developed an erosion trend. Adjacent to the Hobuck RV Campground, on average, the accretion rates increase northward to the Wa'atch River mouth and southward to the Tsoo-Yess River mouth. Average accretion rates also generally increase from south to north along Tsoo-Yess Beach.

Erosion at the Hobuck RV Campground is likely associated with a combination of factors that include undercutting of the dune and existing rip rap by creek flow, wave patterns that tend to transport beach sediment away from the Hobuck RV Campground, and growth of the beach and dunes to the south of Hobuck Creek that promotes northward migration of Hobuck Creek and more routine lowering of the beach profile in front of the Hobuck RV Campground compared to previous decades.

Together with the evidence of a falling sea level, this overall condition of accretion throughout the bay indicates that a nature-based engineering design is a feasible solution for the localized erosion identified at the Hobuck RV Campground. This feasibility assessment is based on evidence of sufficient sediment within the coastal system available for deposition and recovery at the Hobuck RV Campground without negative impact on adjacent areas. The method for creating such a depositional environment leading to a more stable coastline resilient to further retreat is a matter of engineering design for enhanced energy dissipation, sediment deposition and accumulation consistent with the trends along the adjacent shoreline reaches, including stream channel migration (Figure 51).

The available aerial imagery and lidar data for the Ozette Reservation did not allow for detailed annual-scale assessment of coastal change. Rather, the relatively coarse resolution of the data only enabled the identification of a modest erosion trend since 1977, and a possible increase in the rate or prevalence of erosion over the past decade. More study will be required to

understand the mechanisms, magnitude, and extent of the erosion and to develop a resilience strategy to protect the upland from further loss.

For the Ozette Reservation, the coastal setting is much different, and access is much more restricted, such that it will require more thorough consideration for project planning, design, and construction. The Ozette Reservation beaches have significantly less sediment and do not retain sediment supplied by upland erosion, likely due to a high level of turbulence across the rocky platform seaward of the beach as well as wave reflection off the erosion scarp of the upland bench during times of high-water levels with energetic waves (Figure 51).

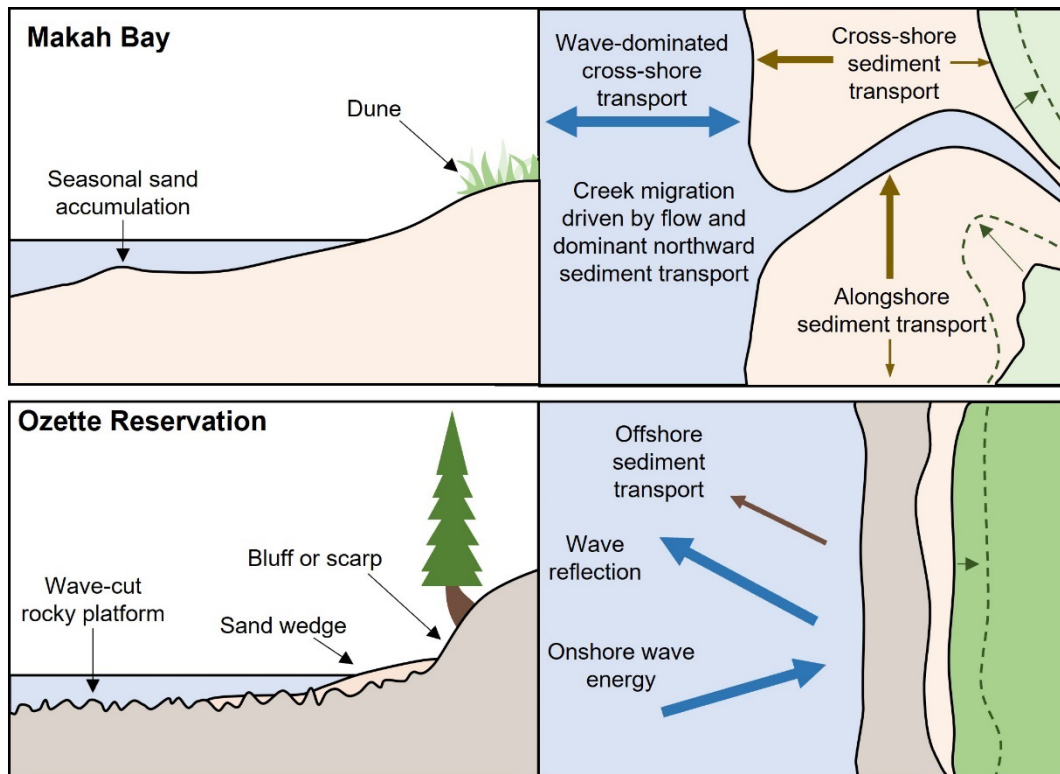


Figure 51. Conceptual drawing of the setting and beach dynamics at Makah Bay and the Ozette Reservation.

Taken together, the analyses conducted herein reveal several insights that are valuable for the Makah Tribe's future coastal planning. First, with the exception of the Hobuck RV Campground, Makah Bay appears to be fairly resilient to coastal erosion processes. The continuation of beach monitoring throughout Makah Bay is recommended to improve the understanding of coastal processes that affect both episodic changes and long-term trends. Studies to further elucidate the sediment transport and supply from the Wa'atch and Tsoo-Yess Rivers as well as studies to understand the erosional patterns that occur at the south ends of Hobuck and Tsoo-Yess Beach will help understand long-term resilience to coastal erosion. Ongoing beach monitoring as well as additional study at the Ozette Reservation will be essential for making a more rigorous assessment of both the evolving erosion conditions as well as the scoping of potential solutions

to reduce or halt continuation of erosion. Erosion at both the Hobuck RV Campground and the Ozette Reservation may be mitigated by nature-based approaches.

This page is purposely left blank

References

- Bayle, P.M., Blenkinsopp, C.E., Martins, K., Kaminsky, G.M., Weiner, H.M., and Cottrell, D. 2023. Swash-by-swash morphology change on a dynamic cobble berm revetment: High resolution cross-shore measurements, *Coastal Engineering*, 184. <https://doi.org/10.1016/j.coastaleng.2023.104341>
- Bayle, P.M., Kaminsky, G.M., Blenkinsopp, C.E., Weiner, H.M., and Cottrell, D. 2021. Behaviour and performance of a dynamic cobble berm revetment during a spring tidal cycle in North Cove, Washington State, USA, *Coastal Engineering*, 167. <https://doi.org/10.1016/j.coastaleng.2021.103898>
- Calder, Brian R. 2003. Automatic Statistical Processing of Multibeam Echosounder Data. *International Hydrographic Review*, 980. <https://scholars.unh.edu/ccom/980>
- Cohn, N., Ruggiero, P., de Vries, S., and Kaminsky, G.M. 2018. New insights on coastal foredune growth: The relative contributions of marine and aeolian processes, *Geophysical Research Letters*, 45, 4965–4973. <https://doi.org/10.1029/2018GL077836>
- Daugherty, R.D. and Fryxell, R. 1967. Archaeological, geochronological, and ecological investigations of the Ozette Village Site Complex on the Northwest Coast of Washington. Manuscript on file. Department of Anthropology, Washington State University, Pullman, WA.
- Drummond, H., Kaminsky, G., Cottrell, D., and Weiner, H. 2021. Integrating nature-based engineering designs and adaptive management strategies for a resilient coast in North Cove, WA. Poster, ASBPA 2021 National Coastal Conference. Available at: https://wacoastalnetwork.com/wp-content/uploads/2021/10/Drummond_ASBPA2021_Poster_NorthCove.pdf
- Friedman, E. 1976. An archaeological survey of Makah territory: A study in resource utilization. Ph.D. dissertation, Department of Anthropology, Washington State University, Pullman, WA.
- Gillins, D.T., Kerr, D., and Weaver, B. 2019. Evaluation of the Online Positioning User Service for Processing Static GPS Surveys: OPUS-Projects, OPUS-S, OPUS-Net, and OPUS-RS, *ASCE Journal of Surveying Engineering*, 145(3): 05019002.
- Google n.d. Google Street View photos of Wedding Rocks, Ozette sub-region from Google Maps. Retrieved November 18 2022, from <https://www.google.com/maps/@48.1509021,-124.7206325,3a,75y,325.54h,80.94t/data=!3m8!1e1!3m6!1sAF1QipOAuWZUINMWlerMoUbXnFqUHSc4iJVXvRgBoEmY!2e10!3e11!6shhttps:%2F%2Flh5.googleusercontent.com%2Fp%2FAF1QipOAuWZUINMWlerMoUbXnFqUHSc4iJVXvRgBoEmY%3Dw203-h100-k-no-pi-0-ya166.85043-ro-0-fo100!7i11264!8i5632>.

- Grier, C. 2022. Indigenous shoreline management in the Salish Sea: The view from archaeology. In: Conway-Cranos, L., Toft, J.D., Trimbach, D.J., Faulkner, H., Krienitz, J., Williams, D., Des Roches, S., editors; 2022. The 2021 Puget Sound Nearshore Restoration Summit Proceedings; 2021 March 10 – 25; Virtual Summit. Olympia, WA: Washington Department of Fish and Wildlife, pp. 180–182. <https://wdfw.wa.gov/publications/02339>; <https://youtu.be/ESf48q7v6Rs?t=1551>
- Grier, C., Angelbeck, B., and McLay, E. 2017. Terraforming and monumentality as long-term social practice in the Salish Sea region of the Northwest Coast of North America, *Hunter Gatherer Research*, 3 (1), pp. 107–132. <https://doi.org/10.3828/hgr.2017.7>
- Janda, R.J. 1971. An evaluation of enhancement of light intensity differences on color aerial photographs and thermal infrared imagery for the Ozette Island - Cape Alava area of the Olympic coast of western Washington. <https://ntrs.nasa.gov/citations/19710023733>
- Kaminsky, G.M., Daniels, R.C., McCandless, D., and Ruggiero, P. 1999. Mapping erosion hazard areas in Pacific County, Washington, *Journal of Coastal Research*, Special Issue #28, pp. 158-170. <http://www.jstor.org/stable/25736193>
- Kaminsky, G., Cottrell, D., and Glore, G. 2020. Nature-based dynamic revetment construction at North Cove, Washington, USA. *Coastal Engineering Proceedings*, (36v), management.38. <https://doi.org/10.9753/icce.v36v.management.38>
- Kaminsky, G.M., Ruggiero, P., Buijsman, M., McCandless, D., and Gelfenbaum, G. 2010. Historical evolution of the Columbia River littoral cell, *Marine Geology*, 273, pp. 96-126. <https://doi.org/10.1016/j.margeo.2010.02.006>
- Miller, I., and Akmajian, A. 2022. Shoreline survey data collected at Hobuck, Tsoo-Yess, and Ozette, on Makah Tribal Lands, 2018–2022, Dryad, Dataset. <https://doi.org/10.5061/dryad.n02v6wx1b>
- Miller, I.M., Morgan, H., Mauger, G., Newton, T., Weldon, R., Schmidt, D., Welch, M., and Grossman, E. 2018. Projected Sea Level Rise for Washington State – A 2018 Assessment. A collaboration of Washington Sea Grant, University of Washington Climate Impacts Group, University of Oregon, University of Washington, and US Geological Survey. Prepared for the Washington Coastal Resilience Project. Updated 07/2019.
- Pacific Conservation District 2018. North Cove, Dynamic Cobble Revetment and Hybrid Slope Reinforcement, Conceptual Drawings. <https://wacoastalnetwork.com/wp-content/uploads/2019/09/North-Cove-Detail-Drawings-DRAFT-for-DC-review.pdf>
- Riedel, J., Sarrantonio, S., and Dorsch, S. 2021. Geomorphology of coastal Olympic National Park. Natural Resource Report NPS/NCCN/NRR—2021/2260. National Park Service, Fort Collins, Colorado. <https://doi.org/10.36967/nrr-2286564>.

- Ruggiero, P., Kaminsky, G.M., and Gelfenbaum, G. 2003. Linking proxy-based and datum-based shorelines on a high-energy coastline: implications for shoreline change analyses, *Journal of Coastal Research*, SI 38, pp. 57–82. <https://www.jstor.org/stable/25736600>
- Ruggiero, P., Kaminsky, G.M., Gelfenbaum, G., and Cohn, N. 2016. Morphodynamics of prograding beaches—A synthesis of seasonal- to century-scale observations of the Columbia River littoral cell. *Marine Geology*, 376, pp. 51–68. <https://doi.org/10.1016/j.margeo.2016.03.012>
- Ruggiero, P., Kaminsky, G.M., Gelfenbaum, G., and Voigt, B. 2005. Seasonal to interannual morphodynamic variability along a high-energy dissipative littoral cell, *Journal of Coastal Research*, (21) 3, pp. 553–578. <https://doi.org/10.2112/03-0029.1>
- Samuels, S.R. and Daugherty, R.D. 1991. Introduction to the Ozette archaeological project. *Ozette Archaeological Project Research Reports, 1*, In: Samuels, S.R., editor 1991. *Ozette Archaeological Project Research Reports, Volume I, House Structure and Floor Midden. Reports of Investigations 63*. Department of Anthropology, Washington State University, Pullman, and National Park Service, Pacific Northwest Regional Office, Seattle. pp. 1–27.
- Snavely, JR, P.D., Niem, A.R., and MacLeod N.S. 1989. Geology of the coastal area between Cape Flattery and Cape Alava, Northwest Washington, Open-File Report 89-141. <https://doi.org/10.3133/ofr89141>
- Snedecor, G.W., and Cochran, W.G. 1989. *Statistical Methods, Eighth Edition*. Iowa state University Press, Ames, Iowa, 503 p.
- Stevens, A.W., Elias, E., Pearson, S., Kaminsky, G.M., Ruggiero, P.R., Weiner, H.M., and Gelfenbaum, G.R., 2020. Observations of Coastal Change and Numerical Modeling of Sediment-Transport Pathways at the Mouth of the Columbia River and its Adjacent Littoral Cell, U.S. Geological Survey Open-File Report 2020-1045, 82 p. <https://doi.org/10.3133/ofr20201045>
- Talebi, B., Kaminsky, G.M., Ruggiero, P., Levkowitz, M., McGrath, J., Serafin, K., and McCandless, D. 2017. Assessment of Coastal Erosion and Future Projections for North Cove, Pacific County, Washington Department of Ecology Publication 17-06-010, 35 p. <https://fortress.wa.gov/ecy/publications/SummaryPages/1706010.html>
- Weissenborn, A.E., and Snavely, JR, P.D. 1968. Summary Report on the Geology and Mineral Resources of the Flattery Rocks, Quillayute Needles, and Copalis National Wildlife Refuges Washington, Geological Survey Bulletin 1260-F. <https://doi.org/10.3133/b1260F>
- Wessen, G.C. 1982. Shell Middens as Cultural Deposits: A Case Study from Ozette. Ph.D. dissertation, Washington State University.
- Weiner, H.M., Kaminsky, G.M., Hacking, A., and McCandless, D., 2019. North Cove Dynamic Revetment Monitoring: Winter 2018-2019. Shorelands and Environmental Assistance

Program, Washington State Department of Ecology, Olympia, WA. Publication #19-06-008.
<https://fortress.wa.gov/ecy/publications/summarypages/1906008.html>

Wright, L.D., and Short, A.D. 1984. Morphodynamic variability of surf zones and beaches: a synthesis, *Marine Geology*, 56(1-4), pp. 93–118. [https://doi.org/10.1016/0025-3227\(84\)90008-2](https://doi.org/10.1016/0025-3227(84)90008-2)

Appendix A. Assessment of Measurement Uncertainties

Base station monument

For purposes of this project, an epoxy monument was installed on Bahobohosh Point on September 4, 2019. The monument was sited directly on the uplifted sandstone outcrop, northwest of the road pullout, about 15-20 ft away from a large spruce tree and fiberglass telephone pole with guy wires.

Each day of the survey, the base station logged its static position at 1 Hz. The raw data were submitted to NOAA's Online Positioning User Service (OPUS; available at: <https://geodesy.noaa.gov/OPUS/>), which provides high-accuracy National Spatial Reference System coordinates.

The final position of the monument was derived from an average of the coordinates output from OPUS for 11 days of static occupations ranging between 6 and 13 hours. Table A-1 lists the geographic coordinates used for data processing in this project. Table A-2 gives the coordinates converted to Washington State Plane North and elevation relative to NAVD88, which is the coordinate system of the final data and deliverables.

Table A-1. Local geographic coordinates for epoxy monument, Bahobohosh, in NAD83 (2011) with ellipsoid height relative to GRS80, meters.

Latitude (DMS)	Longitude (DMS)	Ellipsoid Height (m)
48 19 41.11912	-124 39 36.10066	-12.182

Table A-2. Grid coordinates for epoxy monument, Bahobohosh, in Washington State Plane North, NAD83 (2011), meters, with elevation relative to NAVD88 (GEOID12B), meters.

Easting (m)	Northing (m)	Elevation (m)
216378.308	154714.306	9.058

Positional uncertainty

Positional measurements may be confounded by both systematic and random errors. A reference monument is used in surveying to ascertain measurement accuracy. All data were post-processed relative to a final position of the reference monument on Bahobohosh Point.

The vertical positional uncertainty of the data was assessed through analysis of measurements from the GNSS base station on the Bahobohosh survey monument. The larger the number of measurements, the greater the reduction of random error associated with the measurement (the mean of all measurements). The GNSS base station position at Bahobohosh Point collected measurements over 11 occupations in 2019 each spanning between 6.0 and 12.9 hours (average of 10.9 hours, 115.3 hours total) and 10 occupations in 2021 each spanning between 3.0 and 13.1 hours (average of 10.1 hours, 90.5 hours total). The overall root mean square error

(RMSE) from each individual occupation ranged between 1.2 cm and 1.7 cm (average = 1.5 cm), which is considered a high-quality solution (<https://www.ngs.noaa.gov/OPUS/>; Gillins et al., 2019).

Using this robust data set, the mean elevation of the Bahobohosh monument measured in 2019 was 9.058 m NAVD88 compared to the mean elevation measured in 2021 of 9.078 m NAVD88. Therefore, the Bahobohosh monument was measured to be 1.9 cm higher in July 2021 compared to September 2019. The elevation differences are shown in Figure A-1.

Miller et al. (2018) identifies uplift rates for Makah Bay of ~2.5 mm/yr. The mean elevation gain measured in this work implies an uplift rate about four times higher than reported by Miller et al. (2018) (i.e., ~1.04 cm/yr; 1.83 yrs x 1.04 cm/yr = 1.9 cm). The associated error in the difference of the measurements from the two years was estimated using the standard variance of a difference equation⁴ for propagation of error.

The resulting calculated error (propagated standard deviation for the difference) is 3 mm, and the 95% confidence interval is ±5 mm. Since the measured mean uplift is 10.4 mm/yr, the estimate for the mean uplift during this period ranges from ~5 mm/yr to ~15 mm/yr.

The difference in the mean between the monument measurements for the two years represents a bias between those periods that was removed to determine any measured differences related to erosion and accretion processes. Those reported differences are also subject to the calculated errors or uncertainty of random errors which are propagated for other calculations.

⁴Propagation of error according to the general variance equations for error propagation of differences in statistical methods references, e.g., Snedecor and Cochran (1989):

$$\text{Variance of the difference} = \sigma_{\text{diff}}^2 = \sigma_{2021}^2 + \sigma_{2019}^2 - 2 * \text{COV}_{(2019, 2021)}$$

where $\text{COV}_{(2019, 2021)}$ = covariance of 2019 and 2021 data = correlation coefficient (R) multiplied by the standard deviation of 2021 and the standard deviation of 2019 data sets. So:

$$\sigma_{\text{diff}}^2 = \sigma_{2021}^2 + \sigma_{2019}^2 - 2 * R_{(2019, 2021)} * \sigma_{2021} * \sigma_{2019}$$

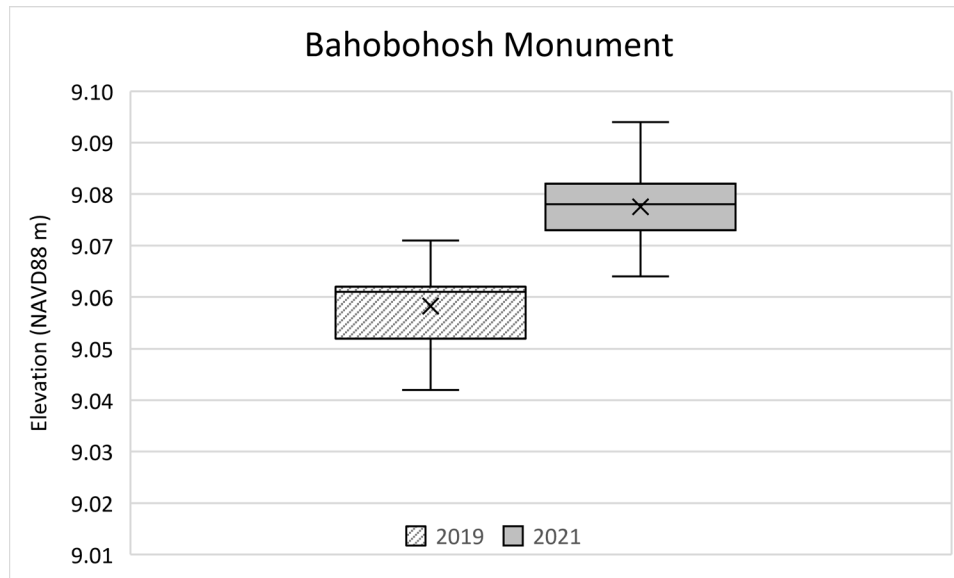


Figure 52. Boxplot showing distribution of elevation measurements at the Bahobohosh survey monument from the 2019 survey (left) and 2021 survey (right). The mean elevation from each survey is marked by an "x" with the median shown as a line across each box.

Topographic measurement uncertainty

The uncertainty in topographic elevation measurements derived from interpolated DEMs can be calculated by differencing DEM surfaces created from separate topographic surveys at locations that remain unchanged between the surveys. In this study there are two areas assumed to have no elevation change between the 2019 and 2021 surveys: a section of upland road surface along Bahobohosh Point; and the upland dune grass area landward of the outcrop separating Hobuck Beach from Tsoo-Yess Beach. These areas represent both relatively smooth beach and irregular upland dune topography contained within Zones A, B, D, F, H, K, M and O (Figure 16). For each area a DEM was created from topography measurements from each survey. Each DEM had an interpolation limit of 21 m. Table A-3 provides the results of the difference between DEM surfaces and topographic point elevations. Weighted by area, the average standard deviation is 0.0508 m.

Table A-3. Summary of topography data used to assess the vertical precision of the topographic DEMs.

Quantity	Road	Dune
DEM Area m ²	638	912
2019 Number of points to create DEM	56	109
2021 Number of points to create DEM	26	229
Maximum absolute difference between DEMs (m)	0.078	0.39
Mean Difference (m)	0.011	0.001
Standard deviation (m)	0.02	0.073

Bathymetric measurement uncertainty

The dual-head dual-mount multibeam sonar system of the R/V George Davidson enables calculation of the relative vertical precision of each bathymetric survey by utilizing the overlap of soundings between the sonars on each survey line. This is similar to the method presented in Stevens et al. (2020) for calculating vertical precision of single-beam bathymetry data collected with multiple survey vessels. For a dual-head multibeam system, the overlap of soundings between the port and starboard sonar heads during each survey line can substitute for replicate lines between survey vessels. A subset of survey lines was chosen to only include data isolated to port and starboard overlap and excluded interference data from adjacent lines. Table A-4 shows the number of lines, area, and percentage of overlap used in the analysis.

Table A-4. Summary of survey lines and survey area used to assess the vertical precision of the bathymetric survey.

	Lines Analyzed	Total Lines	% Lines Analyzed	Area Analyzed	Total Area (m ²)	% Area Analyzed
2019	168	1011	17	325,113	6,044,774	5
2021	148	1184	13	226,275	5,402,680	4

Data from each sonar, each day were gridded utilizing the same CUBE algorithm as the DEMs, at the same resolution (50 cm). The corresponding elevation surfaces were subtracted to find the vertical offset between data collected from each sonar. The standard deviation of the means is 7 mm (1.4 cm at the 95% confidence interval).

Total measurement uncertainty

Total uncertainty for each survey area can be calculated based on the equipment and measurement techniques. Using this approach, the estimated total uncertainty for interpolated topographic DEMs (Zones A, B, D, F, H, K, M and O shown in Figure 16) can be calculated by propagating the positional and topographic uncertainties resulting in a combined uncertainty of 10.2 cm at the 95% confidence interval (Table A-5 and Table A-6). This is consistent with ± 10 cm that appears as a white band in the surface difference figures (e.g., Figure 15, Figure 16, and Figure 17), which indicates no detectable change.

The estimated total uncertainty in bathymetry measurements of offshore areas (Zones J and P shown in Figure 16) can be calculated by propagating the positional and bathymetric uncertainties resulting in a combined uncertainty of 2.1 cm at the 95% interval.

Propagation of error for areas combining both topography and bathymetry measurements (Zones C, E, G, I, L, and N shown in Figure 16) can be calculated by propagating the positional, topographic, and bathymetric uncertainties resulting in a combined uncertainty of 10.4 cm at the 95% interval.

The propagated error for all zones using the above results is relevant to volume change in areas with a common signal of change (i.e., either erosion or accretion.)

Table A-5. Gross accretion and erosion sub-areas, volume changes, and propagated errors derived from September 2019 and July 2021 topo-bathymetric surveys for zones shown in Figure 16 and Figure 20.

Location	Zone	Gross Accretion Area (m ²)	Gross Accretion Volume (1000 m ³)	95th % Confidence Interval for Accretion Volume (1000 m ³)	Estimated Percent Uncertainty %	Gross Erosion Area (m ²)	Gross Erosion Volume (1000 m ³)	95th % Confidence Interval for Erosion Volume (1000 m ³)	Estimated Percent Uncertainty %
Wa'atch River	A	106,901	14.9	3.8	25.5	141,763	-21.4	5.0	23.6
Hobuck North Upper	B	80,781	11.3	2.9	25.5	36,049	-4.5	1.3	28.5
Hobuck North Tidal	C	302,541	102.1	10.9	10.6	199,934	-51.1	7.2	14.1
Hobuck Central Upper	D	48,354	7.2	1.7	23.9	48,990	-11.1	1.7	15.7
Hobuck Central Tidal	E	264,318	54.6	9.5	17.4	226,731	-74	8.1	11.0
Tsoo-Yess River Upper*	F	71,330	16.2	2.5	15.7	68,926	-13.6	2.5	18.0
Tsoo-Yess River Tidal	G	80,224	20.5	2.9	14.1	12,182	-1.2	0.4	36.5
Hobuck South Upper	H	18,175	2.2	0.6	29.4	29,536	-6.6	1.1	15.9
Hobuck South Tidal	I	129,643	33.7	4.7	13.8	143,916	-53.1	5.2	9.7
Hobuck Offshore*	J	1,235,383	149.1	8.8	5.9	1,051,019	-106.8	7.5	7.0
Hobuck North	A-C	490,224	128.3	17.6	13.7	377,746	-77.1	13.6	17.6
Hobuck South	D-I	612,044	127	22.0	17.3	530,279	-148.5	19.0	12.8
Hobuck Beach	A-I	1,102,268	262.5	39.6	15.1	908,025	-236.7	32.6	13.8
Hobuck Bay	A-J	2,337,650	411.6	84.0	20.4	1,959,044	-343.4	70.4	20.5
Tsoo-Yess North Upper	K	39,083	6.7	1.4	20.8	29,908	-4.5	1.1	23.7
Tsoo-Yess North Tidal*	L	236,483	53.9	8.5	15.8	257,607	-74.9	9.3	12.4

Table A-6. Gross accretion and erosion sub-areas, volume changes, and propagated errors derived from September 2019 and July 2021 topo-bathymetric surveys for zones shown in Figure 16 and Figure 21 (continued).

Location	Zone	Gross Accretion Area (m ²)	Gross Accretion Volume (1000 m ³)	95th % Confidence Interval for Accretion Volume (1000 m ³)	Estimated Percent Uncertainty %	Gross Erosion Area (m ²)	Gross Erosion Volume (1000 m ³)	95th % Confidence Interval for Erosion Volume (1000 m ³)	Estimated Percent Uncertainty %
Tsoo-Yess South Upper	M	50,980	9.7	1.8	18.7	49,030	-8.9	1.7	19.6
Tsoo-Yess South Tidal	N	349,393	109.2	12.5	11.5	150,811	-63.9	5.4	8.5
Secret Beach	O	17,132	4.0	0.6	15.3	22,596	-4.3	0.8	18.7
Tsoo-Yess Offshore*	P	920,426	52.1	6.6	12.7	835,312	-54	6.0	11.1
Tsoo-Yess North	K-L	275,566	60.6	9.9	16.3	287,515	-79.4	10.3	13.0
Tsoo-Yess South	M-O	417,505	122.9	15.0		222,436	-77	8.0	10.4
Tsoo-Yess Beach	K-O	693,071	172.8	24.9	14.4	509,951	-147.6	18.3	12.4
Tsoo-Yess Bay	K-P	1,613,497	235.6	58.0	24.6	1,345,263	-210.4	48.3	23.0
Makah Beach	A-I, K-O	1,795,338	446.1	64.5	14.5	1,417,976	-393.1	50.9	13.0
Makah Bay	A-P	3,951,147	647.2	141.9	21.9	3,304,307	-553.8	118.7	21.4

This page is purposely left blank

Appendix B. Historical Vegetation Line Change Tables, Makah Bay

Table 4. Historical vegetation line change rates in Makah Bay based on the 10-m average transects in Cluster 1.

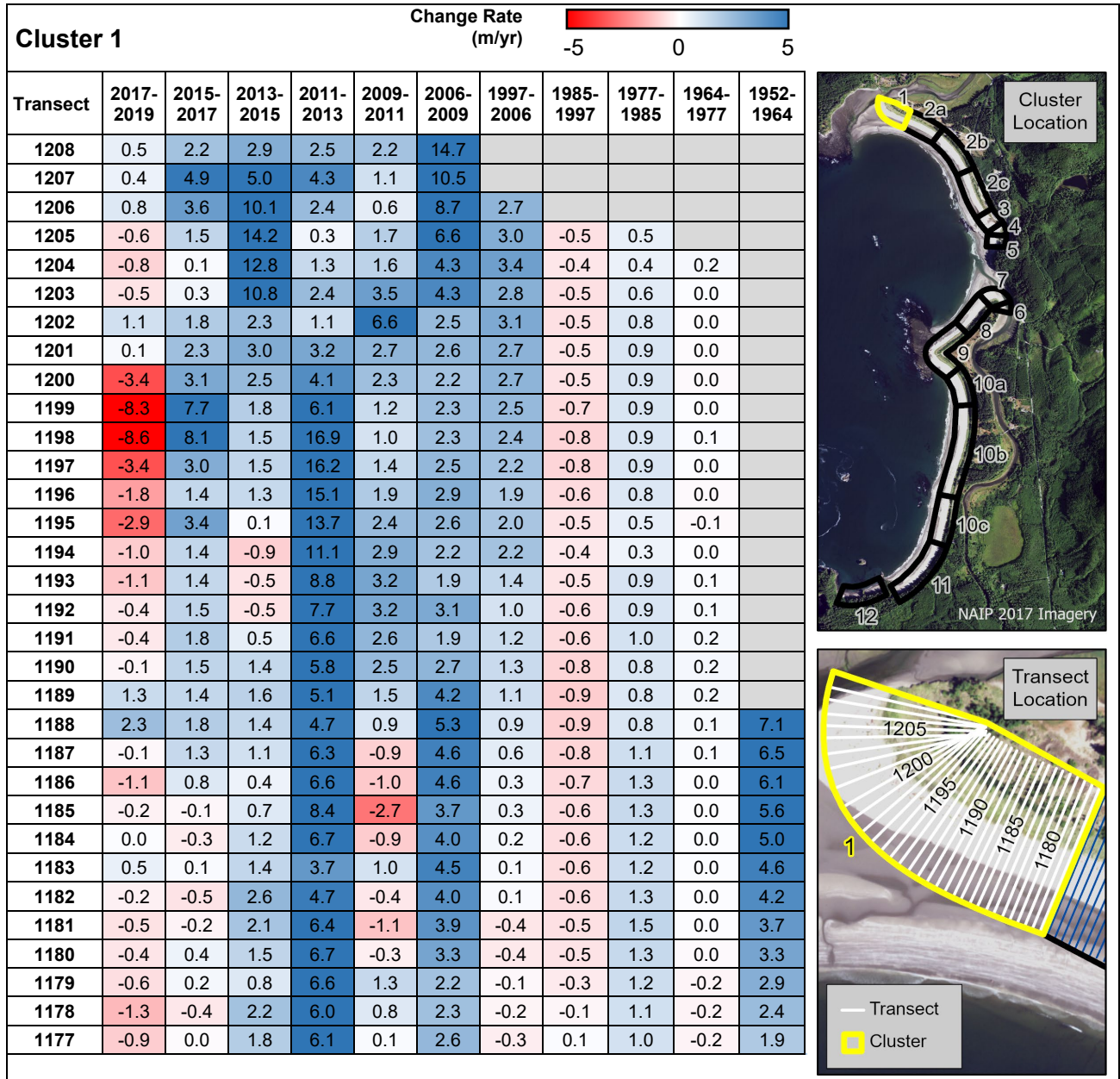


Table 5. Historical vegetation line change rates in Makah Bay based on the 10-m average transects in Cluster 2a.

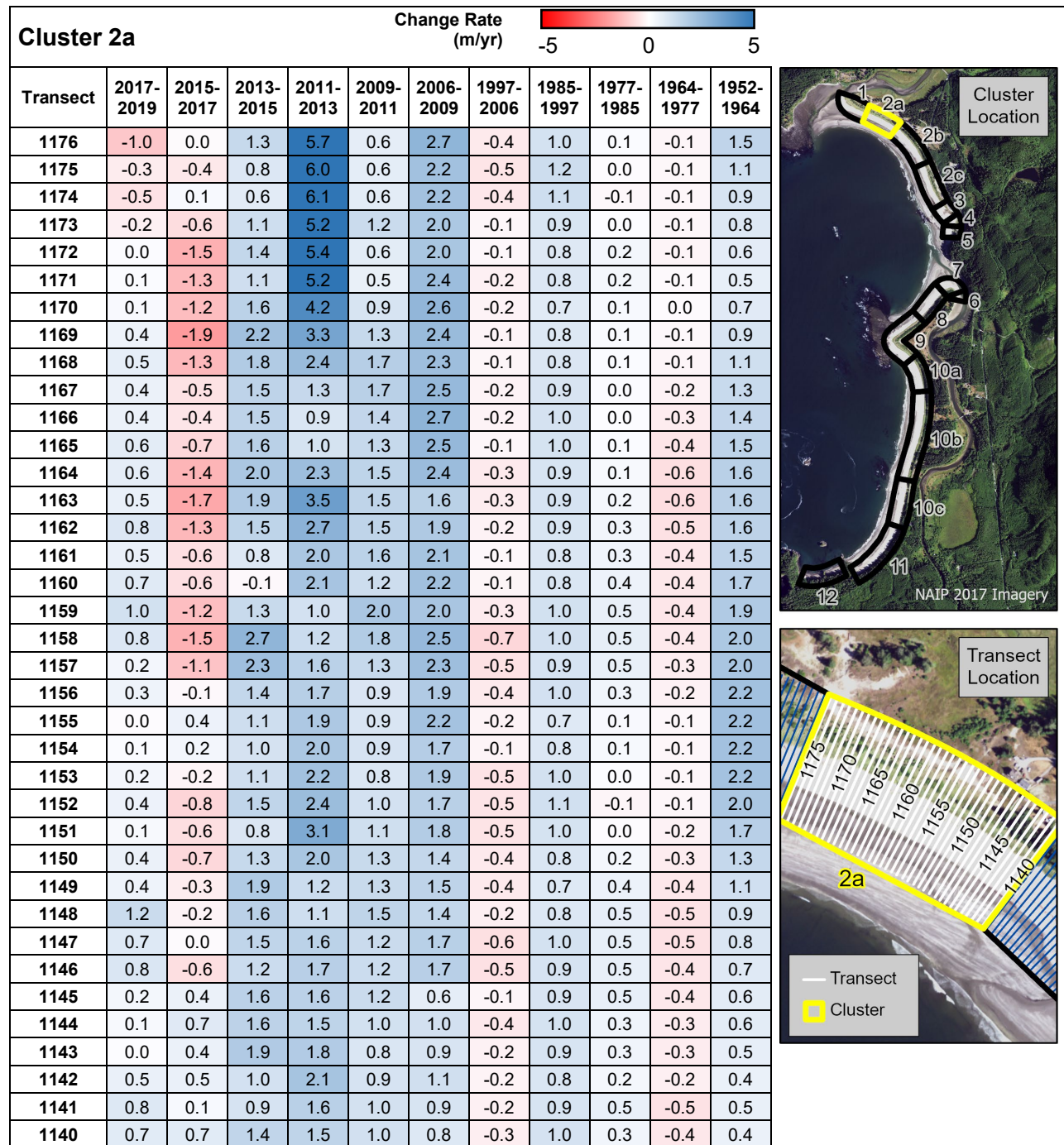


Table 6. Historical vegetation line change rates in Makah Bay based on the 10-m average transects in Cluster 2b.

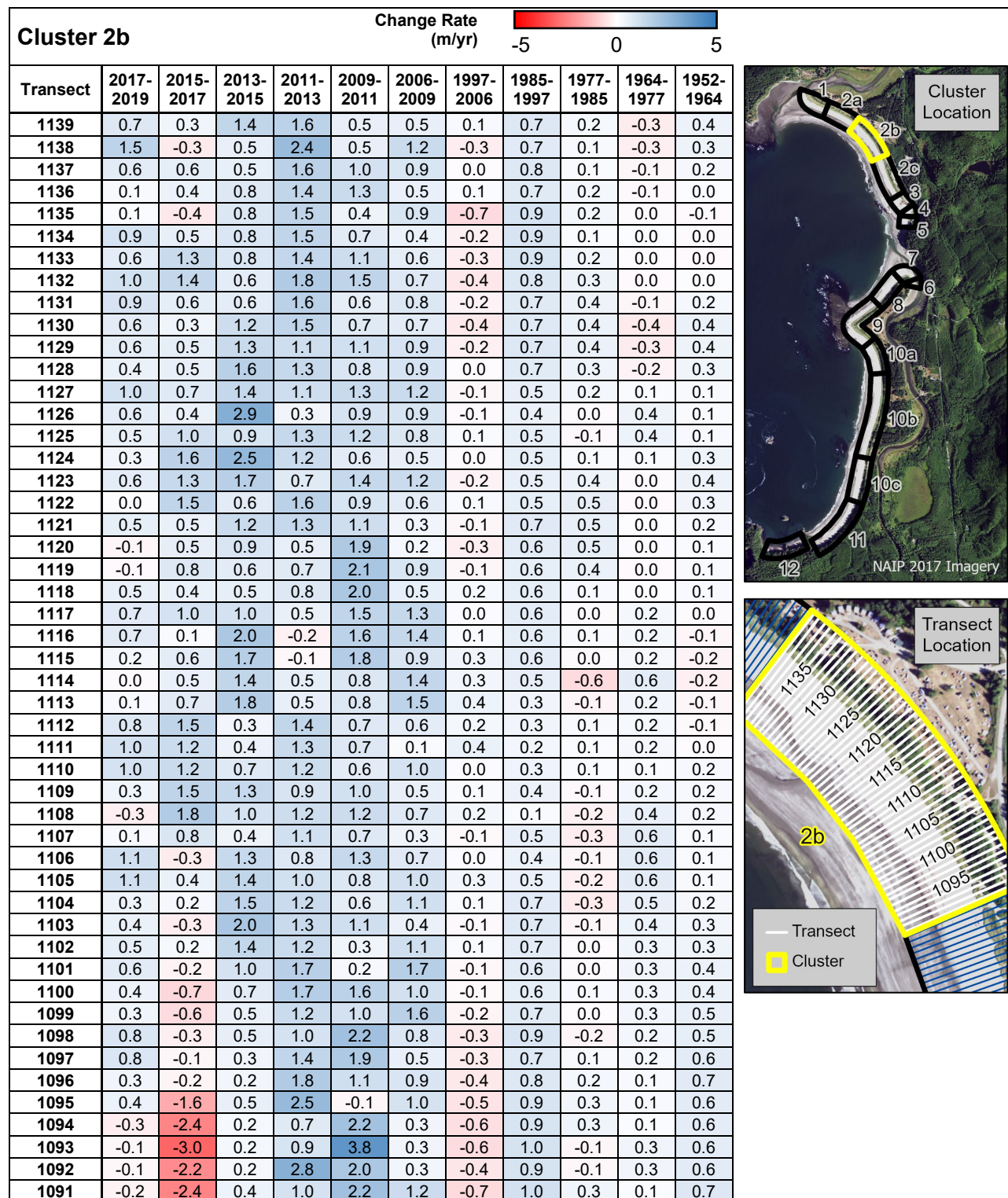


Table 7. Historical vegetation line change rates in Makah Bay based on the 10-m average transects in Cluster 2c.

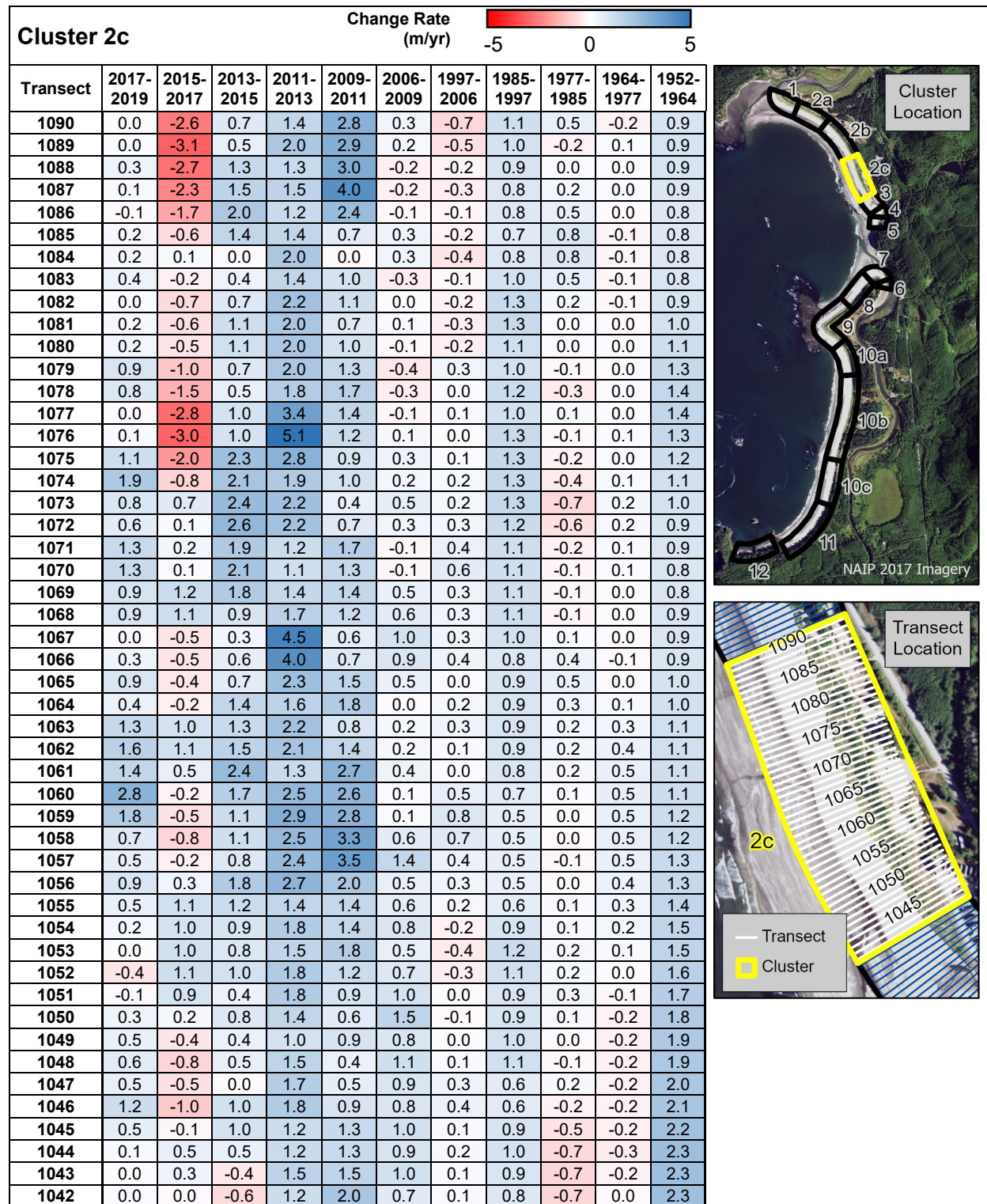


Table 8. Historical vegetation line change rates in Makah Bay based on the 10-m average transects in Clusters 3, 4, and 5.

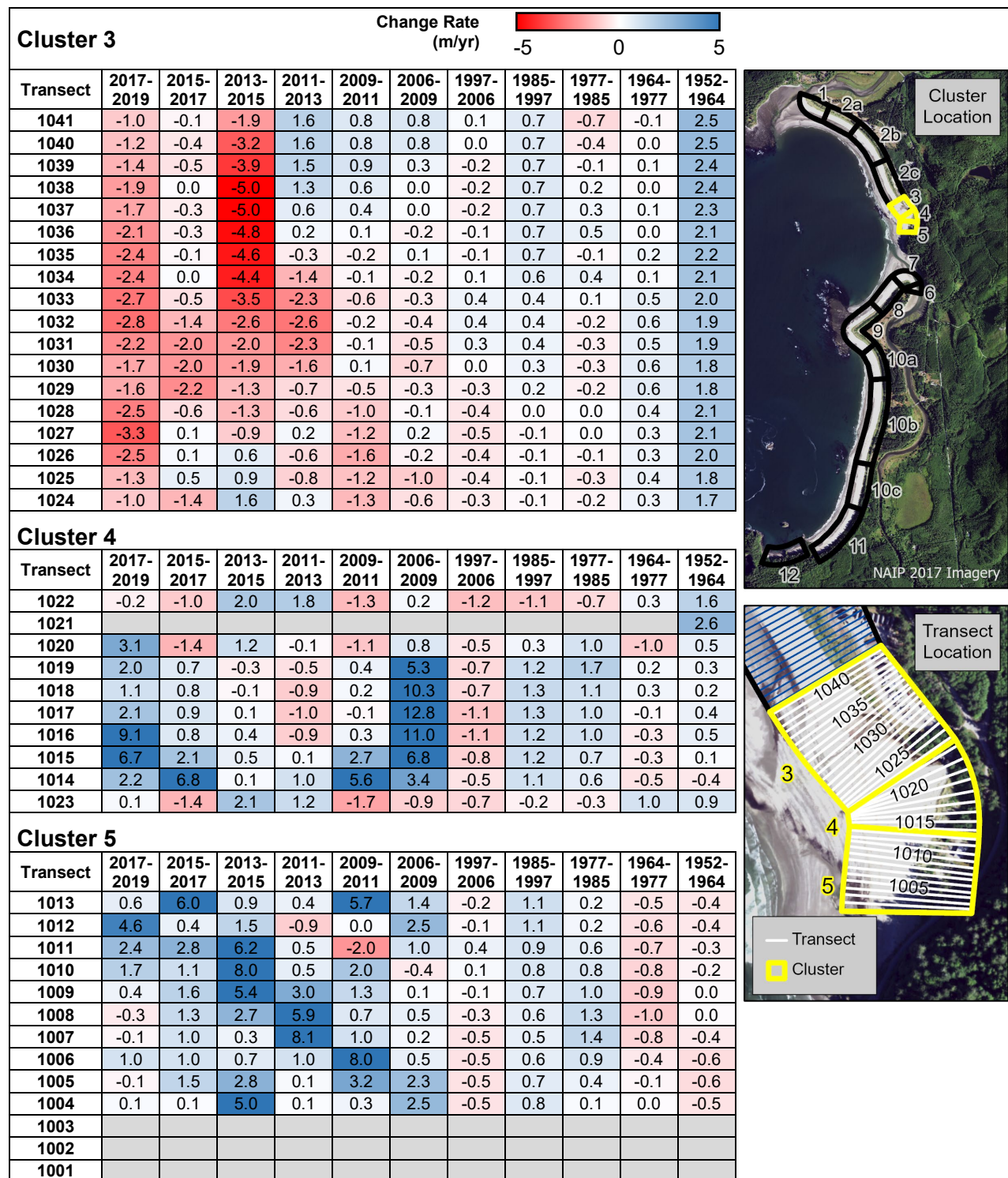


Table 9. Historical vegetation line change rates in Makah Bay based on the 10-m average transects in Clusters 6 and 7.

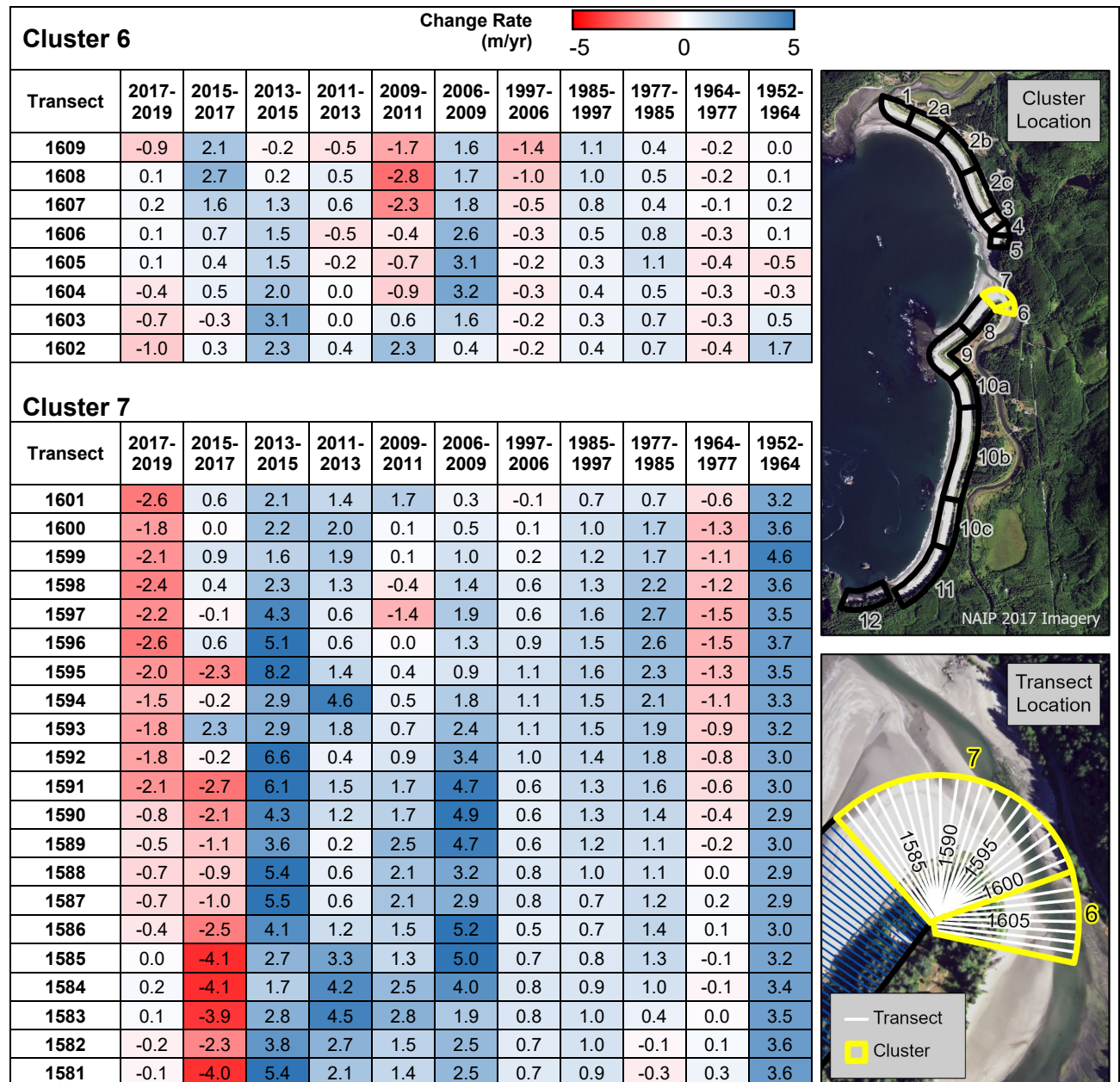


Table 10. Historical vegetation line change rates in Makah Bay based on the 10-m average transects in Cluster 8.

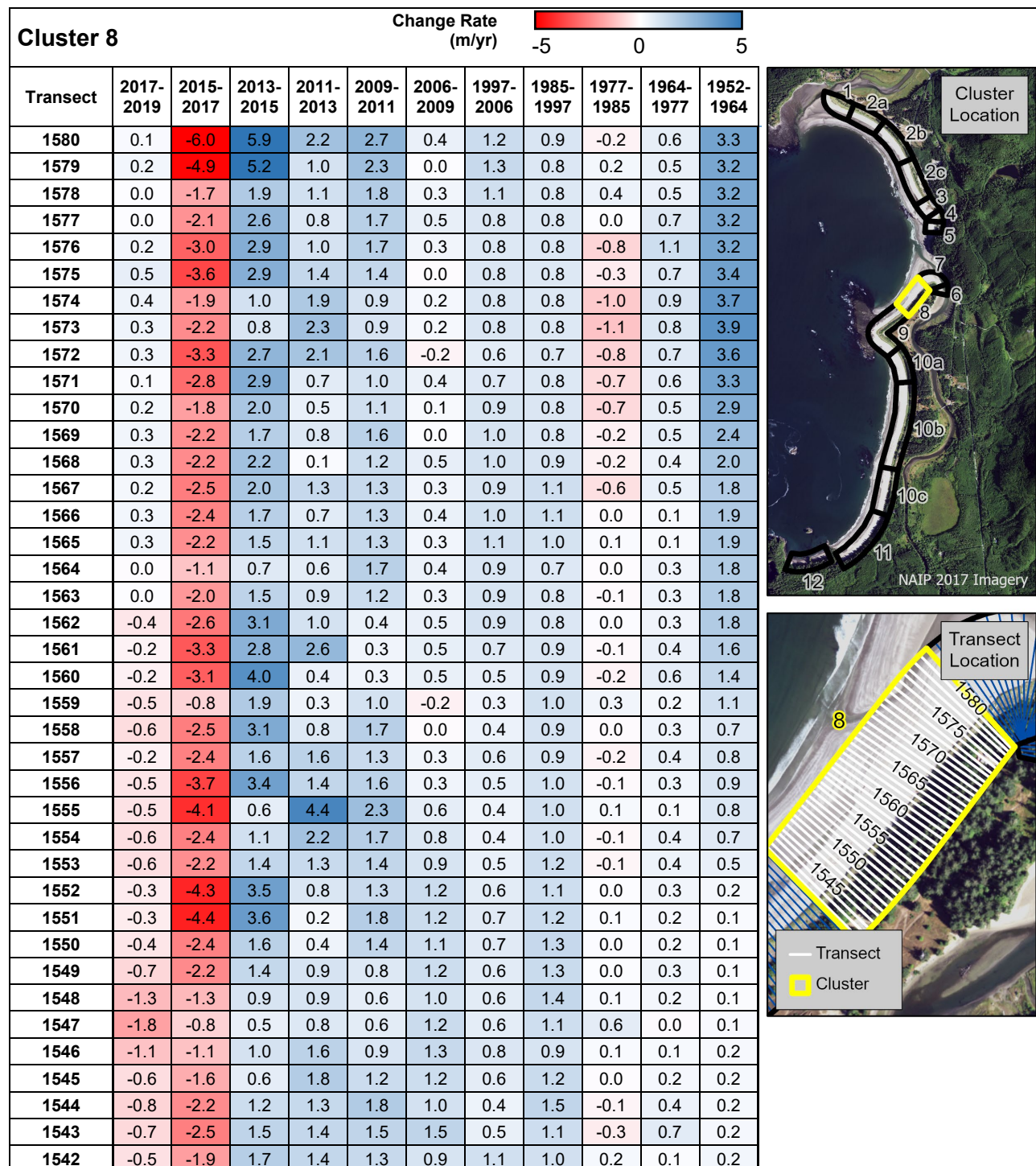


Table 11. Historical vegetation line change rates in Makah Bay based on the 10-m average transects in Cluster 9.

Transect	Change Rate (m/yr)										
	2017-2019	2015-2017	2013-2015	2011-2013	2009-2011	2006-2009	1997-2006	1985-1997	1977-1985	1964-1977	1952-1964
1541	-0.4	-1.9	1.8	0.7	2.9	1.3	1.1	1.1	0.4	-0.4	0.3
1540	-0.6	-2.5	1.1	1.2	4.4	1.0	1.3	1.0	0.3	-0.3	0.3
1539	-0.8	-1.8	0.2	1.8	4.3	1.0	1.2	0.9	0.5	-0.4	0.2
1538	0.0	-1.5	0.9	0.7	1.8	1.5	1.4	0.9	0.4	-0.2	0.1
1537	0.4	-1.0	1.3	0.0	2.0	1.6	1.0	0.8	0.7	-0.1	0.1
1536	0.6	-0.9	1.8	0.7	1.5	1.5	1.0	0.8	0.8	-0.2	0.0
1535	0.2	1.0	0.9	0.9	2.1	2.0	0.6	0.7	1.0	-0.3	-0.1
1534	-0.7	1.2	1.7	-0.9	2.4	1.8	1.0	0.6	1.0	-0.3	-0.2
1533	-1.0	-0.2	1.6	-0.5	2.3	2.6	1.2	0.4	1.3	-0.3	-0.3
1532	-1.0	-3.1	2.5	-0.3	2.7	5.0	0.8	0.5	0.9	-0.3	-0.3
1531	-1.4	-5.0	3.3	-0.1	3.3	5.4	1.0	0.5	0.5	-0.2	-0.4
1530	-1.7	-4.4	4.2	1.1	2.4	3.7	0.8	0.7	0.4	-0.1	-0.4
1529	-0.9	-0.5	1.6	0.7	1.9	1.4	1.3	0.7	0.4	0.1	-0.4
1528	-0.7	0.3	1.0	0.2	1.9	0.9	1.3	0.7	0.6	0.2	-0.3
1527	-0.4	-0.3	0.9	0.2	2.0	0.9	1.0	0.6	1.1	0.2	-0.3
1526	-0.1	0.1	0.1	0.1	2.3	0.0	1.2	0.6	0.9	0.4	-0.2
1525	-0.3	-0.6	0.3	0.0	2.6	0.1	1.3	0.8	0.7	0.3	-0.1
1524	-0.2	-0.6	0.2	1.1	1.2	1.0	1.0	1.1	0.5	0.0	-0.1
1523	-0.1	-0.8	1.7	1.0	1.5	0.8	1.0	1.0	0.3	0.1	-0.1
1522	0.2	-1.4	1.8	0.7	1.4	0.7	1.4	0.8	0.4	0.2	-0.1
1521	1.1	-2.6	1.0	1.5	1.3	0.4	1.5	0.7	0.5	0.1	0.0
1520	0.0	-3.3	1.9	0.8	2.2	0.0	1.5	0.7	0.6	0.0	0.0
1519	0.3	-4.2	2.9	1.6	0.5	0.9	1.5	0.6	0.7	0.1	0.1
1518	0.5	-5.0	3.1	1.4	-0.1	1.9	1.2	0.5	1.2	-0.2	0.1
1517	0.7	-4.5	2.8	0.5	0.5	1.5	1.3	0.4	1.9	-0.4	0.1
1516	0.5	-2.3	1.0	0.6	-2.6	2.2	1.5	0.3	2.2	-0.4	0.1
1515	0.7	-2.0	1.2	0.5	-3.3	3.5	1.1	0.2	2.3	-0.3	0.2
1514	0.6	-2.2	1.5	0.3	-3.4	3.6	1.2	0.0	2.1	0.0	0.2
1513	0.7	-2.9	1.9	0.4	-3.9	3.9	1.2	-0.1	1.9	0.2	0.3
1512	0.7	-3.2	2.4	0.1	-2.7	3.1	1.4	0.0	2.1	0.0	0.4
1511	0.6	-3.1	2.7	-0.6	-1.7	4.0	1.0	0.0	2.3	-0.1	0.6
1510	0.7	-2.9	2.5	-0.7	-0.8	3.6	1.1	0.0	2.5	-0.2	0.6
1509	1.0	-2.7	1.8	-0.1	0.0	3.5	1.0	-0.1	2.7	-0.1	0.7
1508	0.6	-1.3	0.1	0.6	0.3	3.2	1.2	-0.5	3.5	-0.1	0.8
1507	0.4	-1.2	0.2	0.6	1.6	2.1	1.3	-0.4	3.5	-0.1	0.9
1506	0.4	-0.8	-0.2	0.2	3.1	1.1	1.5	-0.5	2.9	0.4	1.0
1505	0.4	0.1	-0.4	0.0	3.3	1.0	1.8	-1.0	3.3	0.4	1.1
1504	0.1	0.6	-0.6	0.2	1.8	2.3	1.7	-1.2	4.0	0.2	1.2
1503	-0.1	1.0	-0.8	0.1	1.8	1.3	2.0	-1.9	5.2	-0.1	1.4
1502	-0.5	1.2	-0.7	0.1	1.5	0.9	1.5	-2.0	5.5	-0.3	1.6
1501	-0.5	1.4	-1.1	0.3	1.4	2.9	1.0	-1.6	4.5	-0.3	1.8
1500	-0.1	1.5	0.3	2.2	0.7	1.1	1.2	-1.4	3.0	-0.1	1.8
1499	-0.1	1.0	0.5	1.3	0.9	0.7	1.3	-1.3	2.4	-0.3	1.8
1498	-1.1	1.8	0.2	-0.5	2.9	0.0	1.5	-1.0	2.1	-0.4	1.7
1497	-0.7	1.1	1.1	-2.9	5.0	0.1	1.2	-0.5	1.5	-0.1	1.4
1496	-1.2	1.1	0.6	-2.6	4.6	0.2	1.2	-0.3	1.2	0.1	1.1
1495	-1.5	2.2	-0.1	-1.9	4.1	0.2	1.1	-0.3	1.7	0.0	0.9
1494	-1.2	2.5	-0.1	-1.3	3.5	0.8	1.1	-0.4	1.9	-0.1	0.8
1493	0.0	1.2	-0.3	0.5	2.2	0.6	1.6	-0.5	2.0	-0.1	0.7
1492	1.4	0.9	0.7	0.4	1.6	1.1	1.3	-0.4	2.0	-0.1	0.7
1491	1.2	0.7	1.4	0.4	1.0	0.9	1.2	-0.1	1.8	-0.1	0.7
1490	0.6	0.6	1.2	0.8	0.3	0.6	1.2	0.1	1.5	0.0	0.7

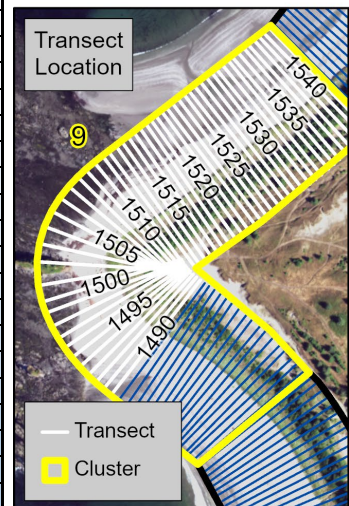


Table 12. Historical vegetation line change rates in Makah Bay based on the 10-m average transects in Cluster 9, continued.

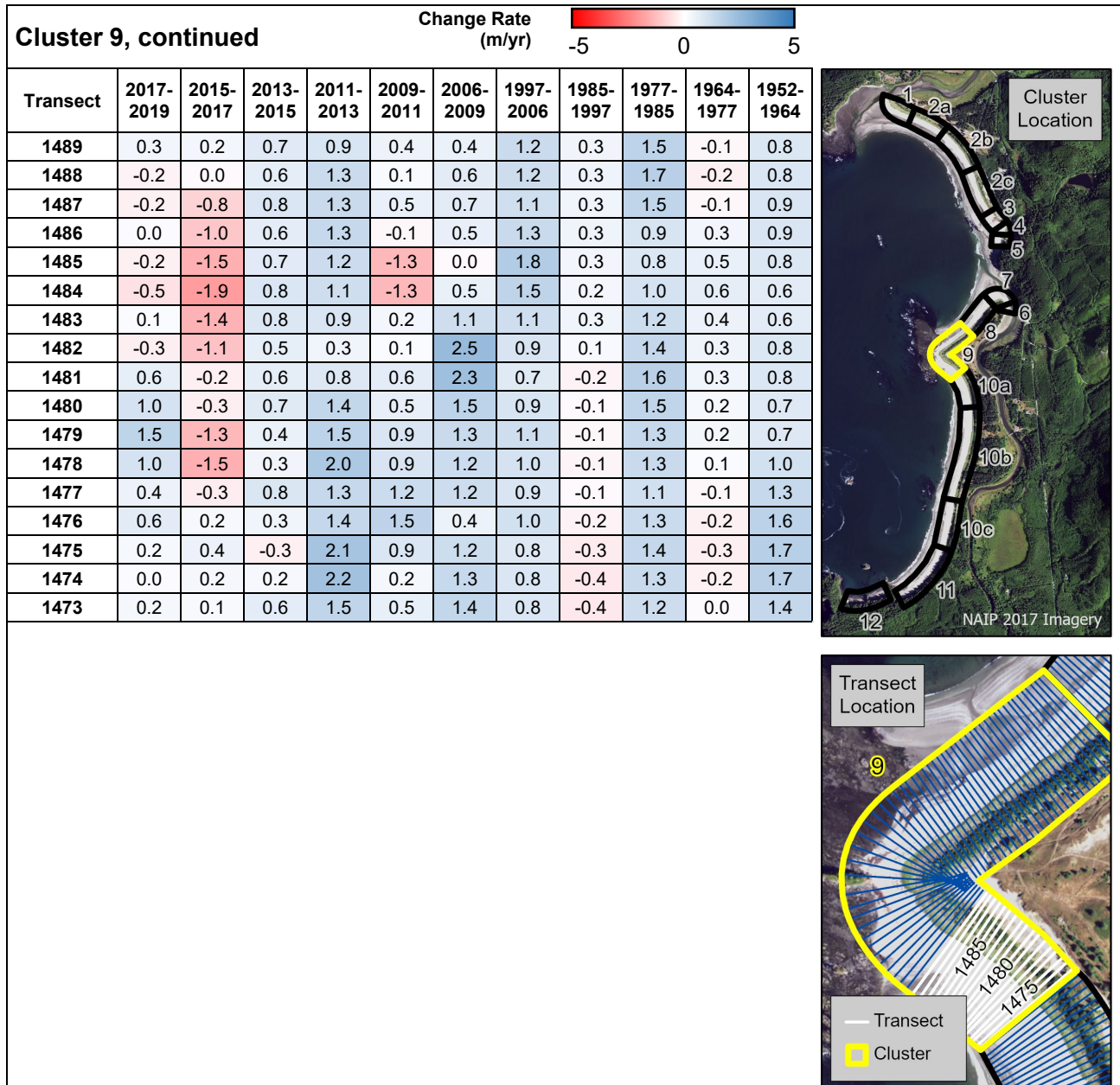


Table 13. Historical vegetation line change rates in Makah Bay based on the 10-m average transects in Cluster 10a.

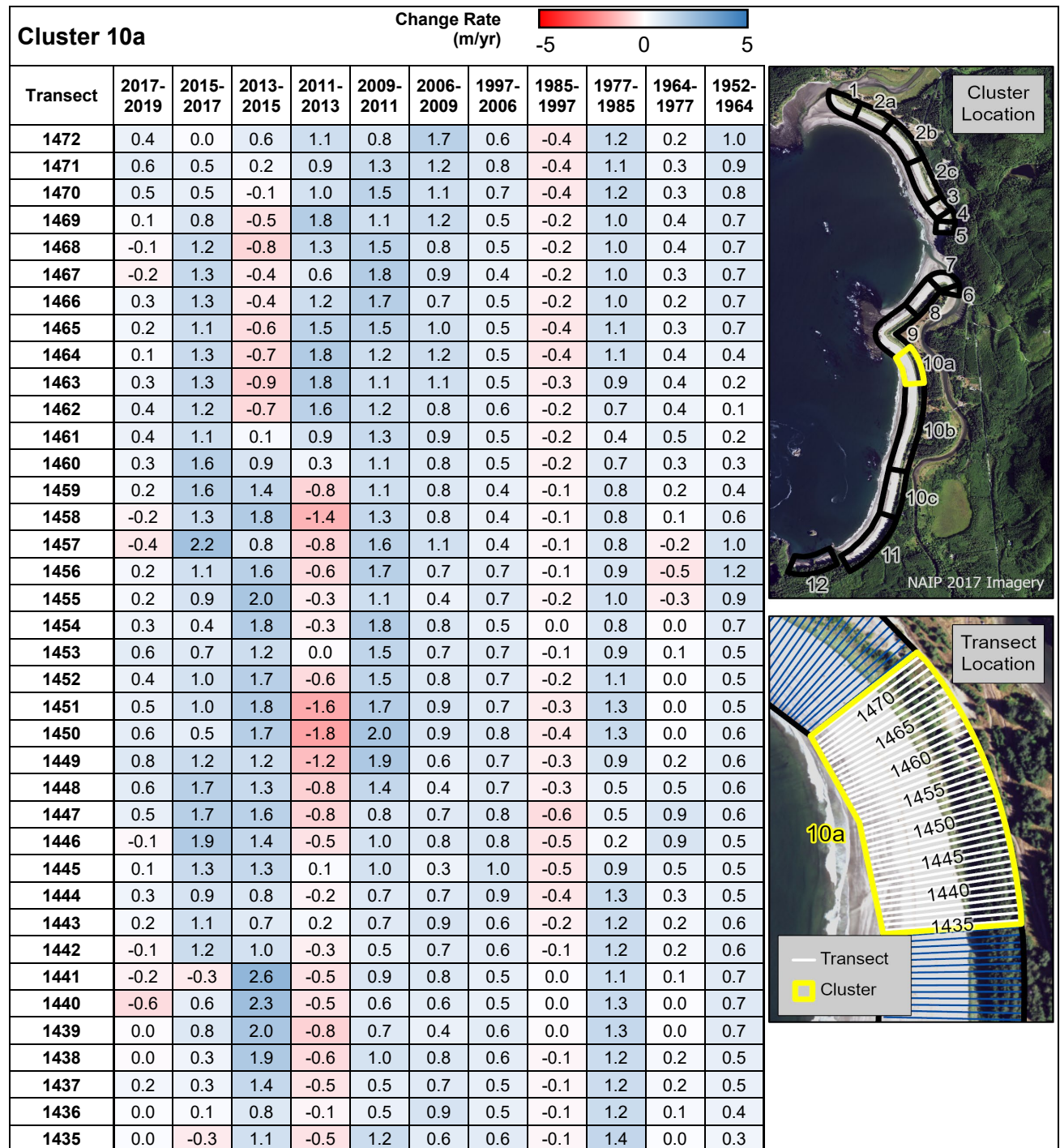


Table 14. Historical vegetation line change rates in Makah Bay based on the 10-m average transects in Cluster 10b.

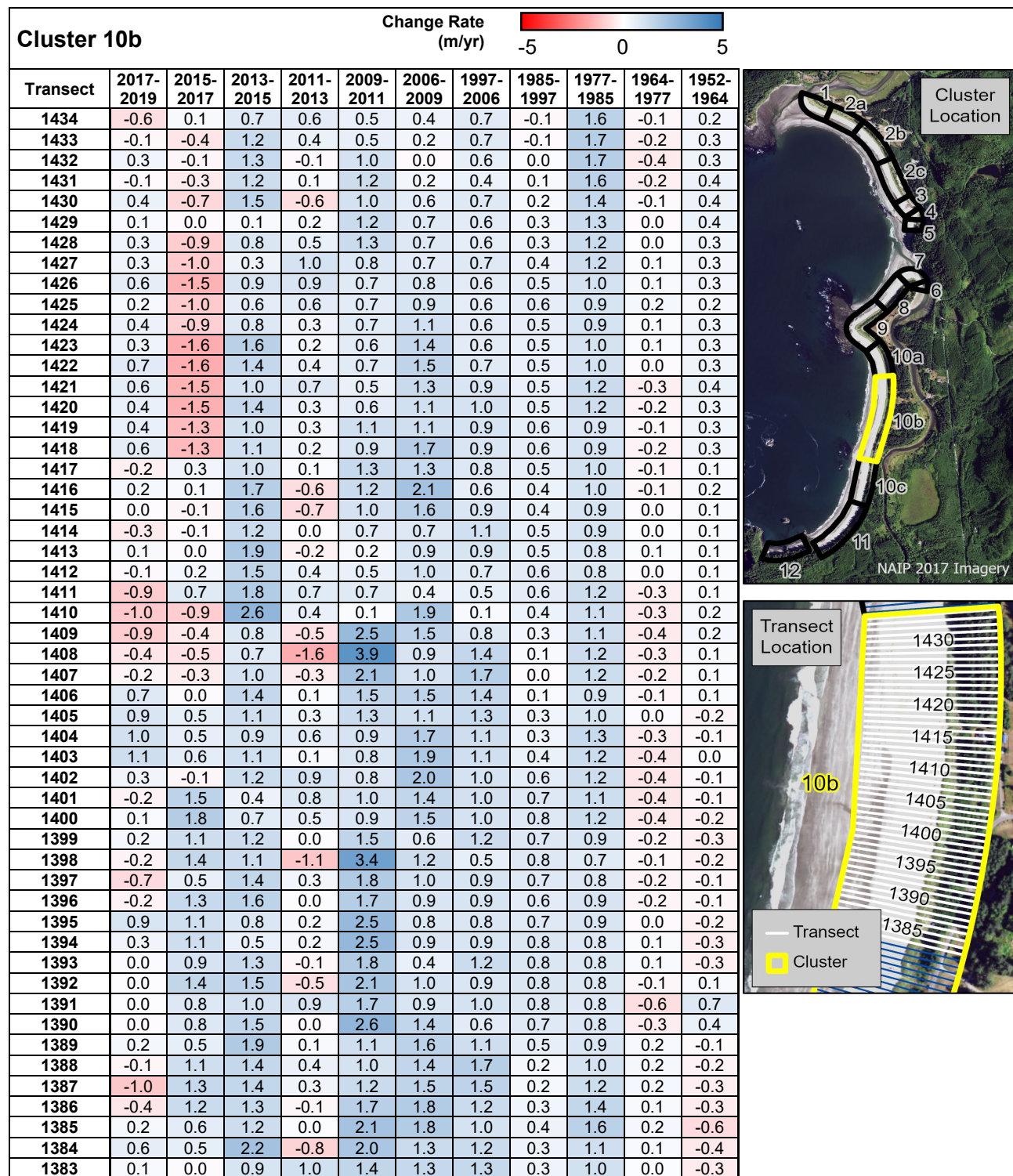


Table 15. Historical vegetation line change rates in Makah Bay based on the 10-m average transects in Cluster 10b, continued.

Transect	Change Rate (m/yr)										
	2017-2019	2015-2017	2013-2015	2011-2013	2009-2011	2006-2009	1997-2006	1985-1997	1977-1985	1964-1977	1952-1964
1382	0.4	-1.0	0.4	2.2	0.7	1.6	1.3	0.4	1.2	0.0	-0.5
1381	1.0	-0.5	1.1	0.2	2.0	1.2	1.3	0.4	1.3	0.0	-0.4
1380	0.0	-0.9	1.0	-0.4	3.1	1.2	1.6	0.2	1.0	0.1	-0.2
1379	-0.1	0.0	1.5	-0.4	2.3	1.3	1.4	0.1	1.3	0.1	-0.2
1378	-0.2	0.9	1.7	-1.2	2.2	1.0	1.3	0.1	1.0	0.3	-0.3
1377	0.2	1.2	2.5	-1.5	2.8	1.4	0.9	0.1	0.7	0.4	-0.3
1376	0.2	0.6	0.7	0.5	1.6	1.6	1.1	0.3	0.5	0.3	-0.1
1375	-0.3	0.1	1.0	1.1	1.6	1.3	1.3	0.4	0.6	0.4	-0.3
1374	0.1	0.0	1.4	0.6	1.8	1.7	1.3	0.3	1.0	0.1	-0.3
1373	0.2	0.5	0.9	0.9	1.9	1.8	1.3	0.4	1.2	0.0	-0.4
1372	0.9	0.6	1.4	0.5	1.7	1.3	1.5	0.5	1.2	0.0	-0.3
1371	0.4	0.6	2.3	-0.4	1.2	1.5	1.4	0.5	0.9	0.1	-0.4
1370	-0.2	1.1	2.0	-0.6	1.3	1.6	1.4	0.6	0.7	0.2	-0.5
1369	-0.2	1.6	1.5	-0.8	1.9	1.2	1.4	0.6	0.8	0.1	-0.3
1368	-0.6	1.5	1.9	0.3	2.4	1.1	1.3	0.3	0.9	0.1	-0.4
1367	0.2	2.3	1.1	0.8	1.5	1.2	1.1	0.2	1.3	0.1	-0.3
1366	0.8	1.7	1.9	-0.3	0.9	1.4	1.1	0.2	1.4	0.1	-0.2
1365	1.2	1.3	1.4	-0.9	1.2	2.1	1.0	0.2	1.3	0.1	-0.1
1364	1.2	0.8	1.8	-1.8	3.2	0.6	1.2	0.3	1.4	0.0	-0.1
1363	0.0	1.6	1.4	-1.3	2.9	0.9	1.1	0.3	1.2	-0.1	-0.1
1362	-1.0	1.8	1.3	-0.6	2.0	1.0	1.0	0.3	0.8	0.1	-0.1
1361	-0.9	1.3	1.3	-0.2	1.7	0.5	1.2	0.3	0.8	0.1	0.0
1360	-1.1	1.0	1.1	0.0	1.4	0.7	1.3	0.2	0.8	0.0	0.0
1359	-1.1	0.6	0.4	1.2	0.6	1.2	1.4	0.0	0.8	0.1	-0.1
1358	-0.8	0.5	0.3	1.4	0.8	0.4	1.4	0.0	1.0	0.0	-0.1
1357	-0.8	1.2	1.4	0.1	1.0	1.1	1.0	0.0	1.1	0.0	-0.1
1356	-1.6	1.6	1.3	0.1	0.6	1.5	0.8	0.1	1.2	0.0	-0.1
1355	-1.5	1.5	1.5	-0.3	1.2	1.0	0.8	0.1	1.3	0.0	0.0
1354	-0.6	0.7	1.0	0.6	1.3	0.4	1.0	0.0	1.4	0.0	0.1
1353	-0.8	1.2	1.7	-0.3	1.5	1.2	0.8	-0.1	1.2	0.0	0.1
1352	0.5	0.7	1.5	0.4	1.2	0.9	1.0	-0.1	1.1	0.0	0.1
1351	0.3	0.5	2.0	0.5	1.0	1.4	0.9	-0.1	1.4	-0.3	0.2
1350	-0.4	1.3	1.3	0.3	1.5	0.6	1.0	-0.2	1.4	-0.2	0.1
1349	-1.5	1.3	1.6	0.1	2.0	2.2	0.3	-0.2	1.3	-0.2	0.1
1348	0.3	-0.1	1.0	0.6	2.0	0.9	1.2	-0.1	1.3	-0.3	0.2
1347	0.5	0.6	0.7	1.0	2.0	1.4	1.0	-0.2	1.4	-0.2	0.1
1346	0.4	1.6	1.1	0.4	1.8	1.3	1.1	-0.2	1.6	-0.4	0.1
1345	0.2	2.1	1.1	0.0	1.7	0.7	1.1	-0.1	1.1	-0.1	0.1
1344	0.5	1.0	1.2	0.6	1.7	0.5	1.1	0.1	1.0	-0.2	0.2
1343	0.1	1.0	0.6	1.2	2.1	0.6	1.1	0.0	0.8	-0.2	0.3
1342	0.6	0.7	1.1	1.2	2.5	0.4	1.1	-0.1	0.9	-0.2	0.2
1341	-0.3	1.5	0.4	1.4	2.4	0.8	1.0	-0.3	1.1	-0.1	0.1
1340	0.2	0.4	1.2	2.2	1.9	0.6	1.0	-0.3	1.2	-0.1	0.1
1339	1.5	-0.9	3.6	1.3	1.4	1.3	0.8	-0.1	1.2	-0.2	0.0
1338	0.3	-2.1	5.1	0.9	1.2	1.0	1.1	-0.1	0.9	-0.1	0.0
1337	-0.2	-1.7	3.2	2.8	1.3	2.4	0.7	-0.1	0.6	0.0	0.0
1336	-0.4	-1.9	2.3	2.5	1.7	1.5	1.3	0.0	0.5	0.1	-0.2
1335	-0.5	-1.3	1.1	2.7	1.7	2.4	1.1	-0.1	0.5	0.0	0.0

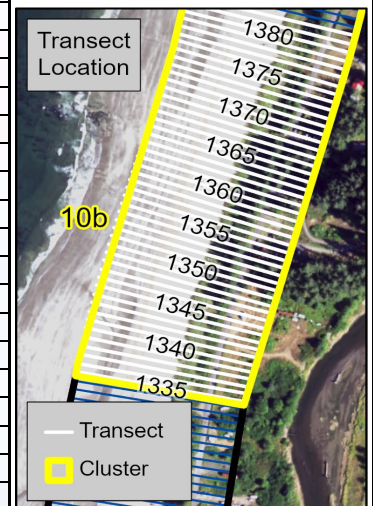
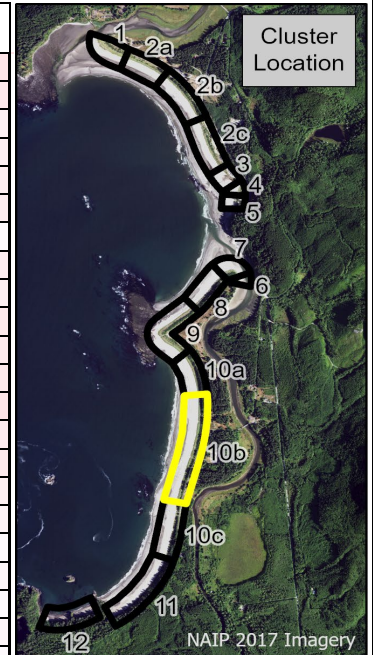


Table 16. Historical vegetation line change rates in Makah Bay based on the 10-m average transects in Cluster 10c.

Cluster 10c	Change Rate (m/yr)										
	2017-2019	2015-2017	2013-2015	2011-2013	2009-2011	2006-2009	1997-2006	1985-1997	1977-1985	1964-1977	1952-1964
1334	-0.2	-0.4	0.4	0.1	1.3	3.1	1.0	0.0	0.3	0.0	0.1
1333	-0.4	-0.6	0.9	0.5	0.3	1.4	0.8	0.0	0.2	0.1	0.0
1332	-0.3	0.1	0.6	1.1	0.5	3.7	0.0	0.2	0.2	0.2	-0.1
1331	0.2	2.2	0.1	0.5	1.9	1.0	0.4	0.2	0.4	0.1	0.0
1330	0.6	0.8	0.8	-0.8	2.0	0.8	0.7	0.2	0.4	-0.1	0.1
1329	0.9	-0.5	0.6	0.1	1.8	1.4	0.5	0.3	0.3	0.0	0.1
1328	0.2	-0.4	0.7	-0.7	1.6	1.5	0.4	0.3	0.1	0.2	0.0
1327	-1.2	1.1	0.4	-0.3	1.4	0.3	0.2	0.4	0.3	0.2	-0.1
1326	0.0	0.5	0.3	-0.5	1.6	0.3	0.2	0.4	0.6	0.0	-0.1
1325	-0.6	1.7	0.2	0.5	0.9	0.4	0.0	0.3	0.8	-0.1	-0.1
1324	0.5	0.0	0.7	-0.3	0.8	1.5	0.3	0.2	0.5	0.1	0.0
1323	0.2	1.3	0.4	-0.5	0.8	0.1	1.1	0.0	1.6	-0.7	0.1
1322	0.4	3.8	1.3	-0.1	0.2	0.5	1.0	-0.6	1.9	-0.8	0.1
1321	-0.5	4.9	0.3	0.5	0.6	0.7	0.3	-0.2	0.6	0.0	0.1
1320	0.7	2.6	0.1	1.1	1.6	0.7	0.0	0.2	0.7	0.0	0.1
1319	0.9	2.4	0.3	1.0	1.0	0.5	0.2	0.3	0.8	-0.1	0.2
1318	0.2	1.7	1.6	0.5	1.7	1.0	0.0	0.3	0.8	-0.1	0.3
1317	-0.4	1.5	1.7	0.3	1.5	1.1	0.3	0.2	0.8	0.0	0.2
1316	0.2	1.6	1.4	0.3	1.6	1.1	0.2	0.3	0.8	0.0	0.3
1315	-0.2	1.6	1.3	0.3	1.6	1.4	0.1	0.4	0.8	0.0	0.4
1314	-0.4	1.2	1.3	0.5	1.5	1.5	0.1	0.4	0.8	0.1	0.4
1313	0.3	1.5	0.5	0.7	1.6	1.7	0.0	0.4	0.8	0.1	0.5
1312	0.9	0.3	0.8	0.6	1.7	1.0	0.1	0.4	0.8	0.2	0.6
1311	1.2	-0.8	1.0	0.9	1.6	0.8	0.0	0.4	0.8	0.2	0.6
1310	1.2	-0.4	0.6	1.5	1.6	0.9	-0.3	0.4	0.7	0.2	0.7
1309	0.2	2.3	-0.2	1.8	1.2	0.3	-0.5	0.3	0.6	0.2	0.8
1308	0.7	0.2	0.9	0.2	1.2	0.9	0.0	0.2	0.7	0.2	0.8
1307	1.3	0.3	0.2	0.4	1.4	1.1	0.2	0.3	0.8	0.2	0.8
1306	1.2	0.4	0.9	0.4	1.1	1.7	-0.1	0.5	0.7	0.2	0.8
1305	1.4	0.6	1.3	0.4	1.2	1.5	-0.2	0.6	0.5	0.3	0.8
1304	0.4	1.2	0.9	0.2	1.3	1.2	-0.2	0.6	0.5	0.2	0.8
1303	0.4	0.5	0.8	0.7	1.0	1.5	-0.2	0.6	0.5	0.3	0.7
1302	0.9	1.1	1.2	0.1	1.4	1.2	-0.1	0.4	0.9	0.1	0.7
1301	1.5	0.8	1.2	0.3	1.1	1.4	-0.2	0.2	1.0	0.0	0.7
1300	1.7	-0.5	1.6	-0.2	1.6	0.9	0.1	0.2	1.0	0.1	0.7
1299	2.1	-0.4	1.3	-0.4	1.8	1.2	0.0	0.2	1.0	0.0	0.8
1298	1.3	-0.1	1.0	-0.2	1.1	1.4	0.1	0.1	1.0	0.0	0.9
1297	1.5	-0.4	1.0	-0.1	1.1	1.4	0.2	0.1	1.0	0.0	0.9
1296	1.8	-0.3	1.5	-0.2	1.5	1.0	0.1	0.1	1.2	-0.1	0.9
1295	1.5	0.0	1.3	-0.3	1.4	1.1	0.2	0.1	1.2	-0.1	0.9
1294	0.9	0.4	0.5	-0.1	1.7	1.3	0.2	0.2	1.2	0.0	0.9
1293	0.1	1.3	0.2	0.2	1.0	1.1	0.2	0.2	1.1	0.1	0.8
1292	-0.5	1.8	0.9	-0.5	1.1	1.2	0.1	0.3	1.0	0.2	0.7
1291	-0.8	1.2	0.1	0.1	1.4	1.6	0.0	0.4	1.0	0.2	0.6
1290	0.3	0.3	0.7	-0.1	1.3	1.3	-0.1	0.5	1.0	0.2	0.6
1289	0.2	0.0	0.9	-0.4	1.6	1.3	-0.2	0.5	1.0	0.1	0.7
1288	0.2	-0.2	0.6	0.1	1.0	1.6	-0.1	0.5	0.7	0.1	0.8
1287	0.3	-0.4	0.5	0.6	0.8	1.5	-0.1	0.5	0.7	0.2	0.9
1286	0.1	-0.3	1.0	-0.3	1.2	1.1	0.0	0.5	0.8	0.1	0.9
1285	0.0	-0.2	1.2	-0.2	0.6	1.4	-0.2	0.5	0.8	0.1	0.8
1284	1.0	-1.4	1.1	-0.2	0.8	0.9	0.0	0.5	0.9	0.1	0.7
1283	1.9	-1.9	1.6	-1.1	1.6	1.3	-0.3	0.5	1.0	0.1	0.7

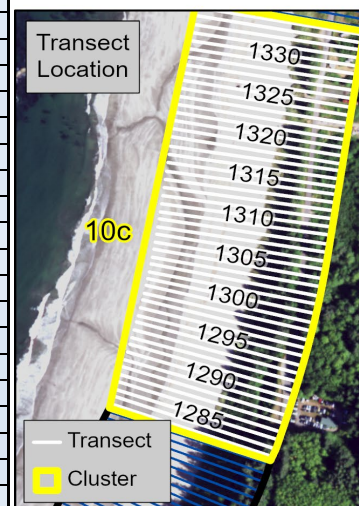


Table 17. Historical vegetation line change rates in Makah Bay based on the 10-m average transects in Cluster 11.

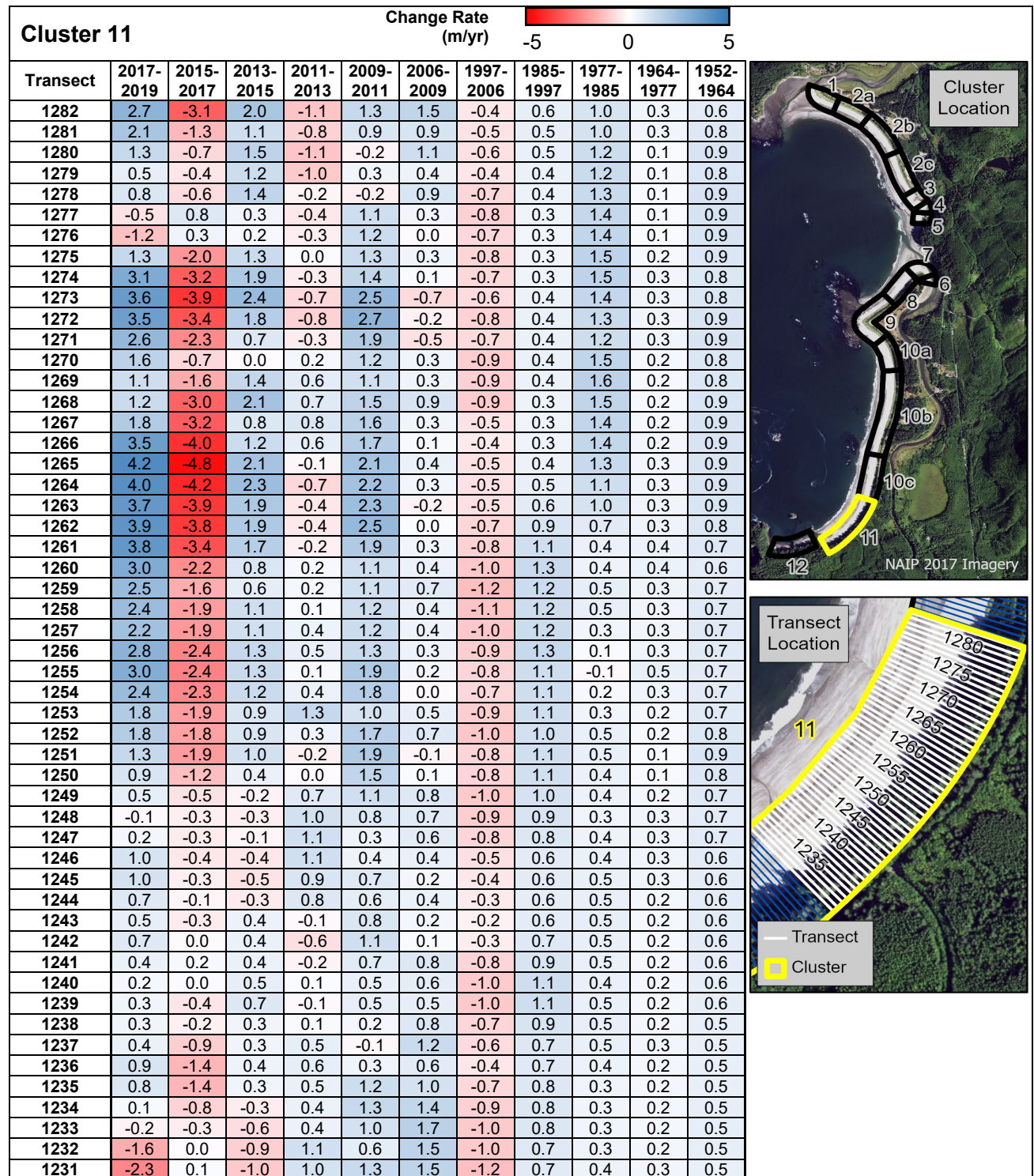


Table 18. Historical vegetation line change rates in Makah Bay based on the 10-m average transects in Cluster 11, continued.

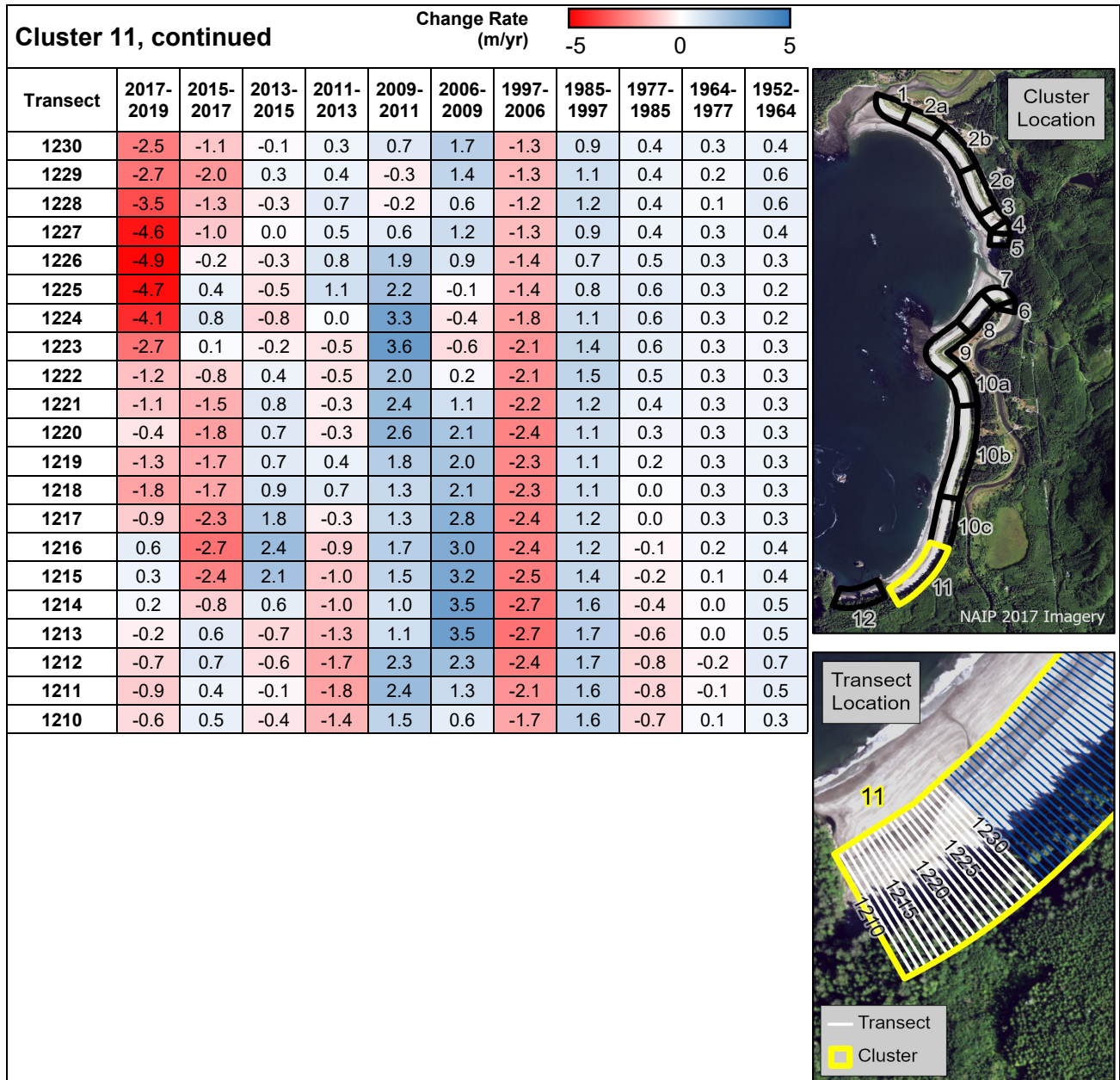
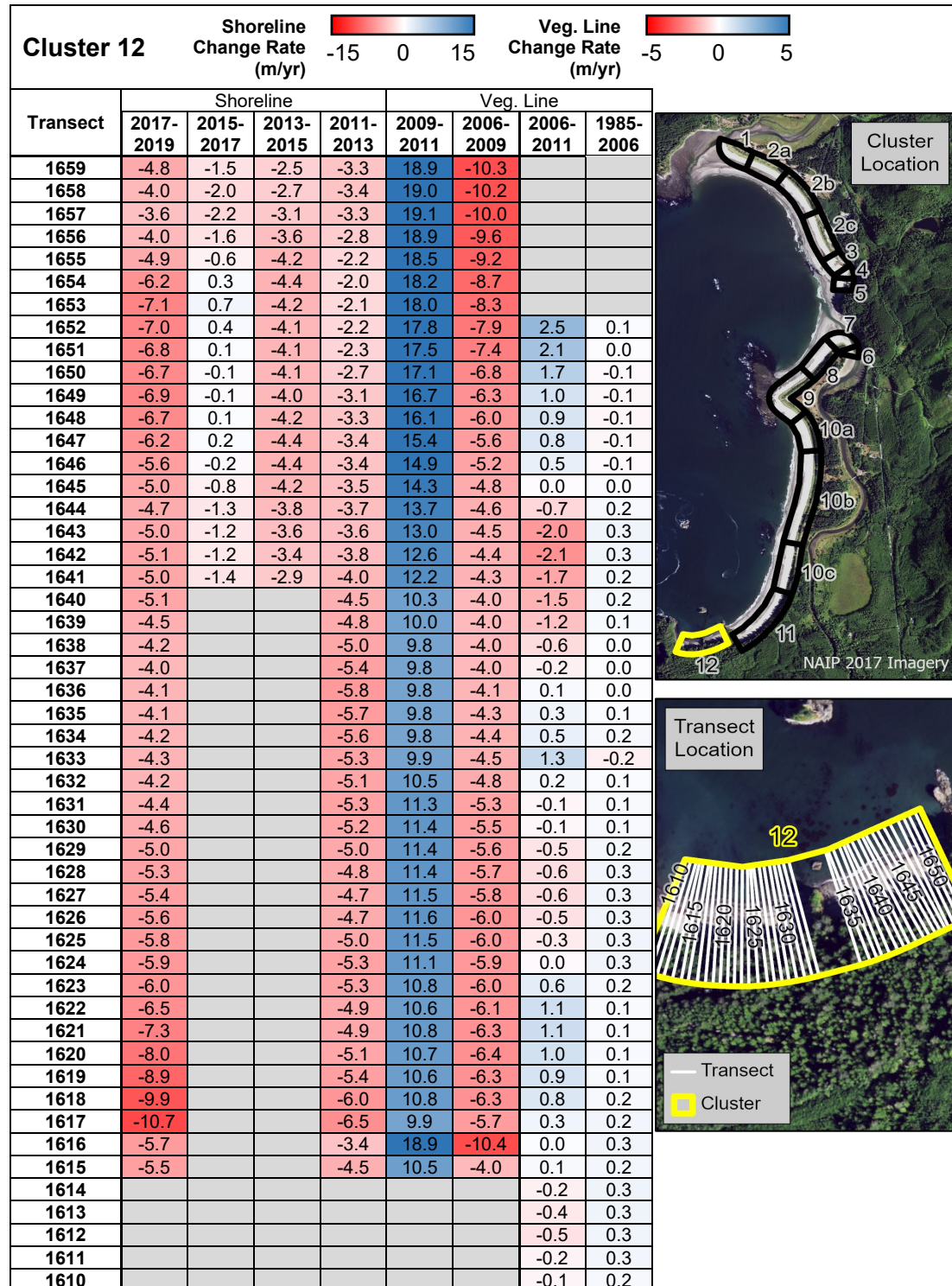


Table 19. Historical vegetation line and shoreline change rates in Makah Bay based on the 10-m average transects in Cluster 12.



Appendix C. Historical Shoreline Change Tables, Makah Bay

Table 20. Historical shoreline change rates in Makah Bay based on the 10-m average transects in Cluster 1.

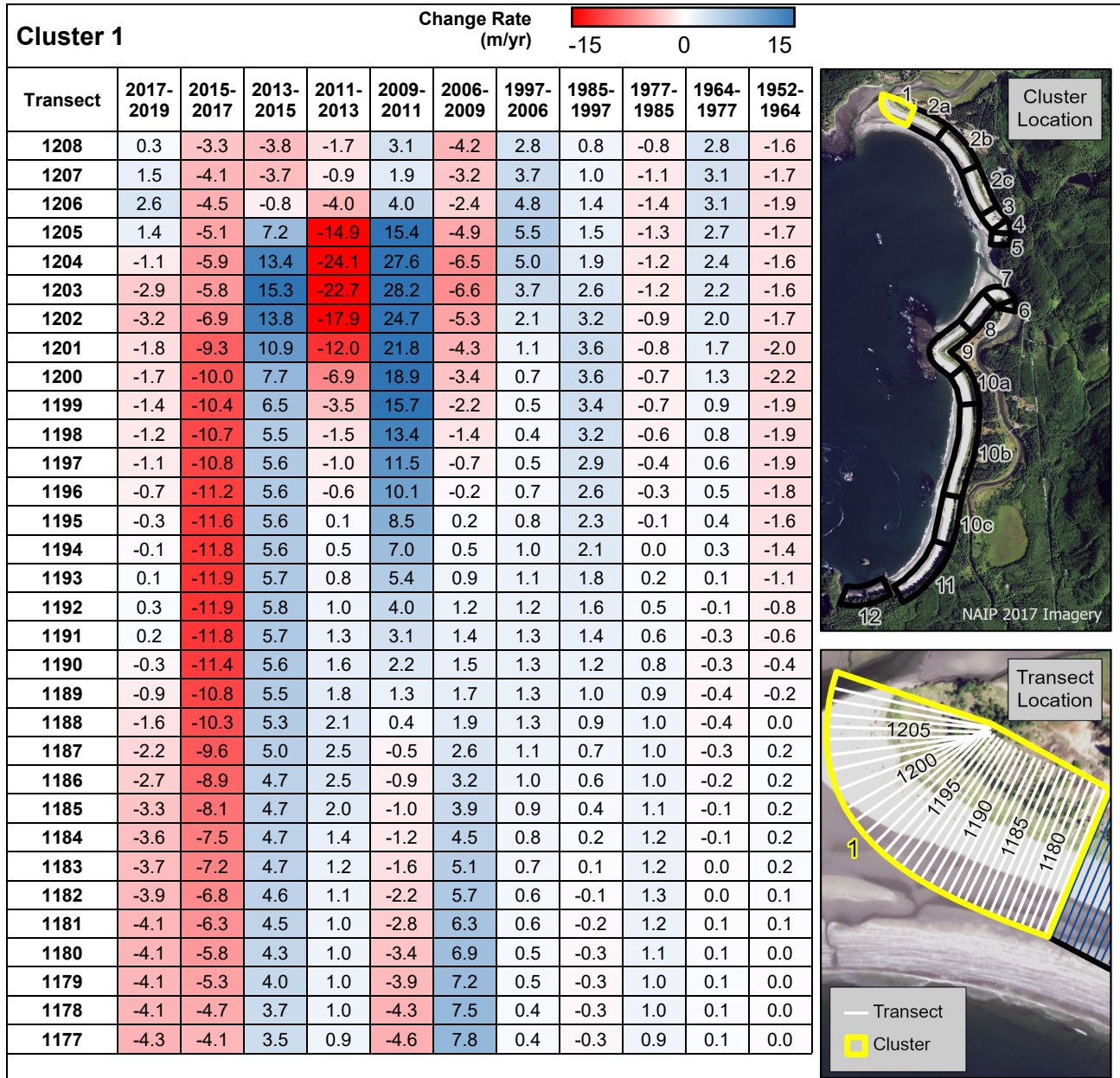


Table 21. Historical shoreline change rates in Makah Bay based on the 10-m average transects in Cluster 2a.

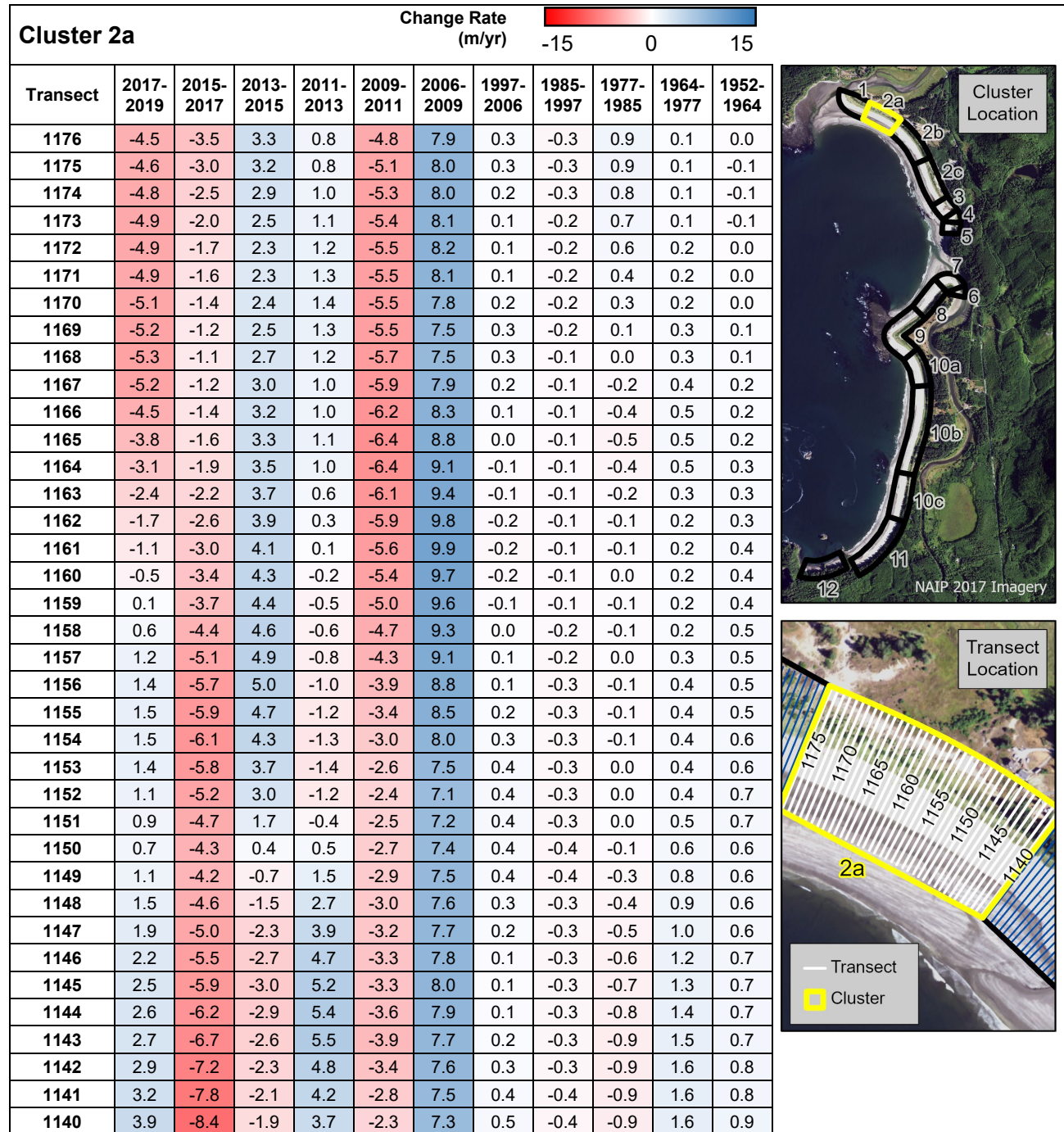


Table 22. Historical shoreline change rates in Makah Bay based on the 10-m average transects in Cluster 2b.

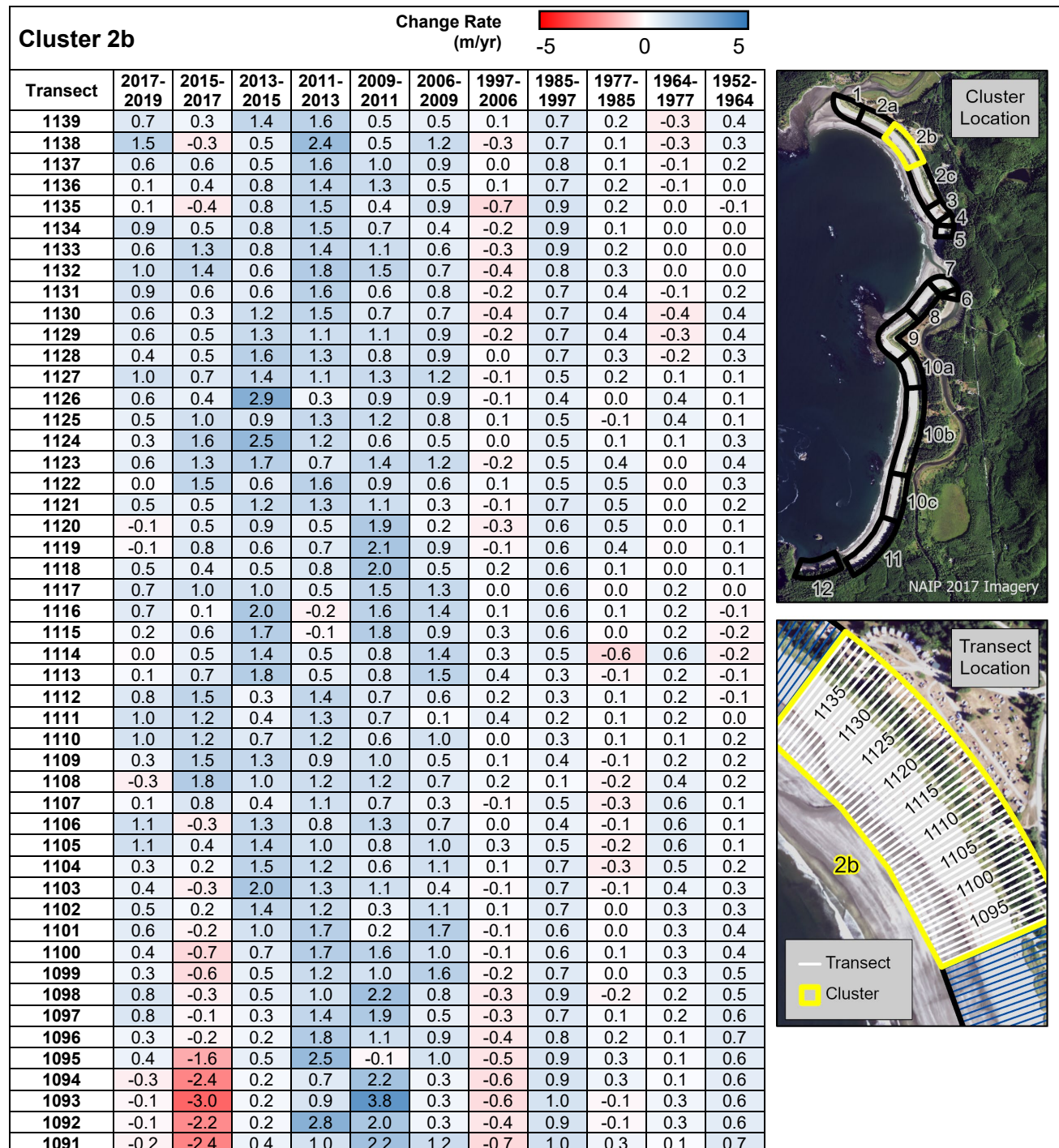


Table 23. Historical shoreline change rates in Makah Bay based on the 10-m average transects in Cluster 2c.

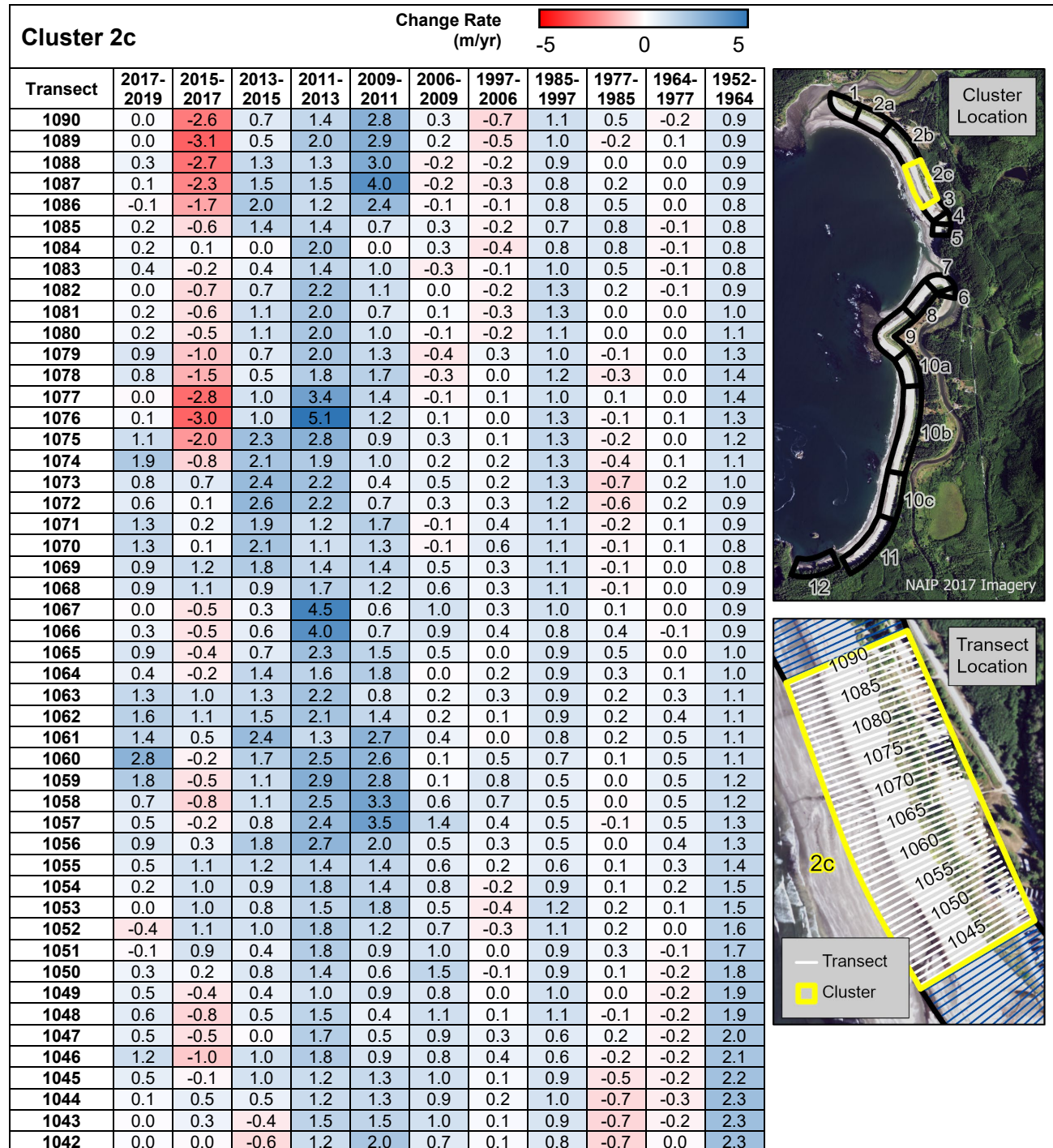


Table 24. Historical shoreline change rates in Makah Bay based on the 10-m average transects in Clusters 3, 4, and 5.

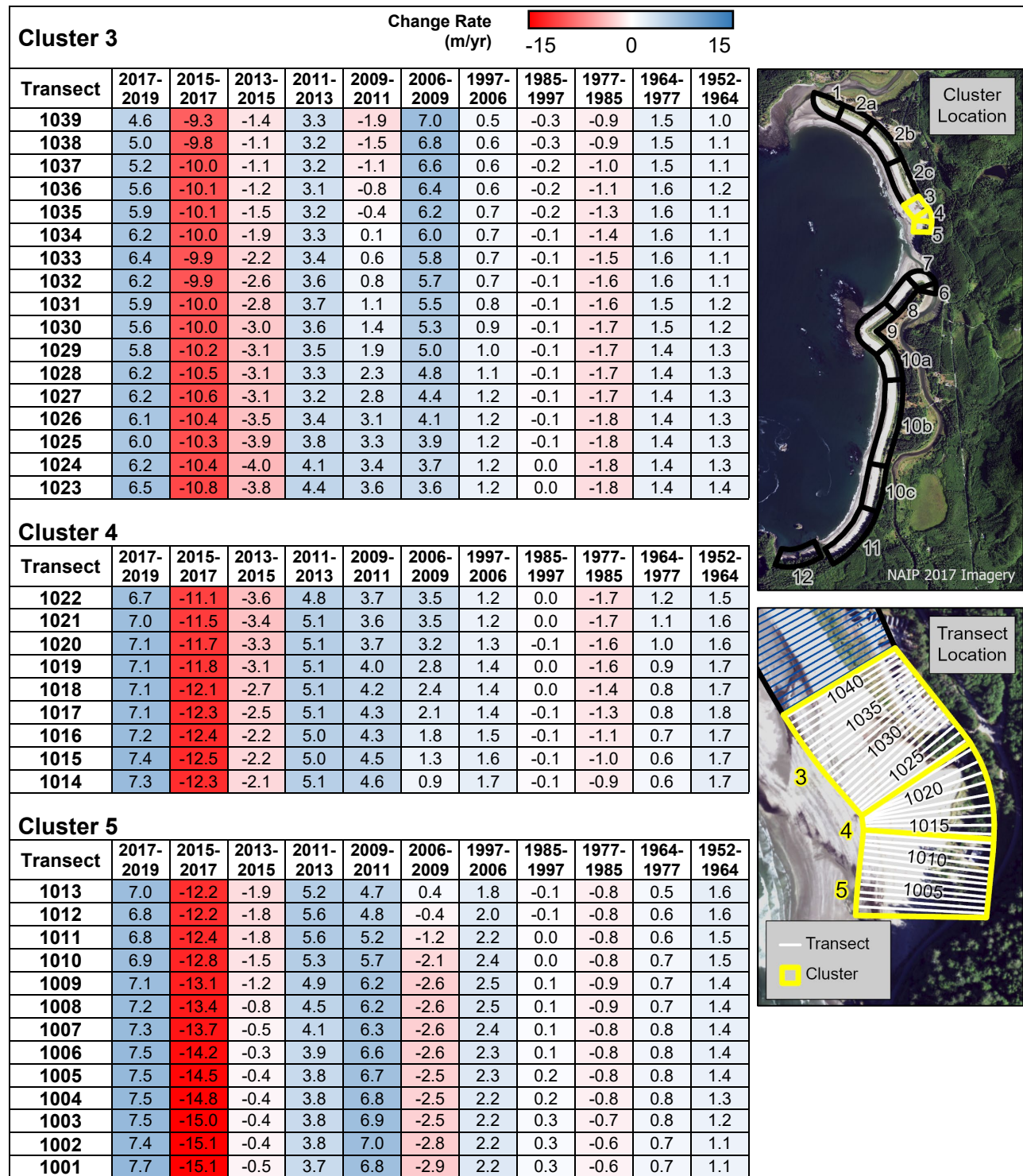


Table 25. Historical shoreline change rates in Makah Bay based on the 10-m average transects in Clusters 6 and 7.

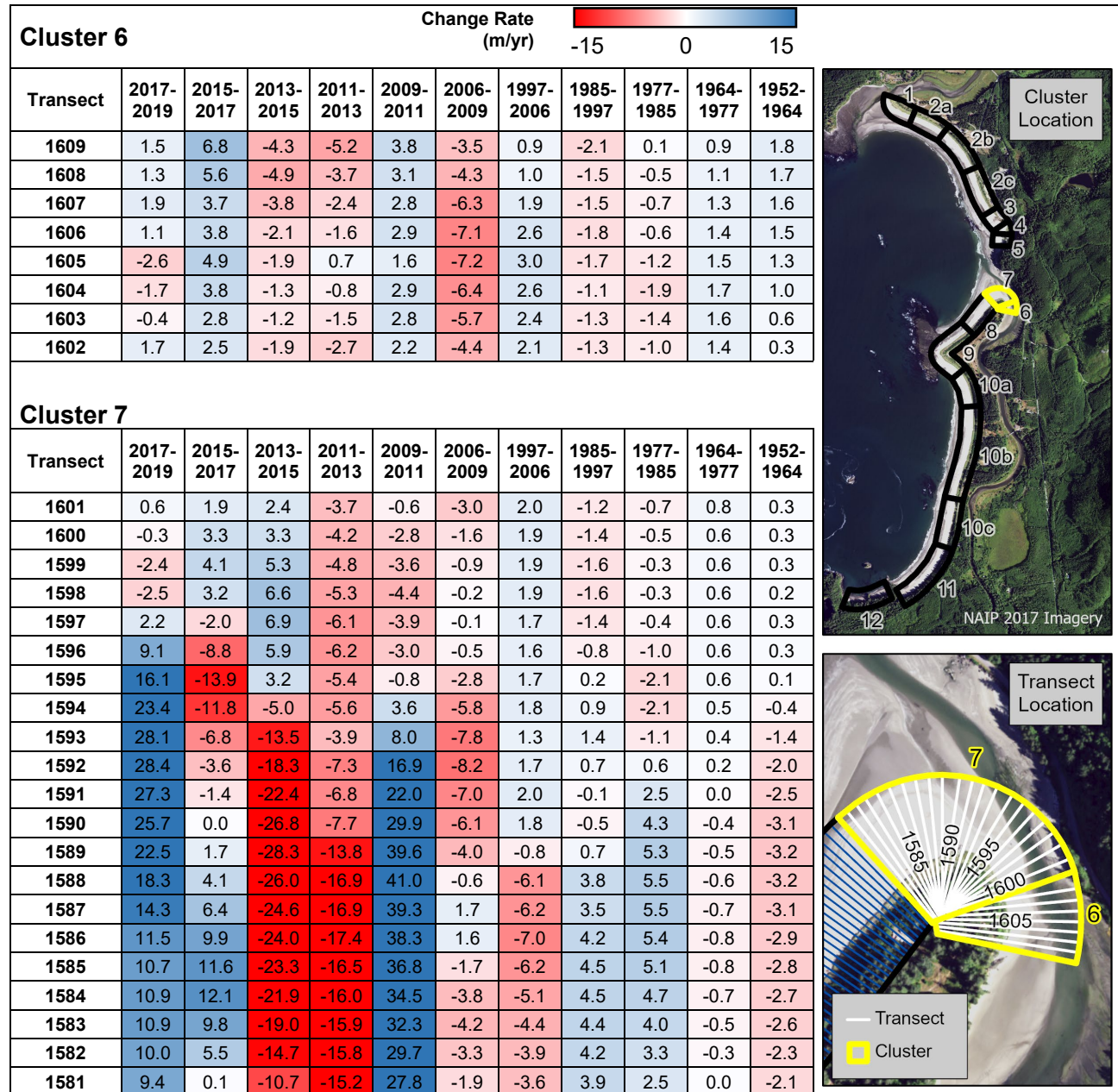


Table 26. Historical shoreline change rates in Makah Bay based on the 10-m average transects in Cluster 8.

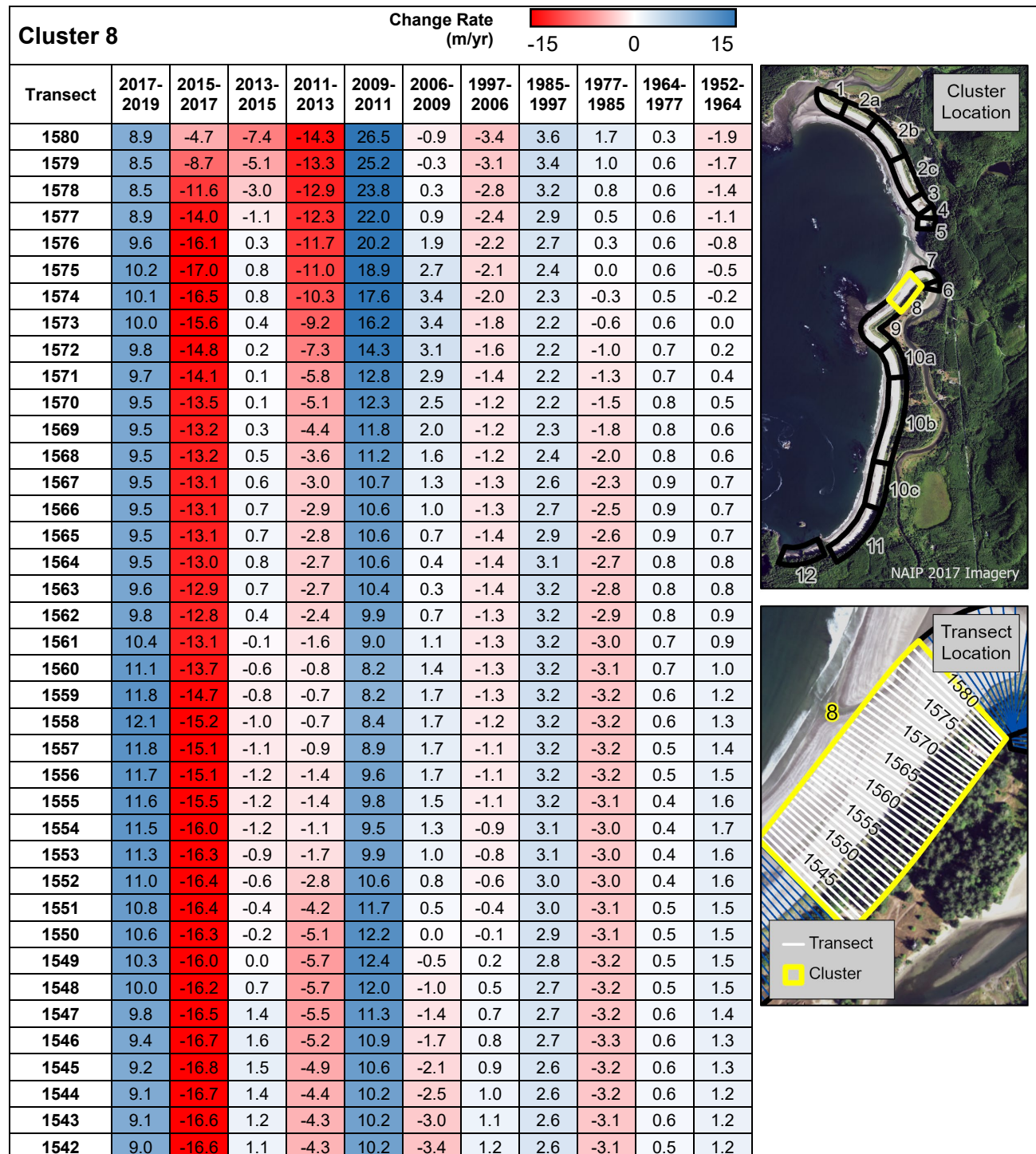


Table 27. Historical shoreline change rates in Makah Bay based on the 10-m average transects in Cluster 9.

Cluster 9	Change Rate (m/yr)										
	2017-2019	2015-2017	2013-2015	2011-2013	2009-2011	2006-2009	1997-2006	1985-1997	1977-1985	1964-1977	1952-1964
1541	9.0	-16.6	1.0	-4.6	10.5	-3.8	1.3	2.6	-3.1	0.5	1.2
1540	9.0	-16.6	1.0	-5.1	11.0	-4.3	1.4	2.6	-3.3	0.6	1.2
1539	8.7	-16.3	1.1	-5.5	11.3	-4.7	1.4	2.6	-3.5	0.7	1.2
1538	7.9	-15.4	1.2	-5.8	11.2	-4.8	1.5	2.6	-3.7	0.8	1.2
1537	7.6	-14.7	1.4	-6.1	11.0	-5.0	1.5	2.6	-3.8	0.9	1.2
1536	7.5	-14.3	1.4	-6.5	11.0	-5.2	1.5	2.6	-4.0	1.0	1.2
1535	7.3	-13.7	1.1	-7.0	11.3	-5.3	1.5	2.6	-4.1	1.1	1.2
1534	6.9	-12.9	0.8	-7.5	11.3	-5.3	1.6	2.6	-4.0	1.1	1.2
1533	6.6	-12.0	0.5	-8.1	11.1	-5.2	1.6	2.5	-4.0	1.1	1.2
1532	6.7	-11.5	0.6	-8.4	10.7	-5.1	1.6	2.5	-3.9	1.1	1.2
1531	6.7	-11.2	0.8	-8.6	10.4	-5.0	1.7	2.4	-3.8	1.0	1.2
1530	6.7	-10.8	0.9	-8.9	10.1	-4.9	1.7	2.3	-3.7	1.0	1.3
1529	6.4	-10.2	0.9	-9.1	10.0	-4.9	1.7	2.2	-3.5	1.0	1.3
1528	6.2	-9.4	0.7	-9.3	9.8	-4.8	1.7	2.1	-3.4	0.9	1.3
1527	6.1	-8.5	0.5	-9.6	9.7	-4.8	1.8	2.0	-3.3	0.9	1.3
1526	5.7	-7.7	0.2	-9.6	9.7	-4.7	1.7	2.0	-3.3	0.9	1.2
1525	5.2	-7.1	-0.7	-8.9	9.6	-4.5	1.7	1.9	-3.2	0.9	1.1
1524	5.0	-6.8	-1.3	-8.0	8.9	-4.0	1.6	1.8	-3.0	0.9	1.1
1523	4.8	-6.3	-1.9	-6.6	7.7	-3.5	1.6	1.8	-2.8	0.9	1.0
1522	4.4	-5.5	-2.6	-5.2	6.6	-3.0	1.5	1.7	-2.7	0.9	0.9
1521	3.9	-4.6	-3.2	-4.1	5.8	-2.6	1.4	1.6	-2.5	0.9	0.8
1520	3.0	-3.4	-3.7	-3.1	5.2	-2.0	1.3	1.5	-2.3	0.8	0.8
1519	2.1	-2.2	-4.1	-2.5	4.9	-1.1	0.9	1.5	-2.3	0.8	0.9
1518	1.4	-1.1	-4.5	-2.1	4.7	0.1	0.5	1.5	-2.4	0.9	0.9
1517	0.8	-0.3	-4.4	-2.2	4.7	1.1	0.2	1.5	-2.5	1.1	0.8
1516	0.4	0.2	-4.1	-2.3	4.8	2.2	-0.1	1.4	-2.7	1.4	0.7
1515	-0.1	0.8	-4.0	-2.1	4.3	3.1	-0.2	1.5	-2.7	1.6	0.5
1514	-1.0	1.7	-3.9	-1.8	3.2	3.9	-0.1	1.4	-2.2	1.5	0.3
1513	-1.8	2.7	-4.0	-1.7	2.3	4.6	-0.1	1.3	-1.2	1.2	0.1
1512	-2.1	3.2	-4.2	-1.8	1.8	5.3	0.0	1.1	-0.2	0.8	0.0
1511	-2.0	3.3	-4.3	-1.9	1.3	5.9	0.1	1.0	0.1	0.8	0.0
1510	-1.1	2.1	-4.3	-1.8	1.1	6.2	0.1	0.9	0.1	0.8	0.1
1509	0.2	0.2	-4.1	-1.3	0.8	6.4	0.1	0.8	0.1	0.8	0.3
1508	1.1	-1.8	-4.0	-0.8	0.4	6.1	0.4	0.6	-0.2	0.9	0.4
1507	1.6	-3.9	-3.4	-0.8	0.8	5.3	0.6	0.6	-0.7	1.0	0.5
1506	1.8	-5.7	-1.5	-2.1	1.5	4.5	0.8	0.6	-1.2	1.1	0.6
1505	1.6	-6.5	-0.1	-3.3	2.5	3.6	1.1	0.6	-1.9	1.1	0.5
1504	1.4	-6.9	0.1	-3.2	3.4	2.4	1.4	0.5	-2.2	0.7	0.7
1503											
1502											
1501	-4.3	5.5	-8.1	-0.8	5.9	4.2	-2.4	2.0	-1.5	-0.3	0.1
1500	-4.7	6.8	-8.8	0.3	5.6	5.0	-3.1	2.2	-1.4	-0.1	-0.2
1499	-4.8	8.0	-9.0	1.8	4.1	5.1	-3.6	2.7	-1.3	0.0	-0.6
1498	-6.2	10.2	-8.9	3.1	1.1	5.6	-3.9	3.0	-1.3	0.3	-0.8
1497	-8.4	11.9	-6.8	2.9	-1.9	6.2	-4.0	3.3	-1.3	0.5	-0.8
1496	-8.9	12.2	-2.9	-0.9	-3.3	3.8	-1.9	2.6	-1.3	0.5	-0.5
1495	-1.3	1.5	4.7	-5.4	-3.5	-3.7	2.3	1.2	-1.1	0.5	0.0
1494	4.5	-9.5	12.1	-6.5	-2.0	-1.3	3.6	0.5	-0.4	0.2	0.3
1493	6.9	-9.0	9.4	-6.1	-0.7	0.1	3.0	0.2	0.0	-0.1	0.5
1492	7.7	-9.2	7.9	-5.2	-0.3	0.3	2.8	0.1	0.3	-0.3	0.7
1491	8.4	-9.4	6.7	-4.3	0.0	0.2	2.7	0.0	0.5	-0.5	0.9
1490	8.9	-9.3	5.6	-3.6	0.1	0.1	2.6	0.1	0.6	-0.5	1.0

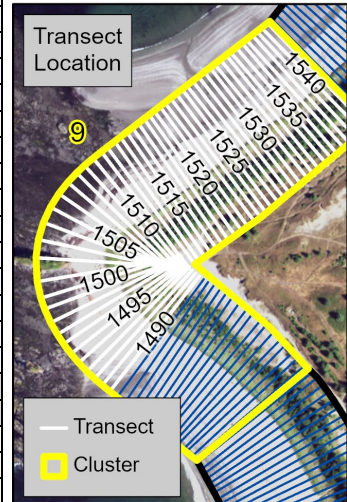


Table 28. Historical shoreline change rates in Makah Bay based on the 10-m average transects in Cluster 9, continued.

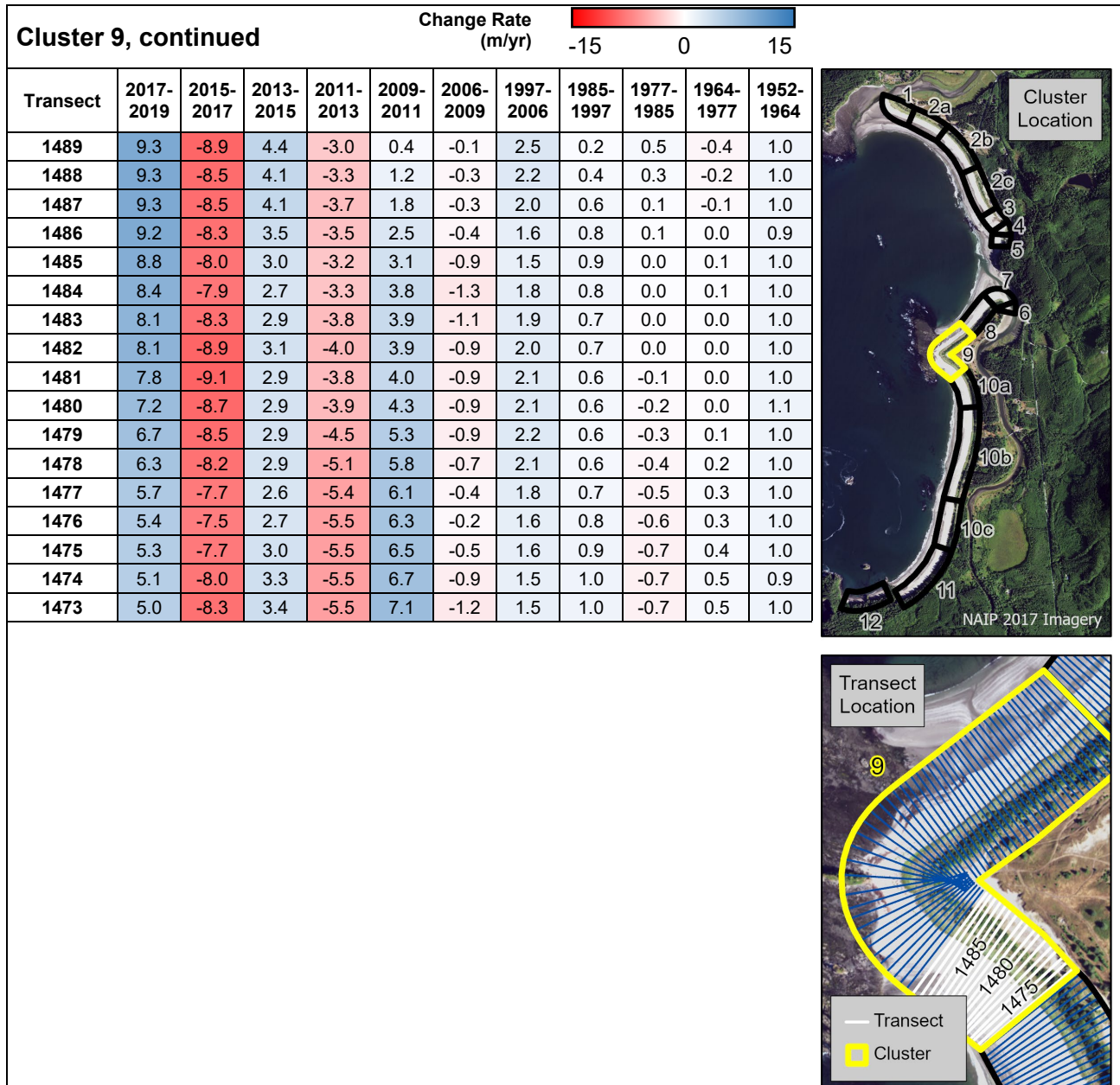


Table 29. Historical shoreline change rates in Makah Bay based on the 10-m average transects in Cluster 10a.

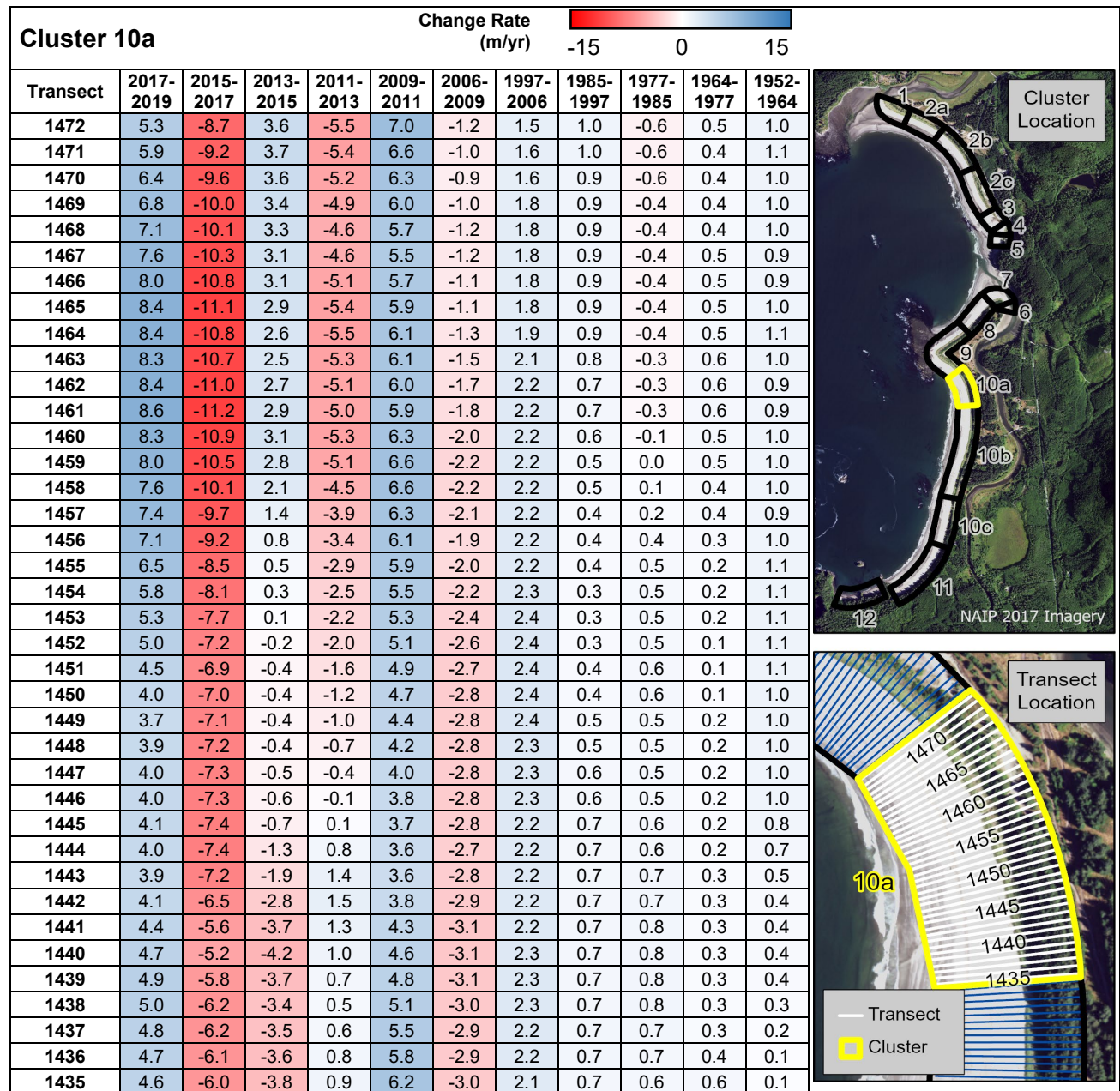


Table 30. Historical shoreline change rates in Makah Bay based on the 10-m average transects in Cluster 10b.

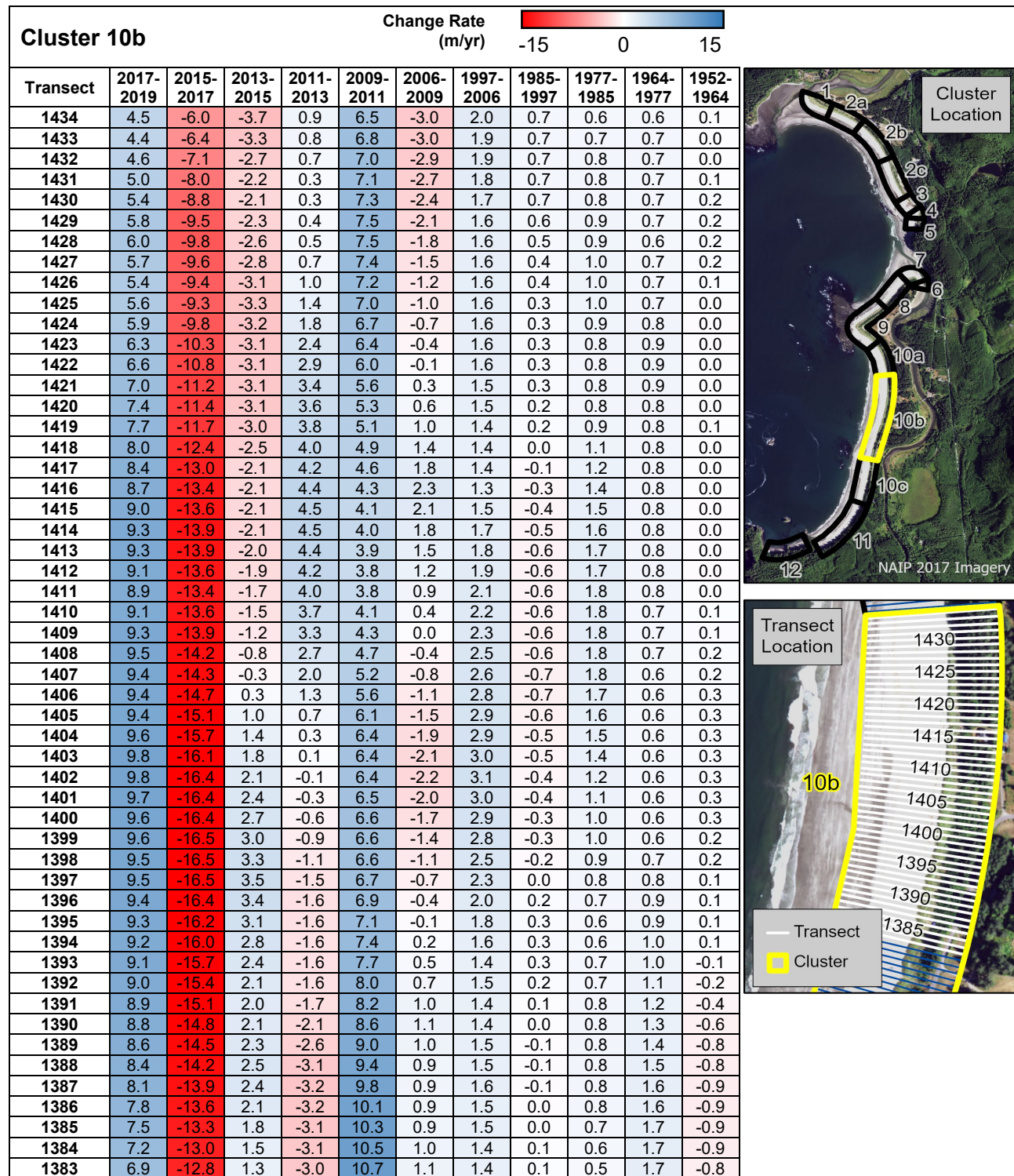


Table 31. Historical shoreline change rates in Makah Bay based on the 10-m average transects in Cluster 10b, continued.

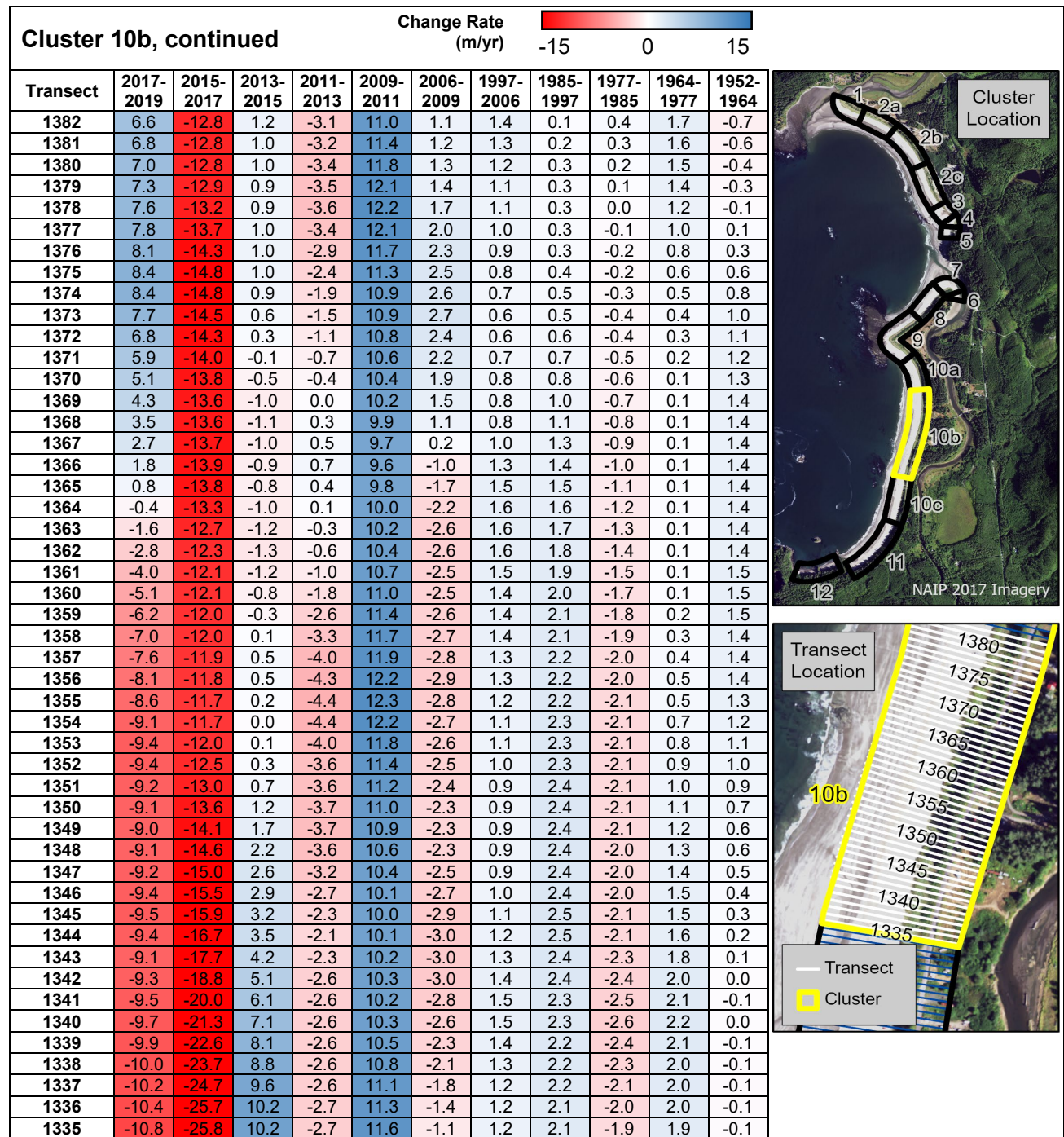


Table 32. Historical shoreline change rates in Makah Bay based on the 10-m average transects in Cluster 10c.

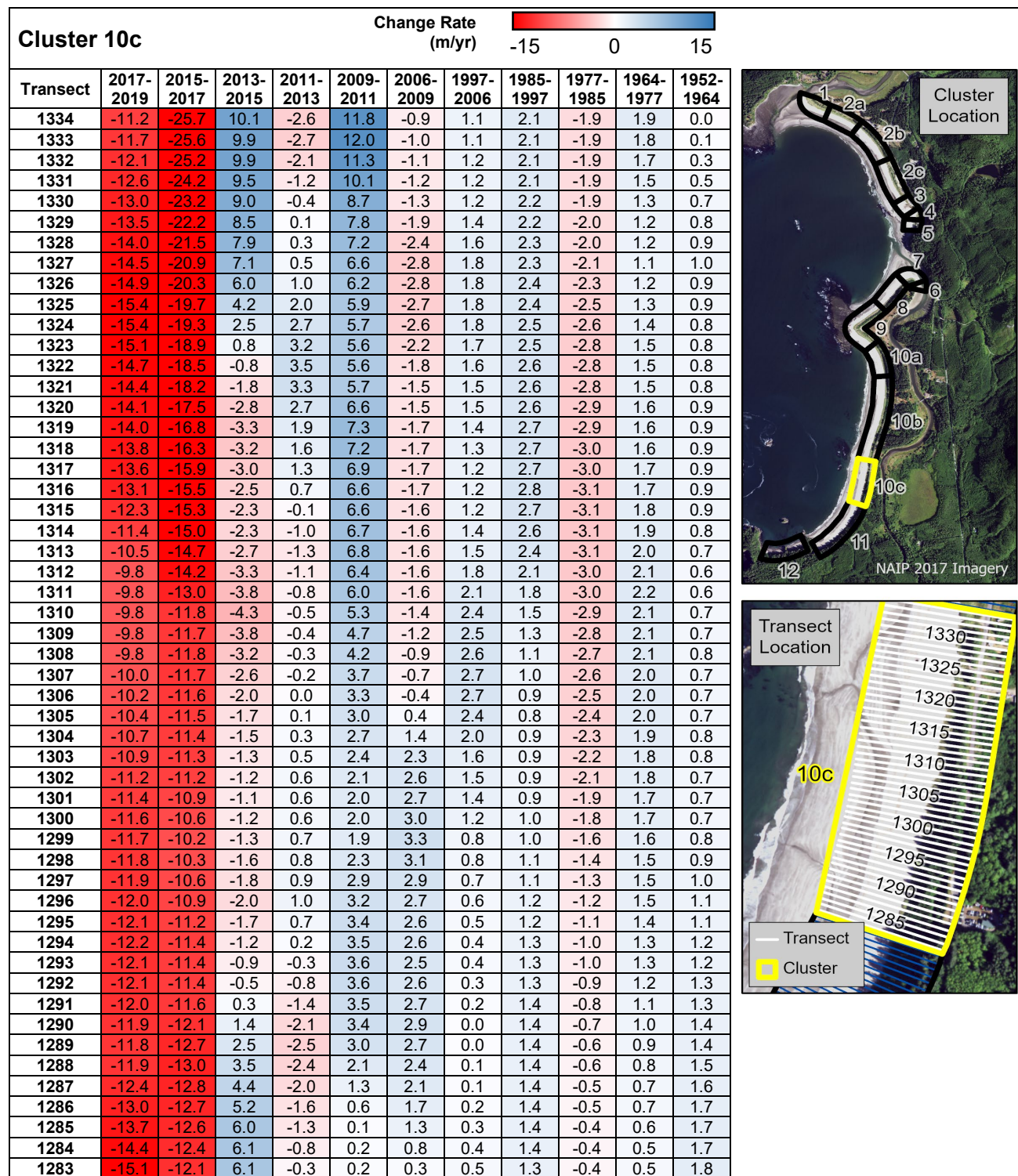


Table 33. Historical shoreline change rates in Makah Bay based on the 10-m average transects in Cluster 11.

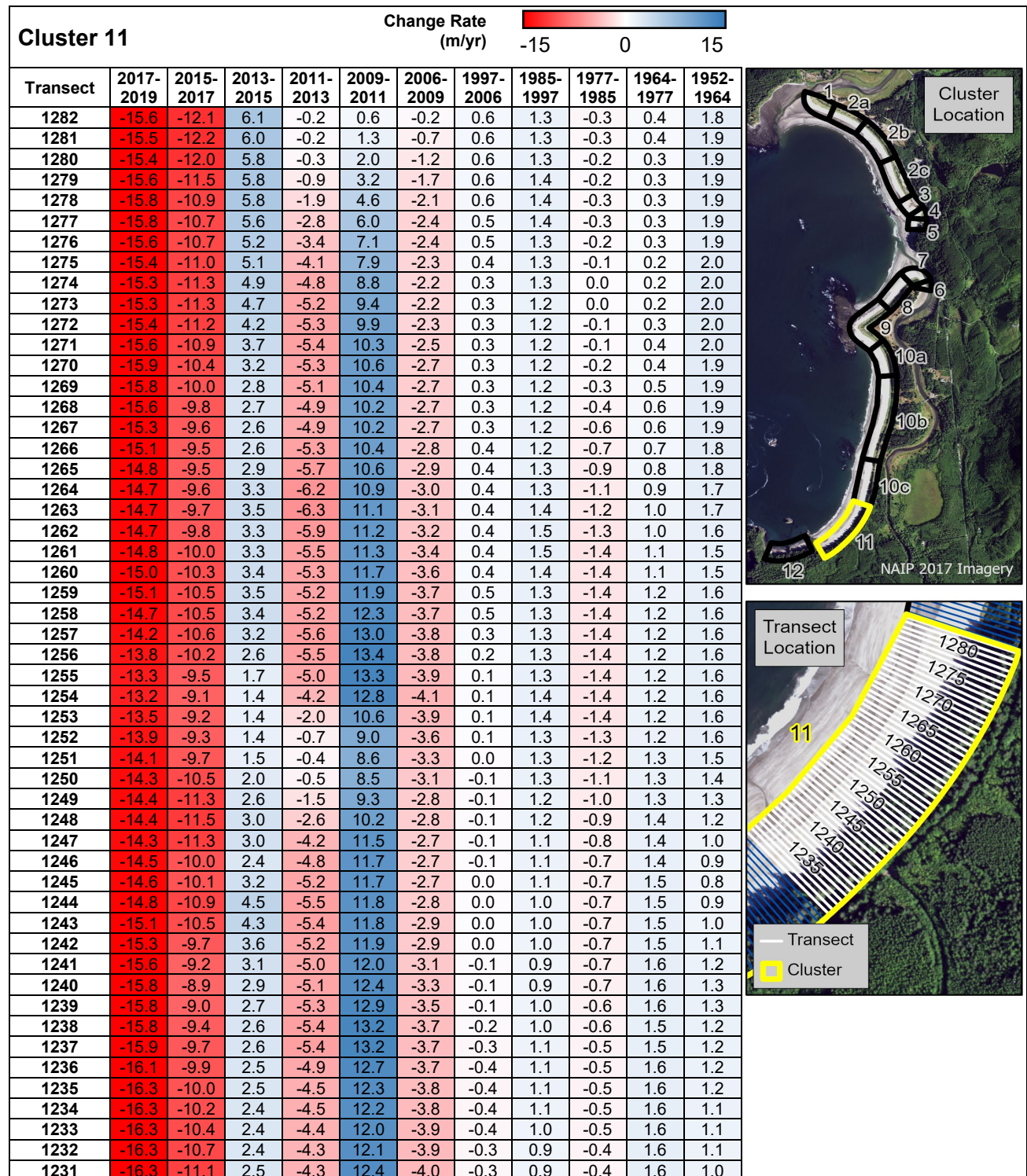
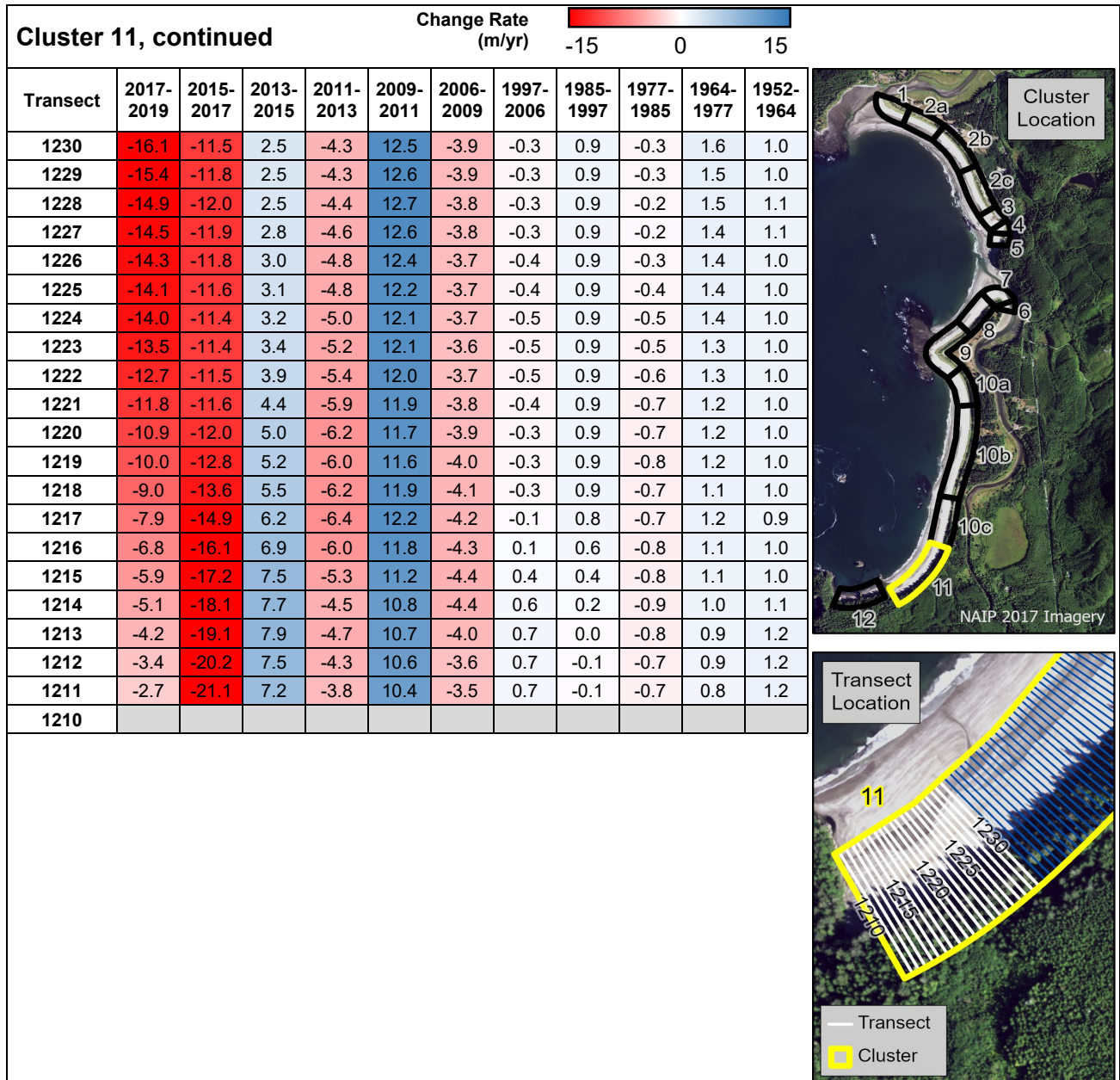


Table 34. Historical shoreline change rates in Makah Bay based on the 10-m average transects in Cluster 11, continued.



This page is purposely left blank

Appendix D. Historical Coastline Change Tables, Ozette Sub-region

Table 35. Summary of imagery years used in each cluster average change rate reported for the Ozette sub-region, with count columns showing the number of years used in each rate, and cells highlighted in green showing rates that were reported. This table shows clusters 21-36.

Cluster	Shoreline			Sand wedge			Vegetation Line		
	Count (long-term)	Count (10-year)	Years	Count (long-term)	Count (10-year)	Years	Count (long-term)	Count (10-year)	Years
21	9	6	1977, 1997, 2006, 2009, 2011, 2013, 2015, 2017, 2019	1	0	1977	0	0	1997
22	8	5	1977, 1997, 2006, 2009, 2011, 2013, 2015, 2017	1	0	1977	0	0	None
23	9	6	1977, 1997, 2006, 2009, 2011, 2013, 2015, 2017, 2019	1	0	1977	0	0	None
24	8	5	1977, 1997, 2006, 2009, 2011, 2013, 2017, 2019	1	0	1977	0	0	None
25	6	4	1977, 2006, 2009, 2011, 2013, 2015	1	0	1977	0	0	None
26	6	4	1977, 2006, 2009, 2011, 2013, 2015	1	0	1977	0	0	None
27	9	6	1977, 1997, 2006, 2009, 2011, 2013, 2015, 2017, 2019	0	0	None	6	5	1977, 2009, 2013, 2015, 2017, 2019
28	8	5	1977, 1997, 2006, 2011, 2013, 2015, 2017, 2019	0	0	None	6	5	1977, 2009, 2013, 2015, 2017, 2019
29	7	5	1977, 2006, 2009, 2011, 2013, 2015, 2019	1	1	2017	0	0	None
30	8	5	1977, 1997, 2006, 2009, 2011, 2013, 2015, 2019	1	1	2017	1	0	1977
31	8	5	1977, 1997, 2006, 2009, 2011, 2013, 2015, 2019	1	1	2017	3	2	1977, 2013, 2017
32	9	6	1977, 1997, 2006, 2009, 2011, 2013, 2015, 2017, 2019	0	0	None	1	1	2017
33	9	6	1977, 1997, 2006, 2009, 2011, 2013, 2015, 2017, 2019	0	0	None	1	1	2017
34	9	6	1977, 1997, 2006, 2009, 2011, 2013, 2015, 2017, 2019	1	0	1977	3	2	1977, 2009, 2017
35	9	6	1977, 1997, 2006, 2009, 2011, 2013, 2015, 2017, 2019	1	0	1977	2	1	1977, 2017
36	9	6	1977, 1997, 2006, 2009, 2011, 2013, 2015, 2017, 2019	4	2	1977, 1997, 2009, 2017	3	2	1977, 2013, 2017

Table 36. Summary of imagery years used in each cluster average change rate reported for the Ozette sub-region, with count columns showing the number of years used in each rate, and cells highlighted in green showing rates that were reported. This table shows clusters 37-49.

Cluster	Shoreline			Sand wedge			Vegetation Line		
	Count (long-term)	Count (10-year)	Years	Count (long-term)	Count (10-year)	Years	Count (long-term)	Count (10-year)	Years
37	9	6	1977, 1997, 2006, 2009, 2011, 2013, 2015, 2017, 2019	4	2	1977, 1997, 2009, 2017	3	2	1977, 2013, 2017
38	9	6	1977, 1997, 2006, 2009, 2011, 2013, 2015, 2017, 2019	5	2	1977, 1997, 2006, 2009, 2017	0	0	None
39	9	6	1977, 1997, 2006, 2009, 2011, 2013, 2015, 2017, 2019	5	2	1977, 1997, 2006, 2009, 2017	1	0	1977
40	9	6	1977, 1997, 2006, 2009, 2011, 2013, 2015, 2017, 2019	5	2	1977, 1997, 2006, 2009, 2017	2	0	1977, 2006
41	9	6	1977, 1997, 2006, 2009, 2011, 2013, 2015, 2017, 2019	6	3	1977, 1997, 2006, 2009, 2015, 2017	2	0	1977, 2006
42	9	6	1977, 1997, 2006, 2009, 2011, 2013, 2015, 2017, 2019	6	3	1977, 1997, 2006, 2009, 2015, 2019	0	0	None
43	9	6	1977, 1997, 2006, 2009, 2011, 2013, 2015, 2017, 2019	6	3	1977, 1997, 2006, 2009, 2015, 2019	0	0	None
44	9	6	1977, 1997, 2006, 2009, 2011, 2013, 2015, 2017, 2019	6	3	1977, 1997, 2006, 2009, 2015, 2019	0	0	None
45	9	6	1977, 1997, 2006, 2009, 2011, 2013, 2015, 2017, 2019	7	4	1977, 1997, 2006, 2009, 2015, 2017, 2019	0	0	None
46	9	6	1977, 1997, 2006, 2009, 2011, 2013, 2015, 2017, 2019	6	4	1977, 1997, 2009, 2015, 2017, 2019	0	0	None
47	9	6	1977, 1997, 2006, 2009, 2011, 2013, 2015, 2017, 2019	7	4	1977, 1997, 2006, 2009, 2015, 2017, 2019	0	0	None
48	9	6	1977, 1997, 2006, 2009, 2011, 2013, 2015, 2017, 2019	7	4	1977, 1997, 2006, 2009, 2015, 2017, 2019	0	0	None
49	9	6	1977, 1997, 2006, 2009, 2011, 2013, 2015, 2017, 2019	7	4	1977, 1997, 2006, 2009, 2015, 2017, 2019	0	0	None

Table 37. Historical shoreline change rates in the Ozette sub-region based on the 10-m average transects in Clusters 21 to 25. The sand wedge and vegetation line could not be evaluated.

						Change Rate (m/yr)		
Cluster 21								
Transect	Shoreline		Sand Wedge		Veg. Line			
	10-Year	Long-Term	10-Year	Long-Term	Long-Term			
10001	-0.79	-0.26						
10002	-1.13	-0.24						
10003	-1.18	-0.23						
10004	-1.26	-0.22						
10005	-1.28	-0.21						
10006	-1.28	-0.19						
10007	-1.32	-0.18						
10008	-1.33	-0.18						
10009	-1.33	-0.17						
10010	-1.37	-0.17						
10011	-1.40	-0.16						
10012	-1.37	-0.15						
10013	-1.21	-0.10						
10014	-1.27	-0.11						
10015	-1.21	-0.09						
10016	-0.89	-0.04						
Cluster 22								
Transect	Shoreline		Sand Wedge		Veg. Line			
	10-Year	Long-Term	10-Year	Long-Term	Long-Term			
10017	0.83	0.21						
10018	1.66	0.66						
Cluster 23								
Transect	Shoreline		Sand Wedge		Veg. Line			
	10-Year	Long-Term	10-Year	Long-Term	Long-Term			
10031	-2.60	0.28						
10032	-2.27	-0.13						
10033	-2.07	-0.14						
10034	-1.80	-0.13						
10035	-1.60	-0.09						
10036	-1.62	-0.08						
10037	-1.79	-0.08						
10038	-1.84	-0.09						
Cluster 24								
Transect	Shoreline		Sand Wedge		Veg. Line			
	10-Year	Long-Term	10-Year	Long-Term	Long-Term			
10039	-1.70	-0.04						
10040	-0.62	0.15						
Cluster 25								
Transect	Shoreline		Sand Wedge		Veg. Line			
	10-Year	Long-Term	10-Year	Long-Term	Long-Term			
10041	1.66	0.26						
10042	1.76	0.23						
10043	1.73	0.19						

Table 38. Historical shoreline change rates in the Ozette sub-region based on the 10-m average transects in Cluster 26. The sand wedge and vegetation line could not be evaluated.

Cluster 26	Change Rate (m/yr)				
	-2 0 2				
	Shoreline		Sand Wedge		Veg. Line
Transect	10-Year	Long-Term	10-Year	Long-Term	Long-Term
10044	-0.63	0.04			
10045	-1.15	-0.07			
10046	-1.18	-0.09			
10047	-1.21	-0.11			
10048	-1.17	-0.12			
10049	-1.13	-0.11			
10050	-1.09	-0.11			
10051	-1.06	-0.11			
10052	-1.08	-0.12			
10053	-1.06	-0.12			
10054	-1.06	-0.11			
10055	-1.09	-0.12			
10056	-1.12	-0.15			
10057	-1.66	-0.17			
10058	-3.02	-0.17			
10059	-2.10	-0.19			
10060	-1.74	-0.20			
10061	-1.74	-0.22			
10062	-1.67	-0.23			
10063	-1.63	-0.23			
10064	-1.56	-0.22			
10065	-1.48	-0.21			
10066	-1.37	-0.19			
10067	-1.34	-0.17			
10068	-1.39	-0.16			
10069	-1.49	-0.17			
10070	-1.57	-0.18			
10071	-1.64	-0.20			
10072	-1.69	-0.20			
10073	-1.58	-0.19			
10074	-1.35	-0.17			
10075	-1.17	-0.16			
10076	-0.46	-0.06			
10077	-0.50	-0.08			
10078	-0.61	-0.08			
10079	-1.03	-0.15			
10080	-1.14	-0.16			
10081	-1.15	-0.16			
10082	-1.14	-0.15			
10083	-1.21	-0.15			
10084	-1.28	-0.15			
10085	-1.31	-0.17			
10086	-1.31	-0.19			
10087	-1.32	-0.20			
10088	-1.36	-0.20			
10089	-1.39	-0.21			
10090	-1.37	-0.20			
10091	-1.45	-0.20			
10092	-1.52	-0.20			
10093	-1.57	-0.20			
10094	-1.53	-0.19			
10095	-1.49	-0.18			
10096	-1.49	-0.16			

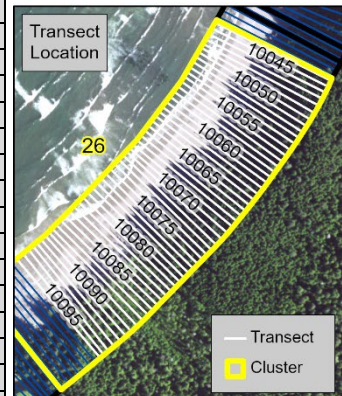
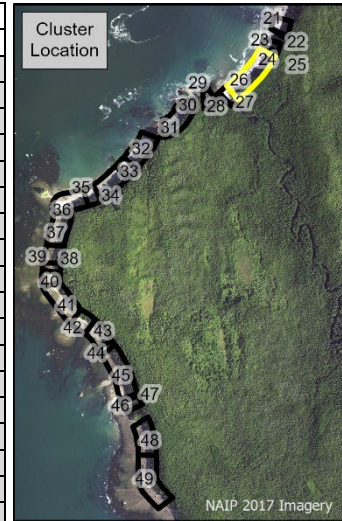


Table 39. Historical shoreline and vegetation line change rates in the Ozette sub-region based on the 10-m average transects in Cluster 26 (continued) through Cluster 29. The sand wedge could not be evaluated.

		Change Rate (m/yr)			
Cluster 26, contd.					
Transect	Shoreline		Sand Wedge		Veg. Line
	10-Year	Long-Term	10-Year	Long-Term	Long-Term
10097	-1.50	-0.13			
10098	-1.54	-0.11			
10099	-1.61	-0.09			
10100	-1.63	-0.07			
10101	-1.62	-0.05			
10102	-1.62	-0.03			
10103	-1.66	-0.01			
Cluster 27					
Transect	Shoreline		Sand Wedge		Veg. Line
	10-Year	Long-Term	10-Year	Long-Term	Long-Term
10104	-1.78	0.01			
10105	-1.96	0.04			-0.22
10106	-1.90	0.06			-0.16
10107	-1.94	0.07			-0.13
10108	-1.84	0.07			-0.13
10109	-1.85	0.08			-0.07
10110	-2.26	0.07			-0.06
10111	-3.02	0.08			-0.04
10112	-3.34	0.12			0.05
10113	-2.62	0.14			0.16
10114	-1.89	0.12			0.20
Cluster 28					
Transect	Shoreline		Sand Wedge		Veg. Line
	10-Year	Long-Term	10-Year	Long-Term	Long-Term
10115	-0.57	-0.20			0.29
10116	-0.73	-0.85			0.22
Cluster 29					
Transect	Shoreline		Sand Wedge		Veg. Line
	10-Year	Long-Term	10-Year	Long-Term	Long-Term
10117		-0.41			
10118		0.11			
10119	-0.57	0.12			
10120	-1.11	0.13			
10121	-1.64	0.12			
10122	-1.45	0.07			
10123	-1.31	0.04			
10124	-1.22	0.02			
10125	-1.15	-0.01			
10126	-1.44	-0.04			
10127	-0.75	-0.09			
10128	-0.65	-0.09			

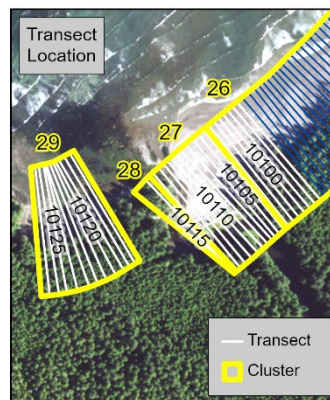
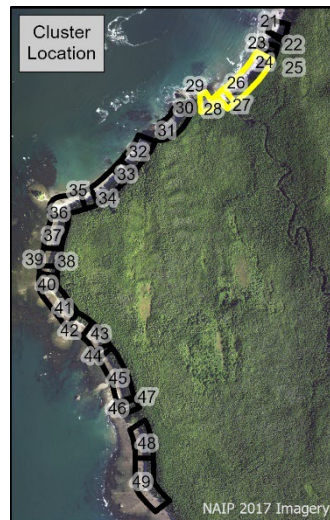


Table 40. Historical shoreline and vegetation line change rates in the Ozette sub-region based on the 10-m average transects in Clusters 30 and 31. The sand wedge could not be evaluated.

						Change Rate (m/yr)	
						-2 0 2	
Cluster 30							
Transect	Shoreline		Sand Wedge		Veg. Line		
	10-Year	Long-Term	10-Year	Long-Term	Long-Term		
10129	-1.66	0.01					
10130	-1.98	-0.04					
10131	-2.02	-0.09					
10132	-1.87	-0.15					
10133	-1.74	-0.19					
10134	-1.68	-0.23					
10135	-1.60	-0.26					
10136	-1.49	-0.29					
10137	-1.36	-0.32					
Cluster 31							
Transect	Shoreline		Sand Wedge		Veg. Line		
	10-Year	Long-Term	10-Year	Long-Term	Long-Term		
10138	-1.29	-0.35					
10139	-1.24	-0.38					
10140	-1.19	-0.39					
10141	-1.13	-0.39					
10142	-1.05	-0.37					
10143	-0.96	-0.37					
10144	-0.93	-0.39					
10145	-0.90	-0.40					
10146	-0.88	-0.39					
10147	-0.96	-0.37					
10148	-1.05	-0.35					
10149	-1.11	-0.35					
10150	-1.12	-0.35					
10151	-1.11	-0.33					
10152	-1.12	-0.30					
10153	-1.16	-0.29					
10154	-1.17	-0.28					
10155	-1.20	-0.26				-0.18	
10156	-1.22	-0.26				-0.18	
10157	-1.09	-0.29				-0.19	
10158	-0.99	-0.30				-0.19	
10159	-0.92	-0.30				-0.18	
10160	-0.83	-0.28				-0.21	
10161	-1.00	-0.27				-0.25	
10162	-1.16	-0.25				-0.27	
10163	-0.79	-0.25				-0.29	
10164	-0.65	-0.23				-0.32	
10165	-0.56	-0.23				-0.32	
10166	-0.44	-0.22				-0.26	
10167		-0.24				-0.22	
10168		-0.22				-0.20	
10169		-0.20					
10170		-0.20					
10171		-0.21					
10172		-0.20					
10173		-0.20					

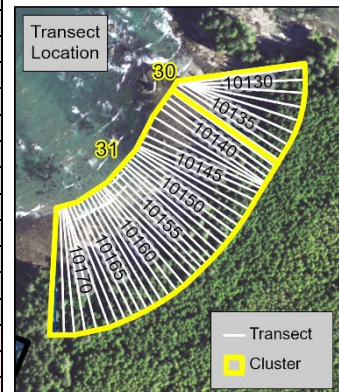
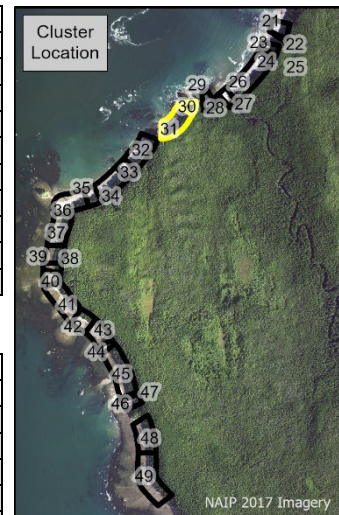


Table 41. Historical shoreline change rates in the Ozette sub-region based on 10-m average transects in Clusters 32 and 33. The sand wedge and vegetation line could not be evaluated.

		Change Rate (m/yr)			
		-2		0	
		2			
Cluster 32					
Transect	Shoreline		Sand Wedge		Veg. Line
	10-Year	Long-Term	10-Year	Long-Term	Long-Term
10193	-0.23	-0.04			
10194	-0.18	-0.02			
10195	-0.16	0.00			
10196	-0.18	0.00			
10197	-0.27	0.01			
10198	-0.81	-0.07			
10199	-0.62	-0.02			
10200	-0.19	0.03			
10201	-0.70	0.05			
10202	-0.77	0.06			
10203	-0.90	0.08			
10204	-1.02	0.09			
10205	-1.08	0.11			
10206	-1.01	0.14			
10207	-0.96	0.17			
10208	-0.90	0.20			
10209	-0.90	0.21			
10210	-0.84	0.21			
10211	-0.75	0.21			
10212	-0.59	0.22			
10213	-0.47	0.23			
10214	-0.47	0.24			
10215	-0.54	0.24			
10216	-0.54	0.23			
10217	-0.55	0.21			
10218	-0.57	0.21			
10219	-0.55	0.21			
10220	-0.50	0.21			
10221	-0.47	0.22			
10222	-0.39	0.23			
10223	-0.32	0.24			
10224	-0.29	0.24			
10225	-0.23	0.25			
10226	-0.17	0.25			
10227	-0.16	0.25			
10228	-0.15	0.26			
10229	-0.97	0.26			
Cluster 33					
Transect	Shoreline		Sand Wedge		Veg. Line
	10-Year	Long-Term	10-Year	Long-Term	Long-Term
10230	-1.48	0.27			
10231	-1.53	0.26			
10232	-1.58	0.24			
10233	-1.72	0.23			
10234	-1.85	0.21			
10235	-1.92	0.19			
10236	-1.85	0.18			
10237	-1.86	0.18			
10238	-1.88	0.18			
10239	-1.81	0.18			
10240	-1.81	0.19			
10241	-1.94	0.19			
10242	-2.16	0.18			
10243	-1.54	0.17			

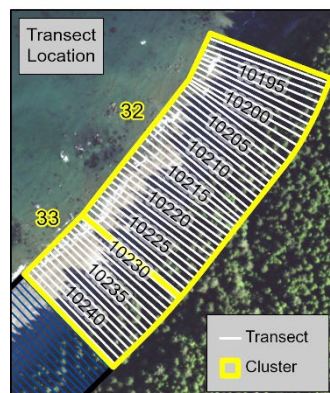
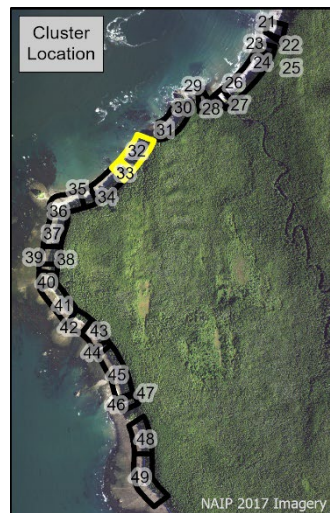


Table 42. Historical shoreline and vegetation line change rates in the Ozette sub-region based on the 10-m average transects in Clusters 34 and 35. The sand wedge could not be evaluated.

		Change Rate (m/yr)			
		-2 0 2			
Cluster 34					
Transect	Shoreline		Sand Wedge		Veg. Line
	10-Year	Long-Term	10-Year	Long-Term	Long-Term
10244	-0.94	0.17			
10245	-0.88	0.19			
10246	-0.77	0.21			
10247	-0.64	0.23			
10248	-0.59	0.24			
10249	-0.60	0.24			
10250	-0.69	0.24			
10251	-0.82	0.24			
10252	-0.85	0.23			
10253	-0.87	0.22			
10254	-0.93	0.20			
10255	-1.12	0.18			
10256	-1.38	0.15			
10257	-1.38	0.15			
10258	-1.32	0.16			
10259	-1.27	0.16			
10260	-1.24	0.14			
10261	-1.21	0.12			
10262	-1.20	0.10			
10263	-1.23	0.08			
10264	-1.25	0.07			
10265	-1.24	0.07			
10266	-1.21	0.07			
10267	-1.17	0.07			
10268	-1.13	0.06			
10269	-1.14	0.05			-0.02
10270	-1.11	0.03			-0.01
10271	-1.06	0.02			0.00
10272	-1.04	0.02			-0.01
10273	-1.04	0.02			0.00
10274	-1.04	0.02			-0.01
10275	-1.07	0.03			-0.02
10276	-1.11	0.02			-0.03
10277	-1.11	0.00			
10278	-1.15	0.00			
10279	-1.25	0.00			
Cluster 35					
Transect	Shoreline		Sand Wedge		Veg. Line
	10-Year	Long-Term	10-Year	Long-Term	Long-Term
10280	-1.34	-0.01			
10281	-1.44	-0.01			
10282	-1.53	-0.01			
10283	-1.62	-0.01			
10284	-1.71	-0.03			
10285	-1.79	-0.05			
10286	-1.78	-0.05			
10287	-1.70	-0.05			
10288	-1.62	-0.06			
10289	-1.53	-0.06			
10290	-1.50	-0.07			
10291	-1.56	-0.08			
10292	-1.64	-0.08			
10293	-1.70	-0.08			

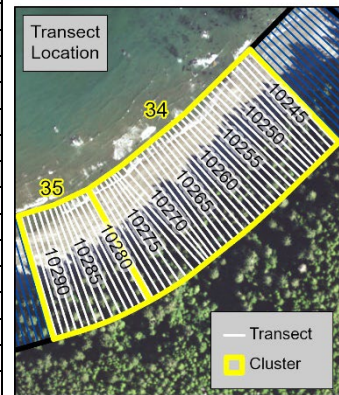
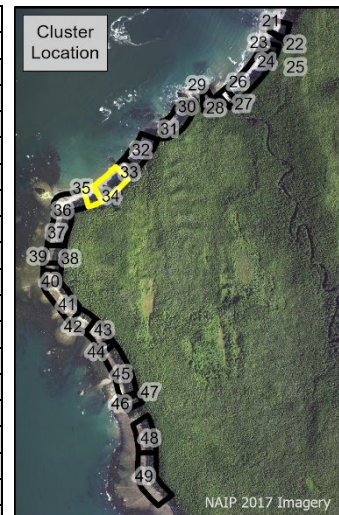


Table 43. Historical shoreline, sand wedge, and vegetation line change rates in the Ozette sub-region based on the 10-m average transects in Cluster 36.

Cluster 36					
Transect	Shoreline		Sand Wedge		Veg. Line
	10-Year	Long-Term	10-Year	Long-Term	Long-Term
10294	-1.73	-0.09			
10295	-1.77	-0.09			
10296	-1.80	-0.08			
10297	-1.86	-0.07			
10298	-1.93	-0.06			
10299	-2.01	-0.06			
10300	-2.04	-0.06			
10301	-2.04	-0.06			
10302	-2.04	-0.10			
10303	-2.07	-0.06			-0.62
10304	-2.16	-0.06			-0.61
10305	-2.27	-0.07			-0.54
10306	-2.37	-0.08			-0.44
10307	-2.42	-0.08			-0.32
10308	-2.47	-0.08			-0.40
10309	-2.44	-0.09			-0.08
10310	-2.39	-0.09			0.04
10311	-2.33	-0.09			0.02
10312	-2.27	-0.09			0.04
10313	-2.19	-0.09			0.05
10314	-2.06	-0.09			0.06
10315	-1.90	-0.09			0.06
10316	-1.74	-0.09			0.04
10317	-1.67	-0.10			0.02
10318	-1.82	-0.12			0.02
10319	-2.47	-0.15			0.03
10320	-3.88	-0.17			0.02
10321	-2.39	-0.34			0.02
10322	-3.88				
10323	-2.66	-0.06			0.02
10324	-2.48	0.07			0.02
10325	-2.06	0.05		0.34	0.03
10326	-1.95	0.07		0.33	-0.03
10327	-1.95	0.06		0.19	-0.04
10328	-1.91	0.03		-0.01	-0.07
10329	-1.77	0.03		0.03	-0.05
10330	-1.61	0.03		-0.03	-0.03
10331	-1.52	0.01		-0.08	-0.01
10332	-1.45	-0.01		-0.14	-0.01

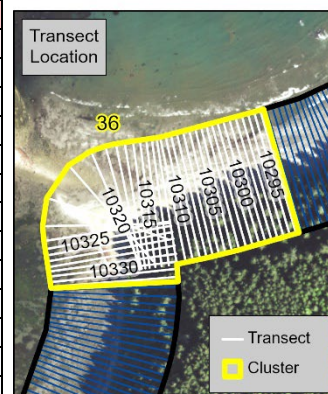
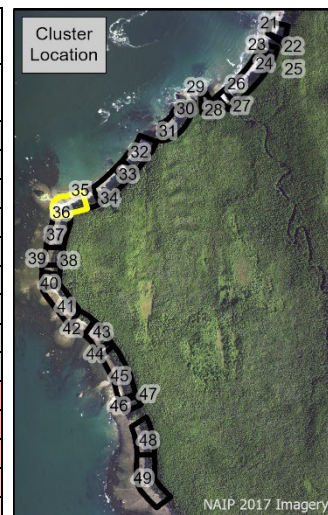


Table 44. Historical shoreline, sand wedge, and vegetation line change rates in the Ozette sub-region based on the 10-m average transects in Cluster 37.

Cluster 37					
Change Rate (m/yr)					
Transect	Shoreline		Sand Wedge		Veg. Line
	10-Year	Long-Term	10-Year	Long-Term	Long-Term
10333	-1.32	-0.01		-0.20	-0.02
10334	-1.17	-0.01		-0.27	-0.04
10335	-1.12	-0.03		-0.27	-0.04
10336	-1.10	-0.04		-0.29	-0.05
10337	-1.08	-0.04		-0.36	-0.06
10338	-1.00	-0.04		-0.41	-0.04
10339	-0.92	-0.05		-0.44	-0.03
10340	-0.87	-0.04		-0.46	-0.02
10341	-0.83	-0.02		-0.46	0.00
10342	-0.83	-0.01		-0.45	-0.01
10343	-0.85	-0.03		-0.47	-0.01
10344	-0.90	-0.04		-0.49	-0.03
10345	-0.99	-0.05		-0.52	0.00
10346	-1.08	-0.06		-0.56	0.00
10347	-1.20	-0.09		-0.58	-0.02
10348	-1.37	-0.11		-0.59	-0.03
10349	-1.54	-0.13		-0.61	-0.06
10350	-1.75	-0.15		-0.62	-0.07
10351	-2.02	-0.19		-0.63	-0.08
10352	-2.17	-0.23		-0.63	-0.07
10353	-1.84	-0.23		-0.63	-0.09
10354	-1.56	-0.25		-0.65	
10355	-1.34	-0.27		-0.71	
10356	-1.17	-0.30		-0.75	
10357	-1.10	-0.33		-0.77	
10358	-1.08	-0.36		-0.77	
10359	-1.07	-0.38		-0.77	
10360	-1.10	-0.41		-0.75	
10361	-1.15	-0.44		-0.75	
10362	-1.21	-0.47		-0.70	
10363	-1.25	-0.49		-0.66	
10364	-1.23	-0.49		-0.64	
10365	-1.22	-0.48		-0.62	
10366	-1.23	-0.46		-0.60	
10367	-1.18	-0.44		-0.60	
10368	-1.11	-0.41		-0.61	
10369	-0.98	-0.39		-0.62	

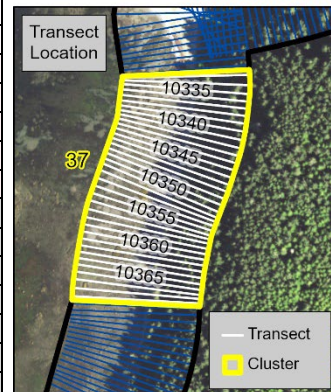
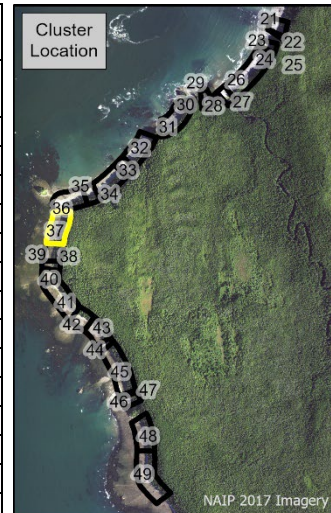


Table 45. Historical shoreline and sand wedge change rates in the Ozette sub-region based on the 10-m average transects in Cluster 37 to 40. The vegetation line could not be evaluated.

Change Rate (m/yr)					
-2 0 2					
Cluster 38					
Transect	Shoreline		Sand Wedge		Veg. Line
	10-Year	Long-Term	10-Year	Long-Term	Long-Term
10370	-0.84	-0.36		-0.60	
10371	-0.84	-0.34		-0.59	
10372	-0.89	-0.34		-0.57	
10373	-0.91	-0.35		-0.54	
10374	-0.86	-0.34		-0.51	
10375	-0.77	-0.32		-0.47	
10376	-0.65	-0.30		-0.45	
10377	-0.60	-0.28		-0.44	
10378	-0.57	-0.27		-0.42	
10379	-0.56	-0.28		-0.39	
10380	-0.55	-0.27		-0.40	
10381	-0.52	-0.26		-0.41	
10382	-0.53	-0.25		-0.42	
10383	-0.52	-0.24		-0.43	
10384	-0.49	-0.22		-0.45	
10385	-0.45	-0.22		-0.47	
10386	-0.42	-0.21		-0.47	
10387	-0.81	-0.21		-0.46	
10388	-1.20	-0.23		-0.42	
10389	-1.20	-0.16		-0.38	
Cluster 39					
Transect	Shoreline		Sand Wedge		Veg. Line
	10-Year	Long-Term	10-Year	Long-Term	Long-Term
10390	-0.34	-0.07		-0.32	
10391	-0.01	-0.04		-0.28	
10392	0.39	-0.03		-0.26	
10393	0.54	-0.01		-0.29	
10394	0.53	0.00		-0.32	
10395	0.61	-0.02		-0.34	
10396	0.66	-0.06		-0.35	
10397	0.68	-0.11		-0.37	
10398	0.71	-0.16		-0.40	
10399	0.70	-0.20		-0.45	
Cluster 40					
Transect	Shoreline		Sand Wedge		Veg. Line
	10-Year	Long-Term	10-Year	Long-Term	Long-Term
10400	0.67	-0.22		-0.48	
10401	0.60	-0.22		-0.46	
10402	0.51	-0.21		-0.43	
10403	0.41	-0.21		-0.42	
10404	0.33	-0.20		-0.43	
10405	0.28	-0.19		-0.43	
10406	0.23	-0.19		-0.43	
10407	0.27	-0.16		-0.41	
10408	0.19	-0.14		-0.38	
10409	0.08	-0.13		-0.34	
10410	0.24	-0.11		-0.32	
10411	0.24	-0.11		-0.32	
10412	0.23	-0.10		-0.30	
10413	0.19	-0.12		-0.30	
10414	0.12	-0.15		-0.33	

Cluster Location

NAIP 2017 Imagery

Transect Location

Transect

Cluster

Table 46. Historical shoreline and sand wedge change rates in the Ozette sub-region based on the 10-m average transects in Cluster 41. The vegetation line could not be evaluated.

Cluster 41					
Transect	Shoreline		Sand Wedge		Veg. Line
	10-Year	Long-Term	10-Year	Long-Term	Long-Term
10415	-0.51	-0.16		-0.39	
10416	-0.62	-0.17		-0.44	
10417	-0.79	-0.17		-0.52	
10418	-0.89	-0.16		-0.61	
10419	-0.86	-0.16		-0.68	
10420	-0.69	-0.13		-0.72	
10421	-0.63	-0.13		-0.61	
10422	-0.53	-0.13		-0.49	
10423	-0.45	-0.16		-0.43	
10424	-0.36	-0.18		-0.40	
10425	-0.34	-0.19		-0.34	
10426	-0.33	-0.20		-0.31	
10427	-0.31	-0.18	-0.55	-0.36	
10428	-0.20	-0.17	-0.18	-0.42	
10429	-0.26	-0.14	-0.08	-0.43	
10430	-0.48	-0.10	-0.87	-0.34	
10431	-0.45	-0.05	-1.09	-0.32	
10432	-0.44	-0.08	-0.61	-0.40	
10433	-0.50	-0.15	-0.72	-0.43	
10434	-0.39	-0.19	-0.81	-0.39	
10435	-0.30	-0.18	-0.74	-0.36	
10436	-0.25	-0.18	-0.66	-0.37	
10437	-0.30	-0.16	-0.60	-0.36	
10438	-0.36	-0.14		-0.33	
10439	-0.32	-0.14		-0.30	
10440	-0.44	-0.14		-0.29	
10441	-0.86	-0.15		-0.29	
10442	-0.39	-0.15		-0.34	
10443	-0.35	-0.20		-0.39	
10444	-0.52	-0.23		-0.42	
10445	-0.59	-0.24		-0.40	
10446	-0.60	-0.24		-0.38	
10447	-0.47	-0.22		-0.39	
10448	-0.40	-0.20		-0.38	
10449	-0.37	-0.18		-0.35	
10450	-0.40	-0.17		-0.35	
10451	-0.56	-0.14		-0.32	
10452	-0.41	-0.11		-0.29	
10453	-0.60	-0.09		-0.27	
10454	-0.77	-0.09		-0.26	
10455	-0.56	-0.06		-0.19	
10456	-0.74	-0.01		-0.17	
10457	-0.97	-0.05		-0.22	
10458	-0.49	-0.05		-0.21	
10459	-0.36	-0.03		-0.20	

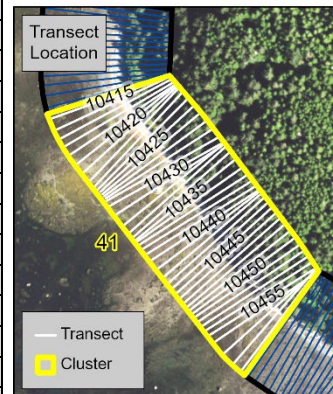
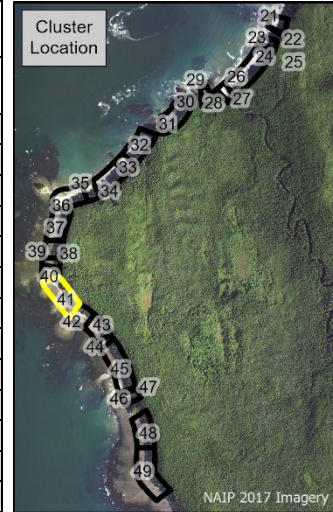
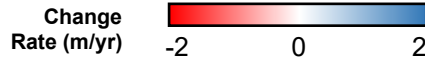


Table 47. Historical shoreline and sand wedge change rates in the Ozette sub-region based on the 10-m average transects in Cluster 42 and 43. The vegetation line could not be evaluated.

		Change Rate (m/yr)			
		-2 0 2			
Cluster 42					
Transect	Shoreline		Sand Wedge		Veg. Line
	10-Year	Long-Term	10-Year	Long-Term	Long-Term
10460	-0.26	-0.04		-0.18	
10461	-0.24	-0.07		-0.17	
10462	-0.31	-0.09		-0.19	
10463	-0.16	-0.12		-0.26	
10464	-0.10	-0.14		-0.28	
10465	-0.07	-0.15	-0.70	-0.38	
10466	-0.12	-0.16	-0.69	-0.43	
10467	0.38	-0.18	-0.69	-0.47	
10468	0.62	-0.20	-0.59	-0.50	
10469	0.26	-0.23	-0.52	-0.52	
10470	0.05	-0.25	-0.50	-0.53	
10471	0.06	-0.27	-0.53	-0.55	
10472	0.03	-0.27	-0.65	-0.57	
10473	0.03	-0.27	-0.80	-0.60	
10474	0.31	-0.26	-0.71	-0.62	
10475	0.79	-0.25	-0.62	-0.61	
10476	0.74	-0.22	-0.60	-0.57	
10477	0.46	-0.19	-0.43	-0.49	
10478	0.77	-0.16	-0.36	-0.43	
10479	0.20	-0.18		-0.41	
Cluster 43					
Transect	Shoreline		Sand Wedge		Veg. Line
	10-Year	Long-Term	10-Year	Long-Term	Long-Term
10480	-0.08	-0.22		-0.47	
10481	-0.14	-0.24	-0.51	-0.51	
10482	-0.21	-0.24	-0.67	-0.52	
10483	-0.24	-0.24	-0.91	-0.46	
10484	-0.29	-0.23	-1.02	-0.39	
10485	-0.28	-0.20	-0.88	-0.31	
10486	-0.27	-0.23	-0.93	-0.30	
10487	-0.36	-0.25	-1.04	-0.31	
10488	-0.37	-0.25	-1.09	-0.30	
10489	-0.47	-0.25	-1.20	-0.31	
10490	-0.45	-0.22	-1.33	-0.30	
10491	-0.34	-0.18	-1.37	-0.25	
10492	-0.30	-0.15	-1.35	-0.23	
10493	-0.55	-0.14	-1.60	-0.26	
10494	-0.66	-0.15	-1.77	-0.28	
10495	-0.67	-0.14	-1.82	-0.26	
10496	-0.68	-0.13	-1.89	-0.27	
10497	-0.65	-0.11	-1.87	-0.26	
10498	-0.58	-0.08	-1.87	-0.28	
10499	-0.48	-0.08	-1.83	-0.29	
10500	-0.34	-0.08	-1.58	-0.27	
10501	-0.27	-0.07	-1.43	-0.29	
10502	-0.35	-0.03	-1.40	-0.29	
10503	-0.45	0.03	-1.45	-0.21	
10504	-0.60	0.06	-1.77	-0.18	
10505	-0.37	0.06	-1.63	-0.15	

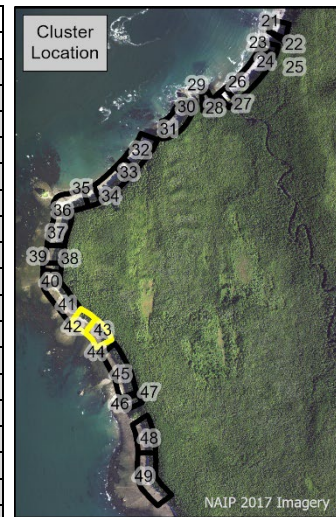


Table 48. Historical shoreline and sand wedge change rates in the Ozette sub-region based on the 10-m average transects in Cluster 44 and 45. The vegetation line could not be evaluated.

		Change Rate (m/yr)				
		-2 0 2				
Cluster 44						
Transect	Shoreline		Sand Wedge		Veg. Line	
	10-Year	Long-Term	10-Year	Long-Term	Long-Term	
10506	0.01	0.05	-1.28	-0.10		
10507	0.23	0.05	-0.60	-0.03		
10508	0.40	0.06	-0.15	-0.04		
10509	0.46	0.06	-0.14	-0.09		
10510	0.51	0.02	-0.12	-0.11		
10511	0.61	-0.01	-0.02	-0.08		
10512	0.66	-0.04	-0.05	-0.08		
10513	0.70	-0.03	0.05	-0.07		
Cluster 45						
Transect	Shoreline		Sand Wedge		Veg. Line	
	10-Year	Long-Term	10-Year	Long-Term	Long-Term	
10514	0.11	-0.05	-0.11	-0.10		
10515	-0.19	-0.08	-0.34	-0.13		
10516	-0.25	-0.09	-0.34	-0.14		
10517	-0.22	-0.08	-0.32	-0.15		
10518	-0.07	-0.05	-0.27	-0.14		
10519	0.10	-0.04	-0.10	-0.11		
10520	0.52	-0.02	-0.10	-0.09		
10521	0.07	-0.03	-0.14	-0.11		
10522	0.08	-0.03	-0.10	-0.12		
10523	0.00	-0.04	-0.14	-0.13		
10524	-0.04	-0.04	-0.29	-0.13		
10525	-0.09	-0.04	-0.42	-0.14		
10526	-0.03	-0.02	-0.31	-0.15		
10527	-0.01	-0.03	-0.25	-0.16		
10528	-0.05	-0.03	-0.20	-0.16		
10529	-0.17	-0.02	-0.29	-0.15		
10530	-0.11	-0.02	-0.31	-0.17		
10531	-0.08	-0.01	-0.29	-0.17		
10532	-0.12	0.01	-0.49	-0.17		
10533	-0.28	0.02	-0.31	-0.15		
10534	-0.41	0.00	-0.20	-0.14		
10535	-0.44	0.01	-0.40	-0.14		
10536	-0.37	0.00	-0.46	-0.14		
10537	-0.28	-0.02	-0.40	-0.15		
10538	-0.27	-0.04	-0.35	-0.15		
10539	-0.15	-0.06	-0.26	-0.16		
10540	-0.12	-0.06	-0.27	-0.16		
10541	-0.27	-0.06	-0.33	-0.17		
10542	-0.33	-0.06	-0.39	-0.19		
10543	-0.23	-0.05	-0.38	-0.18		
10544	-0.16	-0.03	-0.34	-0.16		
10545	-0.21	-0.04	-0.36	-0.14		
10546	-0.14	-0.04	-0.25	-0.12		
10547	-0.09	-0.01	-0.17	-0.11		
10548	-0.11	0.01	-0.28	-0.12		
10549	-0.12	-0.01	-0.29	-0.12		
10550	-0.18	-0.03	-0.32	-0.13		
10551	-0.21	-0.05	-0.32	-0.15		
10552	0.11	-0.02	-0.05	-0.11		
10553	0.36	0.02	0.29	-0.07		
10554	0.54	0.05	0.46	-0.05		
10555	0.59	0.05	0.37	-0.02		

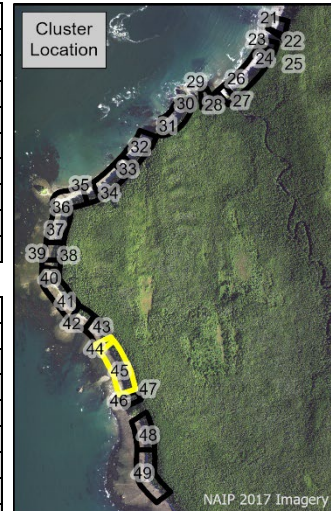


Table 49. Historical shoreline and sand wedge change rates in the Ozette sub-region based on the 10-m average transects in Cluster 45 (continued) through 47. The vegetation line could not be evaluated.

Cluster 45, contd.						Change Rate (m/yr)	-2	0	2
Transect	Shoreline		Sand Wedge		Veg. Line				
	10-Year	Long-Term	10-Year	Long-Term	Long-Term				
10556	0.38	0.03	0.24	-0.03					
10557	-0.13	-0.01	-0.33	-0.06					
10558	-0.23	-0.04	-0.20	-0.10					
10559	-0.39	-0.07	-0.38	-0.12					
10560	-0.32	-0.09	-0.42	-0.11					
10561	-0.27	-0.09	-0.37	-0.12					
10562	-0.34	-0.07	-0.31	-0.13					
10563	-0.22	-0.07	-0.16	-0.12					
10564	-0.32	-0.03	-0.11	-0.07					
10565	-0.28	0.01	-0.15	-0.02					
10566	-0.14	0.03	-0.19	-0.01					
10567	-0.16	0.04	-0.41	-0.02					
10568	-0.16	0.05	-0.21	-0.02					
10569	-0.28	0.06	-0.37	0.02					
10570	-0.37	0.07	-0.72	0.05					

Cluster 46					
Transect	Shoreline		Sand Wedge		Veg. Line
	10-Year	Long-Term	10-Year	Long-Term	Long-Term
10571	-1.29	0.07	-0.56	0.05	
10572	-2.23	0.07	-0.20	0.05	
10573	-1.68	0.08	-0.17	0.06	

Cluster 47					
Transect	Shoreline		Sand Wedge		Veg. Line
	10-Year	Long-Term	10-Year	Long-Term	Long-Term
10574	-0.56	0.10	-0.18	0.06	
10575	-0.41	0.09	-0.20	0.04	
10576	-0.33	0.09	-0.19	0.02	
10577	-0.26	0.08	-0.14	0.01	
10578	-0.22	0.07	-0.01	0.01	
10579	-0.33	0.07	0.02	0.00	
10580	-0.45	0.06	-0.03	0.00	
10581	-0.46	0.05	-0.19	-0.03	
10582	-0.40	0.05	-0.28	-0.04	
10583	-0.37	0.01	-0.09	-0.02	
10584	-0.31	0.01	-0.22	-0.05	
10585	-0.24	-0.02	-0.48	0.07	

Table 50. Historical shoreline and sand wedge change rates in the Ozette sub-region based on the 10-m average transects in Cluster 48. The vegetation line could not be evaluated.

Cluster 48					
Change Rate (m/yr)					
Transect	Shoreline		Sand Wedge		Veg. Line
	10-Year	Long-Term	10-Year	Long-Term	Long-Term
10586	-0.04	0.10	-0.16	-0.05	
10587	-0.09	0.06	-0.13	-0.08	
10588	0.02	0.05	-0.16	-0.11	
10589	0.10	0.02	-0.17	-0.13	
10590	-0.02	0.01	-0.24	-0.14	
10591	-0.05	0.02	-0.34	-0.15	
10592	0.01	0.02	-0.33	-0.14	
10593	-0.05	0.02	-0.34	-0.14	
10594	-0.17	0.03	-0.34	-0.13	
10595	-0.14	0.06	-0.38	-0.13	
10596	-0.08	0.08	-0.44	-0.12	
10597	-0.06	0.10	-0.42	-0.09	
10598	0.04	0.12	-0.30	-0.06	
10599	0.12	0.13	-0.20	-0.05	
10600	0.16	0.13	-0.20	-0.07	
10601	0.15	0.11	-0.27	-0.09	
10602	0.15	0.11	-0.37	-0.10	
10603	0.17	0.11	-0.45	-0.10	
10604	0.11	0.11	-0.50	-0.12	
10605	0.10	0.11	-0.48	-0.12	
10606	0.12	0.12	-0.50	-0.11	
10607	0.11	0.12	-0.54	-0.10	
10608	-0.07	0.11	-0.58	-0.09	
10609	-0.07	0.12	-0.62	-0.09	
10610	0.17	0.16	-0.58	-0.10	
10611	0.32	0.20	-0.45	-0.08	
10612	-0.07	0.17	-0.32	-0.06	
10613	-0.22	0.15	-0.30	-0.04	
10614	-0.13	0.13	-0.14	-0.04	
10615	-0.13	0.11	-0.26	-0.01	
10616	-0.11	0.12	-0.27	-0.01	
10617	-0.10	0.11	-0.24	-0.02	
10618	-0.04	0.10	-0.25	-0.04	
10619	-0.01	0.09	-0.27	-0.07	
10620	-0.04	0.09	-0.24	-0.08	
10621	-0.07	0.09	-0.20	-0.07	
10622	-0.06	0.10	-0.17	-0.02	
10623	-0.04	0.12	-0.17	-0.04	
10624	-0.09	0.11	-0.19	-0.04	

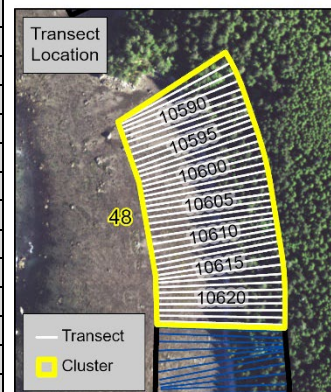


Table 51. Historical shoreline and sand wedge change rates in the Ozette sub-region based on the 10-m average transects in Cluster 49. The vegetation line could not be evaluated.

Cluster 49		Change Rate (m/yr)			Veg. Line
		10-Year	Long-Term	10-Year	
10625	-0.22	0.12	-0.26	-0.02	
10626	-0.22	0.11	-0.46	-0.01	
10627	-0.32	0.10	-0.86	-0.03	
10628	-0.56	0.08	-0.91	-0.04	
10629	-0.67	0.06	-0.67	-0.01	
10630	-0.71	0.04	-0.54	-0.01	
10631	-0.73	0.04	-0.55	-0.03	
10632	-0.63	0.04	-0.83	-0.08	
10633	-0.47	0.04		-0.14	
10634	-0.37	0.02		-0.17	
10635	-0.39	0.02		-0.16	
10636	-0.41	0.04		-0.13	
10637	-0.37	0.05		-0.12	
10638	-0.38	0.05		-0.13	
10639	-0.46	0.06		-0.12	
10640	-0.54	0.07		-0.11	
10641	-0.55	0.08		-0.09	
10642	-0.55	0.07		-0.10	
10643	-0.56	0.06		-0.09	
10644	-0.62	0.06		-0.09	
10645	-0.71	0.06		-0.07	
10646	-0.69	0.06		-0.05	
10647	-0.59	0.05		-0.03	
10648	-0.57	0.05		-0.03	
10649	-0.67	0.04		-0.03	
10650	-1.11	0.01	-0.56	-0.07	
10651	-1.11	0.05	-0.40	-0.05	
10652	-0.26	0.08	-0.31	-0.04	
10653	-0.25	0.10	-0.32	-0.06	
10654	-0.36	0.11	-0.32	-0.01	
10655	-0.33	0.12	-0.50	0.04	
10656	-0.26	0.10	-0.42	-0.01	
10657	-0.23	0.11	-0.38	-0.03	
10658	-0.66	0.04	-0.44	-0.05	
10659	-1.12	-0.07		-0.03	
10660	0.14	0.01	-0.47	-0.17	
10661	-0.26	-0.01	-0.57	-0.23	
10662	-0.23	-0.01	-0.44	-0.21	
10663	-0.42	-0.02	-0.35	-0.18	
10664	-0.43	-0.03	-0.40	-0.19	
10665	-0.48	-0.05	-0.45	-0.20	
10666	-0.33	-0.04	-0.37	-0.19	
10667	-0.13	0.00	-0.47	-0.17	
10668	0.00	0.03	-0.45	-0.16	
10669	0.11	0.04	-0.46	-0.16	
10670	0.18	0.03	-0.42	-0.17	
10671	0.19	0.03	-0.27	-0.19	
10672	0.01	0.02	-0.17	-0.18	
10673	-0.51	0.00	-0.13	-0.16	
10674	-1.03	-0.02	-0.10	-0.15	
10675	-0.26	0.05	-0.18	-0.12	
10676	-0.10	0.08	-0.19	-0.10	
10677	-0.06	0.08	-0.06	-0.10	
10678	-0.20	0.07	-0.16	-0.08	

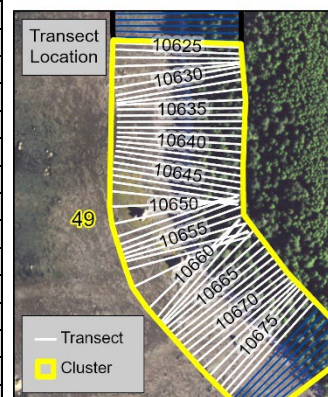
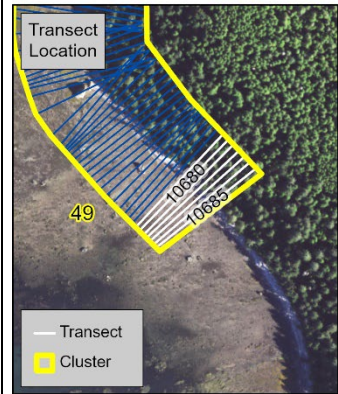
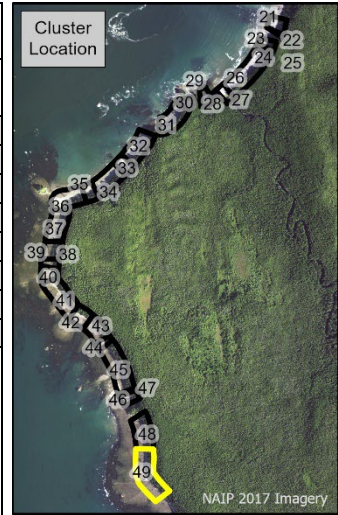


Table 52. Historical shoreline and sand wedge change rates in the Ozette sub-region based on the 10-m average transects in Cluster 49 (continued). The vegetation line could not be evaluated.

Cluster 49, contd.		Change Rate (m/yr)				Veg. Line
		Shoreline		Sand Wedge		
Transect	Change Rate (m/yr)		Change Rate (m/yr)		Long-Term	
	10-Year	Long-Term	10-Year	Long-Term		
10679	-0.50	0.05	-0.29	-0.09		
10680	-0.41	0.06	-0.26	-0.09		
10681	-0.83	0.08	-0.11	-0.07		
10682	-0.75	0.10	-0.18	-0.06		
10683	-0.66	0.10	-0.22	-0.06		
10684	-0.57	0.09	-0.22	-0.05		
10685	-0.37	0.08	-0.28	-0.07		
10686	0.02	0.10		-0.18		



Appendix E. Topo-bathymetric Map of Makah Bay

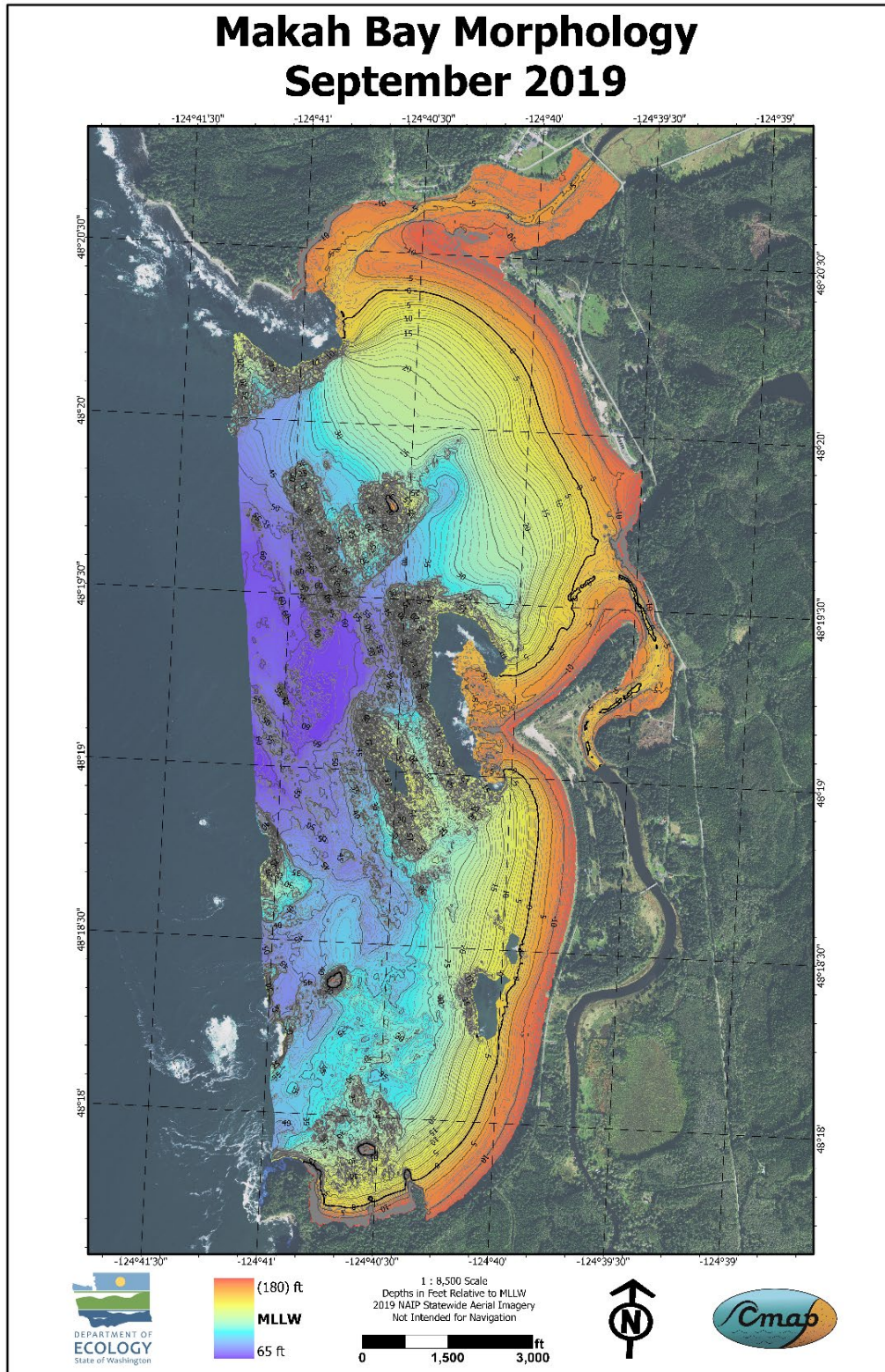


Figure 53. Topo-bathymetric digital elevation model of Makah Bay with contours indicating elevation relative to mean lower low water (MLLW).